Vibrational Spectral Analysis, Electronic Transition and NBO Studies of Tetrazole Derivatives Based on DFT Calculation



Thesis submitted to

Bharathidasan University, Tiruchirappalli

in partial fulfillment of the requirements for the award of the degree of

DOCTOR OF PHILOSOPHY IN PHYSICS

By

Mrs. A.RAJESWARI.M.Sc.,M.Ed.,M.Phil., (Ref. No: 29718/Ph.D.K3/Physics/Full-time/October 2016)

Under the Guidance of

Dr. M.K. MURALI M.Sc., M.Phil., Ph.D.



PG AND RESEARCH DEPARTMENT OF PHYSICS JJ COLLEGE OF ARTS & SCIENCE (AUTONOMOUS)

PUDUKKOTTAI – 22, TAMILNADU, INDIA

MAY - 2022

Dr. M. K. MURALI, M.Sc., M.Phil., Ph.D.,

Assistant Professor and Head,

PG & Research Department of Physics,

JJ College of Arts & Science (Autonomous),

J.J. Nagar, Sivapuram,

Pudukkottai – 622 422.

CERTIFICATE

This is to certify that the thesis entitled, "Vibrational Spectral Analysis, Electronic

Transition and NBO Studies of Tetrazole Derivatives Based on DFT Calculation"

is the bonafide work of Mrs. A. RAJESWARI (Ref. No: 29718/Ph.D.K3/Physics/Full-

time/October 2016) who has carried out the research under my supervision and that

to the best of my knowledge the contents of this thesis have not formed the basis for

the award of any degree, diploma or other similar title of any University or Institution.

Place: Pudukkottai

Date:

(Dr. M. K. MURALI)

Research Supervisor

i

A.RAJESWARI,

Research Scholar,

PG & Research Department of Physics,

JJ College of Arts& Science (Autonomous),

J.J. Nagar, Sivapuram,

Pudukkottai -622 422.

DECLARATION

I hereby declare that the thesis entitled, "Vibrational Spectral Analysis, Electronic

Transition and NBO Studies of Tetrazole Derivatives Based on DFT Calculation"

is a record of work done by me, under the guidance and supervision of

Dr. M. K. MURALI, Assistant Professor and Head, PG & Research Department of

Physics, JJ College of Arts& Science(Autonomous), Sivapuram, Pudukkottai - 22.

I also declare that this work has not formed in part or fully the basis for the award of

any degree or diploma at any University.

Place: Pudukkottai

Date:

A.RAJESWARI

ii

Dr. M. K. MURALI, M.Sc., M.Phil., Ph.D.,

Assistant Professor and Head,

PG & Research Department of Physics,

JJ College of Arts & Science (Autonomous),

J.J. Nagar, Sivapuram,

Pudukkottai – 622 422.



Date:

CERTIFICATE OF PLAGIARISM CHECK

Name of the Research Scholar: A. RAJESWARI

Course of Study: Ph.D., Physics

University Ref. No.: 29718/Ph.D.K3/Physics/Full time/October 2016

Title of the Thesis/Dissertation: Vibrational Spectral Analysis, Electronic

Transition and NBO Studies of Tetrazole

Derivatives Based on DFT Calculation"

Acceptable Maximum Limit: 20%

Percentage of Similarity of

10%

Content Identified:

Software Used: Ouriginal

Date of Verification: 22/09/2021

Report on plagiarism check, item with % of similarity is attached.

Signature of the Research Supervisor

Signature of the Candidate



Document Information

Analyzed document Rajeswari A.pdf (D113160407)

> 2021-09-22 10:47:00 Submitted

Submitted by Srinivasa ragavan S

Submitter email bdulib@gmail.com

> Similarity 10%

Analysis address bdulib.bdu@analysis.urkund.com

Sour	ces included in the report		
W	URL: https://sg.inflibnet.ac.in/jspui/bitstream/10603/201299/11/11-chapter-5.pdf Fetched: 2020-07-12 16:15:22	88	6
W	URL: https://core.ac.uk/download/pdf/229210724.pdf Fetched: 2021-06-22 12:34:10	88	14
W	URL: https://www.ripublication.com/ijoms17spl/ijomsv12n2spl_31.pdf Fetched: 2021-09-03 09:05:09	88	2
W	URL: https://isroset.org/pub_paper/IJSRPAS/12-IJSRPAS-01850-03.pdf Fetched: 2021-06-21 09:40:17	88	14
W	URL: https://docksci.com/nbo-homo-lumo-analysis-and-vibrational-spectra-ftir-and-ft-raman-of-1-amino-4-me_5a9fd685d64ab26cb178b194.html Fetched: 2021-07-23 20:07:35	88	5
W	URL: https://www.pubmedscience.com/article-details/Investigation-on-Spectral-properties-of-3-Chloro-3-Methoxystilbene-for-Anticancer-Drugs-Application-Using-Density-Functional-Theory/558 Fetched: 2021-07-01 09:46:26		3
W	URL: https://rajpub.com/index.php/jac/article/view/1957/1915 Fetched: 2020-02-10 10:22:00		8
W	URL: https://www.elixirpublishers.com/articles/1396517038_69%20(2014)%2022867-22876.pdf Fetched: 2021-07-21 17:05:17		5
W	URL: https://www.longdom.org/open-access/synthesis-and-structural-characterization-of-2hydroxy5phenyldiazenyl-benzaldehyde-oximea-theoretical-approach-2376-130X-1000146.pdf Fetched: 2021-07-29 08:12:45		1
W	URL: http://www.journalcra.com/sites/default/files/issue-pdf/9016.pdf Fetched: 2021-06-22 12:34:16		1

Vibrational Spectral Analysis, Electronic Transition and NBO Studies of Tetrazoie Derivatives Based on DFT Calculation

Abstract

Vibrational spectroscopy is an important tool for the elucidation of molecular structure. It also provides important information about intramolecular force acting between the atoms in a molecule and intermolecular forces in a condensed phase. In the introductory chapter, some of the very basic concepts of vibrational spectroscopy and its applications to polyatomic molcules are discussed. As molecular symmetry and group theory plays an important role in the structure and characteristics of molecules. The instrumentation techniques for infrared and Raman activities are outlined. The application of group of theory in determining the normal modes of vibrations are discussed. The concept of group frequency and the factors influencing the vibrational frequencies of polyatomic molecules are discussed. An overview of DFT and the different types of Basis sets are outlined. The novel organic molecule Tetrazole derivatives were selected to this study. The calculations behind the hyperpolarizability are quoted. Charge distribution among the atoms or surface of the various tetrazole derivatives are explained by Mulliken Atomic charges and Electrosatic Potential are discussed. Frontier molecular orbitals, Quantum chemical parameters and NLO properties are also explained. To analyse the intra-molecular delocatization along with the intermolecular interaction, the NBO study has been done for monomer of the molecules.

ACKNOWLEDGEMENT

I thank the *Almighty God*, for having His Grace and Blessings on me in the successful completion of my research work. I dedicate this work to my beloved parents *Mr. S.P. Arjunan & Mrs. A. Nagu*.

I take this opportunity to express my deep appreciation and sincere gratitude to **Dr. M. K. Murali, M.Sc., M.Phil., Ph.D.,** Assistant Professor and Head, PG and Research Department of Physics, JJ College of Arts & Science (Autonomous), Pudukkottai-22, for his inspiring guidance and encouragement given to me during the entire research tenure. His ever ready attitude to extend help has made my work all the more easier.

I record my sincere thanks to **Mr. N. Subramanian, B.Sc., L.L.B.,** Secretary and **Dr. KavithaSubramanian,** Management Trustee, JJ College of Arts & Science (Autonomous), Pudukkottai-22, who showed keen interest not only in the progress of my work but also in developing the College into a research centre.

I would like to express my sincere gratitude to **Dr. J. Parasuraman**, Principal, JJ College of Arts & Science (Autonomous), Pudukkottai-22, for his support and encouragement.

I express my sincere thanks to the Doctoral Committee MembersDr. Murugan, Assistant Professor, Department of Physics, Government Arts College,
Thiruvarambur and Dr. Janaki, Assistant Professor, PG and Research Department of
Physics, Govt Arts and Science College, Pudukkottai,- for their affectionate care,
encouragement and support to me, since the initiation of my research work.

I wish to express my sense of gratitude to **Dr. Meyyammai** and **Mr. Seetharaman,** JJ College of Arts & Science (Autonomous), Pudukkottai -22.

I would like to express my sincere gratitude to all the staff Members of PG & Research Department of Physics, JJ College of Arts & Science (Autonomous), Pudukkottai -22, and **Dr. A. Ramu**, Assistant Professor & Head, Department of Physics, Ganesar College of Arts And Science, Melaisivapuri, Ponnamaravathi - 622403 for their support and encouragement.

I owe my deepest gratitude and thankfulness to my family members Mr. M. Mathialagan and my kids M. Pavithra and M. Pravin for the warmth and care they have shown during my research work.

I wish to express my thankfulness to the authorities of Bharathidasan University, Tiruchirappalli-620 024 for granting permission to carry out this research work.

I take this opportunity to thank **Global Computers**, Tiruchirappalli, for their kind co-operation in completing my thesis work.

A. Rajeswari

PREFACE

Vibrational spectroscopy continues to be utilized by scientists in the elucidation of molecular structure in spectra-structure identification in qualitative and quantitative analysis. Vibrational spectra can be utilized directly and simply as molecular finger prints to characterize and identify a molecule. Recent developments in Fourier transform spectrometers have led to higher resolution, total wavelengths coverage, higher accuracy in frequency and intensity measurements. Moreover, sophisticated computational methods of theoretical chemistry have also been developed by powerful personal computers. This has made it possible to perform a complete vibrational analysis on relatively large polyatomic molecules.

The assignment of bands in the vibrational spectra of polyatomic molecules is an essential step for solving various structural and chemical problems by applying vibrational spectroscopy. The philosophy of computational methods of vibrational spectroscopy significantly changed after the introduction of quantum chemical calculations. This has opened the way for calculating the frequencies and intensities of spectral bands. The results of the methods also explain the physical and chemical properties of substances present in the compounds.

In the present investigation quantum chemical calculations were carried out by means of the Gaussian 09W program package using B3LYP functional with the 6-31G,6-311+G basis set. The transformation of force field from Cartesian to symmetry co-ordinates, the scaling, the subsequent normal coordinate analysis, calculations of potential energy distribution (PED), IR and Raman intensities were also carried out for some organic compounds using the VEDA program. Furthermore, studies on the

natural bond orbital (NBO), HOMO-LUMO energy, polarizability were carried out using the same level of B3LYP basis set.

Based on the good quality scaled quantum mechanical (SQM) force field, reliable descriptions of the fundamentals were provided and unambiguous assignments have also been made. The infrared and Raman spectra could also be predicted from the calculated intensities. A comparison and reasonable discussions were also made by using the simulated and the experimental spectra.

Chapter One is the general introduction with a brief review of the relevant parts of the existing theories employed in this work to interpret the experimental results. The vibrations of molecules are looked at here, as these are crucial to the interpretation of infrared spectra. In this Chapter some idea about the information to be gained from infrared and Raman spectroscopy should have been gained.

Chapter Two discusses instrumentation and sample handling techniques of fourier transform infrared (FT-IR) and Fourier transform Raman (FT-Raman) spectroscopy which are used in this work.

The theoretical part of quantum chemical calculations, normal coordinate analysis and the scaling procedure employed in this workthe various basis set combination stored in Gaussian 09W program package are reported in *Chapter Three*

Chapter Four deals with spectroscopic signature of Pentylenetetrazole (PTZ)] on the basis of both experimental and theoretical IR and Raman spectra. The normal coordinate analysis and subsequent scaling procedure identify the functional group's wave numbers of the molecule. The complete vibrational assignments, along with the observed and theoretical vibrational wave numbers are presented and interpreted in detail.

In Chapter Five the detailed experimental and theoretical FT-IR and FT-Raman spectra of 5-Methyl-1H-tetrazole(5MTZ). are analysed based on density functional theory (DFT) calculation. Detailed vibrational assignments of observed experimental peaks are done on the basis of PED results. The calculated Mulliken atomic charges at different levels are also presented.

Chapter Six includes the vibrational FT-IR and FT- Raman spectra of 5-Chloro-1-phenyl-1H-tetrazole(5clptz). The completed assignments of vibrational normal modes associated with the molecule are made on the basis of PED results. The electronic properties were studied by DFT calculation with various basis set which helps to determine the chemical hardness, reactivity and softness.

Chapter Seven concerns the detailed experimental and theoretical FT-IR and FT-Raman spectra of 5(4 methyl phenyl)tetrazole (5MPTZ) along with NBO, HOMO-LUMO energy gap. The molecular polarizability and Mulliken properties are also discussed.

I believe that, this research work yields a detailed knowledge about the molecule that will be useful in Medical and Pharmaceutical applications. The optimization method helps us find the free binding energy of molecules, caused by changes in the vibrational mode. The electron binding affinity and HOMO – LUMO energy gap helps to predict the molecular docking capability of the chosen organic compound derivatives.

LIST OF PUBLICATION

- A. Rajeswari, M.K. Murali, A. Ramu. "Quantum mechanics calculation and Vibrational Spectra FT-IR and FT-Raman (theoretical, Experimental) studies of 5-Methyl-1H-tetrazole(5MTZ). (TEST Engineering & Management. ISSN:0193-4120.Nov/Dec 2020. Page No. 139-156)
- 2. A. Rajeswari, M.K. Murali, A. Ramu. "Non Linear Optical Properties, Optimized structure, Global reactivates and Mulliken Atomic Charge studies on 5-Chloro-1-phenyl-1H-tetrazole based on Density functional theory with vibrational assignment. (TEST Engineering & Management. ISSN:0193-4120.Nov/Dec 2020. Page No. 252-268)
- 3. **A. Rajeswari,** M.K. Murali, A. Ramu. "Simulation of FT-IR and FT-Raman Spectra Based on quantum chemical Calculations, Vibrational Assignments, Hyperpolarizability and Homo-Lumo Analysis of 5(4 methyl phenyl) tetrazole (5MPTZ)". **Indian Journal of natural Sciences.** ISSN NO: 0976-0997. Volume 12, Issue 67, August/2021. P:33597- 33607.
- 4. **A. Rajeswari,** M.K. Murali, A. Ramu. "Vibrational Spectra (theoretical, Experimental) and Optimized structure, Frontire Molecular orbital, Mulliken Atomic Charge studies on Pentylenetetrazole (PTZ) based on Density functional theory). **Design Engineering.** ISSN: 0011-9342. Issue 7 2021.P: 10815- 10830.

Papers presented in National/International Conference

- International Conference on Nanomaterials and Molecular Research at PG &Research Department of Physics, St. Joseph's College of Arts & Science (Autonomous), Cuddalore on 8-9th December 2016.
- 2. Spectroscopic FT-IR and FT-Raman analysis NLO, FMO, MEP and Muliken population analysis of 2- Ethoxy-2- phenyl Acetophenone, International conference on Recent Advances in Applied Physics organized by Engineering Physics Section, Faculty of Engineering and Technology, Annamalai University on 21st 22nd September 2017.
- 3. National Level Seminar on Recent Advances in Material Characterization,

 National College (Autonomous), Tiruchirappalli on 02nd March 2018.
- 4. Vibrational studies, molecular Geometry, NBO analysis, frontier molecular orbitals, NLO and DFT calculation on 2- methyl imidazole, National Conference on New Vistas in Material Science, JJ College of Arts and Science (Autonomous), Pudukkottai on 8th & 9th March 2018.
- Vibrational analysis FT-IR and FT- Raman of 2- chloro 3,4 dihydroxy acetophenone, International Conference on Recent Advances in Materials,
 National College (Autonomous), Tiruchirappalli on 22-23 March 2018.

CONTENTS

CHAPTER NO.	TITLE	PAGE NO.
	CERTIFICATE	i
	DECLARATION	ii
	CERTIFICATE OF PLAGIARISM CHECK	iii
	OURIGINAL REPORT	iv
	ACKNOWLEDGEMENT	v
	PREFACE	vii
	LIST OF PUBLICATION	X
	PAPERS PRESENTED IN NATIONAL/INTERNATIONAL CONFERENCE	xi
I	INTRODUCTION TO MOLECULAR SPECTROSCOPY	1
1.1	Introduction	1
1.2	Infrared and Raman Spectroscopy	2
1.3	Selection Rules	4
1.3.	Rule of mutual exclusion	5
1.3.2	Selection rules for an Infrared absorption and for Raman scattering	5
1.4	Normal modes of vibration	6
1.5	Interpretation of group frequencies	8
II	INSTRUMENTATION TECHNIQUES	13
2.1	Introduction	13
2.2	Infrared Spectrometer	14
2.3	Raman Spectrometer	19
2.3.1	FT Raman Spectroscopy	20
III	THEORETICAL AND COMPUTATIONAL METHODS	24
3.1	Introduction	24
3.2	AB Initio calculations	25
3.2.1	Hartree- Fock theory	26
3.2.2	Density functional theory	29
3.3	Basis sets	32
3.4	Calculation of vibrational frequencies	34

3.5	Calculation of vibrational infrared and Raman spectra	36
3.6	Vibrational Hamiltonian	37
3.7	Applications of Quantum chemical calculation	37
3.7.1	Natural Bond orbital Analyis	38
3.7.2	Potential Energy Distribution(PED)	38
3.7.3	Homo-Lumo energy Gap Analysis	39
3.7.4	Dipole moment, Hyperpolarizability	39
IV	VIBRATIONAL SPECTRA (THEORETICAL, EXPERIMENTAL) AND OPTMIZED STRUCTURE, FRONTIER MOLECULAR ORBITAL, MULLIKEN ATOMIC CHARGE STUDIES ON PENTYLENE TERTAZOLE (PTZ) BASED ON DENSITY FUNCTIONAL THEORY	40
4.1	Introduction	40
4.2	Experimental Details	40
4.3	Computational Details	41
4.4	Molecular geometry	41
4.5	Frontier Molecular orbital Analysis	43
4.6	Molecular Electrostatic potential (MEP)	45
4.7	Mulliken Atomic charge	48
4.8	Non linear optical properties	49
4.9	Vibrational assignment	49
4.10	Natural Bond Analysis	53
4.11	Conclusion	54
V	QUANTUM MECHANICS CALCULATION AND VIBRATIONAL SPECTRA FT-IR AND FT-RAMAN (THEORETICAL, EXPERIMENTAL) STUDIES OF 5- METHYL-1H-TETRAZOLE (5MTZ)	64
5.1	Introduction	64
5.2	Experimental Details	65
5.3	Computational Details	65
5.4	Geometrical parameter	66
5.5	Electronic properties	66
5.6	Molecular Electrostatic Potential (MEP)	71
5.7	NLO properties	72

5.8	Mulliken Atomic Charge	74
5.9	Vibrational Assignment	74
5.10	Natural Bond Analysis	78
5.11	Conclusion	79
VI	NON LINEAR OPTICAL PROPERTIES, OPTIMIZED STRUCTURE, GLOBAL REACTIVES AND MULLIKEN ATOMIC CHARGE STUDIES ON 5-CHLORO -1-PHENYL -1H-TETRAZOLE BASED ON DENSITY FUNCTIONAL THEORY WITH VIBRATIONAL ASSIGNMENT	87
6.1	Introduction	87
6.2	Experimental Details	88
6.3	Computational Details	88
6.4	Molecular geometry	90
6.5	Frontier molecular orbital analysis	90
6.6	Molecular Electrostatic Potential(MEP)	93
6.7	Mulliken atomic charge	93
6.8	Nonlinear optical properties	94
6.9	Vibrational assignment	96
6.10	Natural Bond Analysis	100
6.11	Conclusion	101
VII	SIMULATION OF FT-IR AND FT-RAMAN SPECTRA BASED ON QUANTUM CHEMICAL CALCULATIONS, VIBRATIONAL ASSIGNMENTS, HYPERPOLARIZABILITY AND HOMO - LUMO ANALYSIS OF 5 (4 METHYL PHENYL) TETRAZOLE (5MPTZ)	109
7.1	Introduction	109
7.2	Experimental Details	110
7.3	Computational Details	110
7.4	Geometrical parameter	111
7.5	Electronic properties	113
7.6	NLO properties	115
7.7	Mulliken Atomic Charge	116
7.8	Molecular Electrostatic Potential	117
7.9	Vibrational Assignment	120

7.10	Natural Bond Analysis	125
7.11	Conclusion	126
	Summary of Conclusion	135
	References	137

Chapter - I

Introduction to molecular Spectroscopy

Abstract

The general introduction and the characteristic features of the vibrations of polyatomic molecules are discussed. The selection rules for infrared and Raman spectroscopy are explained. Various types of force fields with their merits are dealt with briefly. The group theory, normal modes of vibrations...

Chapter - I

Introduction to Molecular Spectroscopy

1.1. INTRODUCTION

Molecular spectroscopy investigates and quantifies the response of molecules interacting to known amounts of energy (or frequency). Molecules have certain energy levels that can be analyzed by detecting the molecule's energy exchange through absorbance or emission. A transition from a lower level to a higher level with transfer of energy from the radiation field to the atom or molecule is called absorption (IR spectroscopy). A transition from a higher level to a lower level is called emission if energy is transferred to the radiation field or non-radiative decay if no radiation is emitted. Redirection of light due to its interaction with matter is called scattering, and may or may not occur with transfer of energy, i.e., the scattered radiation has a slightly different or the same wavelength (Raman spectroscopy).

In this introductory chapter, the basic ideas and definitions associated with infrared and Raman spectroscopy will be described. The vibrations of molecules will be looked at here, as these are crucial to the interpretation of infrared spectra. In this chapter some idea about the information to be gained from infrared and Raman spectroscopy should have been gained. The following chapter will aid in an understanding of how infrared and Raman spectrometers produce a spectrum.

1.2. INFRARED AND RAMAN SPECTROSCOPY

Infrared and Raman spectroscopy involve the study of the interaction of radiation with molecular vibrations but differs in the manner in which photon energy is transferred to the molecule by changing its vibrational state. IR spectroscopy measures transitions between molecular vibrational energy levels as a result of the absorption of mid-IR radiation. This interaction between light and matter is a resonance condition involving the electric dipole mediated transition between vibrational energy levels. Raman spectroscopy is a two-photon inelastic lightscattering event. Here, the incident photon is of much greater energy than the vibrational quantum energy, and loses part of its energy to the molecular vibration with the remaining energy scattered as a photon with reduced frequency. In the case of Raman spectroscopy, the interaction between light and matter is an off-resonance condition involving the Raman polarizability of the molecule.

Raman Spectroscopy is a routine analytical technique used extensively in semiconductor and pharmaceutical industry. In 1928 Sir C.V. Raman showed that the radiation scattered by molecules, contain photons with same frequency as the incident photon, but may also contain very small number of photons with changed or shifted frequency. The frequency-shifted light is known as Raman radiation.

Some of the Raman radiation is slightly lower in frequency than the incident radiation and is called Stokes-shifted radiation. Another portion of the Raman radiation is higher in frequency than the incident radiation and is called anti-Stokes radiation (Fig 1.1).

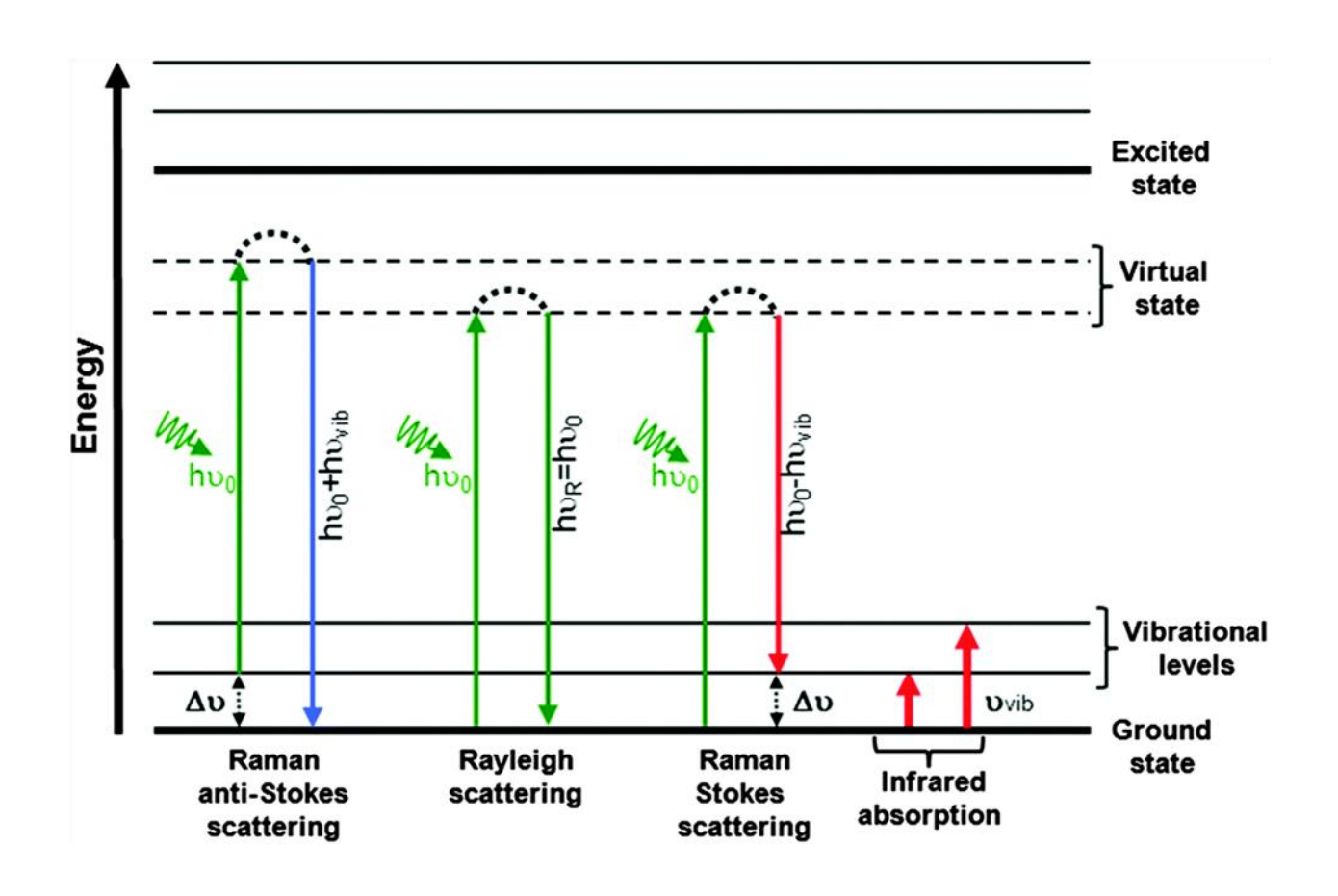


Fig 1.1: Energy levels involved in Raman and Rayleigh scattering

The exact characteristics of Raman radiation depend on the chemical composition of the sample and every compound has unique spectral fingerprint. Since no two molecules give exactly the same Raman spectrum and the intensity of the scattered light is related to the amount of material present, it is easy to obtain both qualitative and quantitative information about the sample. In Raman spectroscopy, monochromatic laser source excites the molecules residing in the ground vibrational and electronic state to a virtual state, equal to the energy of the laser. The molecules relax back to the ground vibrational state, i.e., giving back the same energy. This is Rayleigh scatter. The small portion that relaxes to an upper vibrational state, giving off less energy, is the Raman shift (also known as Stokes shift). Unlike quantized energy level transactions, such as fluorescence or phosphorescence, the Raman scatter event involves virtual excited state and the process is instantaneous. The energy resulting from this shift (initial laser energy minus energy emitted) is equal to the same vibrational energy gap that is excited in infrared spectroscopy. The vibrations that are strong in infrared spectrum, those involving strong dipole moment, are usually weak in Raman spectrum. Similarly, non-polar functional group vibrations that give very strong Raman bands usually result in weak infrared signals.

1.3. SELECTION RULES

Both Raman spectroscopy and infrared spectroscopy provide a unique spectral fingerprint of a material. The patterns of the spectra are caused by molecular or lattice vibrations. Although the spectral features of Raman and infrared spectra can be

interpreted in a similar way the spectra look slightly different. The whole vibrational picture of a material is given by the complementary information of both Raman and infrared spectra.

Using selection rules, it can be predicted whether a molecular vibration is Raman or infrared active. During the interaction between a molecule and a photon the total angular momentum in the electronic ground state has to be conserved. As a consequence of this requirement only specific vibrational transitions are possible.

1.3.1. Rule of mutual exclusion

In general, molecular vibrations symmetric with regard to the centre of symmetry are forbidden in the infrared spectrum, whereas molecular vibrations which are antisymmetric to the centre of symmetry are forbidden in the Raman spectrum. This is known as the rule of mutual exclusion.

1.3.2. Selection rules for an infrared absorption and for Raman scattering

Infrared absorption can be detected if the dipole moment μ in a molecule is changed during the normal vibration. The intensity of an infrared absorption band IIR depends on the change of the dipole moment μ during this vibration:

$$I_{IR} \propto \left[\frac{\partial \mu}{\partial q}\right]_0^2$$

where q is the normal coordinate.

A Raman active vibration can be detected if the polarizability a in a molecule is changed during the normal vibration. The intensity of a Raman active band I_{Raman} depends on the change of polarizability during this vibration:

$$I_{Raman} \propto \left[\frac{\partial \alpha}{\partial q}\right]_0^2$$

As a consequence of the selection rules, infrared spectroscopy provides detailed information about functional groups and Raman spectroscopy especially contributes to the characterization of the carbon backbone of organic substances or polymers.

1.4. NORMAL MODES OF VIBRATION

The interactions of radiation with matter may be understood in terms of changes in molecular dipoles associated with vibrations and rotations. In order to begin with a basic model, a molecule can be looked upon as a system of masses joined by bonds with spring-like properties. Taking first the simple case of diatomic molecules, such molecules have three degrees of translational freedom and two degrees of rotational freedom. The atoms in the molecules can also move relative to one other, that is, bond lengths can vary or one atom can move out of its present plane. This is a description of stretching and bending movements that are collectively referred as vibrations. For a diatomic molecule, only one vibration that corresponds to the stretching and compression of the bond is possible. This accounts for one degree of vibrational freedom. Polyatomic molecules containing many (N) atoms will have 3N degrees of freedom. Looking first at the case of molecules containing three atoms, two groups of tri-atomic molecules may be distinguished, i.e. linear and non-linear. There are 3N-5 degrees of freedom for any linear molecule and 3*N*-6 for any nonlinear molecule.

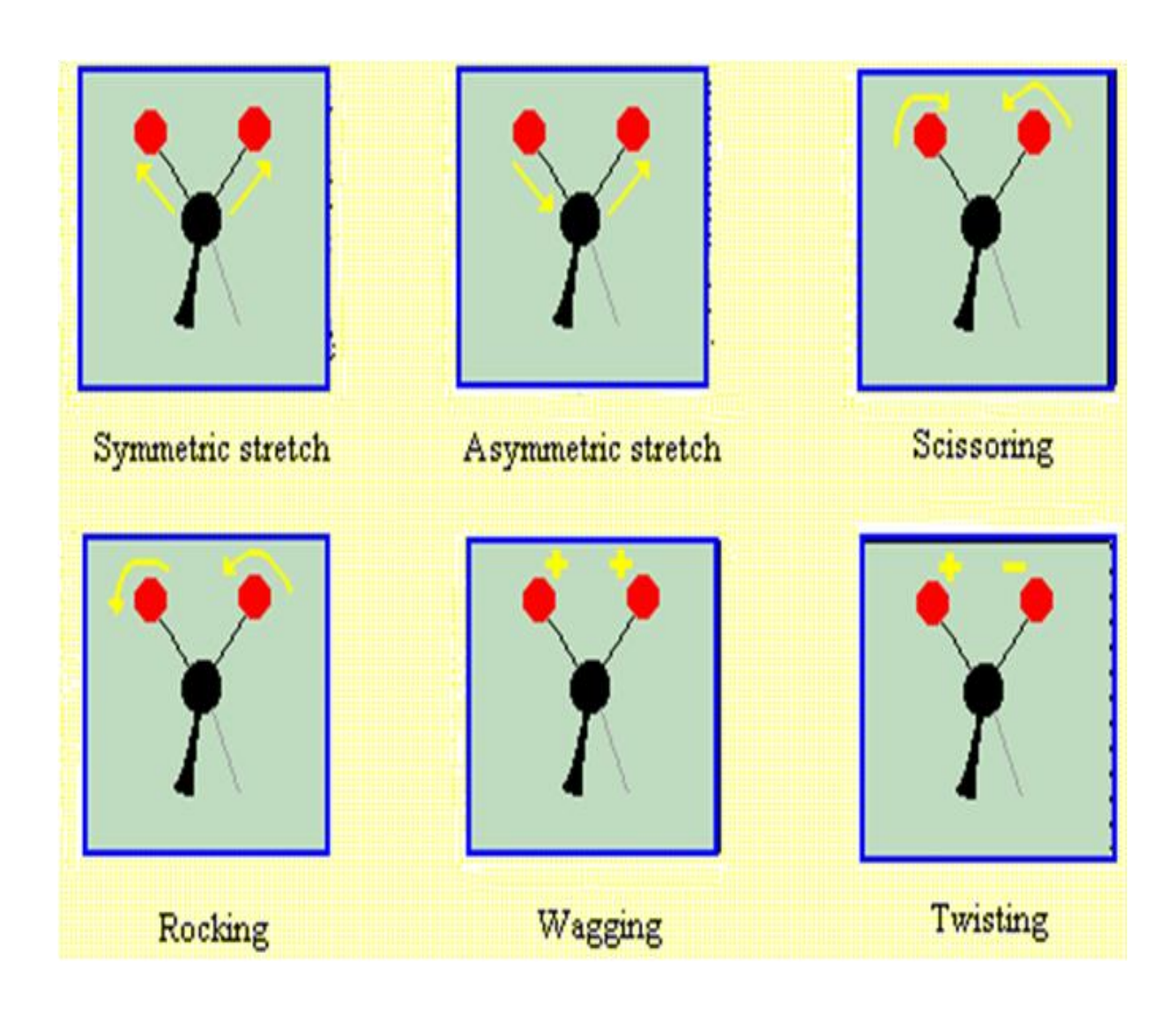


Fig 1.2: Vibrational mode types

Vibrations can involve either a change in bond length (stretching) or bond angle (bending). Some bonds can stretch in-phase (symmetrical stretching) or out-of phase (asymmetric stretching), as shown in Fig 1.2. If a molecule has different terminal atoms such as HCN, ClCN or ONCl, then the two stretching modes are no longer symmetric and asymmetric vibrations of similar bonds, but will have varying proportions of the stretching motion of each group. In other words, the amount of coupling will vary.

Bending vibrations also contribute to spectra. It is best to consider the molecule being cut by a plane through the hydrogen atoms and the carbon atom. The hydrogen can move in the same direction or in opposite directions in this plane, here the plane of the page. For more complex molecules, the analysis becomes simpler since hydrogen atoms may be considered in isolation because they are usually attached to more massive, and therefore, more rigid parts of the molecule. This results in in-plane and out-of-plane bending vibrations, as illustrated in Fig 1.2.

1.5. INTERPRETATION OF GROUP FREQUENCIES

The vibrational spectrum of a molecule is considered to be a unique physical property and is characteristic of the molecule. As such, the infrared spectrum can be used as a fingerprint for identification by the comparison of the spectrum from an "unknown" with previously recorded reference spectra. This is the basis of computer based spectral searching. In the absence of a suitable reference database, it is possible to effect a basic interpretation of the spectrum from first principles, leading to characterization, and possibly even identification of an unknown sample. This first principles approach is

based on the fact that structural features of the molecule, whether they are the backbone of the molecule or the functional groups attached to the molecule, produce characteristic and reproducible absorptions in the spectrum. This information can indicate whether there is backbone to the structure and, if so, whether the backbone consists of linear or branched chains. Next it is possible to determine if there is unsaturation and/or aromatic rings in the structure. Finally, it is possible to deduce whether specific functional groups are present. If detected, one is also able to determine local orientation of the group and its local environment and/or location in the structure.

Infrared spectral interpretation may be applied to both organic and inorganic compounds, and there are many specialized texts dealing with these compounds, in combination and as individual specialized texts. There are too many to reference comprehensively which provides a bibliography of the most important reference texts [1]. However, the most informative general reference texts are included [2–9] with books by Socrates[6] and Lin-Vien [7] being recommended for general organics, and by Nyquist *et al.*, [9] for inorganics (salts and coordination compounds).

The following comments are made relative to the conventions used within this thesis. The term frequency is used for band/peak position throughout, and this is expressed in the commonly used units of wavenumber (cm⁻¹). The average modern infrared instrument records spectra from an upper limit of around 4000 cm⁻¹ (by convention) down to 400 cm⁻¹ as defined by the optics of the instrument (commonly based on potassium bromide, KBr). For this reason, when a spectral region is quoted in this thesis, the higher value will be quoted first, consistent with the normal left-to-right

(high to low cm⁻¹) representation of spectra. Also, the terms infrared band, peak and absorption will be used interchangeably within the thesis to refer to a characteristic spectral feature. Every attempt to ensure accuracy has been taken; however, there will be instances when individual functional groups may fall outside the quoted ranges. This is to be expected for several reasons: the influences of other functional groups within a molecule, the impact of preferred spatial orientations, and environmental effects (chemical and physical interactions) on the molecule.

The preferred format for presenting spectral data for qualitative analysis is in the percentage transmittance format, which has a logarithmic relationship ($-\log 10$) with respect to the linear concentration format (absorbance). This format, which is the natural output of most instruments (after background ratio), provides the best dynamic range for both weak and intense bands. In this case, the peak maximum is actually represented as a minimum, and is the point of lowest transmittance for a particular band.

The group frequencies may be viewed quantitatively, as well as qualitatively. A given absorption band assigned to a functional group increases proportionately with the number times that functional group occurs within the molecule. From a first-order perspective, the idea of the quantitative aspects of the group frequencies carries through for most functional groups, and the overall spectrum is essentially a composite of the group frequencies, with band intensities in part related to the contribution of each functional group in the molecule.

This assumes that thefunctional group does give rise to infrared absorption frequencies (most do), and it is understood that each group has its own unique

contribution based on its extinction coefficient (or infrared absorption cross-section). In reality, one can assign the observed absorption frequencies in the infrared spectrum to much more that just simple harmonic (or anharmonic) stretching vibrations. In practice, one can find that various other deformation motions (angular changes), such as bending and twisting about certain centres within a molecule, also have impact, and contribute to the overall absorption spectrum. By rationalizing the effort needed to move the atoms relative to each other, one can appreciate that it takes less energy to bend a bond than to stretch it. Consequently, one can readily accept the notion that the stretching absorptions of a vibrating chemical bond occur at higher frequencies (wavenumbers) than the corresponding bending or bond deformation vibrations, with the understanding, of course, that energy and frequency are proportionally related. A good example is the C-H set of vibrations, observed in the hydrocarbon spectra, and in virtually all organic compounds. Here, the simple C-H stretching vibrations for saturated aliphatic species occur between 3000 and 2800 cm⁻¹, and the corresponding simple bending vibrations nominally occur between 1500 and 1300 cm⁻¹. Next, it can take slightly more energy to excite a molecule to a asymmetric than a symmetric vibration. While this might be less intuitive, it is still a rational concept, and therefore easy to understand and accept. Again, one can see a good example with the C-H stretch of an aliphatic compound (or fragment), where one can observe the asymmetric C-H stretch of the methyl and methylene groups (2960 and 2930 cm⁻¹, respectively) occurring at slightly higher frequency than symmetric vibrations (2875 and 2855 cm⁻¹, respectively for methyl and methylene). For the most part, this simple rule holds true for most common sets of vibrations. Naturally there are always

exceptions, and a breakdown of the rationale may occur when other effects come into play, such as induced electronic, spatial or entropy-related effects. There are many other spatially related scenarios that tend to follow well-orchestrated patterns, examples being in-plane and out-of-plane vibrations, the differences between *cis* and *trans* spatial relationships, and a variety of multicentered vibrations that are defined as twisting or rocking modes. Many of these are exhibited with the C-H vibrations that occur in saturated, unsaturated and aromatic compounds. Molecular symmetry of the static or the dynamic (during vibration) molecule has a large impact on the spectrum, in addition to factors such as relative electronegativity, bond order and relative mass of the participating atoms.

Chapter - II

Instrumentation Techniques

Abstract

Molecular spectroscopy is study of the absorption or emission of electromagnetic radiation by molecules. The experimental data that such studies provide are the frequencies or wavelength of radiation and the amount of radiation emitted or absorption by the sample. One can often understand...

Chapter - II

Instrumentation Techniques

2.1. INTRODUCTION

Molecular spectroscopy is study of the absorption or emission of electromagnetic radiation by molecules. The experimental data that such studies provide are the frequencies or wavelength of radiation and the amount of radiation emitted or absorption by the sample.

One can often understand the native of the molecular changes that are responsible for the emission or absorption of the radiation. In such cases, the experimental spectroscopic data can be used to determine quantitative values for the various molecular properties. In this way, as will be see, remarkably detailed and exact measurements of the size, shape, flexibility, and electronic arrangement of a molecule can be obtained. It will become apparent that spectroscopy offers one of the most powerful tools for a great variety of molecular structure studies.

Only brief mention will be made of experimental techniques used to obtain spectra that are discussed in this chapter. In practice furthermore, many commercial spectrometers operating in the various spectral regions are available with such equipment, spectra can be obtained and used without a detailed understanding of the behaviour of the components of the instrument.

One can also divide spectroscopy according to the instrumentation used. It happens that the categories obtained in this way are similar to those based on the

molecular energies. The instrumentation classification might be given as microwave spectrometer, infrared spectrometer, visible and ultraviolet spectrometer. It should also be mentioned that vibrational spectra can be obtained by means of Raman spectroscopy. In addition to the types of molecular spectroscopy listed above, there are two closely related types that play a comparable role in spectral study. These are nuclear magnetic resonance (NMR) and electron spin resonance (ESR) spectroscopy that effect of the magnets field is to orient certain nuclei in certain directions with respect to the direction of field.

2.2. INFRARED SPECTROMETER

Infrared spectroscopy (IR spectroscopy) is the spectroscopy that deals with the infrared region of the electromagnetic spectrum, that is light with a longer wavelength and lower frequency than visible light. It covers a range of techniques, mostly based on absorption spectroscopy. As with all spectroscopic techniques, it can be used to identify and study chemicals. A common laboratory instrument that uses this technique is a Fourier transform infrared (FTIR) spectrometer. The infrared portion of the electromagnetic spectrum is usually divided into three regions; the near-, mid- and far-infrared, named for their relation to the visible spectrum. The higher-energy near- IR, approximately 14000 - 4000 cm⁻¹ (0.8 - 2.5 μ m wavelength) can excite overtone or harmonic vibrations. The mid-infrared, approximately 4000 - 400 cm⁻¹ (2.5 - 25 μ m) may be used to study the fundamental vibrations and associated rotational-vibrational structure. The far-infrared, approximately 400 - 10 cm⁻¹ (25 - 1000 μ m), lying adjacent

to the microwave region, has low energy and may be used for rotational spectroscopy. In this study the spectral analysis in the mid-IR region using FT-IR has been studied.

Fourier transform infrared spectroscopy (FT-IR) [10] is a technique which is used to obtain an infrared spectrum of absorption, emission, photoconductivity or Raman scattering of a solid, liquid or gas. An FT-IR spectrometer simultaneously collects spectral data in a wide spectral range. This confers a significant advantage over a dispersive spectrometer which measures intensity over a narrow range of wavelengths at a time. FT-IR has made dispersive infrared spectrometers all but obsolete (except sometimes in the near infrared), opening up new applications of infrared spectroscopy.

The term Fourier transform infrared spectroscopy originates from the fact that a Fourier transform (a mathematical process) is required to convert the raw data into the actual spectrum. Before delving into FT-spectrometry, the review the principles of a classical spectrometer are presented as follow. If an optical or UV spectrometer has been used, the principles are identical as following Fig. 2.1.

In Fig. 2.1 source generates light across the spectrum of interest. A monochromater (in IR this can be either a salt prism or a grating with finely spaced etched lines) separates the source radiation into its different wavelengths. A slit selects the collection of wavelengths that shine through the sample at any given time. In double beam operation, a beam splitter separates the incident beam in two; half goes to the sample, and half to a reference. The sample absorbs light according to its chemical properties. A detector collects the radiation that passes through the sample, and in double-beam operation, compares its energy to that going through the reference. The

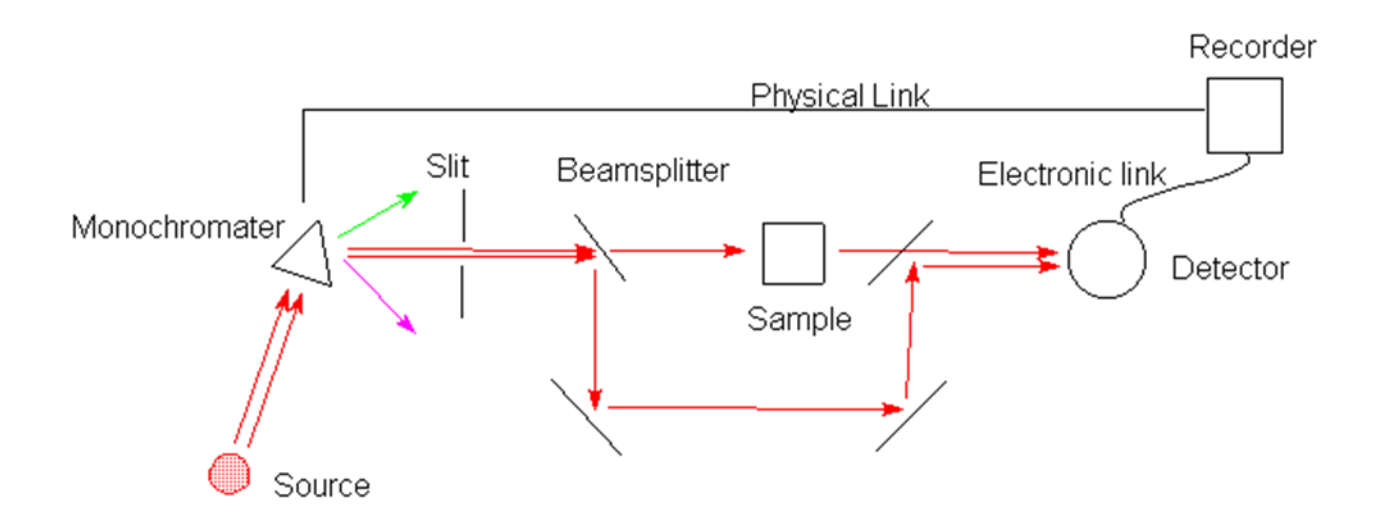


Fig. 2.1: Optical layout of classical spectrometer

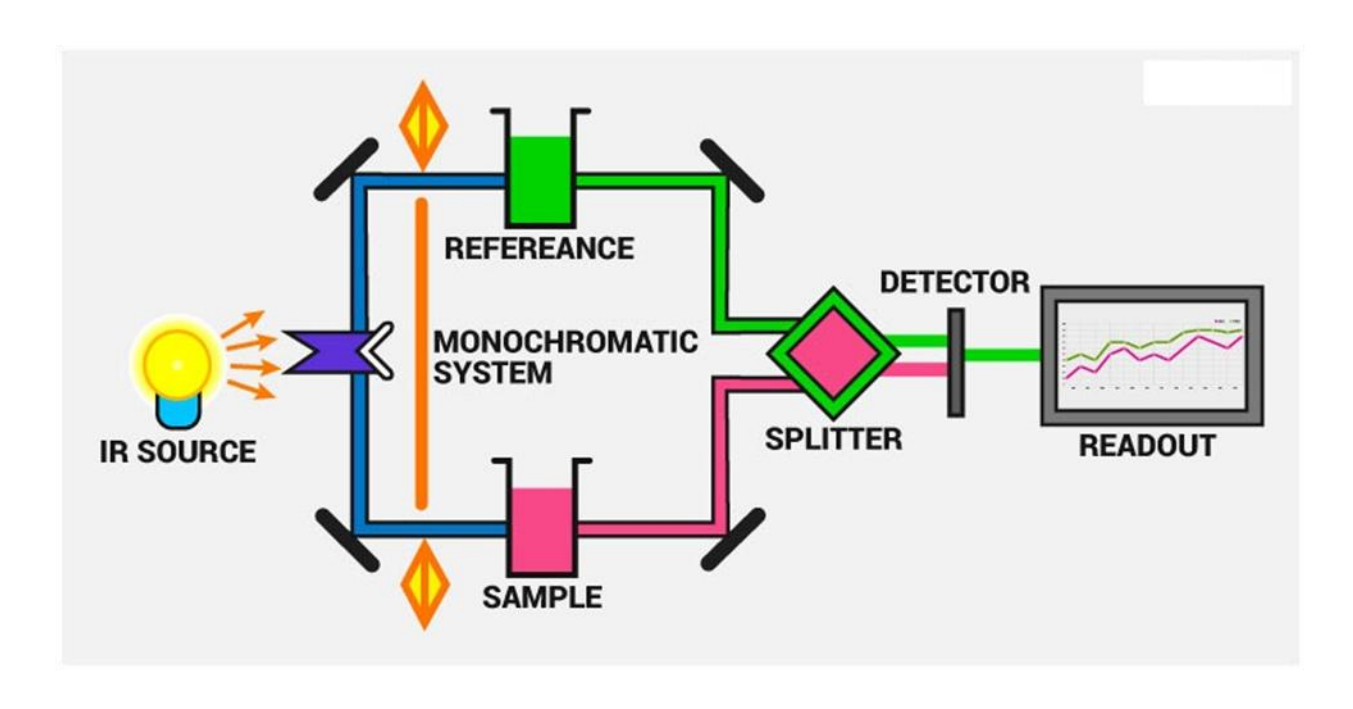


Fig. 2.2: Optical diagram of FT-IR spectrometer

detector puts out an electrical signal, which is normally sent directly to an analog recorder. A link between the monochromater and the recorder allows to record energy as a function of frequency or wavelength, depending on how the recorder is calibrated. Although very accurate instruments can be designed on these principles, there are several important limitations. First, the monochromater/slit limits the amount of signal one can get at a particular resolution. To improve resolution, one must narrow the slit and decrease sensitivity. Second, there is no easy way to run multiple scans to build up signal-tonoise ratios. Finally, the instrument must be repetitively calibrated, because the analog connection between the monochromater position and the recording device is subject to misalignment and wear.

In FT-IR instrument one can still have a source, a sample and a detector, but everything else is different as shown in Fig. 2.2. Now, one can send all the source energy through an interferometer and onto the sample. In every scan, all source radiation gets to the sample. The interferometer is a fundamentally different piece of equipment than a monochromater. The light passes through a beamsplitter, which sends the light in two directions at right angles. One beam goes to a stationary mirror then back to the beamsplitter. The other goes to a moving mirror. The motion of the mirror makes the total path length variable versus that taken by the stationary-mirror beam. When the two meet up again at the beam splitter, they recombine, but the difference in path lengths creates constructive and destructuive interference: an interferogram: The recombined beam passes through the sample. The sample absorbs all the different wavelengths characteristic of its spectrum, and this subtracts specific wavelengths from the

interferogram. The detector now reports variation in energy versus time for all wavelengths simultaneously. A laser beam is superimposed to provide a reference for the instrument operation. Energy versus time is an odd way to record a spectrum, until one recognizes the relationship between time and frequency: they are reciprocals. A mathematical function called a Fourier transform allows to convert an intensity Vs time spectrum into an intensity-vs.-frequency spectrum which is given as follow.

The Fourier transform:
$$A(r) = \sum X(k) \exp\left[\frac{irk}{N}\right]$$

2.3. RAMAN SPECTROMETER

While Raman spectroscopy has been recognized as a valuable research technique in the years since the phenomenon was first observed by Dr. C.V. Raman in 1928, it is only recently that Raman has emerged as an important analytical tool across a number of industries and applications. No longer designed to appeal only to highly specialized and trained experts, the best of today's Raman instruments are fully integrated and come with built-in system intelligence that frees the user to focus on results and not on having to become an expert in the technology itself. Busy analytical laboratories are now able to adopt due to its sensitivity, high information content, and non-destructive nature, Raman is now used in many applications across the fields of chemistry, biology, geology, pharmacology, forensics, pharmaceuticals, materials science, and failure analysis. Spectral libraries in excess of 16,000 compounds are now available for direct compound identification.

In many laboratories, infrared and Raman spectroscopy are used as complementary techniques, because each method looks at different aspects of a given sample. While IR is sensitive to functional groups and to highly polar bonds, Raman is more sensitive to backbone structures and symmetric bonds. Both techniques provide twice the information about the vibrational structure than can be obtained by using either alone. In addition to providing unique information about a sample, Raman offers several additional benefits, including:

- Minimal or no sample preparation
- Sampling directly through glass containers
- Non-destructive analysis, so the same sample can be used in other analyses
- Non-intrusive analysis, permitting study of more labile sample features,
- Minimal water interference
- \forall No interference from atmospheric CO₂ or H₂O

Raman spectrometers are based on one of two technologies: dispersive Raman and Fourier transform Raman. Each technique has its unique advantages and each is ideally suited to specific types of analysis. Fourier transform Raman spectrometer has been used for the spectral study and discussed as follow.

2.3.1. FT-Raman Spectroscopy

In place of visible excitation lasers, an FT-Raman spectrometer (Fig. 2.3) uses a laser in the near infrared - usually at 1064 nm. At this wavelength fluorescence is almost completely absent, however because of the $1/\lambda^4$ relationship between Raman scattering intensity and wavelength, the Raman signal is weak. In addition, silicon CCD detectors

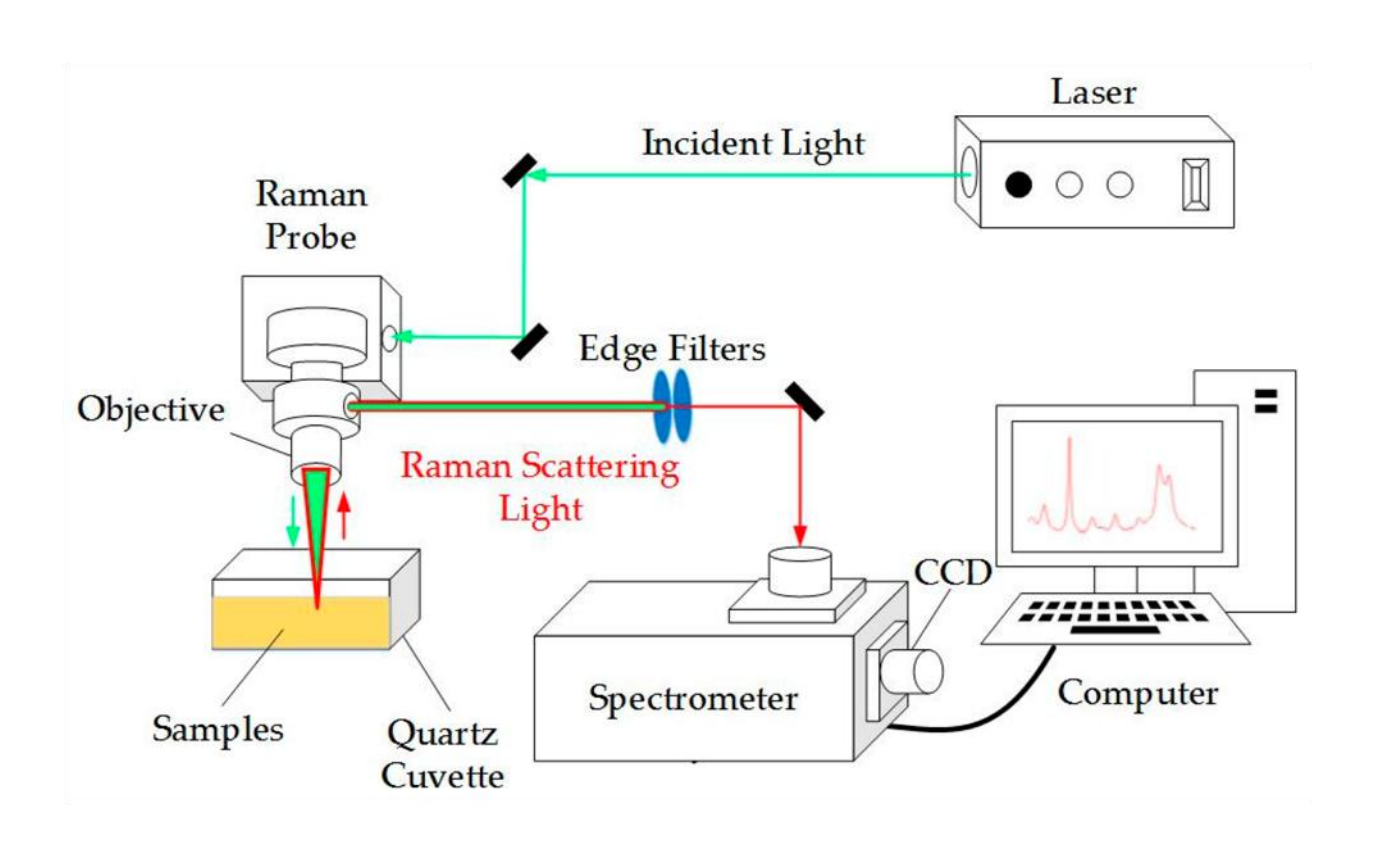


Fig. 2.3: The schematic diagram of FT-Raman spectrometer

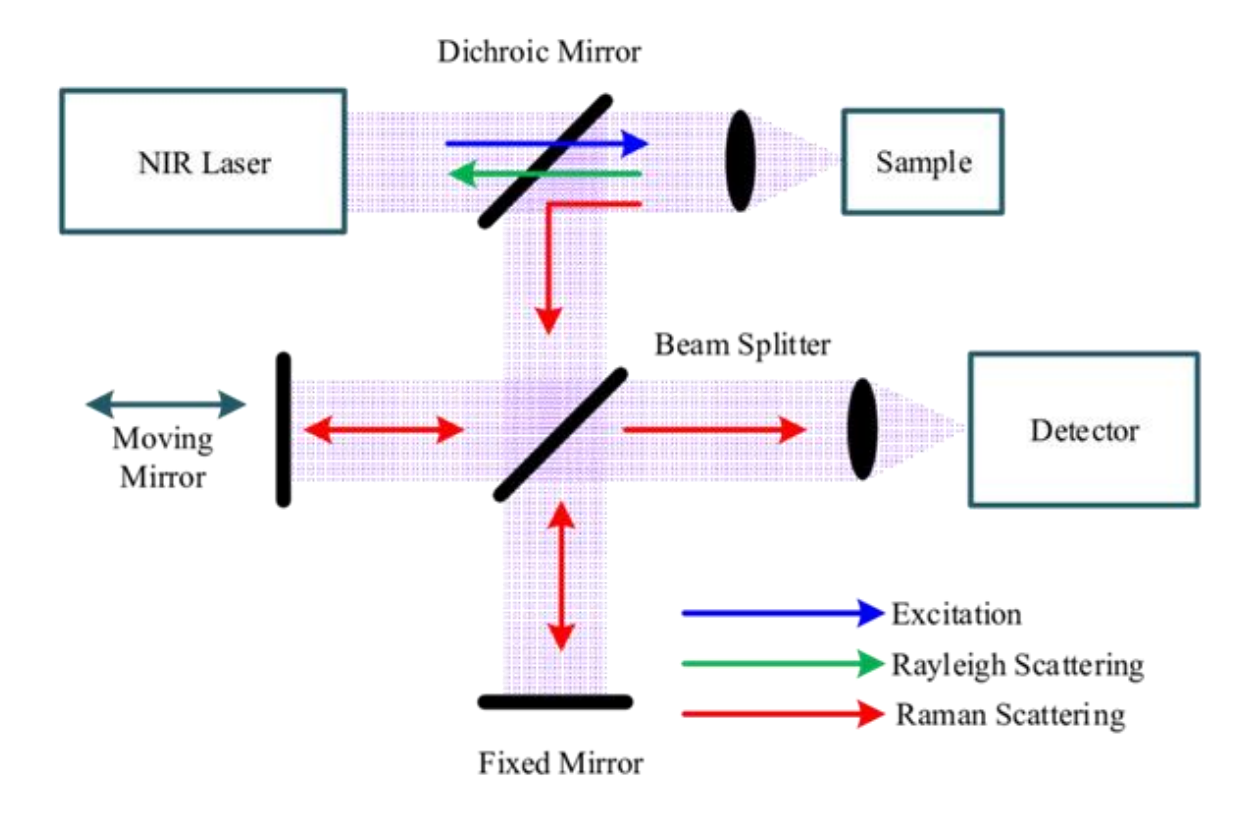


Fig. 2.4: The internal arrangement of interferometer

cannot be used in this region of the spectrum. FT-Raman uses sensitive, single-element, near-infrared detectors such as indium gallium arsenide (InGaAs) or liquid nitrogen-cooled germanium (Ge) detectors.

An interferometer (Fig. 2.4) converts the Raman signal into an interferogram, permitting the detector to collect the entire Raman spectrum simultaneously. Since at low signal levels the spectral noise is predominantly detector dark noise and is independent of the intensity of the Raman signal, delivering the entire spectrum at once onto the detector greatly improves the signal to-noise ratio. Application of the Fourier transform algorithm to the interferogram converts the results into a conventional Raman spectrum. In addition to freedom from fluorescence interference, another advantage of FT-Raman spectroscopy is its exceptionally good x-axis (shifted wavenumber) accuracy as a result of the internal interferometer calibration supplied by the built-in helium-neon laser. Both of these attributes make FT-Raman the ideal technique for collecting spectra for reference libraries.

In this study, Bruker IFS 66V spectrometer has been used for recording the FT-IR spectral data. The same instrument with FRA 106 Raman module equipped with Nd:YAG laser source has been used for recording FT-Raman spectrum.

Chapter - III

Theoretical and Computational Methods

Abstract

In recent years, computational quantum chemistry has been very widely used not only by theoretical research groups but also by experimental chemists in various fields of chemistry, including molecular spectroscopy and structure. The rapid developments in molecular simulation software packages and the presence of powerful computing facilities...

Chapter - III

Theoretical and Computational Methods

3.1. INTRODUCTION

In recent years, computational quantum chemistry has been very widely used not only by theoretical research groups but also by experimental chemists in various fields of chemistry, including molecular spectroscopy and structure. The rapid developments in molecular simulation software packages and the presence of powerful computing facilities have greatly aided many areas of both research and teaching and have helped solve many problems in science.

Limitations that computational tools had in the past which led to faulty conclusions have been overcome in recent years. Nowadays, new research problems in different areas of chemistry can be supported and properly guided by making use of available computational techniques. Moreover, quantum chemical techniques can help resolve issues that cannot be practically achieved due to instrumentation limits. Computational chemistry, especially high-level theories and calculations, can also help refine, and perhaps change, some of the old concepts and understanding of chemical phenomena.

Quantum-mechanical calculations in chemistry started early in the last century with the use of empirical and semiemperical molecular orbital approaches, such as the Hückel method. These methods applied a simplified Hamiltonian rather than the

complete molecular Hamiltonian and used parameters whose values were adjusted to fit the experimental data or even the results from other *ab initio* calculations.

3.2. AB INITIO CALCULATIONS

Ab initio is Latin for "from the beginning". The name implies that the computations in ab initio quantum mechanical methods are based on theoretical principles and universal physical constants without involving experimental data. Ab initio calculations also utilize the correct Hamiltonian to investigate the properties of the molecule. Some useful approximations are needed in order for the calculations not to consume an intensive amount of time and to be more reliable with the computer facilities available for use. Examples of these types of approximations are the use of the time-independent Schrödinger equation, assuming the non-relativistic behavior of the wavefunctions describing the molecular system, and applying the Born-Oppenheimer approximation.

Since early in the last century, the developments in quantum mechanics evolved several theoretical approaches to find the approximate solutions of the Schrödinger equation and to calculate the chemical and physical properties for the molecules. In this chapter, brief highlights in simple mathematical formats will be presented to explain the density-functional (DFT) theories. These computational methods have been implemented in this research work. The following descriptions were mainly taken from Refs. [11-14].

3.2.1. Hartree-Fock theory

The Hartree-Fock (HF) calculation is a very commonly used method of *ab initio* calculations. The Hartree-Fock method has not been used in this work except for a few cases. However, since it is the first step for the Møller-Plesset perturbation theory and other more sophisticated approaches, some discussion about the nature of HF calculations will be presented. The molecular time-independent Schrödinger equation is given by

$$\left\{-\frac{\hbar^2}{2}\sum_{m_k} (\nabla_k^2) + V\right\} \Psi(\bar{\mathbf{r}}, \bar{\mathbf{R}}) = \mathbf{E}\Psi(\bar{\mathbf{r}}, \bar{\mathbf{R}}) \psi$$

where \hbar is Planck's constant divided by 2, m_k is the mass of the particle k, ψ is the total wavefunction, \bar{r} and \bar{R} represent the positions of the electrons and nuclei, respectively, V is the potential energy component of the Hamiltonian and is given by the Coulomb repulsion or interaction between the electrons and nuclei, E is the total energy of the system a and ∇^2 or "del squared" is the Laplacian operator and is defined by

$$\nabla_k^2 = \frac{\partial^2}{\partial x_k^2} + \frac{\partial^2}{\partial y_k^2} + \frac{\partial^2}{\partial z_k^2}$$

The exact solution of the Schrödinger equation for many-electron systems is not possible. Some assumptions, however, can be made in order to approximate the solutions for the total molecular wavefunction, ψ . Based on the molecular orbital theory the total wavefunction can be represented by individual molecular orbitals (ϕ 1, ϕ 2, ϕ 3,..., ϕ n) that are chosen to be normalized and orthogonal with respect to each other to fulfil some of the conditions for ψ . The simplest wavefunction built from these molecular orbitals is a Hartree product:

$$\Psi(\bar{r}) = \phi_1(\bar{r}_1)\phi_2(\bar{r}_2) \dots \phi_n(\bar{r}_n)$$

One advantage of this method is that it breaks the many-electron systems into many simpler one-electron hydrogen-like problems each of which can be solved independently to give a single-electron wave function called an orbital and an energy called an orbital energy. This was the basis of the HF method which was introduced by Douglas Hartree in 1928 [17]. Later, more modifications were made to that approach to improve the outcome eigenvalues. For example, Slater- and Gaussiantype orbitals (STOs and GTOs) were used as mathematical functions to describe the wavefunctions in order to produce more reliable results.

An essential requirement of ϕ (r) is that it much be antisymmetric with respect to exchange, meaning that it must change its sign when two identical particles are swapped within the system. The function shown in Equation does not fulfill the requirement of antisymmetry. The common way of having that requirement satisfied is by expressing the wavefunction in a form of a determinant. Switching any two electrons corresponds to swapping two rows of the determinant, which causes the sign to change.

The Hartree-Fock method is a variational calculation. Variational methods provide an upper bound to the ground-state energy for a specific system [16]. In other words, the exact wavefunction (ψ 0) becomes a lower bound to the energy calculated by another normalized, antisymmetric wavefunction (ψ ϕ).

$$E_0(\Psi_0) \le E_\phi \big(\Psi_\phi \big)$$

The closer the trial function (ψ_0) to extract function (ψ_{Φ}) , the closer E_{Φ} will be to E0. This illustrates the importance of having a good approximation of the trial function at the start of the calculation.

In 1951 C.J. Roothaan [17] applied the variational principle to the solution from the Slater determinant to derive the following equation describing molecular orbital expansion coefficient,

$$\sum_{\substack{\nu=1\\\mu=1}}^{N} (F_{\mu\nu} - \varepsilon_i S_{\mu\nu}) c_{\nu i} = 0$$

This Equation can be also written in matrix form as

where ϵ is a diagonal matrix of orbital energies whose elements are the one-electron orbital energies, ϵ_i 's, F is the Fock matrix, and S is the overlap matrix indicating the overlap between the orbitals. The Fock matrix, F, accounts for the Coulomb repulsion of each electron with the static field of all of the other electrons. Roothaan's approach was critical because he was the first to describe the matrix algebraic equations of the HF procedure using a basis set representation for the molecular orbitals as shown above Equation.

The steps in a Hartree-Fock calculation start with an initial guess of the orbital coefficients. This function is used to calculate energy and a new set of orbital coefficients, which can then be used to obtain a smaller energy value with an improved set of coefficients. This optimization procedure continues until no more improvement can be

obtained within the predefined convergence criteria. This iterative procedure is said to be the self-consistent field (SCF). In the Hartree-Fock description, the molecular orbitals are the solutions of one- electron equations with each electron moving in the average field of all the other electrons. This accounts for the static interaction between the electrons but neglects the correlation between the motions of the electrons. The inadequate description of the electron correlation is the main deficiency of the HF theory. The methods that go beyond the Hartree-Fock theory in treating the electron-electron interaction more precisely are known as electron-correlation methods. These types of calculations begin with the HF calculation and then correct for correlation. Some of these methods are the Møller-Plesset perturbation theory (MPn, where n is the order of correction), configuration interaction (CI), and coupled cluster (CC) theory.

3.2.2. Density functional theory

In recent years density functional theory (DFT) has become a popular choice for investigating the chemical properties of different types of molecules. The advantage of the DFT-based calculations is that they result in very satisfactory output and use less computational time than many other traditional quantum mechanical techniques. In 1964 Kohn and Hohenberg [18] proposed that there exists a unique functional that determines the ground state energy and density exactly. However, the Kohn-Hohenberg theorem does not provide a specific form for this functional. This theorem was the basis of DFT which describes the energy of the molecule not from evaluating the total wavefunction but from solving for the electron density. Therefore, DFT can be classified as a method that is different from *ab initio* calculations.

In simple format, DFT methods split up the total electronic energy into smaller term according to

$$E = E^T + E^V + E^J + E^{XC}$$

where E^T is the kinetic energy term associated with the electron motions, E^V is the potential energy term associated with the nucleus-electron attraction and nucleusnucleus repulsion, E^J is the average electron-electron repulsion term, and E^{XC} is the exchange-correlation term which includes the rest of the electron-electron repulsion. All of the four energy terms in above Eq. except for the nucleus-nucleus repulsion, are functions of the electron density, $\rho(r)$. The DFT method determines one function in terms of another function, which is basically the meaning of the word *functional*. The density functional obtains the energy for the system from its electron density.

The non-classical term in Eq. is the exchange-correlation term E^{XC} . The E^{XC} term is approximated by integrals involving mainly the spin densities. The E^{XC} is

$$E^{XC}(\rho) = E^X(\rho) + E^C(\rho)$$

In above Eqn. $E^X(\rho)$ is the exchange functional which corresponds to the same spin electron-electron interaction, while $E^C(\rho)$ is the correlation functional which corresponds to the mixed-spin electron-electron interaction. There is no exact form for the functional. However, there are many forms of several functionals which have been developed and implemented to explore the chemical properties of different molecules. Some functionals were developed from fundamental quantum mechanics and some were developed by fitting them to experimental results. These different types of approaches are

referred to as *ab initio* and semi empirical DFT methods, respectively. Examples of developed and commonly used functionals are B3LYP, B3P86, and PW91. These functionals have advantages and disadvantages when they are incorporated in the calculations. The B3LYP method utilizes a three-term Becke functional [19] combined with the Lee, Yang, Parr [20,21] exchange functional.

The B3LYP functional is said to be hybrid, which means it includes Hartree-Fock and DFT exchange term in addition to the DFT correlation terms. That is

$$E_{hybrid}^{XC} = C_{HF}E_{HF}^{XC} + C_{DFT}E_{DFT}^{XC}$$

where the confinements c's are constants. The B3LYP hybrid functional is currently the most widely used type of DFT calculation, especially for organic molecules.

More complicated types of density functionals are those incorporating the electron density and their gradients as well. Such methods are known as gradient-corrected methods. The gradient-corrected methods are usually hybrid. An example of gradient-corrected functionals is PW91 (Perdew and Wang 1991) [22, 23]. The DFT method was found to predict the vibrational frequencies in very good agreement with experimental results, especially for hydrocarbons. DFT results are not as accurate for heavy elements, highly-charged systems, or systems sensitive to electron correlation. One technique for improving the efficiency of the density functionals is by minimizing the integration grid size of the electron density. Finer grids result in a greater number of integration points per unit volume of density, and thus more accurate results are obtained.

3.3. BASIS SETS

A basis set is a set of linear combinations of mathematical functions that describe the shapes of the orbitals in a molecule. In order to be able to perform an *ab initio* calculation, basis sets must be used. The larger the basis set, the more accurate these descriptions are, and the fewer the restrictions imposed on the locations of the electrons will be. The basis sets use linear combinations of Gaussian-type functions to form the orbitals. Basis sets assign a group of basis functions to each atom within a molecule to describe its orbitals. There is a long list of existing basis sets that can be used to perform *ab initio* calculations. The choice of basis sets is a major factor in determining the amount of computation time and the degree of accuracy for a specific type of calculation.

A minimal basis set uses the minimum number of basis functions per atom. This has only three Gaussian primitives per basis function (3GTOs). The size of the basis set can be increased by incorporating a larger number of basis functions for each atom. For example, instead of using one basis function to describe the 1s orbital for the hydrogen atom, two basis functions of different sizes are used. These types of basis sets are known as split-valence or sometimes as double-zeta (double-) basis sets. Examples of split-valence basis sets are the 3-21G and 6-31G. When three different types of basis functions are used to describe each atomic orbital, it is known as triplesplit- valence or triple-zeta (triple-) basis sets. An example of a triple-split-valence basis set is the 6-311G. The basis sets such as 6-31G, 6-311G are known as the Pople basis sets. Split-valence and triple-split-valence basis sets allow the changes not only in the size of the orbitals but also in their shape. When an angular momentum function is added to the basis function

description, it gives the orbital the correct symmetry (s, p, d, etc.), and the basis set is said to be polarized. Polarization functions add more accuracy to ab initio result because they give the orbitals more flexibility to change their shape. Polarization functions are used to predict more accurate geometry and vibrational frequencies. Examples of polarized basis sets include the 6-31G(d) and 6-31(d,p). The notation 6-31G(d) implies that a set of d primitives has been added to each atom other than hydrogens, whereas the 6-31G(d,p) means that a set of d primitives has been added to each atom other than hydrogens and a set of p primitives has been added to the hydrogen atoms as well. Extra numbers of sets of polarization functions may also be added, depending on the need and the level of accuracy being sought. However, polarization functions are generally expensive in terms of the required computational time. Other types of functions used with Pople basis sets are diffuse functions, and they are indicated with plus signs, such as 6-31+G(d) and 6-31++G(d) basis sets. Diffuse functions are primitives with small exponents and give a better description for the wavefunction far from the nucleus. They are helpful in several cases, such as for predicting the geometry for anions, for calculations involving molecules with lone pairs of electrons, for investigating the types of interactions that occur over long distances, and for calculations related to electronic excited states. Adding diffuse functions also changes the relative stabilities of different conformations within a molecule. The "plus" means a set of diffuse functions is added to nonhydrogen atoms.

The additional plus implies that another set of diffuse functions is added to hydrogen atoms. In terms of computational time, diffuse functions are not as expensive as polarization functions.

Other commonly used basis sets are those developed by Dunning, Huzinaga, Duijneveldt and others. Two examples of widely used basis functions of the Dunning type are VDZ and VTZ which stand for double-zeta valence and triple-zeta valence types, respectively. A very commonly used basis set of this type is the cc-pVTZ. The "cc" means it is a correlation-consistent basis set. In other words, the basis functions are optimized for the best performance with correlated calculations. The letter "p" implies the use of polarization functions of a large angular momentum. Dunning made a major contribution in developing different types of correlation-consistent basis functions. It has been noted that these large correlation-consistent basis sets with high angular-momentum polarization functions greatly improve the level of accuracy of the calculations.

3.4. CALCULATION OF VIBRATIONAL FREQUENCIES

Ab initio calculations use the harmonic oscillator approximation to compute the vibrational frequencies because the harmonic oscillator approach is more affordable as compared to other more accurate methods. Harmonic oscillator calculations are useful for predicting the frequencies for the fundamental vibrations. For a diatomic molecule the potential energy, U(r) from a Taylor series expansion truncated after the second after the second order is given by

$$U(r_{AB}) = \frac{1}{2}k_{AB}(r_{AB} - r_{AB,eq})^2$$

where r_{AB} is the distance between the atoms A and B, req is the equilibrium distance at the energy minimum and k_{AB} is the force constant which is defined as

$$k_{AB} = \frac{d^2 U}{dr^2} \bigg|_{r=req}$$

To predict the rotational and vibrational frequencies for a molecule with N atoms, the Schrödinger equation in terms of nuclear motions:

$$\left[-\sum_{i}^{N}\frac{1}{2m_{i}}\nabla_{i}^{2}+V(q)\right]\Psi^{nuc}\left(q\right)=E\Psi^{nuc}\left(q\right)$$

needs to be solved. Most of the parameters have been described above.

The other terms are q, the nuclear coordinate (a total of 3N vibrational coordinates have to be considered), and wnuc, the nuclear wavefunction expressed in terms of the nuclear coordinate. Above Eq. allows the rotational and vibrational frequencies to be calculated within the harmonic oscillator model. In the case of vibrational frequency calculations for a polyatomic molecule of N atoms,

$$\left[-\sum_{i}^{3N}\frac{1}{2m_{i}}\nabla_{i}^{2}+V(q-q_{eq})H(q-q_{eq})\right]\Psi^{nuc}(q)=E\Psi^{nuc}(q)$$

where q represents the mass-dependent spatial coordinate vector and H is the Hessian matrix which is defined by

$$H = \frac{\partial^2 U}{\partial q^2} \bigg|_{q = q_{eq}}$$

It can be seen that above Equation is 3N-dimensional, but it can be divided into 3N one-dimensional Schrödinger equations. Each component of the vector q corresponds to a molecular vibration which is called a normal mode. For each normal mode, a set of harmonic oscillator eigenfunctions and eigenvalues are expressed in terms of square roots

of force constants in the Hessian matrix and in terms of atomic masses as well. This can be applied to structures other than the minimum conformations. In this case, one or more imaginary frequencies will result from the calculations. These result from negative force constants of normal modes indicating that the displacements of specific molecular vibrations lead to lowering of the energy on the potential energy surface. Since the harmonic oscillator vibrational frequencies are computed from the square root of the force constants, this gives rise to imaginary, or sometimes called negative, frequencies. Thus, vibrational frequency calculations can be used to examine the optimized structure whether it is a minimum or a saddle point.

In any case, the level of theory and basis set used to compute the vibrational frequencies must not be changed from the one used to optimize the geometry for the molecule.

3.5. CALCULATION OF VIBRATIONAL INFRARED AND RAMAN SPECTRA

Infrared and Raman intensities can be calculated from *ab initio* calculations. The IR intensities are proportional to the change in dipole moments as a function of vibrational displacements. *Ab initio* methods compute several properties using mixed derivatives originating from the energy expansion, and the infrared intensities can be predicted from

IR intensity
$$\propto \left[\frac{\partial \mu}{\partial q}\right]^2 \propto \left[\frac{\partial^2 E}{\partial R \partial F^2}\right]^2$$

where μ is the electric dipole moment, q is, as defined above, the vibrational normal coordinate, R is the change in the nuclear geometry, and F is the external electric field. The Raman intensities based on the harmonic oscillator approximation are proportional to the polarizability change (α) with respect to the vibrational coordinate and can be given by

Raman intensity
$$\propto \left[\frac{\partial \alpha}{\partial q}\right]^2 \propto \left[\frac{\partial^3 E}{\partial R \, \partial F^2}\right]^2$$

This equations show that the infrared intensity is a second-order property while the Raman intensity is a third-order property that requires longer time to be computed. Computed infrared and Raman intensities are semi-quantitative. The level of accuracy for intensities is not as good as for the vibrational frequencies. However, they are very helpful and are found to generally agree with experimental results.

3.6. VIBRATIONAL HAMILTONIAN

The potential energy surfaces governing the conformational changes in nonrigid molecules can be determined from spectroscopic data in conjunction with quantum mechanics. Consider the time-independent vibrational Schrödinger equation:

$$H^{vib}\Psi^{vib} = E^{vib}\Psi^{vib}$$

where H^{Vib} is the vibrational Hamiltonian operator, ψ^{vib} is the vibrational wavefunction and E^{vib} represents the eigenvalues associated with the vibrational Wavefunction. The vibrational Hamiltonian is defined by

$$H^{vib} = T^{vib} + V^{vib}$$

where T^{vib} and V^{vib} are the kinetic and potential energy operators, respectively.

3.7 APPLICATIONS OF QUANTUM CHEMICAL CALCULATION

3.7.1 Natural Bond Orbital Analysis

The hyper conjugative interplay and electron density shift are effectively explained by The NBO analysis. The NBO studies [24] were carried out by NBO 3.1 program as executed in the Gaussian 09 package, which is used to understand various second order interplays between the filled orbitals of one sub system and empty orbitals of another subsystem, which is a measure of the intermolecular delocalization (or) hyper conjugation. The hyper conjugative interaction energy was derived from the second – order perturbation approach

$$E^{(2)} = \Delta E_{ij} = q_i \frac{F(ij)^2}{\varepsilon_j - \varepsilon_i}$$

where q_i is the i^{th} donor orbital occupancy, ϵ_i and ϵ_j are diagonal elements (orbital energies) and F(i,j) is the off-diagonal NBO fock matrix element .

3.7.2 Potential Energy Distribution (PED)

The PED has used to check whether selected set of symmetric coordinates provides maximum to the potential energy associated with the molecule. The vibrational problem was set up in term of internal and symmetry co-ordinates. The Cartesian representation of the theoretical force constants has been calculated at the optimized geometry by assuming C_1 (or) C_s point group symmetry. The symmetry of the molecule assumption was also enhancing in vibrational assignment. The transformation of force field, subsequent normal coordinate studies and computation of the PED are a crucial for

determining vibrational characteristics of a molecule. The calculation of PED can be done with the help of VEDA program.

3.7.3 HOMO-LUMO Energy Gap Analysis

The frontier molecular orbitals (FMO_S) theory is immense to explain the chemical stability and the reactivity of pericyclic reactions. This theory deals about filled and unfilled orbital in a molecule [25].hence, the highest occupied molecular orbital (HOMO) donate an electron and lowest unoccupied molecular orbital (LUMO) accept an electron. The energy gap calculation between HOMO and LUMO also crucial for understand the chemical reactivity, optical polarizability and chemical hardness-softness of the molecule [26].

3.7.4 Dipole moment, Hyper polarizability

In the present work dipole moment (μ) and polarizability (α) and first static hyperpolarizability(β) have been calculated by Gaussian 09 software, using the finite field approach. According to Buckingham's definition [27], these quantities are given by

$$\mu = \left(\mu_x^2 + \mu_y^2 + \mu_z^2\right)^{\frac{1}{2}}$$

$$\langle \alpha \rangle = \frac{1}{3} \left(\alpha_{xx} + \alpha_{yy} + \alpha_{zz} \right)$$

$$\beta_{tot} = (\beta_x^2 + \beta_y^2 + \beta_z^2)^{\frac{1}{2}}$$

Where,

$$\beta_x = (\beta_{xxx} + \beta_{xyy} + \beta_{xzz})$$

$$\beta_{y} = (\beta_{yyy} + \beta_{yzz} + \beta_{yxx})$$

$$\beta_z = (\beta_{zzz} + \beta_{zxx} + \beta_{zvv})$$

Chapter - IV

Vibrational Spectra (theoretical, Experimental) and Optimized structure, Frontire Molecular orbital, Mulliken Atomic Charge studies on Pentylenetetrazole (PTZ) based on Density functional theory

Abstract

The vibrational spectra of Pentylenetetrazole (PTZ) have been recorded in the regions $4000-400 \text{ cm}^{-1}$ for FT-IR and $3500-100 \text{ cm}^{-1}$ for FT-Raman. The molecular structure, geometry optimization, vibrational frequencies were obtained by the density functional theory (DFT) using B3LYP method with 6-31G and 6-311+G basis sets. The complete assignments were performed on the basis of the potential energy distribution (PED) of the vibrational modes, calculated and the scaled values were compared with experimental FT-IR and FT-Raman spectra. The HOMO and LUMO energy gap reveals that the energy gap reflects the chemical activity of the molecule. The dipole moment (μ), polarizability (α), anisotropy polarizability ($\Delta \alpha$) and first hyperpolarizability (β_{tot}) of the molecule have been reported. Information about the size, shape, charge density distribution and site of chemical reactivity of the molecule has been obtained by molecular electrostatic potential (MEP).

Chapter - IV

Vibrational Spectra (theoretical, Experimental) and Optimized structure, Frontire Molecular orbital, Mulliken Atomic Charge studies on Pentylenetetrazole (PTZ) based on Density functional theory

4.1 INTRODUCTION

The biological potential molecule Pentylenetetrazole (PTZ) is a tetrazole derivative and inhibitor of the γ aminobutyric acid (GABAA) and its receptor complex[28,29]. PTZ is a convulsing agent used for inducing seizures. It can traverse the blood-brain barrier[30]. As well as Pentylenetetrazole has been used to induce seizures in zebra fish larvae[31], mice[32], and male wistar rats[33]. This extensive applications of tetrazoles derivatives stimulated research in areas such as the reactivity of various tetrazolyl derivatives and the design of synthetic methodologies. In these studies, the molecular structure, vibrational spectra and HOMO-LUMO energy gap of Pentylenetetrazole (PTZ) were investigated by a concerted approach using matrix isolation vibrational spectroscopy and high-level DFT-based theoretical calculations. Regarding their studies, tetrazoles have been found to be extremely interesting and challenging molecules.

4.2 EXPERIMENTAL DETAILS

The fine sample of PTZ was obtained from Lancaster Chemical Company.UK, with a stated purity of 99% and it was used as such without further purification.The FT-

Raman Spectrum of PTZ was recorded using 1064 nm line of ND: YAG laser for excitation wavelength in the region 3500-100 cm⁻¹ on Thermo Electron Corporation model Nexus spectrometer equipped with FT-Raman module accessory. The FT-IR Spectrum of the title compound was recorded in the region 4000-400 cm⁻¹ on Perking Elmer Spectrophotometer in KBr pellet.

4.3. COMPUTATIONAL DETAILS

The combination of Vibration spectra with quantum chemical calculation is effective for understanding the fundamental mode of vibration of the compound. The structural characteristic, stability and energy of the compound under investigation are determined by DFT with the three-parameter hybrid functional (B₃) for the exchange part and the Becke Three Lee Yong-Pare (LYP) and 6-31G ,6-311+G basis sets with Gaussian 09 Program Package. The Cartesian representation of the theoretical force constants has been compound at the fully optimized geometry by assuming the molecule belongs to C₁ point group symmetry. The Transformation of force field from Cartesian to internal local symmetry coordinates, the scaling, and the subsequent normal coordinate analysis (NCA) Calculation of potential energy distributions (PED) has been done on a PC with the VEDA program.

4.4 MOLECULAR GEOMETRY

The optimized structures of the title compounds along with numbering of atoms are shown in Figure 4.1. Due to the global minimum energy all the calculated vibrational wavenumbers using the optimized geometry were found to be positive for the title

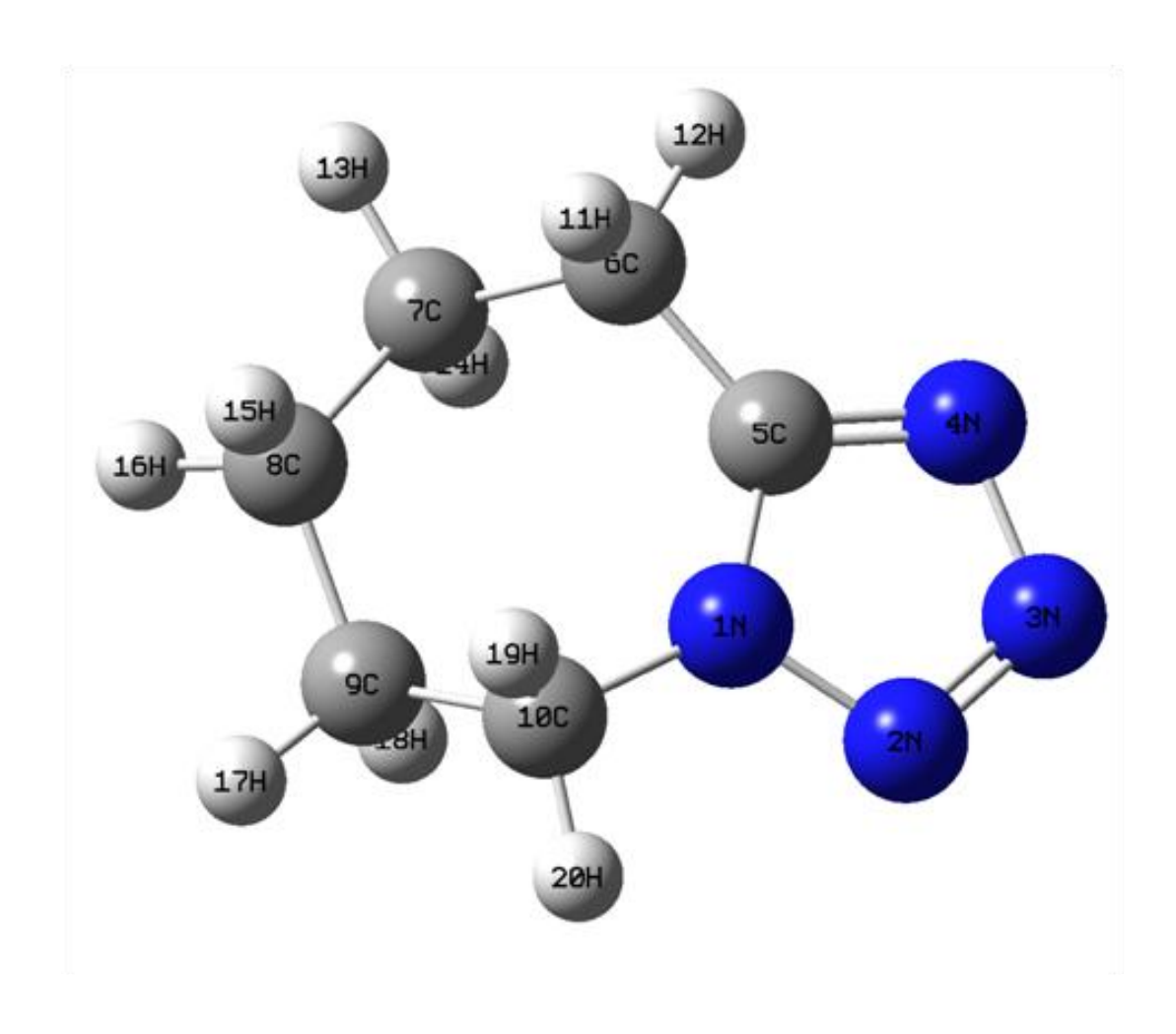


Fig. 4.1. The theoretical geometry structure and atomic numbering scheme of Pentylenetetrazole (PTZ) $\,$

compounds. The bond lengths, bond angles and the optimized parameters calculated using the DFT method is shown in the Supplementary material (Tables 4.1).

An organic heterobicyclic compound that is 1H-tetrazole in which the hydrogens at positions 1 and 5 are replaced by a pentane-1, 5-diyl group. Further, in PTZ, the bond lengths of C6-C7, C7-C8, C8-C9, C9-C10, C8-C10 were found to be elongated to 1.55 Å, 1.54 Å, 1.54 Å respectively compared to pentamethylene and tetrazole connection bond C5-C6 values of 1.49 Å. In this structure, C-C bond length has longer value and C-H bond length has shorter value (1.10 Å). The bond lengths of N3-N4, N1-N2 were found to be elongated to 1.40 Å, 1.39 Å respectively, compared to N2-N3 values of 1.32 Å. Because bond order of N2-N3 is higher than N3-N4, N1-N2 bond order [34]. The two different basis set have good agreement with each other.

4.5 FRONTIER MOLECULAR ORBITAL ANALYSIS

The highest occupied molecular orbital (HOMO) and lowest unoccupied molecular orbital (LUMO) and their properties are very useful to analyze the chemical reaction of molecule. The HOMO and LUMO energies are directly related to the ionization potential and electron affinity respectively [35, 25].those is also used by the frontier electron density for predicting the most reactive position in pi-electron systems and also explains several types of reaction in conjugated system [36]. The conjugated molecules are characterized by a small energy gap, which is the result of a significant degree of intra-molecular charge transfer from the endcapping electron-donor groups to the efficient electron-acceptor group through pi-conjugated path [37]. The HOMO and

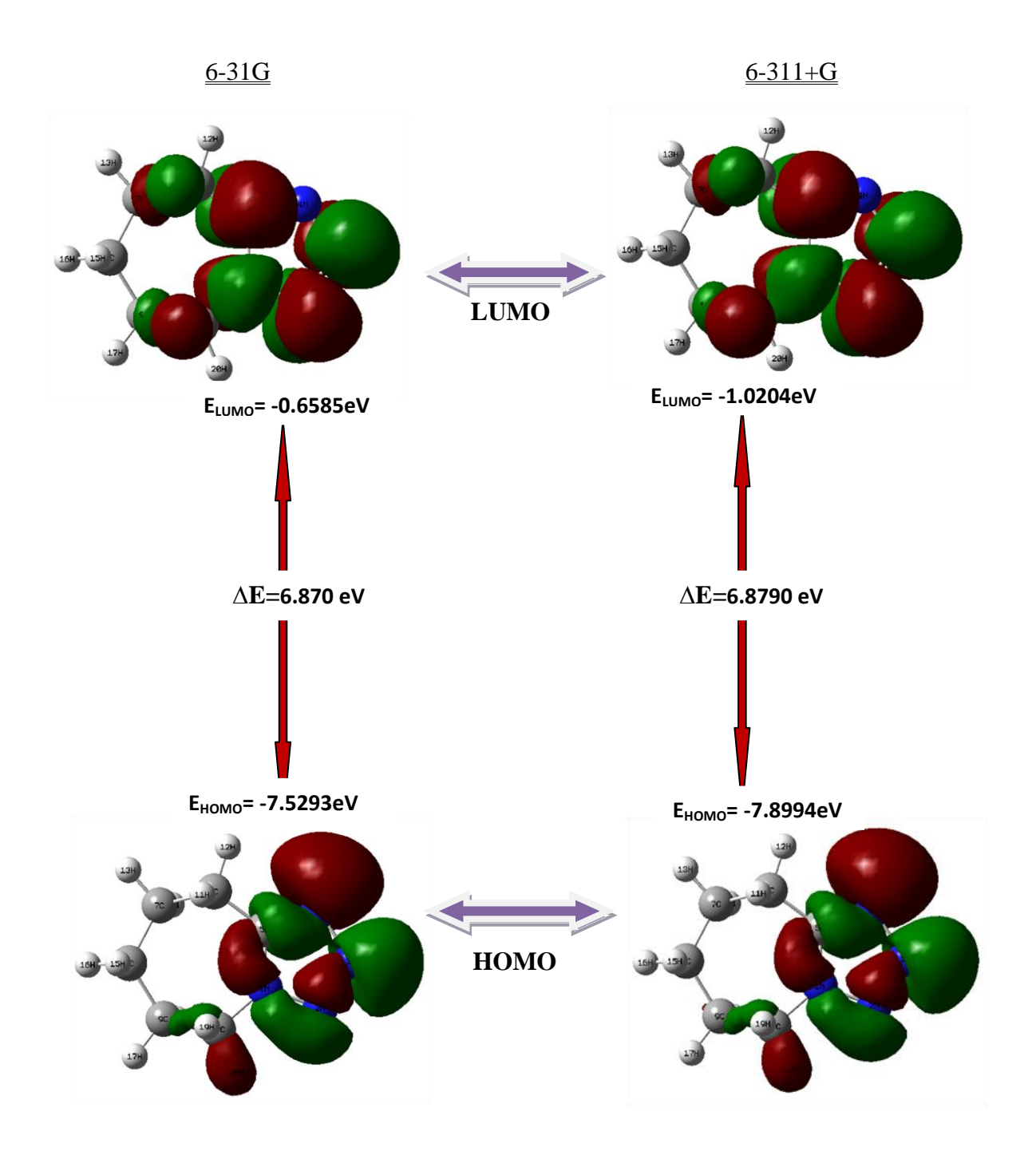


Fig 4.2: The atomic orbital compositions of the frontier molecular orbital for pentelyenetetrazole (PTZ)

LUMO plots of the title compound are shown in Figs. 4.2. The energy gap (ΔE) is a critical parameter in determining molecular electrical transport properties because it is a measure of electron conductivity. By using the HOMO and LUMO energy values, the global chemical reactivity descriptors such as hardness, chemical potential, electronegativity and electrophilicity index as well as local reactivity have been defined. Pauling introduced the concept of electronegativity as the power of an atom in a molecule to attract electrons to it. Hardness (η) , chemical potential (μ) , electrophilicity (ω) and electronegativity (χ) are defined using Koopman's theorem as $\eta = (I - A)/2$, $\mu = -(I + A)/2$ and $\chi = (I + A)/2$, where $I = -E_{HOMO}$ and $A = -E_{LUMO}$ are the ionization potential and electron affinity of the molecule. Considering the chemical hardness, large energy gap denotes a hard molecule and small gap denotes a soft molecule. One can also relate the stability of the molecule to hardness, which means that the molecule with least energy gap means, it is more reactive. Parr et al. [38] have defined a descriptor to quantify the global electrophilic power of the molecule as electrophilicity index, $\omega = \mu^2/2\eta$. The usefulness of this new reactivity quantity has been recently demonstrated in understanding the toxicity of various pollutants in terms of their reactivity and site selectivity [39–45]. The global parameters of compound PTZ are given in Table 4.2.

4.6 MOLECULAR ELECTROSTATIC POTENTIAL (MEP)

The molecular electrostatic potential (MEP) method is used to study the interaction of a molecular system with its surroundings which is used for predicting sites and relative reactivity towards electrophilic attack and in studies of biological recognition.

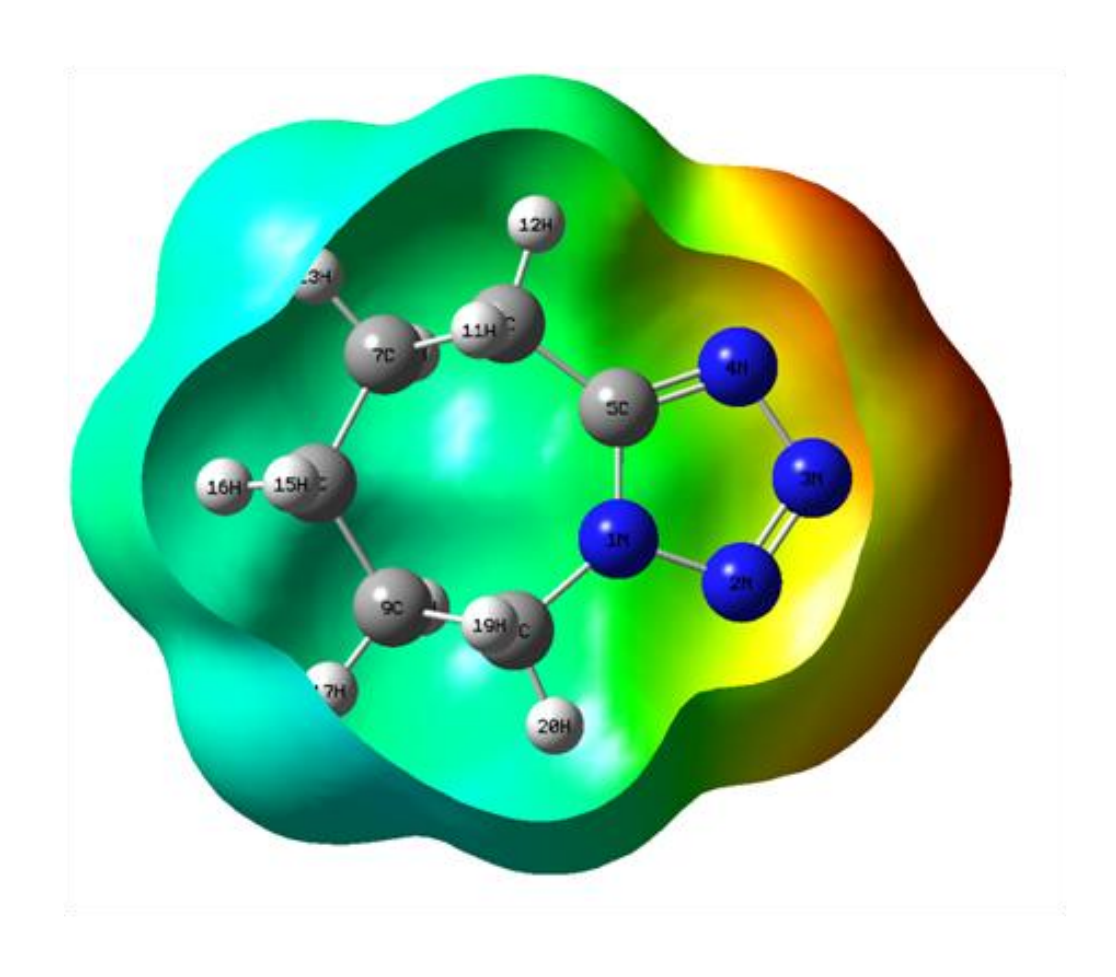


Fig. 4.3. The total electron density surface mapped with of Pentylenetetrazole (PTZ).

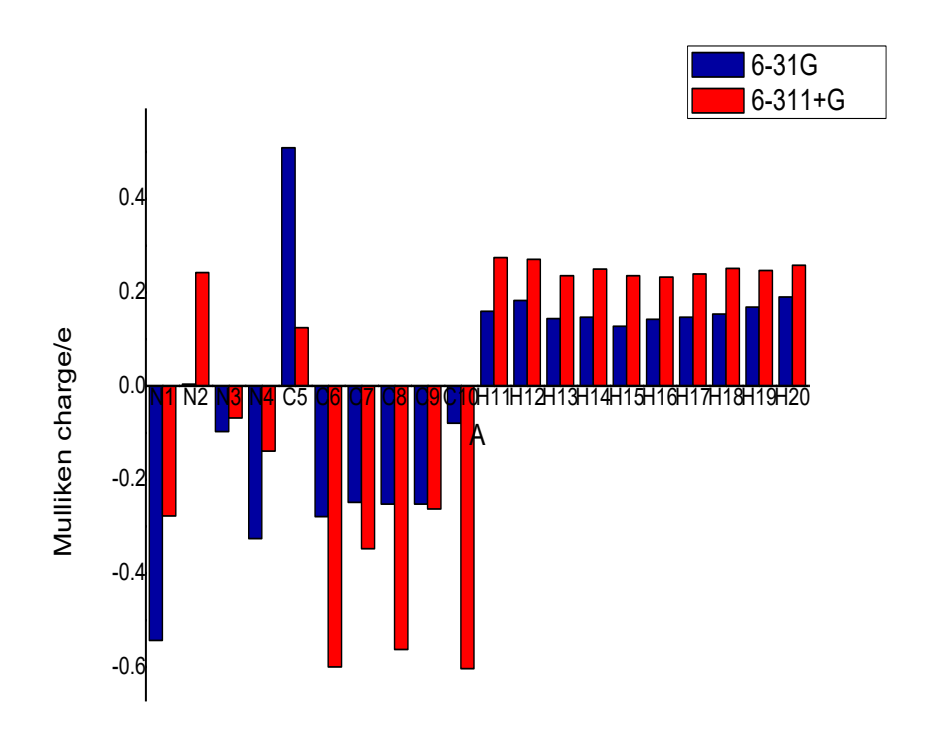


Fig. 4.4 Bar diagram representing the Mulliken atomic charge distribution of Pentylenetetrazole (PTZ) $\,$

•

The MEP surface which is a method of mapping electrostatic potential on to the isoelectron density surface and it provides a visual method to understand the relative polarity [46]. To predict reactive sites of electrophilic and nucleophilic attacks for the investigated molecule, MEP at the B3LYP level optimized geometry was calculated. The different values of the electrostatic potential at the MEP surface are represented by different colors; red, blue and green represent the regions of most negative, most positive and zero electrostatic potential respectively. The MEP plots of the title compound PTZ is shown in Fig. 4.3 and it provides a visual representation of the chemically active sites and comparative reactivity of atoms. The negative electrostatic potential corresponds to an attraction of proton by the aggregate electron density in the molecule (shades of red and yellow) and the positive electrostatic potential corresponds to the repulsion of proton by the nuclei (shades of blue). The electrophilic attack,nucleophilic attack and zero region of the title compound are depicted by Fig. 4. 3.

4.7 MULLIKEN ATOMIC CHARGE

The Mulliken atomic charge calculation has vital role in the application of quantum mechanics calculations to molecular system: the calculation of effective atomic charge plays an important role [47]. The electron distribution in PTZ is compared in two different quantum chemical methods and the sensitivity of the calculated charges to charge in the choice of methods is studies. By determining the electron population of each atom in the define basis function, the Mulliken charges are calculated. An estimated

Mulliken charges at both levels are lists in Table 4.3. The results can be represented in graphical form as given in Fig. 4. 4.

4.8 NONLINEAR OPTICAL PROPERTIES

Theoretical evaluation of the polarizability (a), and the first order hyperpolarizabilities (b) is used to the design of new compounds for nonlinear optical applications and to understand the interaction between electromagnetic field and matter [48]. The calculation of hyperpolarizability and related properties have been carried out at DFT level by finite field approach.

The dipole moment, the mean polarizability of the title compound are calculated using Gaussian 09 software and are found to be 7.1416,7.3831 Debye 6-31G,6-311+G basis set respectively. The magnitude of the first hyperpolarizability from Gaussian 09 output is 0.6177X10⁻³⁰, 0.6692 X10⁻³⁰ esu 6-31G, 6-311+G basis set respectively.

4.9 VIBRATIONAL ASSIGNMENT

The title compound belongs to C1 symmetry, consists of 20 atoms species and get 54 fundamental vibrations. The detailed vibration assignments of fundamental modes of PTZ with observed and calculated frequencies and normal modes description are reported in Table 4.5. The observed experimental FT-IR, FT-Raman spectra are shown in Fig 4.5 and 4.6 respectively. The higher value of theoretical vibrations have been reduced by scaled factor 0.9555 for >1500 cm⁻¹,0.9826 for <1500cm⁻¹ in 6-31G basis set. as well as 0.9642 for >1500 cm⁻¹,0.9860 for <1500cm⁻¹ in 6-311+G basis set.

B3LYP computation gives mode arising from the N-N stretching at 1129 cm⁻¹ in 6-31G and 1119 cm⁻¹ in 6-311+G basis set corresponding to the peak at 1115 cm⁻¹ in IR spectrum. The C-N vibrations is a very critical task, since the mixing of vibrations is possible in this region. Silverstein et al. [49] attributed C-N stretching absorption in the region 1266–1382 cm⁻¹ for aromatic amines. In benzamide the band observed at 1368 cm⁻¹ is assigned to the CN stretching band [50]. In 1,2,4-triazole the band observed at 1390 and 1327 cm⁻¹ are assigned to CN stretching [51]. The C-N stretching modes are reported in the range 1000–1400 cm⁻¹ [52] and in the present case these bands are assigned at 1194, 1269, 1533 (6-31G) 1191,1268, 1530 (6-311+G) cm⁻¹ theoretically. 1171, 1246, 1530 cm⁻¹ in IR and 1242,1531 cm⁻¹ in Raman.

The vibrations of the CH_2 group (attached with the tetrazole ring), the asymmetric stretch CH_2 , symmetric stretch CH_2 , scissoring vibration CH_2 and wagging vibration CH_2 appear in the regions, 3000 ± 50 , 2965 ± 30 , 1455 ± 55 and 1350 ± 85 cm⁻¹, respectively [53,54]. The B3LYP calculations give stretching vibration of CH_2 at 3007-2885 cm⁻¹ in 6-31G basis set, 3003- 2860 cm⁻¹ in 6-311+G basis set. Experimentally bands are observed at 2946-2821 cm⁻¹ in IR and at 3005-2869 cm⁻¹ in the Raman spectrum as CH_2 stretching modes. All the bands were also found well within the characteristic region and presented in.

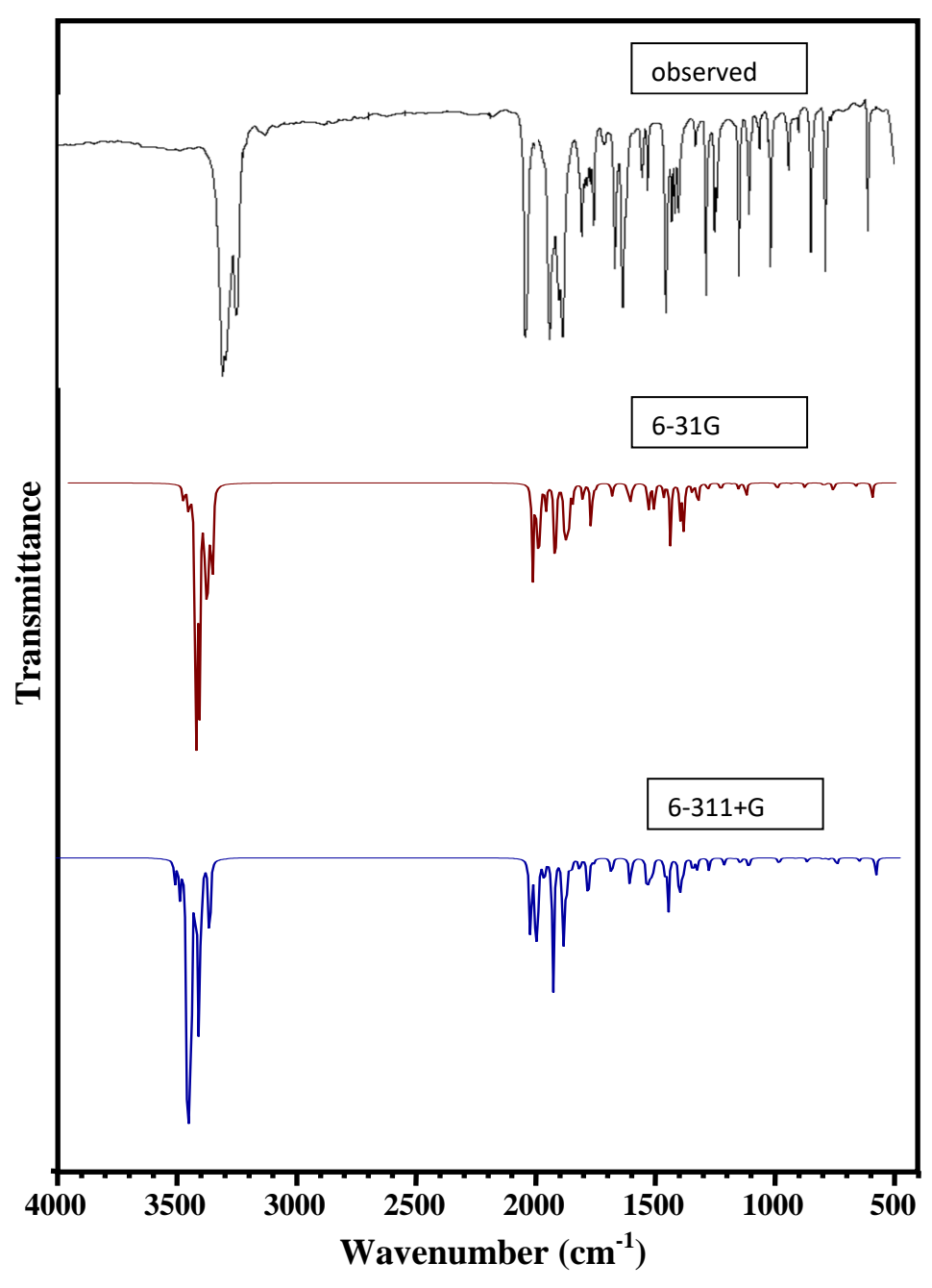


Fig. 4.5. Comparative representation of FT-IR spectra for Pentylenetetrazole (PTZ)

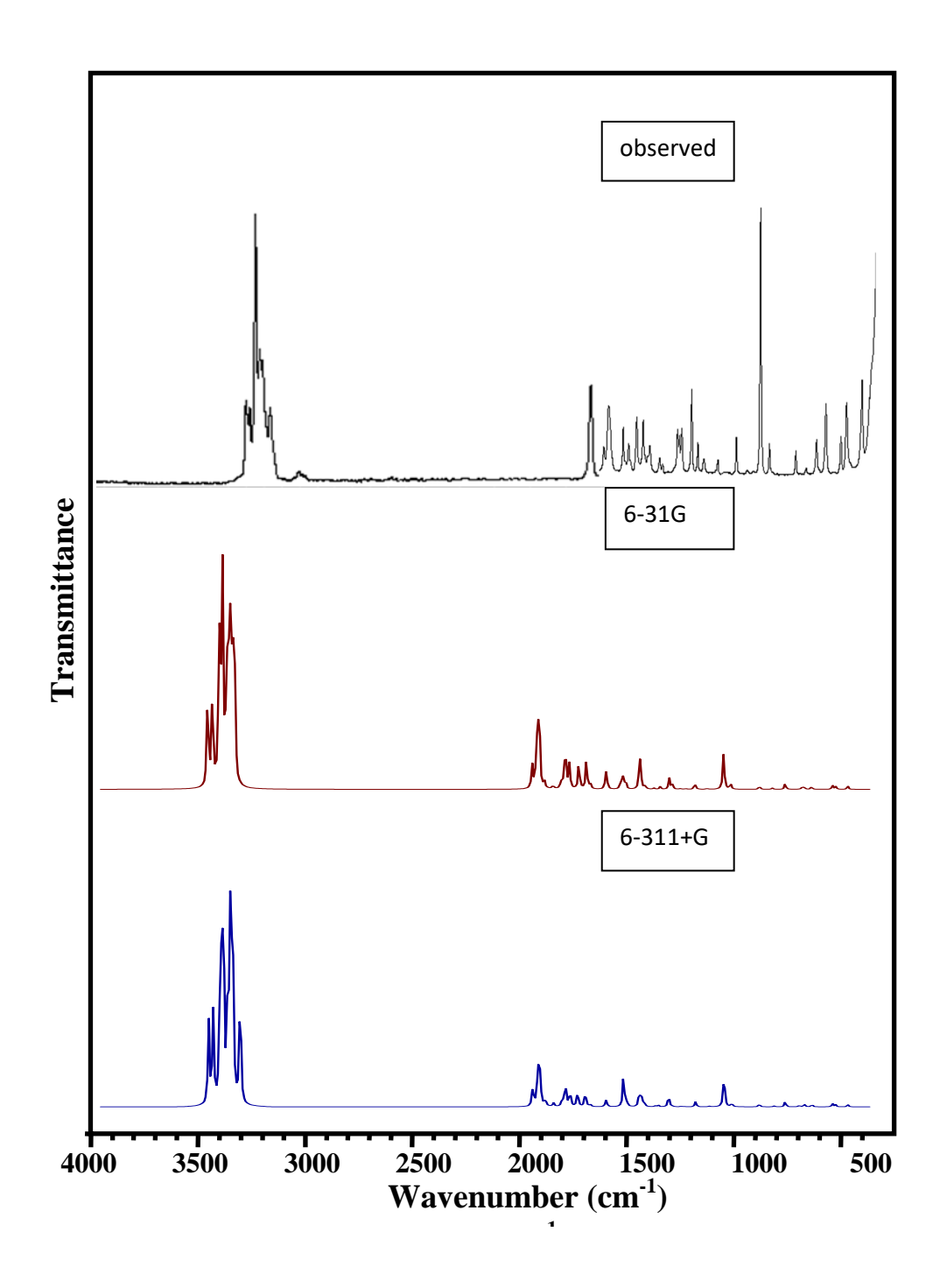


Fig.4.6. Comparative representation of FT-Raman spectra for Pentylenetetrazole (PTZ)

4.10 Natural Bond Analysis

The Natural bond ortbital [55] analyzes is used to understand the delocalization of electron density and second order donor-acceptor energy. Typically, the stabilization of orbital interaction is high for higher energy differences between interacting orbitals. Effective donor and effective acceptor have this strong stabilization [56-59]. According to the second order perturbation approach, the stabilization energy is derived [60]. The energy from (donor) $i \rightarrow$ (acceptor) j is calculated as

$$E^{2} = \Delta E_{ij} = q_{i} \frac{F(i, j)^{2}}{\varepsilon_{i} - \varepsilon_{i}}$$

Where, q_i is the donor orbital occupancy, ε_i , ε_j are diagonal elements (orbital energies) and F(i,j) is the off-diagonal NBO Fock matrix element. The NBO analysis gives valuable information about the intra and inters molecule interaction of the molecule [61].

The current work summarizes second order perturbative calculation donor-acceptor interactions based on NBO. This analysis was carried out by observing all possible interaction between lewis and non-lewis NBOs and calculated their stabilization energy (E2). Donor NBO (i), acceptor NBO (j) and stabilization energy (E2) are tabulated in Table 4.6 From this table, it is show that the interaction between the bonded N2-N3 (NBO 92) and N4-C5 antibond (NBO 95) gives the strongest stabilization, 30.11 kcal/mol and also, lonepair N1 (NBO 34) \rightarrow N4-C5 antibond (NBO 95), lonepair N1 (NBO 34) \rightarrow N2-N3 antibond (NBO 92) has the highest stabilization energy are 23.09, 21.94, 16.68kcal/mol Respectively.`

4.11 CONCLUSION

The present investigation thoroughly analyzed the HOMO-LUMO, and vibration spectra, both infrared and Raman of PTZ molecules with B3LYP method with standard 6-31G and 6-311+G basis sets. All the vibration bands are observed in the FT-IR and FT-Raman spectra of the compound are assigned to various modes of vibration and most of the modes have wave numbers in the expected range. The complete vibration assignments of wave numbers are made on the basis of potential energy distribution (PED). The electrostatic potential surfaces (MEP) together with complete analysis of the vibration spectra, both IR and Raman spectra help to identify the structure and symmetry. The excellent agreement of the calculated and observed vibration spectra reveals the advantages over the other method. Finally, calculated HOMO-LUMO energies show that the charge transfer occurs in the molecule, which are responsible for the bioactive properly of the biomedical compound PTZ.

Table 4.1: Geometry Optimization Parameter of Pentelyenetetrazole (PTZ) based on B3LYP/6-31G and B3LYP/6-311+G method and basis set.

]	BondLength(Å)	В	BondAngle(°)	
Atom	6-31G	6-311+G	Atom	6-31G	6-311+G
C6-C7	1.55	1.55	C5-N1-C10	130.49	130.37
C7-C8	1.54	1.54	N4-C5-C6	125.87	125.85
C8-C9	1.54	1.54	N1-C5-C6	125.56	125.56
C9-C10	1.54	1.53	N2-N1-C10	120.94	120.97
C5-C6	1.49	1.49	C7-C8-C9	115.96	116.05
N1-C10	1.46	1.46	C8-C9-C10	115.2	115.20
N3-N4	1.40	1.40	C6-C7-C8	115.07	115.10
N1-N2	1.39	1.39	C5-C6-C7	114.17	114.14
N1-C5	1.36	1.36	N1-C10-C9	112.95	112.91
N4-C5	1.34	1.34	C9-C10-H20	111.04	111.04
N2-N3	1.32	1.32	N2-N3-N4	110.61	110.69
C6-H11	1.10	1.10	C9-C10-H19	110.56	110.41
C7-H13	1.10	1.10	C8-C9-H18	110.16	110.23
C7-H14	1.10	1.09	C7-C6-H12	110.12	110.04
C8-H15	1.10	1.09	C8-C7-H14	109.77	109.81
C8-H16	1.10	1.09	C5-C6-H11	109.73	109.77
C9-H17	1.10	1.09	C6-C7-H14	109.21	109.26
C9-H18	1.10	1.09	C7-C6-H11	109.13	109.24
C10-H19	1.10	1.09	C7-C8-H15	109.13	109.12
C6-H12	1.09	1.09	C9-C8-H15	109.06	109.06
C10-H20	1.09	1.09	C10-C9-H18	108.94	108.97
			N1-C10-H19	108.76	108.68
			N2-N1-C5	108.58	108.66
			N1-C5-N4	108.56	108.58

C8-C9-H17	108.56	108.54
C8-C7-H13	108.31	108.30
C7-C8-H16	108.14	108.14
H19-C10-H20	108.00	107.99
C9-C8-H16	107.97	107.86
C6-C7-H13	107.59	107.58
C10-C9-H17	106.94	106.96
H11-C6-H12	106.8	106.71
H17-C9-H18	106.66	106.63
C5-C6-H12	106.62	106.55
H13-C7-H14	106.53	106.42
N3-N4-C5	106.2	106.26
H15-C8-H16	106.14	106.09
N1-N2-N3	106.04	106.02
N1-C10-H20	105.28	105.40

Table 4.2: HOMO-LUMO energy (eV) and other related properties of Pentelyenetetrazole (PTZ) based on B3LYP/6-31G and B3LYP/6-311+G method and basis set

Parameters	6-31G	6-311+G
rarameters	(eV)	(eV)
Homo(I)	-7.5293	-7.8994
Lumo(A)	-0.6585	-1.0204
Energy gap(ΔE)	6.8708	6.8790
Electronegativity	4.0939	4.4599
Global hardness	3.4354	3.4395
Global softness(eV ⁻¹)	0.2910	0.2907
Chemical potential	-4.0939	-4.4599
Electriphilicity	2.4393	2.8915

Table 4.3: Mulliken charge (charge/e) of Pentelyenetetrazole (PTZ) based on B3LYP/6-31G and B3LYP/6-311+G method and basis set

Atom	6-31G	6-311+G				
Atom	Charge/e					
N1	-0.5433	-0.2775				
N2	0.0042	0.2422				
N3	-0.0973	-0.0681				
N4	-0.3257	-0.1392				
C5	0.5090	0.1250				
C6	-0.2788	-0.5999				
C 7	-0.2482	-0.3476				
C8	-0.2519	-0.5628				
C9	-0.2522	-0.2626				
C10	-0.0793	-0.6035				
H11	0.1598	0.2747				
H12	0.1825	0.2706				
H13	0.1440	0.2357				
H14	0.1471	0.2496				
H15	0.1277	0.2357				
H16	0.1427	0.2325				
H17	0.1474	0.2393				
H18	0.1539	0.2510				
H19	0.1683	0.2467				
H20	0.1901	0.2581				

Table 4.4: Dipole moment(μ), Polarizability(α), Anisotropy polaraizability($\Delta\alpha$) and First order polarizability(β_{tot}) of Pentelyenetetrazole (PTZ) based on B3LYP/6-31G and B3LYP/6-311+G method and basis set

Parameters	6-31G	6-311+G
μ_{x}	-6.9613	-7.1981
$\mu_{ m y}$	-0.8587	-0.8722
μ_z	1.3437	1.3917
$lpha_{ ext{XX}}$	-73.8034	-75.6721
$lpha_{ m YY}$	-59.1621	-60.6258
α_{ZZ}	-58.4211	-59.6432
$a_{ ext{XY}}$	-0.9227	-0.9443
α_{XZ}	2.2679	2.3738
$lpha_{YZ}$	-0.0276	-0.0363
eta_{XXX}	-52.1379	-55.563
eta_{YYY}	-5.5846	-5.9735
β_{ZZZ}	1.3902	1.8947
$eta_{ ext{XYY}}$	-16.5269	-18.1617
eta_{XXY}	-3.4782	-3.5951
eta_{XXZ}	5.5513	5.6818
β_{XZZ}	-1.3562	-2.1705
eta_{YZZ}	-1.0458	-1.2285
eta_{YYZ}	3.3821	3.5901
eta_{XYZ}	0.3376	0.2452
μ(debye)	7.1416	7.3831
a(esu)	-9.4417X10 ⁻²⁴	-9.6664 X10 ⁻²⁴
$\Delta \alpha(esu)$	19.0493X10 ⁻²⁴	19.5343 X10 ⁻²⁴
$\beta_{tot}(esu)$	0.6177X10 ⁻³⁰	0.6692 X10 ⁻³⁰

Table 4.5: Observed Frequency (cm⁻¹), Theoretical Frequency (cm⁻¹) and Vibrational assignment with PED(%) of Pentelyenetetrazole (PTZ) based on B3LYP/6-31G and B3LYP/6-311+G method and basis set.

	Observed Frequency(cm ⁻¹)		Theoretical				
cis			Frequency(cm ⁻¹)			¹)	- Vibrational assignment (PED %)
Spe cis	FT-IR	FT-Raman	6-	31G	6-3	11+G	- Vibrational assignment (1 ED 70)
	r 1-ik	r 1 - Kaman	Calc	Scaled	Calc	Scaled	
A	-	3005	3147	3007	3114	3003	ν CH (91)
A	-	2983	3125	2986	3094	2983	ν CH (94)
A	-	-	3094	2956	3060	2951	ν CH (82)
A	-	-	3088	2951	3054	2945	ν CH (88)
A	-	-	3077	2940	3045	2936	ν CH (76)+ ν CH (15)
A	2946	2951	3056	2920	3024	2916	ν CH (84)
A	2929	2927	3044	2909	3013	2905	ν CH (93)
A	-	2911	3042	2907	3010	2902	ν CH (12)+ ν CH (78)
A	2863	2869	3029	2894	3000	2893	ν CH (88)
A	2821	-	3019	2885	2987	2860	ν CH (84)+ ν CH (11)
A	1530	1531	1560	1533	1552	1530	ν NC (27)+ β HCH (12)+ β HCH (25)
A	-	-	1541	1514	1531	1510	β HCH (59)
A	-	-	1536	1509	1527	1506	β HCH (70)

A	-	-	1530	1503	1521	1500	β HCH (58)
A	1468	1474	1527	1500	1517	1496	β HCH (68)
A	1439	1449	1524	1477	1514	1473	β HCH (54)+ β HCH (10)
A	1428	-	1463	1438	1456	1436	v CC (17)+ τ HCNC (19)
A	1378	1375	1427	1402	1420	1400	β HCC (12)+ $τ$ HCCC (60)
A	1370	-	1420	1395	1413	1393	β HCC (13)+ $τ$ HCCN (14)+ $τ$ HCCN (13)+ $τ$ HCNC (12)
A	1382	-	1408	1382	1402	1382	β HCC (12)+ $τ$ HCCC (33)
A	1355	-	1407	1382	1398	1378	β HCN (25)+ $τ$ HCCN (21)
A	1344	1347	1388	1364	1380	1361	β HCC (26)+ τ HCCN (30)
A	1334	-	1344	1321	1346	1327	β HCC (44)+ $τ$ HCNC (18)
A	1302	1307	1310	1287	1309	1291	β HCC (14)+ $β$ HCN (12)+ $τ$ HCNC (13)
A	1271	1274	1306	1283	1305	1287	β HCC (10)+ $β$ HCC (12)+ $β$ HCC (17)+ $τ$ HCCN (13)
A	1246	1241	1292	1269	1286	1268	ν NC (10)+ $β$ HCC (12)+ $τ$ HCCC (12)
A	1187	-	1219	1198	1215	1198	β HCC (16)
A	1171	-	1215	1194	1208	1191	v NC (31)
A	1115	-	1210	1129	1206	1119	v NN (55)
A	1097	1100	1138	1118	1132	1116	τ CCCC (30)
A	1088	1092	1128	1108	1119	1103	v CC (56)
A	1078	1079	1064	1045	1062	1047	β NNN (66)
A	-	1028	1059	1041	1053	1038	ν CC (41)+ β CNN (11)

A	993	997	1038	1020	1040	1025	ν NN (24)+ β CCC (11)+ τ HCCC (10)
A	968	-	996	979	988	974	v CC(15)
A	962	-	968	951	973	959	ν NN (22)
A	894	-	925	909	926	913	v NC (14)+ β NCN (44)
A	864	-	911	895	912	899	β NNC (22)
A	832	-	873	858	869	857	ν CC (14)+ β CCN (15)
A	805	802	870	835	863	841	τ HCCC (31)+ τ NCNN (14)
A	799	-	807	793	801	790	v CC (51)
A	744	-	751	738	738	728	τ NNNC (13)+ δ CNNC (53)
A	676	679	704	692	699	689	τ NNNC (74)+ δ CNNC (12)
A	633	635	675	663	670	661	ν NC (54)
A	504	501	643	632	635	626	ν CC (21)+ $β$ NNC (11)+ $τ$ NCNN (11)
A	-	-	509	500	507	500	β CCC (38)+ τ HCCC (10)
A	-	395	449	441	448	432	β CNN (19)
A	-	349	390	383	388	383	β CCC (28)+ τ CCNC (12)
A	-	273	355	309	354	319	β CCN (40)
A	-	-	343	298	341	296	β CCN (12)+ $β$ CNN (27)+ $τ$ HCCC (10)
A	-	245	268	263	265	261	β CCN (21)+ β CCC (13)+ τ CCNC (18)
A	-	155	234	168	234	168	τ CCNC (13)+ δ CCNN (21)
A	-	-	156	153	155	153	τ CCCN (65)
A	-	-	101	99	100	99	τ NCNN (10)+ τ CCCN (10)+ δ CCNN (30)

Table 4.6: Natural Bond Orbital Calculation of Pentelyenetetrazole (PTZ)

S.No	Don	or NRO (i)	Λ.	AccentarNRO (i)		E(2)	E(j)-E(i)	F(i,j)
5.110	Donor NBO (i)		A	AcceptorNBO (j)		kcal/mol	a.u.	a.u.
1	92 B	D N2-N3	95	BD*	N4-C5	30.11	0.04	0.06
2	34 L	P N1	95	BD*	N4-C5	23.09	0.36	0.083
3	34 L	P N1	92	BD*	N2-N3	21.94	0.32	0.076
4	8 B	D N4-C5	92	BD*	N2-N3	16.68	0.3	0.066
5	36 L	P N3	88	BD*	N1-N2	12.55	0.68	0.082

Chapter - V

Quantum mechanics calculation and Vibrational Spectra FT-IR and FT-Raman (theoretical, Experimental) studies of 5-Methyl-1H-tetrazole(5MTZ)

Abstract

The spectra of 5-Methyl-1H-tetrazole(5MTZ) have been recorded in the regions $4000-400 \text{ cm}^{-1}$ for FT-IR and $3500-100 \text{ cm}^{-1}$ for FT-Raman. The geometry optimization, vibrational frequencies were obtained by the density functional theory (DFT) using B3LYP method with 6-31G and 6-311+G basis sets. The complete assignments were performed on the basis of the potential energy distribution (PED) of the vibrational modes, calculated and the scaled values were compared with experimental FT-IR and FT-Raman spectra. The HOMO and LUMO energy gap reveals that the energy gap reflects the chemical activity of the molecule. The dipole moment (μ), polarizability (α), anisotropy polarizability ($\Delta \alpha$) and first hyperpolarizability (β_{tot}) of the molecule have been reported. Information about the size, shape, charge density distribution and site of chemical reactivity of the molecule has been obtained by molecular electrostatic potential (MEP).

Chapter-V

Quantum mechanics calculation and Vibrational Spectra FT-IR and FT-Raman (theoretical, Experimental) studies of 5-Methyl-1H-tetrazole (5MTZ)

5.1 INTRODUCTION

The Quantum mechanics is used as a tool to learn the molecular forces determining drug activity. This information can be used to infer the nature of the biological substances with which the drug reacts and hopefully as a guide to the synthesis of useful new agents[62].the complete investigation of the 5-Methyl-1H-tetrazole(5MTZ) has been carried by DFT method, which belongs to the quantum mechanics.

In recent years, tetrazole and their derivatives have been extensively studied as they exhibit effective biological activities such as anti-inflammatory[63], antiviral[64], analgesic[65], antibacterial[66], antitubercular[67], anticonvulsant[68] etc. the title molecule 5-Methyl-1H-tetrazole is one of the tetrazole derivatives which used in the preparation of novel antifungal agents based derived from N-iodopropargylazoles and N-triiodoallylazoles. 5-Methyl Tetrazole also in the preparation of novel quinoline derivatives against mycobacterium tuberculosis. In these studies, the molecular structure, vibrational spectra and HOMO-LUMO energy gap of 5-Methyl-1H-tetrazole(5MTZ) were investigated by a concerted approach using matrix isolation vibrational spectroscopy and high-level DFT-based theoretical calculations. Regarding their studies, tetrazoles have been found to be extremely interesting and challenging molecules.

5.2 EXPERIMENTAL DETAILS

The fine sample of 5-Methyl-1H-tetrazole(5MTZ) was obtained from Lancaster Chemical Company.UK, with a stated purity of 99% and it was used as such without further purification.The FT-Raman Spectrum of 5MTZ was recorded using 1064 nm line of ND: YAG laser for excitation wavelength in the region 3500-100 cm⁻¹ on Thermo Electron Corporation model Nexus spectrometer equipped with FT-Raman module accessory. The FT-IR Spectrum of the title compound was recorded in the region 4000-400 cm⁻¹ on Perking Elmer Spectrophotometer in KBr pellet.

5.3 COMPUTATIONAL DETAILS

The combination of Vibration spectra with quantum chemical calculation is effective for understanding the fundamental mode of vibration of the compound. The structural characteristic, stability and energy of the compound under investigation are determined by DFT with the three-parameter hybrid functional (B₃) for the exchange part and the Becke Three Lee Yong-Pare (LYP) and 6-31G ,6-311+G basis sets with Gaussian 09 Program Package. The Cartesian representation of the theoretical force constants has been compound at the fully optimized geometry by assuming the molecule belongs to C₁ point group symmetry. The Transformation of force field from Cartesian to internal local symmetry coordinates, the scaling, and the subsequent normal coordinate analysis (NCA) Calculation of potential energy distributions (PED) has been done on a PC with the VEDA program.

5.4 GEOMETRICAL PARAMETER

The calculated C-N distances areN1-C7 = 1.36 Å, N4-C5=1.34 Å, this value indicate that the bond N4-C5 is stronger than the bond N1-C7 and these values indicate that the bond distances were found to be much smaller than the average value for a single C-N bond (1.47 Å) [68]. The bond lengths of N3-N4, N1-N2 were found to be elongated to 1.40 Å, 1.39 Å respectively, compared to N2-N3 values of 1.32 Å. Because bond order of N2-N3 is higher than N3-N4, N1-N2 bond order [34]. table-5.1 report the detailed data of geometrical optimization of the isolated title molecule. Functional group methyl substituted in ring structure with C5 atom which made longest bond length in that molecule structure because C-C bond shaped a nonpolar covalent bond[69] and the hyper conjugation causes the interaction of the orbital of the methyl group with the π orbital of a ring. in methyl group ,C-H bond length1.10Å, (6-31G),1.09 Å, (6-311+G) are good agreement with other literature values 1.09 Å [70]1.08 Å,1.09 Å [71]1.09 Å [72]. this cooperation caused to discharging electronic charge from methyl group[73].highest bond angle occurred at C5-N1-H6 whereas lowest bond angle occurred at N1-N2-N3.

5.5 ELECTRONIC PROPERTIES

To explain several types of reactions and for predicting the most reactive position in conjugated systems, molecular orbital and their properties such as energy are used [74]. The highest occupied molecular orbital (HOMO) and lowest unoccupied molecular orbital (LUMO) are the most important orbital in a molecule. The eigen values of HOMO and LUMO and their energy gap reflect the biological activity of the molecule.

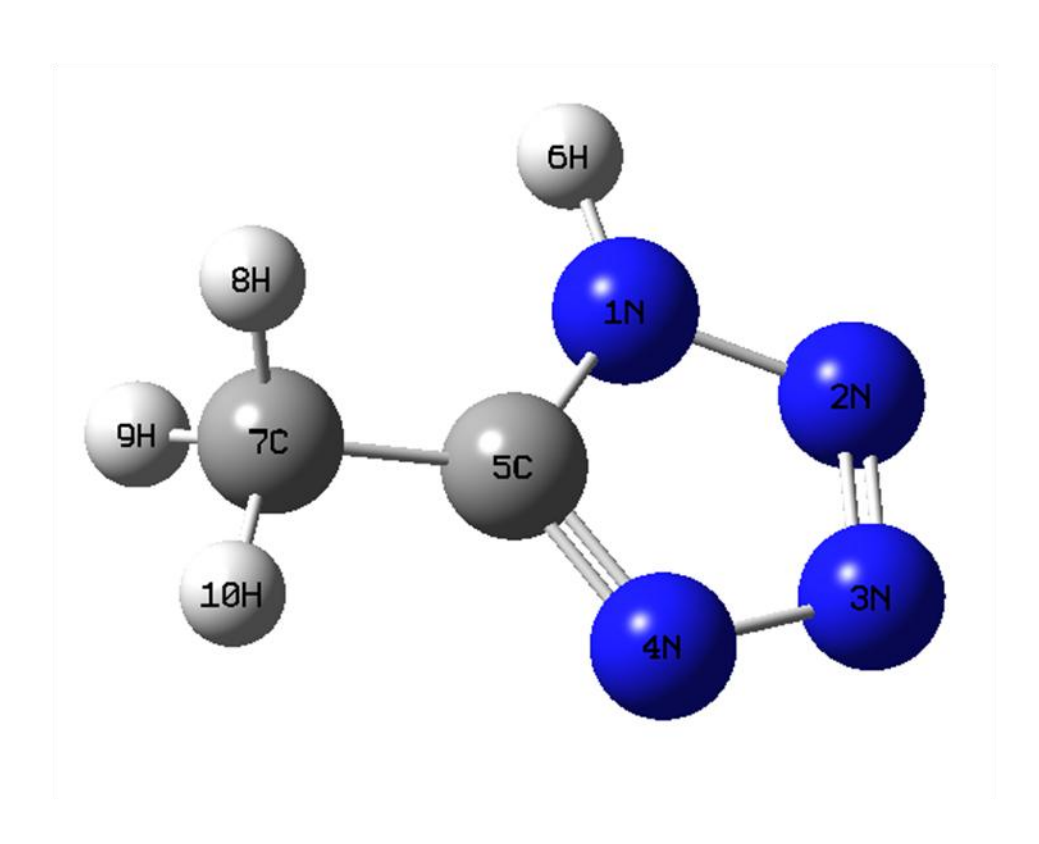


Fig 5.1. The theoretical geometry structure and atomic numbering scheme of 5-Methyl-1H-tetrazole (5MTZ)

<u>6-31G</u> <u>6-311+G</u>

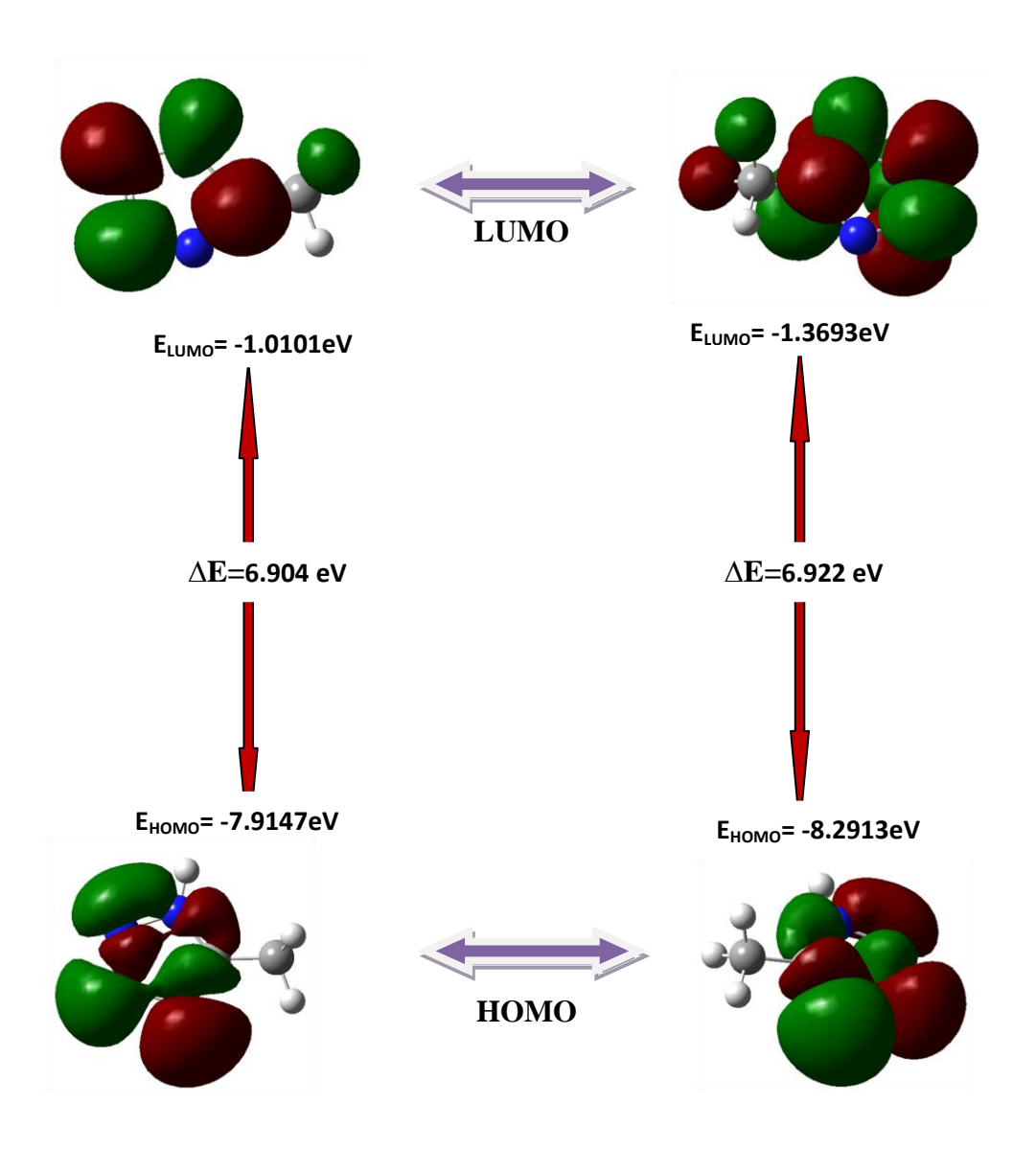


Fig 5.2: The atomic orbital compositions of the frontier molecular orbital for 5-Methyl-1H-tetrazole (5MTZ)

A molecule having a small frontier orbital gap is more polarizable and is generally associated with a high chemical reactivity and low kinetic stability [75,76]. HOMO, which can be thought the outer orbital containing electrons, tends to give these electrons as an electron donor and hence the ionization potential is directly related to the energy of the HOMO. On the other hand LUMO can accept electrons and the LUMO energy is directly related to electron affinity [26]. Two important molecular orbital (MO) were examined for the title compound, the highest occupied molecular orbital (HOMO) and the lowest unoccupied molecular orbital (LUMO) which are given in Fig.5.2. In the title compound, the HOMO of π nature is delocalized over the tetrazole ring. By contrast, the LUMO is located over the tetrazole ring and methyl group. For understanding various aspects of pharmacological sciences including drug design and the possible ecotoxicological characteristics of the drug molecules, several new chemical reactivity descriptors have been proposed. Conceptual DFT based descriptors have helped in many ways to understand the structure of molecules and their reactivity by calculating the chemical potential, global hardness and electrophilicity. Using HOMO and LUMO orbital energies, the ionization energy and electron affinity can be expressed as: I = E_{HOMO} , $A = E_{LUMO}$. Table. 5.2 shows global reactor values of the title compound. It is seen that the chemical potential of the title compound is negative and it means that the compound is stable. They do not decompose spontaneously into the elements they are made up of. The hardness signifies the resistance towards the deformation of electron cloud of chemical systems under small perturbation encountered during chemical process. The principle of hardness works in Chemistry and Physics but it is not physical

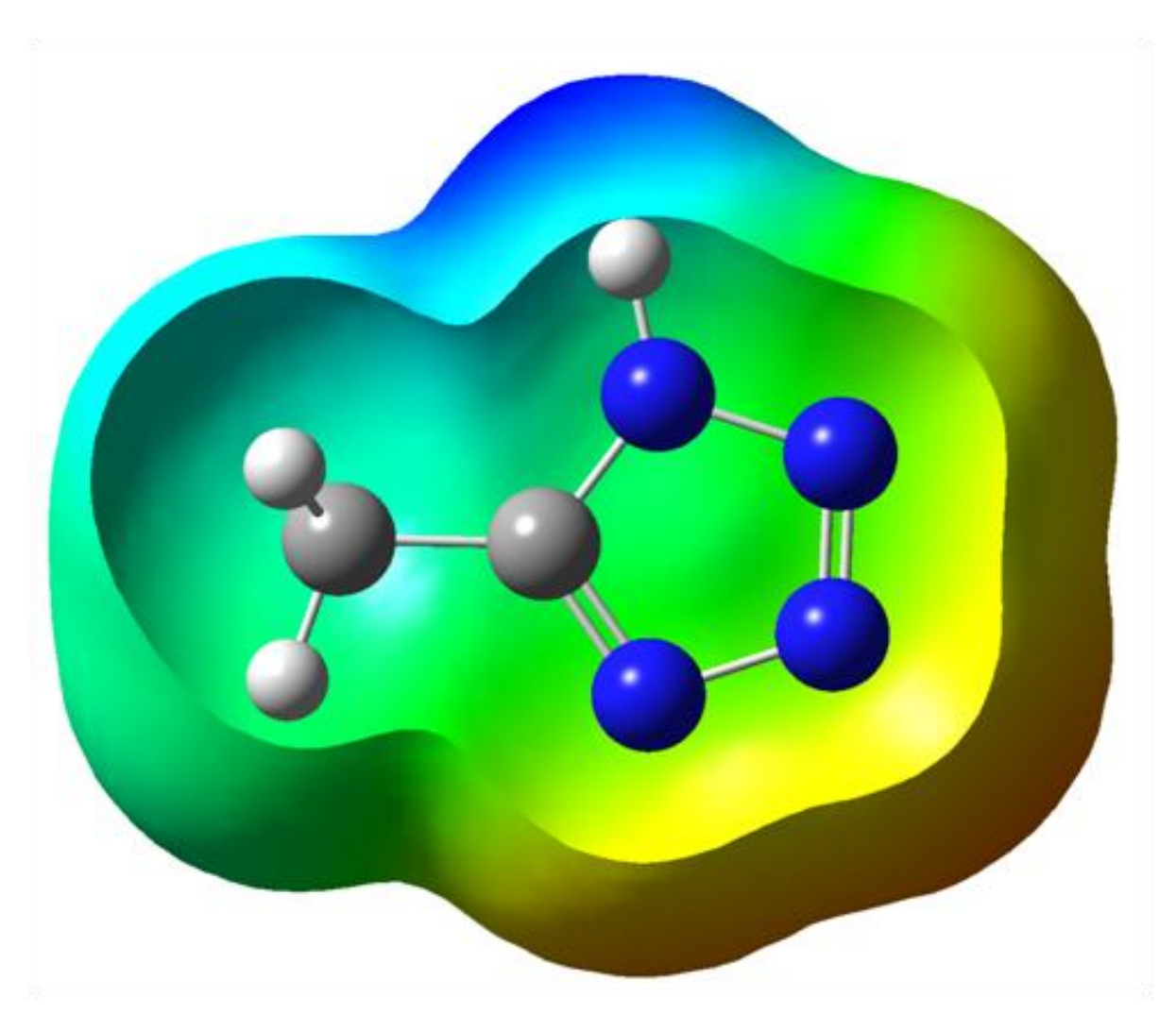


Fig. 5.3. The total electron density surface mapped with of 5-Methyl-1H-tetrazole $(5\mathrm{MTZ})$

observable. Soft systems are large and highly polarizable, while hard systems are relatively small and much less polarizable.

5.6 MOLECULAR ELECTROSTATIC POTENTIAL (MEP)

MEP is related to the Electron Density and is a very useful descriptor in understanding sites for electrophilic and nucleophilic reactions as well as hydrogen bonding interactions [77,78]. The electrostatic potential V(r) is also well suited for analyzing processes based on the "recognition" of one molecule by another, as in drugreceptor, and enzyme-substrate interactions, because it is through their potentials that the two species first "see" each other [79,80]. To predict reactive sites of electrophilic and nucleophilic attacks for the investigated molecule, MEP at the B3LYP level optimized geometry was calculated. The different values of the electrostatic potential at the MEP surface are represented by different colours red, blue and green represent the regions of most negative, most positive and zero electrostatic potential respectively. The negative electrostatic potential corresponds to an attraction of the proton by the aggregate electron density in the molecule (shades of red), while the positive electrostatic potential corresponds to the repulsion of the proton by the atomic nuclei (shade of blue). The negative (red and yellow) regions of MEP were related to electrophilic reactivity and the positive (blue) regions to nucleophilic reactivity (Fig. 5.3). From the MEP it is evident that the negative charge covers the N atoms which presence in tetrazole group. the positive region is over the H atoms. The value of the electrostatic potential is largely responsible for the binding of a substrate to its receptor binding sites since the receptor and the corresponding ligands recognize each other at their molecular surface [81,82].

5.7 NLO Properties

Nonlinear optics deals with the interaction of applied electromagnetic fields in various materials to generate new electromagnetic fields, altered in wavenumber, phase, or other physical properties [83]. Organic molecules able to manipulate photonic signals efficiently are of importance in technologies such as optical communication, optical computing, and dynamic image processing [84,85]. In this context, the dynamic first hyperpolarizability of the title compound is also calculated in the present study. The first hyperpolarizability (b0) of this novel molecular system is calculated using DFT method, based on the finite field approach. In the presence of an applied electric field, the energy of a system is a function of the electric field. First hyperpolarizability is a third rank tensor that can be described by a 3 X 3X 3 matrix. The 27 components of the 3D matrix can be reduced to 10 components due to the Kleinman symmetry [86]. The components of b are defined as the coefficients in the Taylor series expansion of the energy in the external electric field. When the electric field is weak and homogeneous, this expansion become

$$E = E_0 - \mu_\alpha F_\alpha - 1/2\alpha_{\alpha\beta} F_\alpha F_\beta - 1/6\beta_{\alpha\beta\gamma} F_\alpha F_\beta F_\gamma + \dots$$

where E_0 is the vitality of the unperturbed atoms, F_{α} the field at the source μ_{α} , $\alpha_{\alpha\beta}$ and $\beta_{\alpha\beta\Upsilon}$ are the segments of dipole moment, polarizability and the first order hyper polarizabilities. The aggregate static dipole moment (μ), polarizability(α), anisotropy polarizability ($\Delta\alpha$) and the mean first order hyperpolarizability (β_{tot}) utilizing x,y,z,

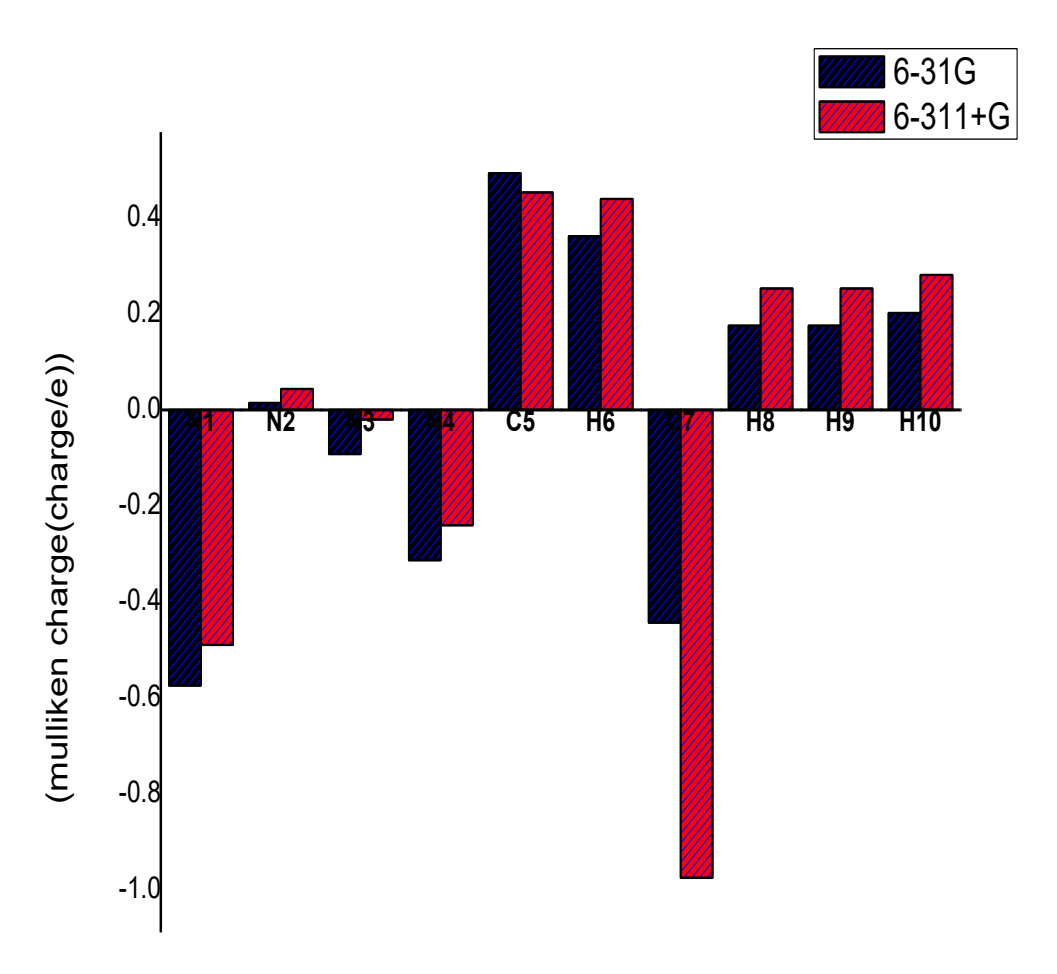


Fig. 5.4 Bar diagram representing the Mulliken atomic charge distribution of 5-Methyl-1H-tetrazole (5MTZ)

The segments are characterized as follows ,The calculated first order hyperpolarizability of the title compound is 0.3199×10^{-30} esu/6-31G,0.3458 $\times 10^{-30}$ esu/6-311+G. The calculated hyperpolarizability of the title compound is superior than that of the standard NLO material urea (0.13 $\times 10^{-30}$ esu) [47]. We conclude that the title compound is an attractive object for future studies of nonlinear optical properties.

5.8 MULLIKEN ATOMIC CHARGE

The Mulliken atomic charge calculation has important role in the application of quantum mechanics calculations to molecular system: the atomic charge calculation of molecule plays an important role [47]. The electron distribution in 5MTZ is compared in two different quantum chemical methods and the sensitivity of the calculated charges to charge in the choice of methods is studies. By determining the electron population of each atom in the define basis function, the Mulliken charges are calculated. An estimated Mulliken charges at both levels are lists in Table 5.3. The results can be represented in graphical form as given in Fig 5.4. In this molecule all the hydrogen atoms have got positive charge. N1, N3 and N4 have negative charge. Tetrazole carbon atom has negative charge and methyl carbon atom has positive charge.

5.9 VIBRATIONAL ASSIGNMENT

The detailed vibrational data of the c1 point group title molecule were tabulated in table5.5. The higher value of theoretical vibrations have been reduced by scaled factor 0.9555 for >1500 cm⁻¹,0.9826 for <1500cm⁻¹ in 6-31G basis set. as well as 0.9642 for >1500 cm⁻¹,0.9860 for <1500cm⁻¹ in 6-311+G basis set.

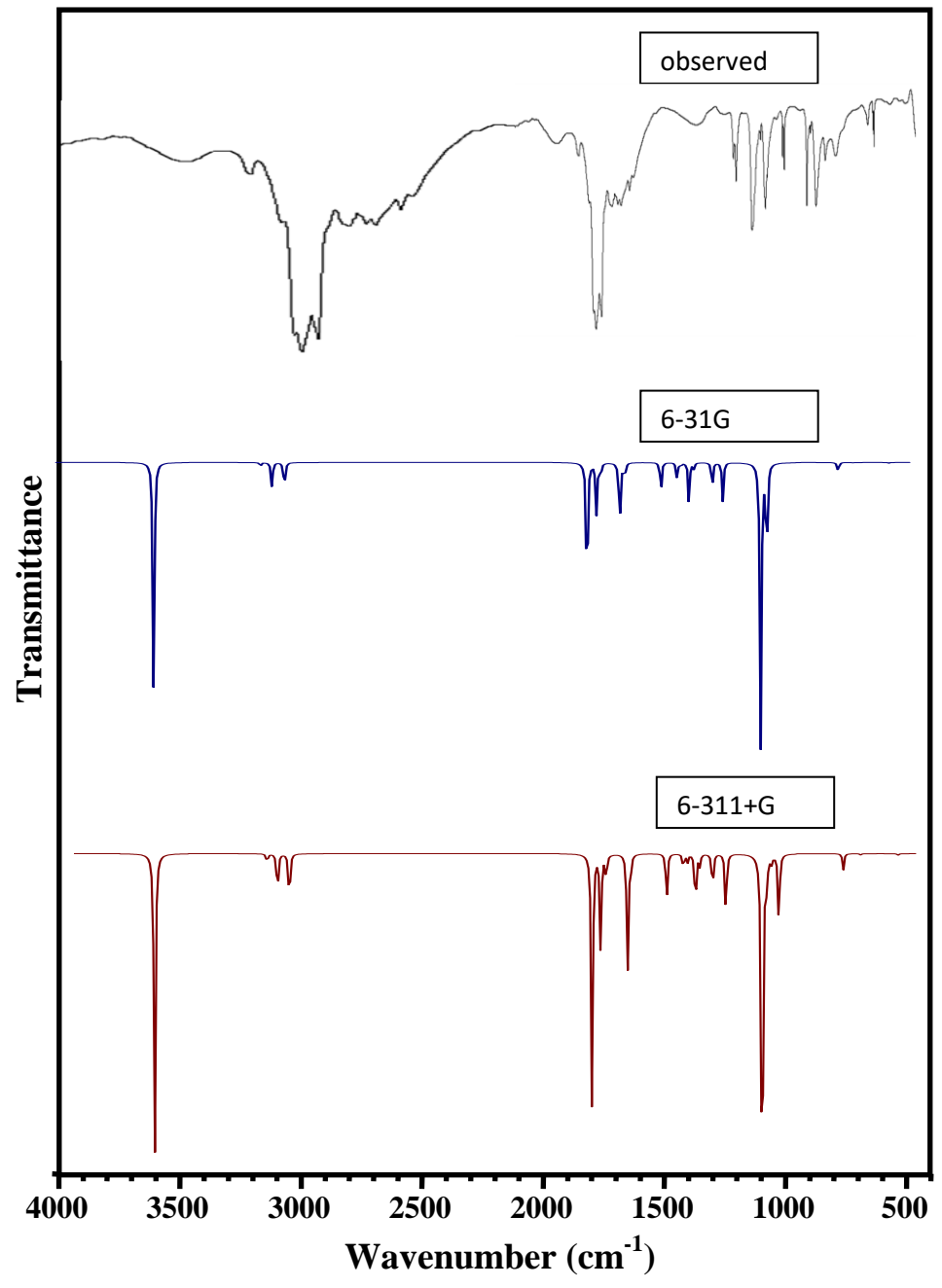


Fig. 5.5. Comparative representation of FT-IR spectra for 5-Methyl-1H-tetrazole (5MTZ)

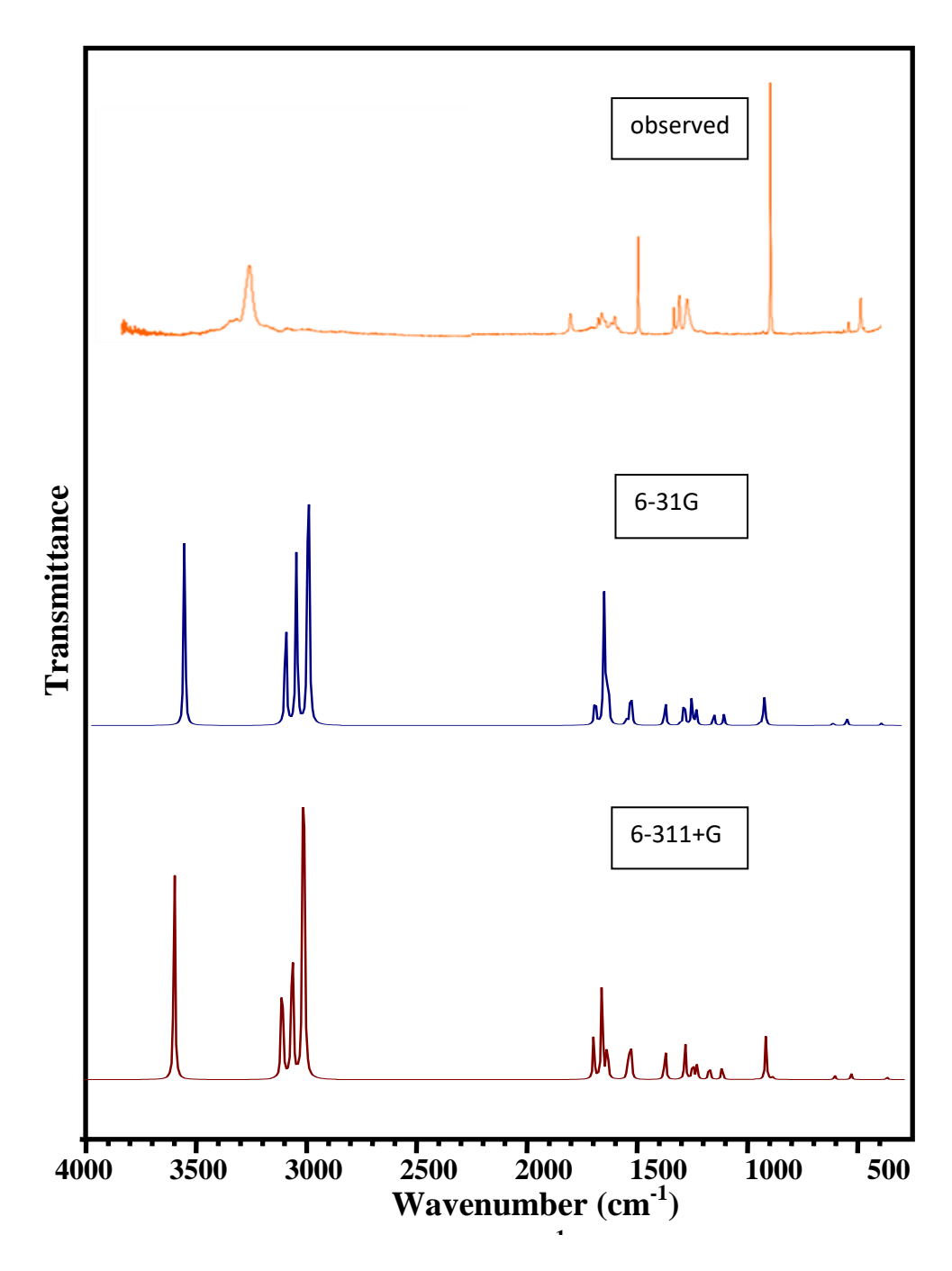


Fig. 5.6. Comparative representation of FT-Raman spectra for 5-Methyl-1H-tetrazole (5MTZ)

The C-H linear vibration in methyl group occurs in the range 3000 - 2900 cm⁻¹ [73]. The methyl groups vibrational frequencies depend upon the connecting atom. For example, the stretching frequency of C-OCH₃ is higher than that of C-CH₃ [87]. The C-H vibration frequencies also differ in their position. K.Parimala et al [88] assigned asymmetric C-H stretching frequency band at 2943 cm⁻¹,2896 cm⁻¹ and,2940 cm⁻¹,2900 cm⁻¹ respective in the FT-IR and FT-Raman. Other literature values assigned to the frequency band stretching for CH₃ molecule is 2833cm⁻¹, 2875cm⁻¹, 2991cm⁻¹ in FT-IR 2937, 2975 cm⁻¹ in FT-Raman[73], 2967 cm⁻¹, 2925 cm⁻¹ in FT-IR, 2976 cm⁻¹, 2930 cm⁻¹ in FT-Raman(89). In this investigation all the vibration frequencies of the methyl group are in accordance with literature values those found in the characteristic group frequency as shown in Table 5.5. The calculated values by B3LYP methods are fit with experimental values.

NH stretching is in the region 3500-3400cm⁻¹ [90] and theoretically assigned at 3490cm⁻¹ and 3458cm⁻¹ [91]. In this molecule,in this work,the NH band occurred at 3420 cm⁻¹ in FT-IR,3550 cm⁻¹ in FT-Raman.theoretically,this band observed at 3535 cm⁻¹ (6-31G),3553 cm⁻¹ (6-311+G).

B3LYP computation gives mode arising from the N-N stretching at 1162 cm⁻¹ in 6-31G and 1162 cm⁻¹ in 6-311+G basis set corresponding to the peak at 1113 cm⁻¹ in IR spectrum.

The C-N vibrations is a very critical task, since the mixing of vibrations is possible in this region. Silverstein et al. [92] attributed C-N stretching absorption in the region 1266–1382 cm⁻¹ for aromatic amines. In benzamide the band observed at 1368 cm⁻¹ is

assigned to the CN stretching band [50]. In 1,2,4-triazole the band observed at 1390 and 1327 cm⁻¹ are assigned to CN stretching [93]. The C-N stretching modes are reported in the range 1000–1400 cm⁻¹ [52] and in the present case these bands are assigned at 1008, 1354, 1508 (6-31G) 1007,1345, 1510 (6-311+G) cm⁻¹ theoretically. 1001, 1366, 1566 cm⁻¹ in IR and 1380, 1570 cm⁻¹ in Raman.

5.10 Natural Bond Analysis

The Natural bond ortbital [58] analyzes is used to understand the delocalization of electron density and second order donor-acceptor energy. Typically, the stabilization of orbital interaction is high for higher energy differences between interacting orbitals. Effective donor and effective acceptor have this strong stabilization [56-59]. According to the second order perturbation approach, the stabilization energy is derived [60]. The energy from (donor) $i \rightarrow$ (acceptor) j is calculated as

$$E^{2} = \Delta E_{ij} = q_{i} \frac{F(i, j)^{2}}{\varepsilon_{i} - \varepsilon_{i}}$$

where, q_i is the donor orbital occupancy, ε_i , ε_j are diagonal elements (orbital energies) and F(i,j) is the off-diagonal NBO Fock matrix element. The NBO analysis gives valuable information about the intra and inters molecule interaction of the molecule [61].

The current work summarizes second order perturbative calculation donor-acceptor interactions based on NBO. This analysis was carried out by observing all possible interaction between lewis and non-lewis NBOs and calculated their stabilization energy (E2). Donor NBO (i), acceptor NBO (j) and stabilization energy (E2) are

tabulated in Table 5.6. From this table, it is show that the interaction between the bonded N2-N3 (NBO 55) and N4-C5 antibond (NBO 58) gives the strongest stabilization, 27.74 kcal/mol and also, lonepair N1 (NBO 19) \rightarrow N2-N3 antibond (NBO 55), lonepair N1 (NBO 19) \rightarrow N4-C5 antibond (NBO 58), bonded N4-C5 (NBO 8) \rightarrow N2-N3 antibond (NBO 55) has the highest stabilization energy are 18.98, 18.32, 16.27kcal/mol Respectively.

5.11 CONCLUSION

The present investigation thoroughly analyzed the HOMO-LUMO, and vibration spectra, both infrared and Raman of 5MTZ molecules with B3LYP method with standard 6-31G and 6-311+G basis sets. All the vibration bands are observed in the FT-IR and F-Raman spectra of the compound are assigned to various modes of vibration and most of the modes have wave numbers in the expected range. The complete vibration assignments of wave numbers are made on the basis of potential energy distribution (PED). The electrostatic potential surfaces (MEP) together with complete analysis of the vibration spectra, both IR and Raman and help to identify the structure and symmetry. The excellent agreement of the calculated and observed vibration spectra reveals the advantages over the other method. Finally, calculated HOMO-LUMO energies show that the charge transfer occurs in the molecule, which are responsible for the bioactive properly of the biomedical compound 5MTZ.

Table 5.1: Geometry Optimization Parameter of 5-Methyl-1H-tetrazole (5MTZ) based on B3LYP/6-31G and B3LYP/6-311+G method and basis set

	BondLength(Å	7)		BondAngle(°)	
Atom	6-31G	6-311+G	Atom	6-31G	6-311+G
C5-C7	1.49	1.48	C5-N1-H6	130.75	130.85
N3-N4	1.40	1.40	N1-C5-C7	126.12	126. 10
N1-N2	1.39	1.39	N4-C5-C7	125.90	126.01
N1-C5	1.36	1.36	N2-N1-H6	119.91	119.60
N4-C5	1.34	1.34	С5-С7-Н8	111.56	111.62
N2-N3	1.32	1.32	С5-С7-Н9	111.54	111.57
C7-H9	1.10	1.09	N2-N3-N4	110.77	110.54
C7-H8	1.10	1.09	N2-N1-C5	109.35	109.55
C7-H10	1.09	1.09	C5-C7-H10	108.65	108.81
N1-H6	1.01	1.00	H8-C7-H10	108.47	108.30
			H9-C7-H10	108.47	108.29
			Н8-С7-Н9	108.06	108.15
			N1-C5-N4	107.98	107.89
			N3-N4-C5	106.36	106.49
			N1-N2-N3	105.54	105.54

Table 5.2: HOMO-LUMO energy (eV) and other related properties of 5-Methyl-1H-tetrazole (5MTZ) based on B3LYP/6-31G and B3LYP/6-311+G method and basis set $\frac{1}{2}$

Parameters	6-31G	6-311+G
rarameters	(eV)	(eV)
Homo(I)	-7.9147	-8.2913
Lumo(A)	-1.0101	-1.3693
Energy gap(ΔE)	6.9046	6.9220
Electronegativity	4.4624	4.8303
Global hardness	3.4523	3.4610
Global softness(eV ⁻¹)	0.2897	0.2889
Chemical potential	-4.4624	-4.8303
Electriphilicity	2.8840	3.3706

Table 5.3: Dipole moment(μ), Polarizability(α), Anisotropy polaraizability($\Delta\alpha$) and First order polarizability(β_{tot}) of 5-Methyl-1H-tetrazole (5MTZ) based on B3LYP/6-31G and B3LYP/6-311+G method and basis set

Parameters	6-31G	6-311+G
μ_{x}	-4.7921	4.9639
μ_{y}	4.0155	4.1044
μ_z	0.0001	0.0003
α_{XX}	-37.5178	-38.5207
α_{YY}	-34.8592	-35.9312
α_{ZZ}	-34.6744	-35.4883
α_{XY}	0.054	0.0135
α_{XZ}	-0.001	-0.001
α_{YZ}	0.0002	0.0007
eta_{XXX}	-23.2569	24.9565
eta_{YYY}	21.6646	22.7176
β_{ZZZ}	0.0017	0.0013
eta_{XYY}	-5.3476	5.8671
eta_{XXY}	-0.165	-0.2122
eta_{XXZ}	0.0009	-0.0028
β_{XZZ}	-0.6815	1.2008
β_{YZZ}	1.1585	1.5009
eta_{YYZ}	-0.0006	0.0004
eta_{XYZ}	-0.0007	-0.001
μ(debye)	6.2521	6.4410
a(esu)	-5.2812X10 ⁻²⁴	-5.4237 X10 ⁻²⁴
$\Delta \alpha(esu)$	65.0411X10 ⁻²⁴	66.7801 X10 ⁻²⁴
$\beta_{tot}(esu)$	0.3199×10^{-30}	0.3458X10 ⁻³⁰

Table 5.4: Mulliken charge (charge/e) of 5-Methyl-1H-tetrazole (5MTZ) based on B3LYP/6-31G and B3LYP/6-311+G method and basis set

A 4 0	6-31G	6-311+G		
Atom	Cl	Charge/e		
N1	-0.5748	-0.4897		
N2	0.0143	0.0438		
N3	-0.0924	-0.0203		
N4	-0.3128	-0.2401		
C5	0.4934	0.4534		
Н6	0.3618	0.4396		
C 7	-0.4437	-0.9744		
Н8	0.1759	0.2534		
Н9	0.1759	0.2534		
H10	0.2023	0.2809		

Table 5.5: Observed Frequency (cm⁻¹)- Theoretical Frequency (cm⁻¹) and Vibrational assignment with PED(%) of 5-Methyl-1H-tetrazole (5MTZ) based on B3LYP/6-31G and B3LYP/6-311+G method and basis set.

Spe cis	Observed	Theoretical							
				Frequen	cy(cm ⁻¹)	Vibrational aggignment (DED 9/)		
	FT-IR	FT-Raman	6-,	31G	6-311+G		Vibrational assignment (PED %)		
			Calc	scaled	Calc	Scaled			
A	3420	3550	3700	3535	3684	3553	ν NH (100)		
A	3146	-	3176	3035	3140	3028	ν CH(86)+ν CH(14)		
A	2955	-	3121	2982	3090	2979	v CH(99)		
A	2923	-	3060	2923	3032	2924	ν CH(14)+ν CH(86)		
A	1566	1570	1578	1508	1566	1510	v NC(23)+v CC(23)		
A	1464	-	1532	1464	1526	1471	β HCH(78)+τ HCCN(21)		
A	-	-	1529	1461	1523	1469	β HCH(71)+ $τ$ HCCN(21)		
A	1409	1410	1469	1444	1465	1444	β HCH(97)		
A	1366	1380	1378	1354	1364	1345	v NC(30)+v NC(19)+β NNC(11)		
A	1269	1270	1355	1331	1350	1331	$v CC(14) + \beta HNN(57)$		
A	1113	1105	1182	1162	1178	1162	v NN(73)		
A	1089	1090	1106	1087	1099	1084	β HCH(20)+ $τ$ HCCN(60)+ $τ$ HCCN(10)		
A	1064	1070	1087	1068	1080	1065	$\nu NC(32) + \nu NC(14) + \beta NCN(14)$		

A	-	-	1049	1031	1042	1027	β NNN(71)
A	1001	-	1026	1008	1022	1007	$\nu NC(11) + \beta HCH(15) + \beta NNC(15)$
A	928	-	939	922	961	947	ν NN(68)+β NCN(11)
A	723	-	888	872	897	885	$\nu NC(19) + \beta NCN(43) + \beta NNN(16)$
A	690	-	711	699	726	716	τ NNNC(31)+ τ NNCN(58)
A	683	-	706	694	703	694	τ HNNN(79)+τ NNNC(19)
A	-	-	686	674	681	672	$\nu NC(10)+\nu CC(52)+\beta NCN(11)$
A	-	490	679	667	646	637	τ HNNN(15)+τ NNNC(44)+τ NNCN(19)
A	-	330	339	333	341	336	β CCN(86)
A	-	270	270	265	260	256	τ NNCN(19)+ δ CNNC(65)
A	-	-	96	94	83	81	τ HCCN(77)+δ CNNC(11)

Table 5.6: Natural Bond Orbital Calculation of 5-Methyl-1H-tetrazole (5MTZ)

S.No	Donor NBO (i)		A 4	noontor	·NBO (j)	E (2)	E(j)-E(i)	F(i,j)	
5.110	Donor ADO (1)			A	ceptor	NBO (J)	kcal/mol	a.u.	a.u.
1	55	BD	N2-N3	58	BD*	N4-C5	27.74	0.04	0.04
2	19	LP	N1	55	BD*	N2-N3	18.98	0.34	0.34
3	19	LP	N1	58	BD*	N4-C5	18.32	0.38	0.38
4	8	BD	N4-C5	55	BD*	N2-N3	16.27	0.3	0.3
5	21	LP	N3	51	BD*	N1-N2	12.15	0.68	0.68

Chapter - VI

Non Linear Optical Properties, Optimized structure, Global reactivates and Mulliken Atomic Charge studies on 5-Chloro-1-phenyl-1H-tetrazole based on Density functional theory with vibrational assignment

Abstract

The vibrational spectra of 5-Chloro-1-phenyl-1H-tetrazole (5ClPTZ) have been recorded in the regions 4000-400 cm⁻¹ for FT-IR and 3500-100 cm⁻¹ for FT-Raman. The molecular structure, geometry optimization, vibrational frequencies were obtained by the density functional theory (DFT) using B3LYP method with 6-31G and 6-311+G basis sets. The complete assignments were performed on the basis of the potential energy distribution (PED) of the vibrational modes, calculated and the scaled values were compared with experimental FT-IR and FT-Raman spectra. The HOMO and LUMO energy gap reveals that the energy gap reflects the chemical activity of the molecule. The dipole moment (μ), polarizability (α), anisotropy polarizability ($\Delta \alpha$) and first hyperpolarizability (β_{tot}) of the molecule have been reported. Information about the size, shape, charge density distribution and site of chemical reactivity of the molecule has been obtained by molecular electrostatic potential (MEP).

Chapter-VI

Non Linear Optical Properties, Optimized structure, Global reactivates and Mulliken Atomic Charge studies on 5-Chloro-1-phenyl-1H-tetrazole based on Density functional theory with vibrational assignment

6.1 INTRODUCTION

5-Chloro-1-phenyl-1H-tetrazoles are widely used in several disparate areas of research and, commercially, in a variety of drug and herbicide manufactures[94]. Biological activity is encountered due to the special metabolism of disubstituted tetrazoles and also because, in 5-substituted tetrazolyl compounds, the heterocyclic ring is isosteric with a carboxy group and of similar acidity[96]. Some typical uses of such tetrazoles are in anti-inflammatory drugs[95], herbicides[97], rocket propellants[98] and photography and polymers[99]. Due to this importance, the title molecule 5-Chloro-1-phenyl-1H-tetrazole (5ClPTZ) was investigated by DFT method. since density functional theory (DFT) has recently emerged as a compromise between the desired level of accuracy and the demand on computational time.

In these studies, the molecular structure, vibrational spectra and HOMO-LUMO energy gap of 5-Chloro-1-phenyl-1H-tetrazole (5ClPTZ) were investigated by a concerted approach using matrix isolation vibrational spectroscopy and high-level DFT-based theoretical calculations. Regarding their studies, tetrazoles have been found to be extremely interesting and challenging molecules.

6.2 EXPERIMENTAL DETAILS

The fine sample of 5ClPTZ was obtained from Lancaster Chemical Company.UK, with a stated purity of 99% and it was used as such without further purification. The FT-Raman Spectrum of 5ClPTZ was recorded using 1064 nm line of ND: YAG laser for excitation wavelength in the region 3500-100 cm⁻¹ on Thermo Electron Corporation model Nexus spectrometer equipped with FT-Raman module accessory. The FT-IR Spectrum of the title compound was recorded in the region 4000-400 cm⁻¹ on Perking Elmer Spectrophotometer in KBr pellet.

6.3 COMPUTATIONAL DETAILS

The combination of Vibration spectra with quantum chemical calculation is effective for understanding the fundamental mode of vibration of the compound. The structural characteristic, stability and energy of the compound under investigation are determined by DFT with the three-parameter hybrid functional (B₃) for the exchange part and the Becke Three Lee Yong-Pare (LYP) and 6-31G ,6-311+G basis sets with Gaussian 09 Program Package. The Cartesian representation of the theoretical force constants has been compound at the fully optimized geometry by assuming the molecule belongs to C₁ point group symmetry. The Transformation of force field from Cartesian to internal local symmetry coordinates, the scaling, and the subsequent normal coordinate analysis (NCA) Calculation of potential energy distributions (PED) has been done on a PC with the VEDA program.

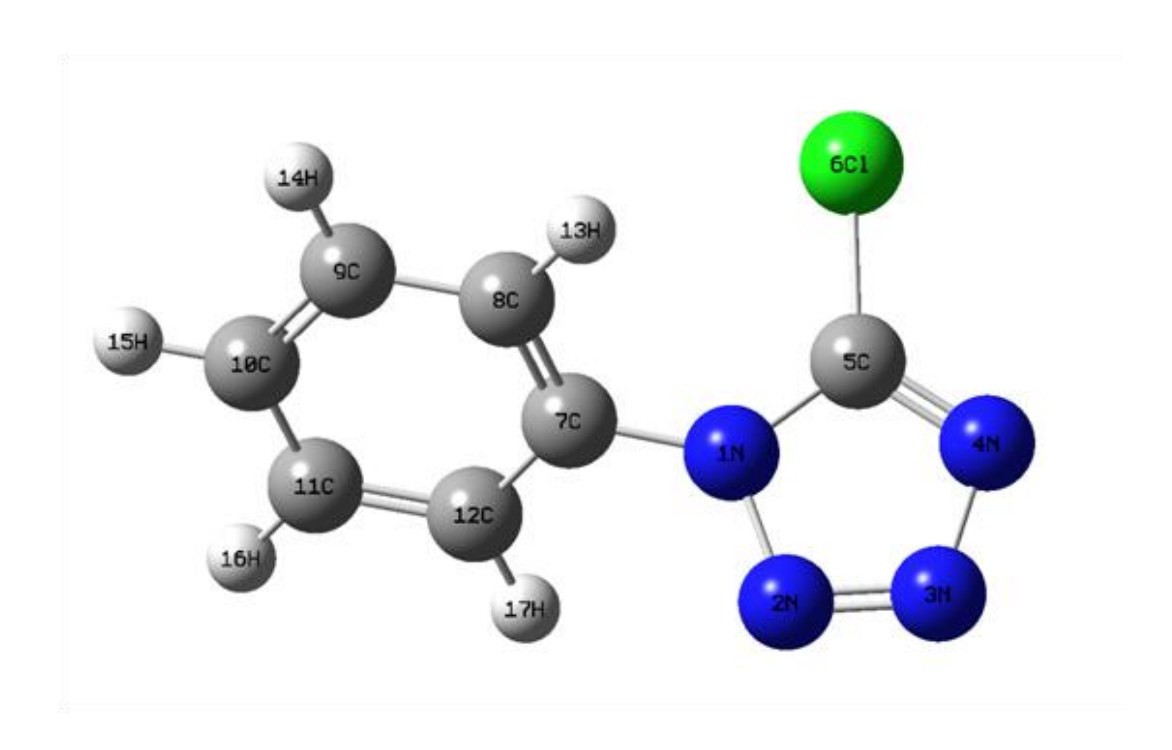


Fig. 6.1. The theoretical geometry structure and atomic numbering scheme of 5-Chloro-1-phenyl-1H-tetrazole (5ClPTZ)

6.4 MOLECULAR GEOMETRY

The optimised geometry of 5CIPTZ with atom numbering is shown in Fig. 6.1. The more stable 5CIPTZ molecule has C1 point group symmetry. The theoretical and experimental C–C bond lengths in the benzene ring of 5CIPTZ are in the range of 1.40 Å. The Alcala [100] and Derissen [101] reported that the C–C bond length of the isophthalic acid was in the range of 1.391–1.402 Å and well agreed with the theoretical bond length of the title molecule. The C–H bond lengths are calculated as 1.09-1.08 Å, experimentally reported as 0.930 Å. The substitution of halogen reduces the electron density at the ring carbon atom. The C-Cl bond length is calculated as 1.76 Å which is longest bond length in the molecule. The theoretical bond angles are in harmony with the experimental bond angles. In particular, the C–C–C bond angles of benzene ring in the title molecule is in range of 120.253–121.162 and well agreed with the experimental range of bond angles 116.2–124.80. The calculated C-N distance in the tetrazole ring is 1.36 Å. Whereas 1.43 Å for C7-N1 bond. The N-N bonds are assigned at 1.40 Å.

6.5 FRONTIER MOLECULAR ORBITAL ANALYSIS

The study of frontier molecular orbital is important that ionization potential (I), electron affinity (A), electrophilicity index (ω), chemical potential (μ), electronegativity (χ) and hardness (η) to be put into a MO frame work [38]. These global descriptors η , μ and χ are defined as η = (I -A)/2, μ = -(I + A)/2, χ = (I + A)/2, where I and A denote the ionization potential and electron affinity of the compounds respectively. The ionization energy (I) and electron affinity (A) can be expressed through HOMO and LUMO orbital

<u>6-31G</u> <u>6-311+G</u>

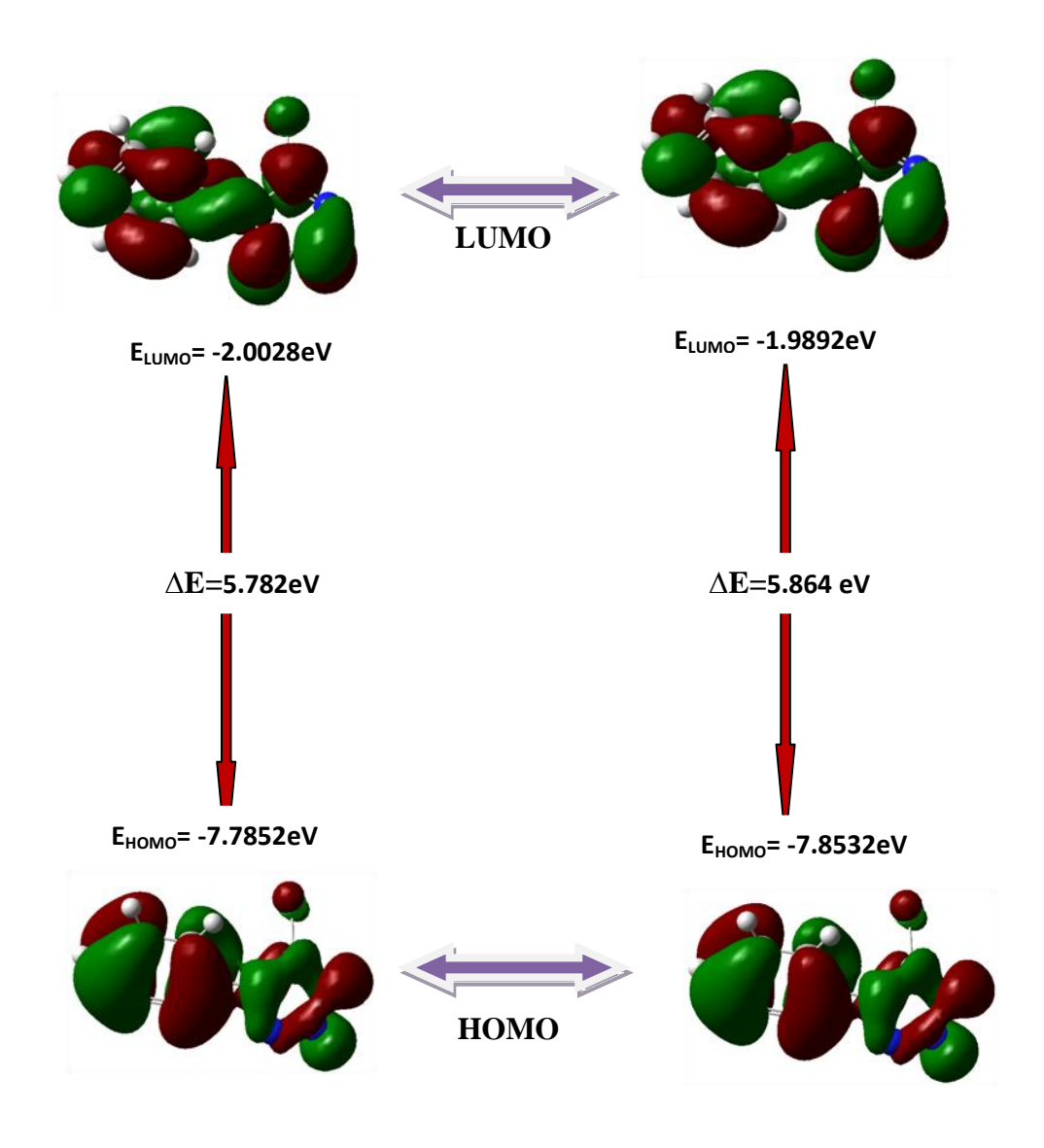


Fig. 6.2 The atomic orbital compositions of the frontier molecular orbital for5-Chloro-1-phenyl-1H-tetrazole (5ClPTZ)

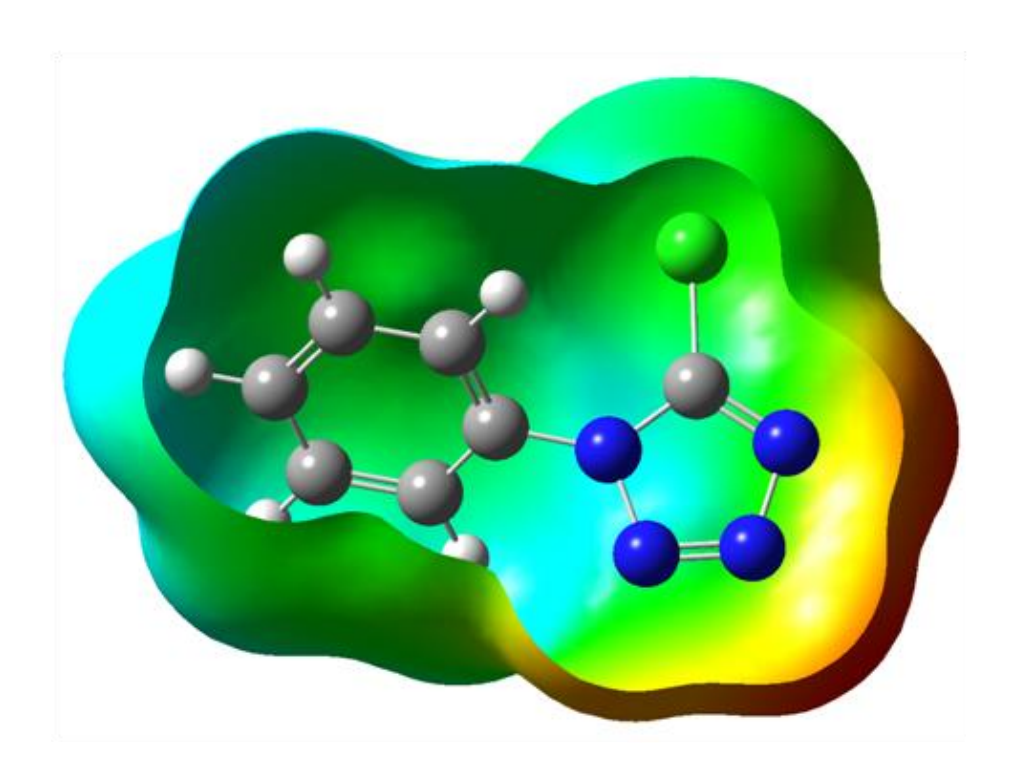


Fig. 6.3 The total electron density surface mapped with of 5-Chloro-1-phenyl-1H-tetrazole (5ClPTZ)

energies as I = -EHOMO and A = -ELUMO. Parr et al. [38] have defined a new descriptor to quantity the global electrophilic power of the compound as electrophilicity index ($\omega = \mu 2/2\eta$) which defines a quantitative classification of global electrophilic nature of a compound. The calculated values have tabulated in table6.2. HOMO is localized over the entire molecule and LUMO is localized over the entire compound .the small value of energy gap reveals the title molecule has more reactive.

6.6 MOLECULAR ELECTROSTATIC POTENTIAL (MEP)

Molecular electrostatic potential (MEP) is most helpful descriptor in understanding sites for electrophilic attack and nucleophilic reactions and for the study of biological recognition process [102] and to predict reactive sites of electrophilic and nucleophilic attacks for the title molecule, MEP at the B3LYP optimized geometry was calculated. Potential value increases in the order red < orange < yellow < green < blue. The negative (red and yellow) regions of MEP were related to electrophilic reactivity and the positive (blue) regions to nucleophilic reactivity. From the MEP of the title compound it is evident that the negative charge covers the N atoms which belongs to tetrazole molecule group and the positive region is over the H group in phenyl ring.

6.7 MULLIKEN ATOMIC CHARGE

Although atomic charges in a molecule are not experimentally observable quantities, they are fundamental and useful tools to understand and relate properties of molecules to their structures. Even though Various methods are available to assigning charges have been proposed, Mulliken method is widely used due to its convenient.

Mulliken atomic charge [47,103,104] is defined based on orbitals. For each atom, all electronic charge contributions from orbitals centered at that atom are summed up, and electronic overlap clouds between two atoms are divided equally to the two atoms. However, they are extremely basis-function dependent: changing basis functions could result in a big difference for the charge on the same atom[105,106]. In this study two different basis sets were used to find the muliiken atomic charge of title molecule. They are tabulated in table 6.3. All the N atoms got negative charge except N2 atom. As well as all the C atoms got negative charge except C12 atom. Further, all the H atoms got positive charge and Cl atom got negative charge.

6.8 NONLINEAR OPTICAL PROPERTIES

In the current study, the nonlinear optical (NLO) effect is considered most important because it provides key functions of optical modulation, optical switching, optical logic, and optical memory for the emerging technologies in the areas of telecommunications, optical interconnections, and signal processing [107]. In order to investigate the effects of the HF and DFT/B3LYP methods on the NLO properties of the studied compound, the dipole moments (μ), the polarizabilities (α), the anisotropy of the polarizabilities (α), and the mean first- order hyperpolarizabilities (α) of 5ClPTZ were calculated using the finite-field approach and are presented in Table 6.4.

The dipole moment, the mean polarizability of the title compound are calculated using Gaussian 09 software and are found to be 6.4941,6.4675 Debye 6-31G,6-311+G basis set respectively. The magnitude of the first hyperpolarizability from Gaussian 09

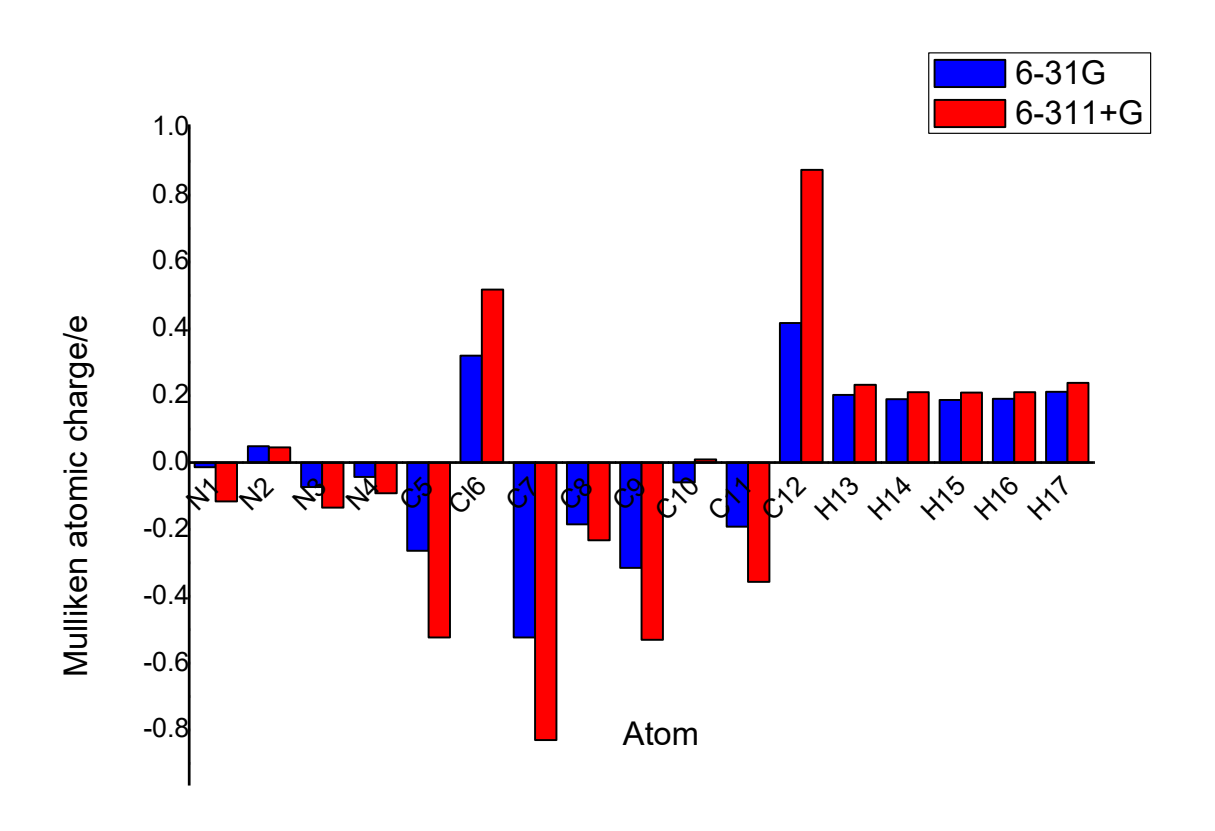


Fig. 6.4 Bar diagram representing the Mulliken atomic charge distribution of 5-Chloro-1-phenyl-1H-tetrazole (5ClPTZ)

output is $0.9636X10^{-30}$, $0.9552~X10^{-30}$ esu 6-31G, 6-311+G basis set respectively. The β value calculated by the DFT/B3LYP method shows that the title compound is an attractive molecule for future studies of NLO properties. Based on NLO properties of (common values) urea; the mean first-order hyperpolarizability and polarizability values of the studied molecule are bigger than those of urea.

6.9 VIBRATIONAL ASSIGNMENT

The detailed vibration assignments of fundamental modes of 5ClPTZ with observed and calculated frequencies and normal modes description are reported in Table 6.5. The observed experimental FT-IR, FT-Raman spectra are shown in Fig 6.5 and 6.6 respectively. The higher value of theoretical vibrations have been reduced by scaled factor 0.9555 for >1500 cm⁻¹,0.9826 for <1500cm⁻¹ in 6-31G basis set. As well as 0.9642 for >1500 cm⁻¹,0.9860 for <1500cm⁻¹ in 6-311+G basis set.

Typically, the C-Cl frequency band is absorbed between 850 and 550 cm⁻¹ [108]. For the title compound the bands occured at 490 cm⁻¹ in the IR spectrum are assigned as C-Cl stretching mode. According to the DFT theory, these bands are calculated at 479,440 cm⁻¹ (6-31G) and 465,430(6-311+G) cm⁻¹. The PED value of the CCl stretching modes is 45 and 16%. In this case the deformation modes of C-Cl are assigned at 235 cm⁻¹ at Raman spectrum, whereas this bands have been observed at 228,218 cm⁻¹ (6-31G),218,212 cm⁻¹ (6-311+G) in theoretically.

The C-H stretching vibrational modes of the title compound are expected in the region 3120-3000 cm⁻¹[109]. This study reveals the CH stretching modes are assigned at

3073 cm⁻¹ in the Raman spectrum, 3065 cm⁻¹ in the IR spectrum and at 3096, 3091, 3081, 3072, 3062 cm⁻¹ (6-31G) and 3166, 3160, 3150, 3140, 3129 cm⁻¹ (6-311+G) theoretically. The ring stretching vibrational modes are expected in the region 1615-1260 cm⁻¹[109]. In the present case, the ring modes are occured at 1691, 1339, 1116 cm⁻¹ in the IR spectrum and 1599 cm⁻¹ in the Raman spectrum. The theoretical calculation showed that mode at 1578, 1569,1104 cm⁻¹ (6-31G) and 1616, 1606, 1291cm⁻¹(6-311+G). PED contribution of the phenyl ring stretching modes were assigned at 29%, 44% and 62%.

The C-H in-plane deformation of this molecule is expected in the range 1270-1045 cm⁻¹[109]. For the title compound the phenyl C-H in-plane deformation CH(Phenyl) are observed at 1244, 1174 cm⁻¹ in the in the IR spectrum. The DFT calculation gives modes at 1209,1202 cm⁻¹ (6-31G) and 1179,1171cm⁻¹ (6-311+G). The C-H out-of-plane deformations are expected in the range [109] 980-740 cm⁻¹[109]. These CH Phenyl modes are observed at 853 cm⁻¹ in the IR spectrum, corresponding calculated values are 1022, 1000, 860 cm⁻¹ (6-31G) and 998,980,873 cm⁻¹ (6-311+G).

DFT computational method gives mode arising from the N-N stretching at 966, 937 cm⁻¹ in 6-31G and 957,923 cm⁻¹ in 6-311+G basis set corresponding to the peak at 975,924 cm⁻¹ in IR spectrum. The C-N vibrations is a very critical task, since the mixing of vibrations is possible in this region. Silverstein et al. [49] attributed C-N stretching absorption in the region 1266–1382 cm⁻¹ for aromatic amines. In benzamide the band observed at 1368 cm⁻¹ is assigned to the CN stretching band [50]. In 1,2,4-triazole the band observed at 1390 and 1327 cm⁻¹ are assigned to CN stretching [93].

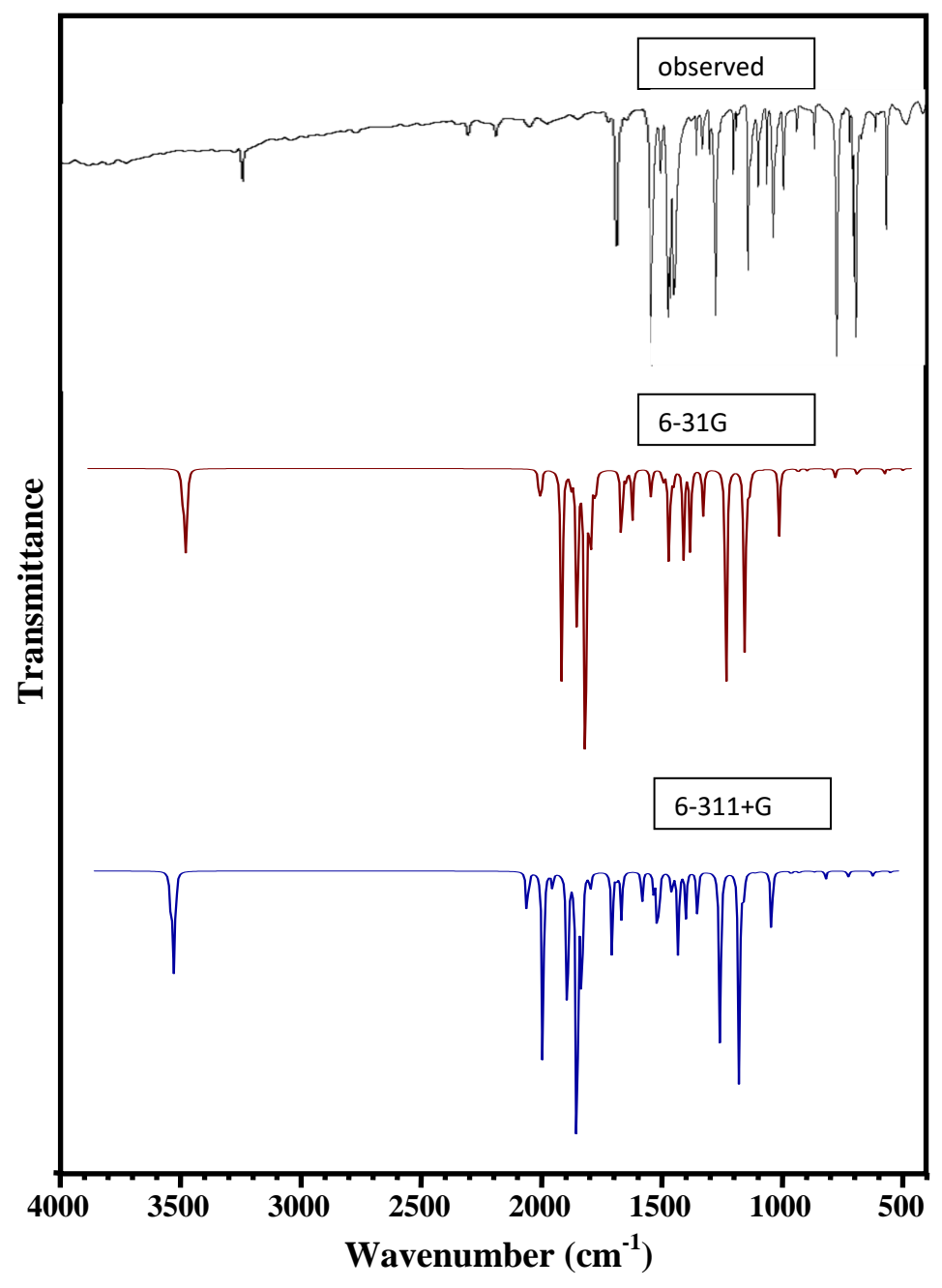


Fig. 6.5. Comparative representation of FT-IR spectra for 5-Chloro-1-phenyl-1H-tetrazole (5ClPTZ)

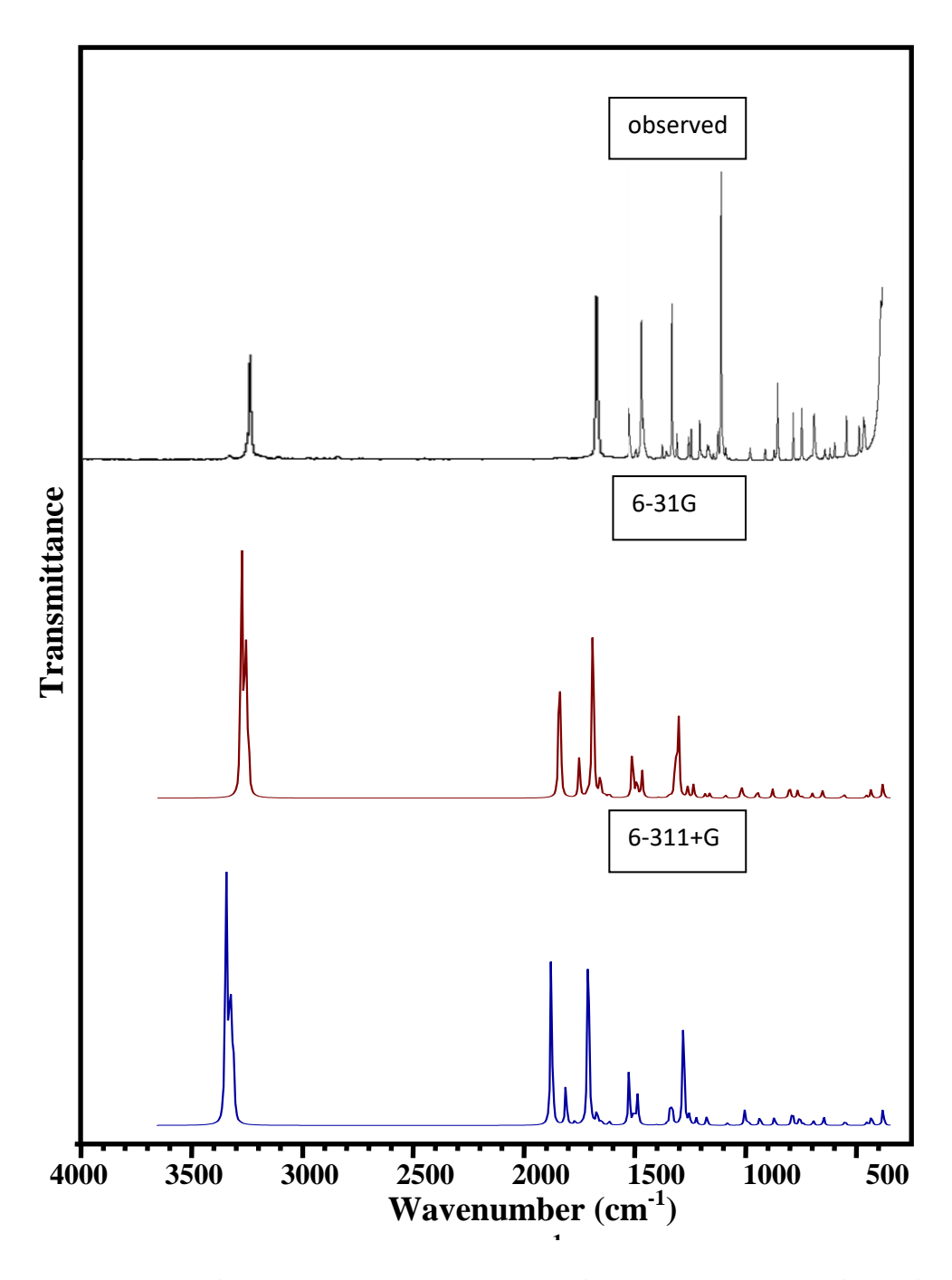


Fig. 6.6. Comparative representation of FT-Raman spectra for 5-Chloro-1-phenyl-1H-tetrazole (5ClPTZ)

The C-N stretching modes are reported in the range 1000–1400 cm⁻¹ [52] and in the present case these bands are assigned at 1418,1382 (6-31G) and 1387, 1347 (6-311+G) cm⁻¹ theoretically. 1431,1410 cm⁻¹ in IR and 1433 cm⁻¹ in Raman.

6.10 NATURAL BOND ANALYSIS

The Natural bond ortbital [55] analyzes is used to understand the delocalization of electron density and second order donor-acceptor energy. Typically, the stabilization of orbital interaction is high for higher energy differences between interacting orbitals. Effective donor and effective acceptor have this strong stabilization [56-59]. According to the second order perturbation approach, the stabilization energy is derived [60]. The energy from (donor) $i \rightarrow$ (acceptor) j is calculated as

$$E^{2} = \Delta E_{ij} = q_{i} \frac{F(i, j)^{2}}{\varepsilon_{i} - \varepsilon_{i}}$$

where, q_i is the donor orbital occupancy, ε_i , ε_j are diagonal elements (orbital energies) and F(i,j) is the off-diagonal NBO Fock matrix element. The NBO analysis gives valuable information about the intra and inters molecule interaction of the molecule [61].

The current work summarizes second order perturbative calculation donor-acceptor interactions based on NBO. This analysis was carried out by observing all possible interaction between lewis and non-lewis NBOs and calculated their stabilization energy (E2). Donor NBO (i), acceptor NBO (j) and stabilization energy (E2) are tabulated in Table 6.6. From this table, it is show that the interaction between the Antibonded N2-N3 (NBO 152) and N4-C5 antibond (NBO 155) gives the strongest

stabilization, 79.87 kcal/mol and also, antibond C7-C8 (NBO 158) \rightarrow C11-C12 antibond (NBO 168), antibond C7-C8 (NBO 158) \rightarrow C9-C10 antibond (NBO 163), lone pair N1 (NBO 40) \rightarrow N2-N3 antibond (NBO 152) has the highest stabilization energy are 72.4, 69.1, 20.72kcal/mol Respectively.`

6.11 CONCLUSION

The present investigation thoroughly analyzed the HOMO-LUMO, and vibration spectra, both infrared and Raman of 5CIPTZ molecules with B3LYP method with standard 6-31G and 6-311+G basis sets. All the vibration bands are observed in the FT-IR and FT-Raman spectra of the compound are assigned to various modes of vibration and most of the modes have wave numbers in the expected range. The complete vibration assignments of wave numbers are made on the basis of potential energy distribution (PED). The electrostatic potential surfaces (MEP) together with complete analysis of the vibration spectra, both IR and Raman spectra help to identify the structure and symmetry. The excellent agreement of the calculated and observed vibration spectra reveals the advantages over the other method. Finally, calculated HOMO-LUMO energies show that the charge transfer occurs in the molecule, which are responsible for the bioactive properly of the biomedical compound 5CIPTZ.

Table 6.1: Geometry Optimization Parameter of 5-Chloro-1-phenyl-1H-tetrazole (5ClPTZ) based on B3LYP/6-31G and B3LYP/6-311+G method and basis set

	BondLength(Å	7)	BondAngle(°)				
Atom	6-31G	6-311+G	Atom	6-31G	6-311+G		
C5-Cl6	1.76	1.76	C5-N1-C7	131.744	131.538		
N1-C7	1.43	1.43	N1-C5-C16	124.968	124.831		
N3-N4	1.40	1.40	N4-C5-C16	124.536	124.704		
C10-C11	1.40	1.40	N2-N1-C7	121.239	121.269		
C9-C10	1.40	1.40	C8-C7-C12	121.214	121.202		
N1-N2	1.40	1.40	C11-C12-H17	121.162	121.134		
C7-C8	1.40	1.40	C9-C8-H13	120.584	120.593		
C7-C12	1.40	1.40	C7-C8-H13	120.296	120.269		
C8-C9	1.40	1.40	C8-C9-C10	120.253	120.232		
C11-C12	1.40	1.40	C10-C9-H14	120.224	120.213		
N1-C5	1.36	1.36	C10-C11-H16	120.217	120.211		
N4-C5	1.33	1.32	C10-C11-C12	120.238	120.204		
N2-N3	1.32	1.32	C9-C10-C11	120.018	120.039		
C10-H15	1.09	1.08	N1-C7-C8	120.087	120.033		
C9-H14	1.08	1.08	C11-C10-H15	120.011	120.001		
C11-H16	1.08	1.08	C9-C10-H15	119.970	119.959		
C8-H13	1.08	1.08	C7-C12-H17	119.687	119.683		
C12-H17	1.08	1.08	C12-C11-H16	119.544	119.585		
			C8-C9-H14	119.519	119.551		
			C7-C12-C11	119.150	119.181		
			C7-C8-C9	119.118	119.134		
			N1-C7-C12	118.678	118.754		
			N2-N3-N4	110.949	110.785		
			N1-C5-N4	110.470	110.443		
			N2-N1-C5	107.004	107.178		
			N1-N2-N3	106.266	106.175		
			N3-N4-C5	105.311	105.419		

Table 6.2: HOMO-LUMO energy (eV) and other related properties of 5-Chloro-1-phenyl-1H-tetrazole (5ClPTZ) based on B3LYP/6-31G and B3LYP/6-311+G method and basis set

Parameters	6-31G	6-311+G (eV)	
rarameters	(eV)		
Homo(I)	-7.7852	-7.8532	
Lumo(A)	-2.0028	-1.9892	
Energy gap(ΔE)	5.7824	5.8641	
Electronegativity	4.8940	4.9212	
Global hardness	2.8912	2.9320	
Global softness(eV ⁻¹)	0.3459	0.3411	
Chemical potential	-4.8940	-4.9212	
Electriphilicity	4.1420	4.1299	

Table 6.3: Mulliken charge (charge/e) of 5-Chloro-1-phenyl-1H-tetrazole (5ClPTZ) based on B3LYP/6-31G and B3LYP/6-311+G method and basis set

A 4	6-31G	6-311+G				
Atom	Charge/e					
N1	-0.0142	-0.1162				
N2	0.0482	0.0448				
N3	-0.0734	-0.1347				
N4	-0.0431	-0.0923				
C5	-0.2643	-0.5233				
Cl6	0.3190	0.5174				
C7	-0.5227	-0.8294				
C8	-0.1844	-0.2327				
C9	-0.3151	-0.5296				
C10	-0.0595	0.0095				
C11	-0.1920	-0.3567				
C12	0.4169	0.8746				
H13	0.2016	0.2319				
H14	0.1899	0.2097				
H15	0.1873	0.2090				
H16	0.1906	0.2103				
H17	0.2117	0.2381				

Table 6.4: Dipole moment(μ), Polarizability(α), Anisotropy polaraizability($\Delta\alpha$) and First order polarizability(β_{tot}) of 5-Chloro-1-phenyl-1H-tetrazole (5ClPTZ) based on B3LYP/6-31G and B3LYP/6-311+G method and basis set

Parameters	6-31G	6-311+G
μ_{x}	-5.8148	-5.8211
μ_{y}	2.8346	2.7621
μ_{z}	-0.5722	-0.5609
α_{XX}	-81.805	-81.9707
α_{YY}	-80.4211	-80.7151
α_{ZZ}	-75.0133	-74.632
α_{XY}	5.8718	5.6262
$lpha_{ ext{XZ}}$	-0.2512	-0.202
$lpha_{ m YZ}$	6.3594	6.4021
eta_{XXX}	-85.5234	-85.3691
$oldsymbol{eta_{YYY}}$	31.8908	31.1578
eta_{ZZZ}	-1.4118	-1.2158
$oldsymbol{eta_{XYY}}$	-13.4878	-12.2542
$oldsymbol{eta_{XXY}}$	21.7629	21.499
eta_{XXZ}	-7.532	-7.3829
eta_{XZZ}	4.4195	3.4289
eta_{YZZ}	3.2261	3.0377
$oldsymbol{eta_{YYZ}}$	-7.1489	-7.2038
$oldsymbol{eta_{XYZ}}$	-7.499	-7.6444
μ(debye)	6.4941	6.4675
α(esu)	-11.7038 X10 ⁻²⁴	-11.7077 X10 ⁻²⁴
$\Delta \alpha(esu)$	141.8267 X10 ⁻²⁴	142.1401 X10 ⁻²⁴
$\beta_{tot}(esu)$	0.9636 X10 ⁻³⁰	0.9552 X10 ⁻³⁰

Table 6.5: Observed Frequency (cm⁻¹), Theoretical Frequency (cm⁻¹) and Vibrational assignment with PED(%) of 5-Chloro-1-phenyl-1H-tetrazole (5ClPTZ) based on B3LYP/6-31G and B3LYP/6-311+G method and basis set.

		Ol	oserved	Theoretical				X7:1
	cis	Frequency(cm ⁻¹)		Frequency(cm ⁻¹)				Vibrational
S.No.	Spe cis	FT-IR	FT-Raman	6	6-31G 6-311+G		Assignment	
				Calc	scaled	Calc	Scaled	(PED %)
1	A	-	-	3240	3096	3211	3166	ν CH(55)
2	A	-	-	3235	3091	3205	3160	ν CH(44)
3	A	-	-	3225	3081	3194	3150	ν CH(50)
4	A	-	3073	3215	3072	3185	3140	ν CH(72)
5	A	3065	-	3204	3062	3173	3129	ν CH(85)
6	A	1691	-	1651	1578	1639	1616	v CC(29)
7	A	-	1599	1642	1569	1629	1606	ν CC(44)
8	A	-	-	1552	1483	1545	1524	β HCC(36)
9	A	1502	1503	1511	1444	1503	1482	β HCC(32)
10	A	1431	1433	1443	1418	1439	1387	v NC(35)
11	A	1410	-	1406	1382	1397	1347	v NC(44)
12	A	1404	-	1384	1360	1376	1327	β HCC(22)
13	A	1339	-	1363	1340	1339	1291	v CC(62)
14	A	1267	1269	1251	1229	1245	1200	β NCN(18)
15	A	1244	-	1231	1209	1223	1179	β HCC(37)
16	A	1174	-	1223	1202	1215	1171	β HCC(61)
177	A	1124	1165	1202	1100	1202	1160	$v NN(65) + \beta$
17	A	1164	1165	1203	1182	1203	1160	CNN(16)
18	A	1116	1119	1123	1104	1114	1074	v CC(21)
19	A	1041	-	1071	1052	1064	1026	β CCC(27)

20	A	1015	-	1046	1028	1047	1010	β NNN(54)
21	A	1003	1004	1042	1024	1039	1002	β CCC(53)
22	A			1040	1022	1035	998	τ HCCC(50)+ τ
22	A	-	-	1040	1022	1033	990	CCCC(31)
23	A	-	-	1028	1010	1021	984	ν CC(61)
24	A	-	-	1018	1000	1017	980	τ HCCC(37)
25	A	975	-	983	966	992	957	v NN(39)
26	A	924	-	953	937	957	923	ν NN(19)
27	A	-		898	882	905	873	ν NCN(41)
28	A	853	-	876	860	877	873	τ HCCC(55)
29	A	755	-	799	785	803	774	τ HCCC(52)
30	A	-	-	718	705	718	696	τ CCCC(28)
31	A	714	-	717	710	717	694	τ CCCC(38)
32	A	702	-	709	697	701	676	β CCN(47)
33	A	696	699	696	684	696	671	δ NNNC(60)
34	A	612	614	644	633	643	620	τ CCC(46)
35	A	570	568	569	559	571	551	β NCCC(19)
36	A	490	-	487	479	483	465	ν ClC(45)
37	A	-	-	448	440	446	430	ν ClC(16)
38	A	-	-	427	420	428	413	ν CCCC(69)
39	A	-	-	377	370	379	365	β NCC(13)
40	A	-	327	327	322	327	315	τ CCCC(18)
11	٨		225	222	220	226	210	β ClCN(21)+ δ
41	A	-	235	232	228	226	218	CINNC(39)
42	A	-	-	222	218	220	212	β ClCN(20)
12	٨			115	112	111	110	β NCC(24)+ δ
43	A	-	-	115	113	114	110	NCNC(37)
44	A	-	-	92	90	91	88	β NNC(30)
45	A	-	-	34	33	34	33	δ NNCC(86)

Table 6.6: Natural Bond Orbital Calculation of 5-Chloro-1-phenyl-1H-tetrazole (5ClPTZ)

S.No Donor NBO (i)			AcceptorNBO (j)			E(2)	E(j)-E(i)	F(i,j)	
5.110	υ	OHOL	ADO (I)	A	Acceptor (1)		kcal/mol	a.u.	a.u.
1	152	BD*	N2-N3	155	BD*	N4-C5	79.87	0.02	0.059
2	158	BD*	C7-C8	168	BD*	C11-C12	72.4	0.01	0.062
3	158	BD*	C7-C8	163	BD*	C9-C10	69.1	0.01	0.063
4	40	LP	N1	152	BD*	N2-N3	20.72	0.33	0.075
5	40	LP	N1	155	BD*	N4-C5	19.44	0.34	0.074
6	8	BD	N4-C5	152	BD*	N2-N3	14.11	0.32	0.062
7	45	LP	Cl6	161	BD*	C8-H13	14.11	0.88	0.1
8	46	LP	Cl6	161	BD*	C8-H13	14.02	0.87	0.1
9	16	BD	C9-C10	158	BD*	C7-C8	11.82	0.28	0.052
10	21	BD	C11-C12	158	BD*	C7-C8	11.69	0.29	0.052
11	46	LP	Cl6	155	BD*	N4-C5	11.25	0.33	0.057
12	16	BD	C9-C10	168	BD*	C11-C12	11.1	0.3	0.051
13	40	LP	N1	158	BD*	C7-C8	10.92	0.41	0.062
14	21	BD	C11-C12	163	BD*	C9-C10	10.83	0.3	0.051
15	42	LP	N3	148	BD*	N1-N2	10.66	0.69	0.076
16	11	BD	C7-C8	168	BD*	C11-C12	10.39	0.32	0.051

Chapter - VII

Simulation of FT-IR and FT-Raman Spectra Based on quantum chemical Calculations, Vibrational Assignments, Hyperpolarizability, and Homo-Lumo Analysis of 5(4 methyl phenyl)tetrazole (5MPTZ)

Abstract

The spectra of 5(4 methyl phenyl) tetrazole (5MPTZ) have been recorded in the regions $4000-400 \text{ cm}^{-1}$ for FT-IR and $3500-100 \text{ cm}^{-1}$ for FT-Raman. The geometry optimization, vibrational frequencies were obtained by the density functional theory (DFT) using B3LYP method with 6-31G and 6-311+G basis sets. The complete assignments were performed on the basis of the potential energy distribution (PED) of the vibrational modes, calculated and the scaled values were compared with experimental FT-IR and FT-Raman spectra. The HOMO and LUMO energy gap reveals that the energy gap reflects the chemical activity of the molecule. The dipole moment (μ), polarizability (α), anisotropy polarizability ($\Delta \alpha$) and first hyperpolarizability (β_{tot}) of the molecule have been reported. Information about the size, shape, charge density distribution and site of chemical reactivity of the molecule has been obtained by molecular electrostatic potential (MEP).

Chapter-VII

Simulation of FT-IR and FT-Raman Spectra Based on quantum chemical Calculations, Vibrational Assignments, Hyperpolarizability, and Homo-Lumo Analysis of 5(4 methyl phenyl)tetrazole (5MPTZ)

7.1 INTRODUCTION

Tetrazole-related molecules have attracted considerable attention due to their biological activities. The synthesis of new members of this family of ligands is an important direction in the development of modern coordination chemistry [110,111]. Tetrazole compounds have a wide range of applications in coordination chemistry, medicinal chemistry and material science[112,113]. Tetrazole derivatives are used as antibiotics and optically active tetrazole-containing antifungal preparations of azole type was reported. There is always a need for new and effective antifungal and antibacterial agents with broad-spectrum activities. It was decided to develop this interest by ascertaining the molecules features essential for activity and utilizing them to develop a new class of potential drugs[114].

The dertailed investigations of the **5(4 methyl phenyl)tetrazole (5MPTZ)** were carried out with Gaussian 09 software package [115] using the Beeke-3-Lee-Yang-Parr (B3LYP) functional[19,20] supplemented with the standard 6-31G and 6-311+G basis set.

7.2 EXPERIMENTAL DETAILS

The fine sample of **5(4 methyl phenyl)tetrazole** (**5MPTZ**) was obtained from Lancaster Chemical Company.UK, with a stated purity of 99% and it was used as such without further purification.The FT-Raman Spectrum of 5MPTZ was recorded using 1064 nm line of ND: YAG laser for excitation wavelength in the region 3500-100 cm⁻¹ on Thermo Electron Corporation model Nexus spectrometer equipped with FT-Raman module accessory. The FT-IR Spectrum of the title compound was recorded in the region 4000-400 cm⁻¹ on Perking Elmer Spectrophotometer in KBr pellet.

7.3 COMPUTATIONAL DETAILS

The combination of Vibration spectra with quantum chemical calculation is effective for understanding the fundamental mode of vibration of the compound. The structural characteristic, stability and energy of the compound under investigation are determined by DFT with the three-parameter hybrid functional (B₃) for the exchange part and the Becke Three Lee Yong-Pare (LYP) and 6-31G ,6-311+G basis sets with Gaussian 09 Program Package. The Cartesian representation of the theoretical force constants has been compound at the fully optimized geometry by assuming the molecule belongs to C₁ point group symmetry. The Transformation of force field from Cartesian to internal local symmetry coordinates, the scaling, and the subsequent normal coordinate analysis (NCA) Calculation of potential energy distributions (PED) has been done on a PC with the VEDA program.

7.4 GEOMETRICAL PARAMETER

The molecular structure along with numbering of atoms of 5(4 methyl phenyl)tetrazole (5MPTZ) was as shown in the Fig 7.1. The Global minimum energies of the title molecule calculated by Density Functional Theory structure optimization for different basis sets such as B3LYP/6-31+ G(d,p), B3LYP/6-31++ G(d,p), B3LYP/6-311+ G(d,p) and B3LYP/6-311++ G(d,p) are given in Table 7.1. Geometry optimization is the procedure that attempts to find the configuration of minimum energy of the molecule. The procedure calculates the wave function and the energy at a starting geometry and then proceeds to search a new geometry of a lower energy. This is repeated until the lowest energy geometry is found. The procedure calculates the force on each atom by evaluating the gradient or the first derivative of the energy with respect to atomic positions. Sophisticated algorithms are then used at each step to select a new geometry, aiming for rapid convergence to the geometry of the lowest energy. In the final, minimum energy geometry the force on each atom is zero. The optimized geometric parameters like bond length, bond angles of 5(4 methyl phenyl)tetrazole (5MPTZ) were calculated and given in Table 7.1.

The title compound is a tetrazole ligand with a toluene substituent in position 5 (Fig. 7.1). In the solid state structure the molecule possesses crystallographic mirror symmetry, with four C atoms lying on the reflecting plane, which bisects the phenyl and tetrazole rings[116]. The C-C bond lengths in the benzene ring obtained from B3LYP ranges from 1.41 to 1.40 Å and C-H bond length ranges from 1.09 to 1.08 Å. The C-N

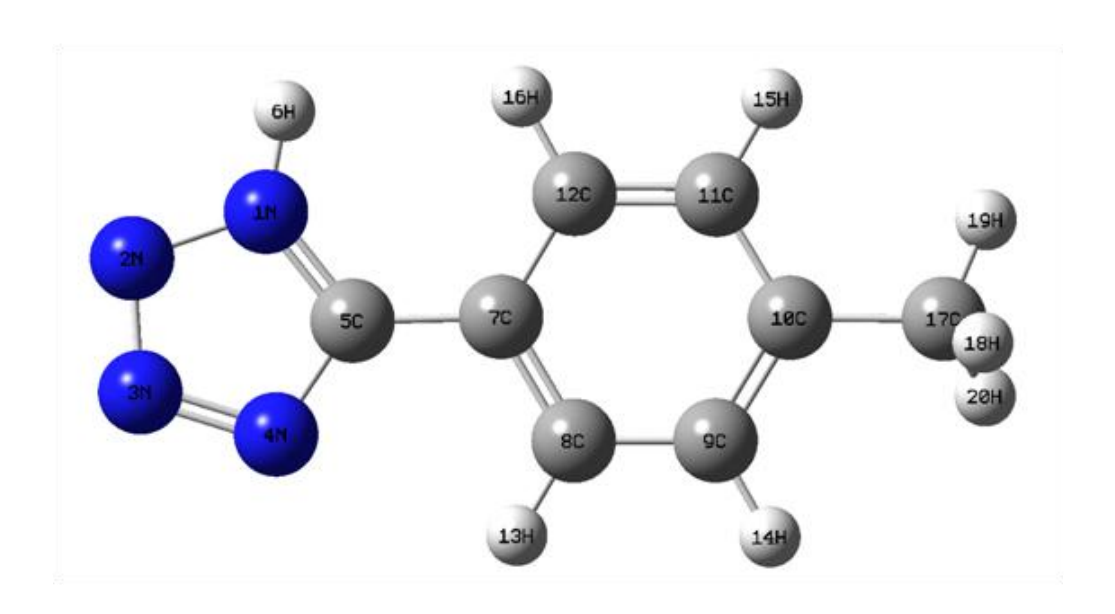


Fig. 7.1. The theoretical geometry structure and atomic numbering scheme of 5(4 methyl phenyl)tetrazole (5MPTZ)

bond lengths in the tetrazole ring have calculated as 1.36 and 1.35 Å. the N1-N2 and N3-N4 bond length of the tetrazole ring has longer than the N2-N3 bond length in the same ring.the C-H bond lenths of the methyl group were 1.10-1.09 Å. The bond angle of the phenyl ring does not have equal value .it varied from 118° to 121°. All the values were compared with experimental values[9], those are good agreement with each other.

7.5 ELECTRONIC PROPERTIES

When we are dealing with interacting molecular orbitals, the two that interact are generally The Highest energy Occupied Molecular Orbital (HOMO) of one molecule, The Lowest energy Unoccupied Molecular Orbital (LUMO) of the other molecule. These orbitals are the pair that lie closest in energy of any pair of orbitals in the two molecules, which allows them to interact most strongly. These orbitals are sometimes called the frontier orbitals, because they lie at the outermost boundaries of the electrons of the molecules. The energy gap between the HOMOs and LUMOs called as energy gap. It is a critical parameter in determining molecular electrical transport properties because it is a measure of electron conductivity [76]. The HOMO energy characterizes the ability of electron giving, the LUMO characterizes the ability of electron accepting, and the gap between HOMO and LUMO characterizes the molecular chemical stability [117]. Surfaces for the frontier orbital's were drawn to understand the bonding scheme of present compound. The features of these Molecular Orbitals can be seen in Figure 7.2.

<u>6-31G</u> <u>6-311+G</u>

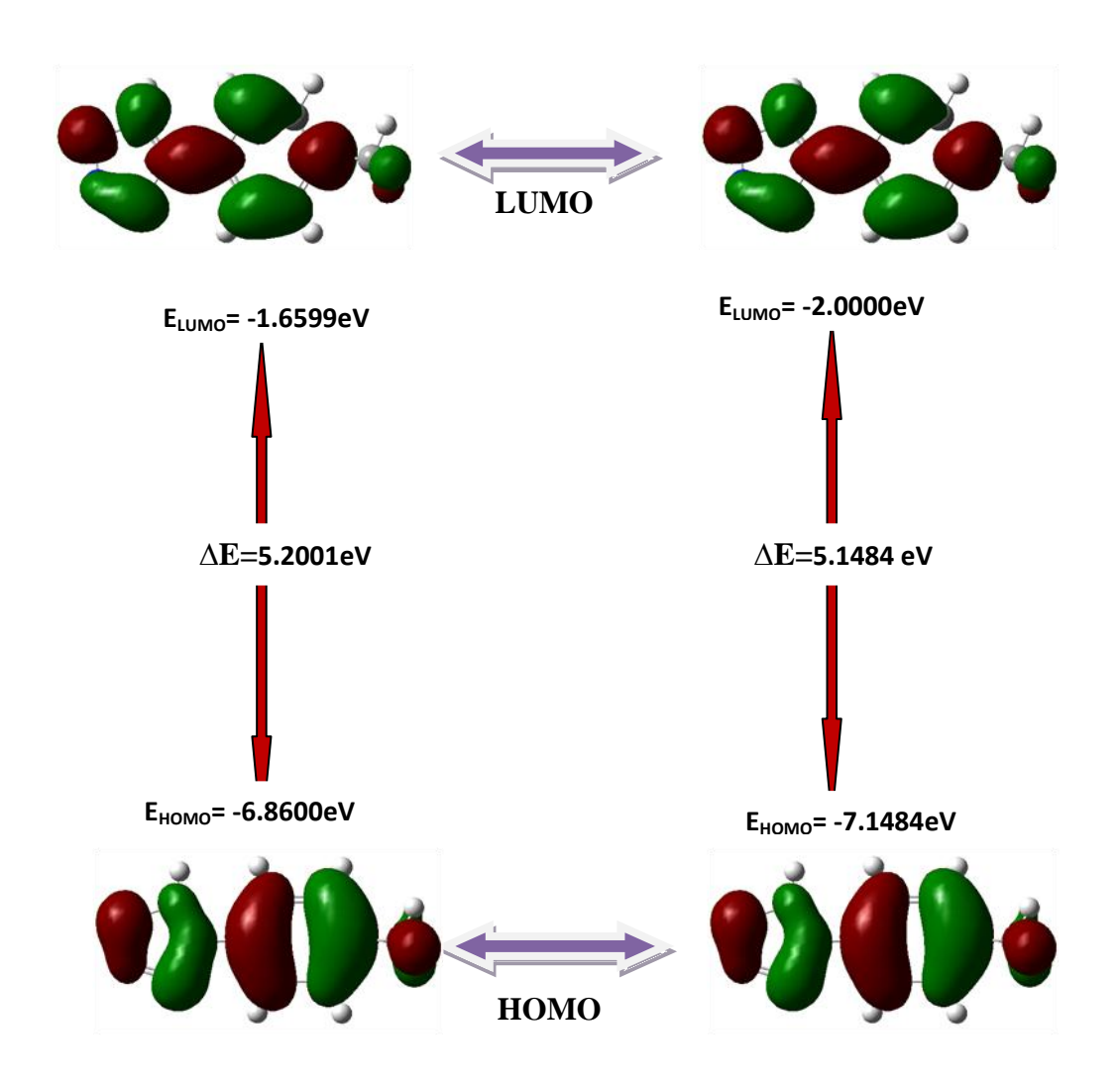


Fig. 7.2: The atomic orbital compositions of the frontier molecular orbital for 5(4 methyl phenyl)tetrazole (5MPTZ)

This electronic absorption corresponds to the transition from the ground state to the first excited state and is mainly described by one electron excitation from HOMO to LUMO. While the energy of the HOMO is directly related to the ionization potential, LUMO energy is directly related to the electron affinity. There are lots of applications available for the use of HOMO and LUMO energy gap as a quantum chemical descriptor. It establishes correlation in various chemical and bio-chemical systems [118]. The HOMO–LUMO energy gap is an important value for stability index. A large HOMO–LUMO gap implies high stability for the molecule in the sense of its lower reactivity in chemical reactions [119]. According to B3LYP calculation, EHOMO, ELUMO and the energy band gap (translation from HOMO to LUMO) of the title molecule in electron Volt are presented in Table 7.2.

Considering the chemical hardness, large HOMO-LUMO gap represent a hard molecule and small HOMO-LUMO gap represent a soft molecule. From the Table 7.2, it is clear that the molecule under investigation is very soft since it has a small HOMO-LUMO gap and also having a high value for softness.

7.6 NLO PROPERTIES

The NLO activity provide the key functions for frequency shifting, optical modulation, optical switching and optical logic for the developing technologies in areas such as communication, signal processing and optical interconnections [107]. The first static hyperpolarizability (β tot) and its related properties (β , α and $\Delta\alpha$) have been calculated using B3LYP/6-31G and 6-311+G level based on finite field approach. In the

presence of an applied electric field, the energy of a system is a function of the electric field and the first order hyperpolarizability is a third rank tensor that can be described by a $3\times3\times3$ matrix. The 27 components of the 3D matrix can be reduced to 10 components because of the Kleinman symmetry [86]. The matrix can be given in the lower tetrahedral format. It is obvious that the lower part of the $3\times3\times3$ matrices is a tetrahedral.

The values of the polarizabilities (α) and first hyperpolarizability (β tot) of the Gaussian 09 output are reported in atomic units (a.u.). All the calculated values then have been converted into electrostatic units (esu). (For α : 1a.u. = 0.1482 × 10⁻²⁴ esu; For β : 1a.u. = 8.639 ×10⁻³³ esu). The total molecular dipole moment and first order hyperpolarizability are 7.0628 and 7.2331 Debye and 1.1830x10⁻³⁰ and 1.241010⁻³⁰ esu , respectively and are depicted in Table 7.4.Total dipole moment of title molecule is greater than that of urea and first order hyperpolarizability is very much greater than that of urea (μ and β of urea are 1.3732 Debye and 0.3728×10⁻³⁰ esu) obtained by B3LYP/6-31G and 6-311+G method. This result indicates the nonlinearity of the title molecule.

7.7 MULLIKEN ATOMIC CHARGE

Atomic charges has been used to describe the process of electronegativety equalization and charge transfer in chemical reactions [120,121]. Mulliken atomic charge calculation has an important role in the application of quantum chemical calculation to molecular system because atomic charges affect dipole moment, molecular polarizability, electronic structure and a lot of properties of electronic systems. The Mulliken atomic

charges are calculated at B3LYP/6-31G and 6-311+G level by determining the electron population of each atom as defined by the basis function and collected in Table7. 3.

A Graph of Mulliken atomic charge on individual atom of 5MPTZ was drawn and given in Figure 7.4. It is worthy to mention that N3, N4 and C8, C9, C11and C12, C17 atoms of the title molecule exhibit negative charge where all hydrogen atoms exhibit positive charges.

7.8 MOLECULAR ELECTROSTATIC POTENTIAL

The molecular electrostatic potential is the potential that a unit positive charge would experience at any point surrounding the molecule due to the electron density distribution in the molecule. The electrostatic potential generated in space by charge distribution is helpful to understand the electrophilic and nucleophilic regions in the title molecule. Electrostatic potential maps, also known as electrostatic potential energy maps, or molecular electrical potential surfaces, illustrate the charge distributions of molecules three dimensionally. Knowledge of the charge distributions can be used to determine how molecules interact with one another. Molecular electrostatic potential (MEP) mapping is very useful in the investigation of the molecular structure with its physiochemical property relationships [122-125].In the electrostatic potential map, the semispherical blue shapes that emerge from the edges of the above electrostatic potential map are hydrogen atoms.

The molecular electrostatic potential surface (MEPS) which is a 3D plot of electrostatic potential mapped onto the iso electron density surface simultaneously

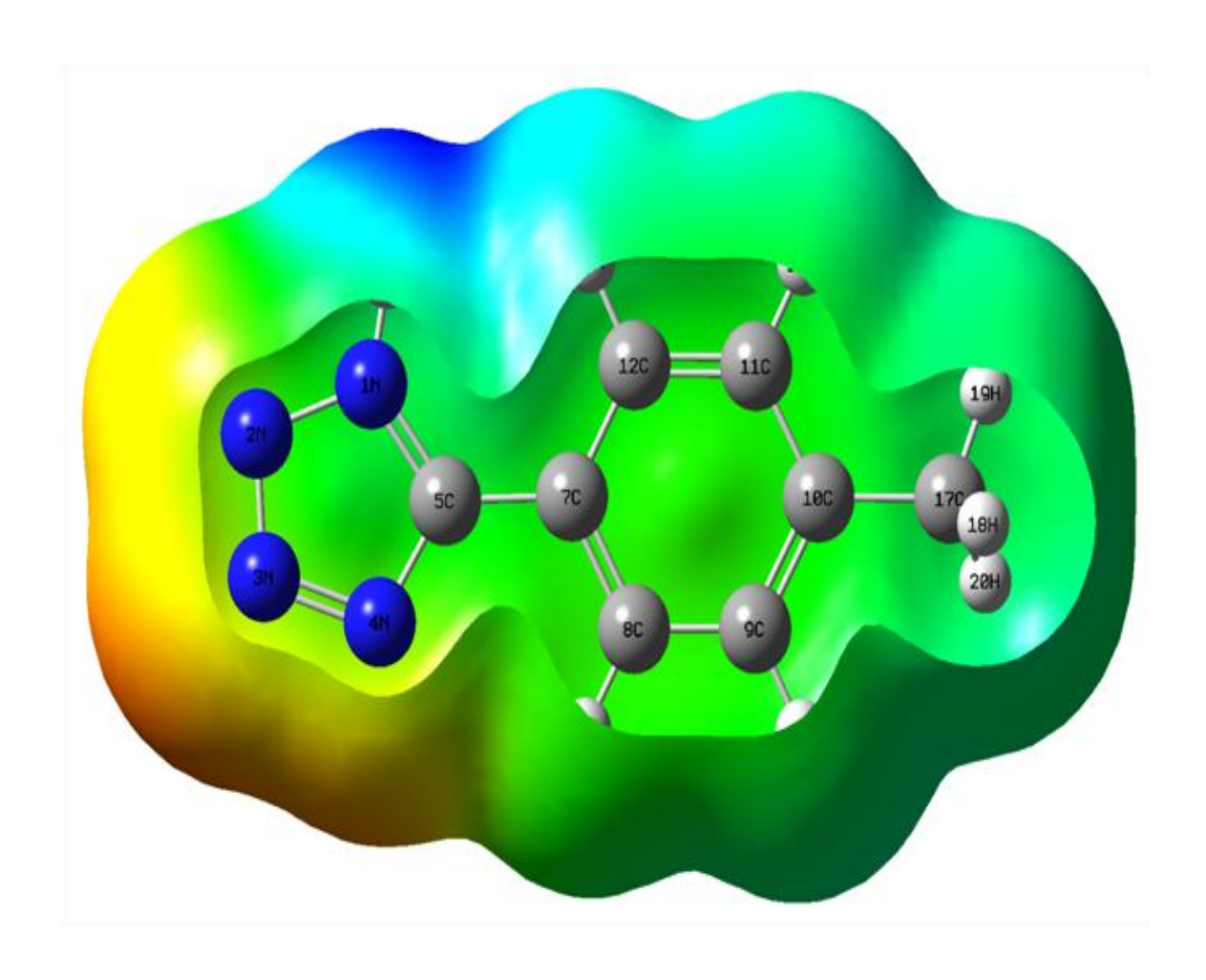


Fig. 7.3. The total electron density surface mapped with of 5(4 methyl phenyl)tetrazole (5MPTZ)

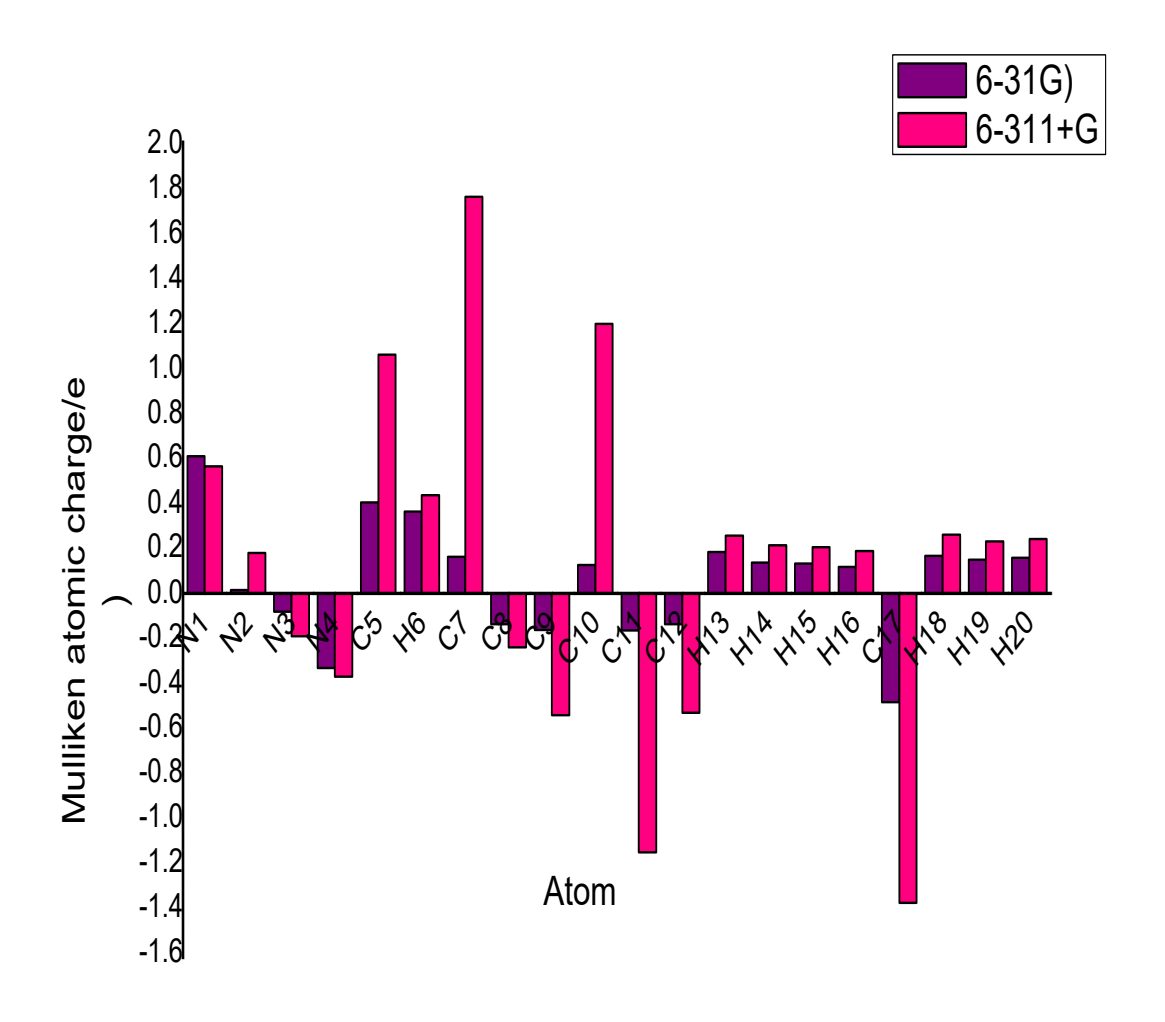


Fig. 7.4 Bar diagram representing the Mulliken atomic charge distribution of 5(4 methyl phenyl)tetrazole (5MPTZ)

_

displays molecular shape, size and electrostatic potential values. The Electrostatic potential surface of 5MPTZ is shown in Figure 7.4.

The colour scheme for the MEPS surface is red - electron rich or partially negative charge; blue - electron deficient or partially positive charge; light blue-slightly electron deficient region; yellow–slightly electron rich region, respectively. Areas of low potential, red, are characterized by an abundance of electrons. Areas of high potential, blue are characterized by a relative absence of electrons. That is negative potential sites are on the electronegative atoms like nitrogen while the positive potential sites around the hydrogen and carbon atoms. Green area covers parts of the molecule where electrostatic potentials are nearly equal to zero. This is a region of zero potential enveloping the π systems of aromatic ring leaving a more electrophilic region in the plane of hydrogen atom. Nitrogen has a higher electronegativity value would consequently have a higher electron density around them. Thus the spherical region that corresponds to nitrogen atom would have a red portion on it. The MEPS of 5MPTZ clearly indicates the electron rich centers of nitrogen atom.

7.9 VIBRATIONAL ASSIGNMENT

Vibrational spectroscopy has been shown to be effective in the identification of functional groups of organic compounds as well as in studies on molecular conformations and reaction kinetics [126] The symmetry possessed by the title molecule helps to determine and classify the actual number of fundamental vibrations of the system. The observed spectrum is explained on the basis of C1 point group symmetry. The title

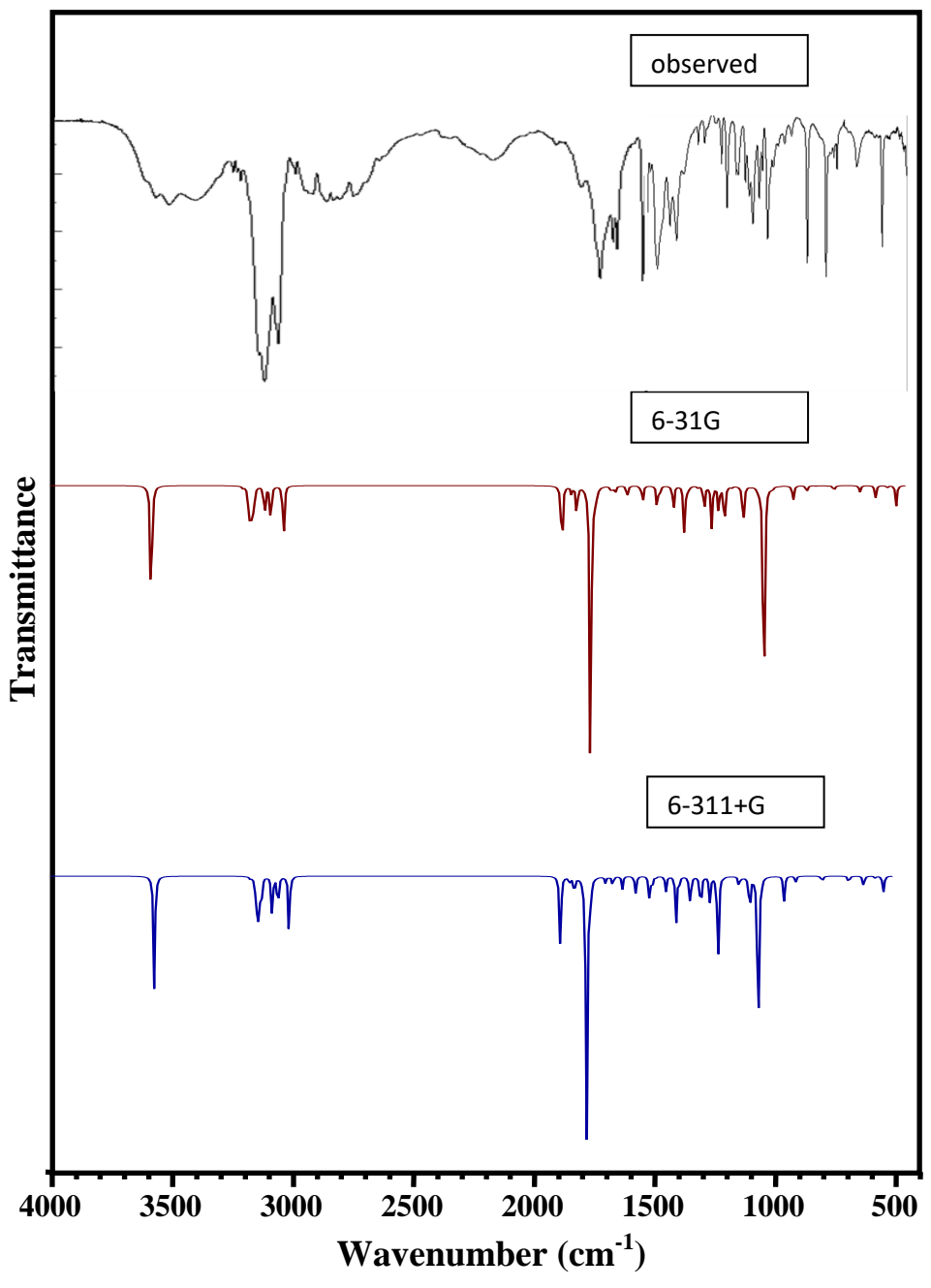


Fig 7.5. Comparative representation of FT-IR spectra for 5(4 methyl phenyl)tetrazole (5MPTZ))

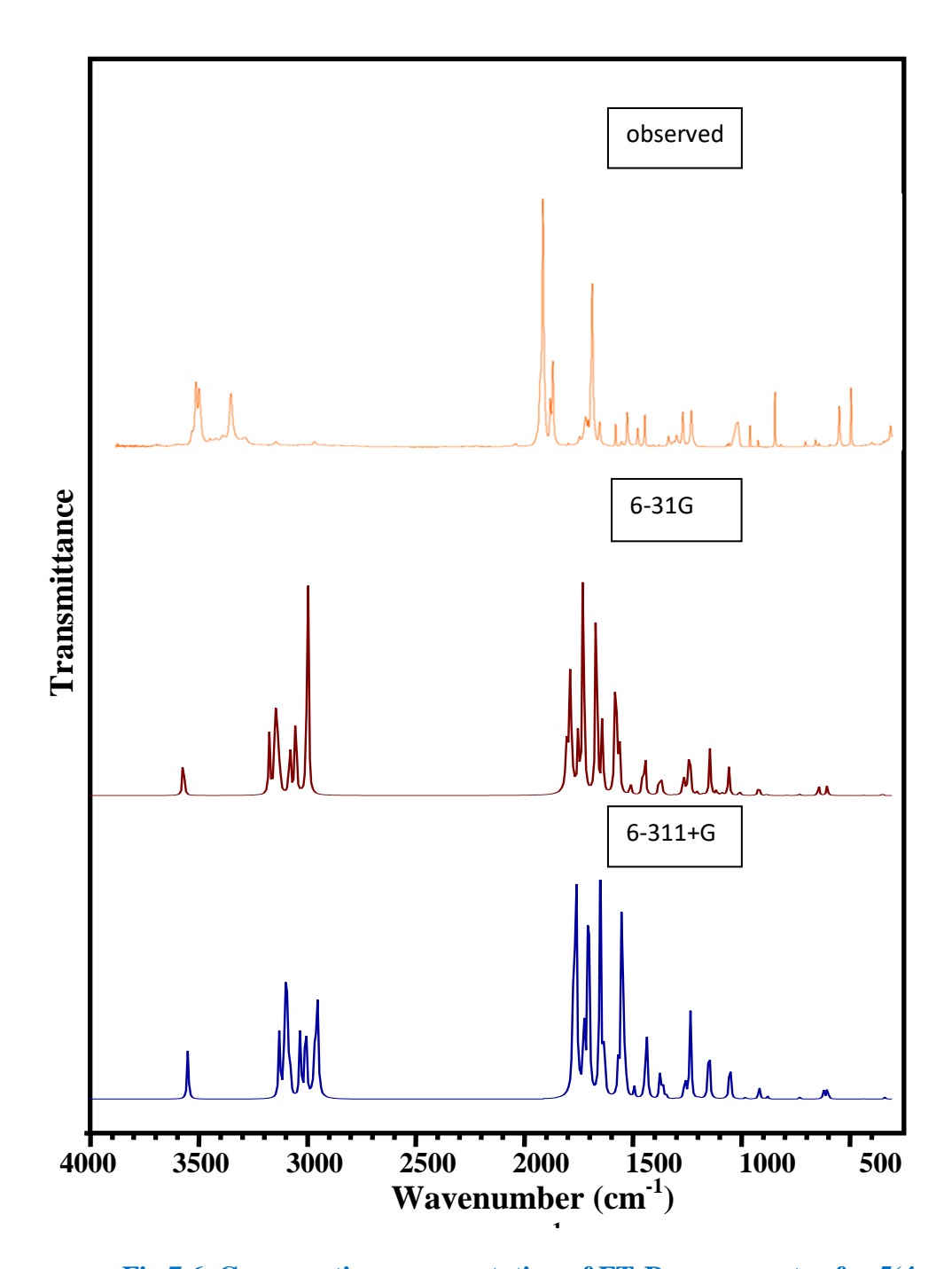


Fig 7.6. Comparative representation of FT-Raman spectra for 5(4 methyl phenyl)tetrazole (5MPTZ)

molecule consists of 20 atoms, which undergo 36 normal modes of vibrations . The total number of 54 fundamental vibrations (3N-6, where N is the number of atoms) are distributed as Γ vib = 37 A' (In plane vibrations;2N-3) 17 A''(out of plane vibrations;N-3) All vibrations are active both in Raman and infrared absorption. The detailed vibrational assignment of fundamental modes of 5MPTZ along with the calculated IR and Raman frequencies, normal mode descriptions using PED (Potential Energy Distribution) are reported in Table 7.5. The calculated frequencies are usually higher than the corresponding experimental quantities, due to the combination of electron correlation effects and basis set deficiencies.

C-H vibrations: The presence of C-H stretching vibrations in the region 3000 – 3200 cm⁻¹ is common for heteroaromatic structure. In the present study the C-H stretching vibrations of the title compound are observed at 3082 and 3045 cm⁻¹ in the FT-IR spectrum and 3050cm⁻¹ in the FT-Raman spectrum. The calculated wave numbers at 3097, 3067, 3058, 3044 cm⁻¹ are assigned to C-H stretching vibrations. The C-H out of plane bending vibrations are occurring in the region 900-667 cm⁻¹ [127].In the present investigation the computed wave numbers at 1073,1009,1008 are assigned to C-H out of plane vibrations and the scaled values are in good agreement with the experimental values. The assignments of other in-plane and out-of-plane C-H bending vibrations are as shown in Table 7.5.

Ring vibrations: There are six equivalent C-C bonds in benzene and consequently there will be six C-C stretching vibrations. In addition, there are several C-C-C in-plane and out-of-plane bending vibrations of the ring carbons. However, due to high symmetry

of benzene, many modes of vibrations are infrared inactive. In general, the bands around 1400 to 1650 cm⁻¹ in benzene derivatives are assigned to skeletal stretching C-C bands[128]. In the case of title compound the carbon stretching vibrations have been observed at 1613,1580,1505 cm⁻¹ in the FT-IR spectrum and 1630.1595 cm⁻¹ in FT-Raman spectrum were assigned to C-C stretching vibration which show good agreement with scaled frequencies. The measured wavenumbers at 1603, 1558, 1533 cm⁻¹ are assigned to C-C stretching vibrations. It is clear from the above values that the difference between observed and scaled frequencies is very small. In general, the C-C-C out-of-plane and in-plane-bending vibrational wavenumber observed in FTIR spectrum and FT-Raman spectrum shows good agreement with theoretically computed wavenumber.

C-N Vibrations: The mixing of several bands are possible in this region. The C-N stretching frequency is a rather difficult task. In the present study the band observed at 1285,1116 cm⁻¹ in FT-IR spectrum is attributed to C-N bending vibration. The theoretically calculated value of corresponding C-N bending vibration is predicted at 1298,1131 cm⁻¹. B3LYP computation gives mode arising from the N-N stretching at 1158,1147 cm⁻¹ corresponding to the peak at 1187,1163 cm⁻¹ in IR spectrum.

The methyl group CH stretching vibrational frequency band is found in 5MPTZ at 2924, 2910 cm⁻¹ respectively, in the FT-Raman, FT-IR spectrum. The CH stretching mode for methyl is in the zone of 3000-2800 cm⁻¹ [129,130].theoretically found at 2994, 2965, 2906 cm⁻¹.

7.10 NATURAL BOND ANALYSIS

The Natural bond ortbital [55] analyzes is used to understand the delocalization of electron density and second order donor-acceptor energy. Typically, the stabilization of orbital interaction is high for higher energy differences between interacting orbitals. Effective donor and effective acceptor have this strong stabilization [56-59]. According to the second order perturbation approach, the stabilization energy is derived [60]. The energy from (donor) $i \rightarrow$ (acceptor) j is calculated as

$$E^{2} = \Delta E_{ij} = q_{i} \frac{F(i, j)^{2}}{\varepsilon_{i} - \varepsilon_{i}}$$

Where, q_i is the donor orbital occupancy, ε_i , ε_j are diagonal elements (orbital energies) and F(i,j) is the off-diagonal NBO Fock matrix element. The NBO analysis gives valuable information about the intra and inters molecule interaction of the molecule [61].

The current work summarizes second order perturbative calculation donor-acceptor interactions based on NBO. This analysis was carried out by observing all possible interaction between lewis and non-lewis NBOs and calculated their stabilization energy (E2). Donor NBO (i), acceptor NBO (j) and stabilization energy (E2) are tabulated in Table 7.6. From this table, it is show that the interaction between the Antibonded C7-C12 (NBO 110) and C10-11 antibond (NBO 117) gives the strongest stabilization, 275.79 kcal/mol and also, antibond C7-C12 (NBO 110) \rightarrow C8-C9 antibond (NBO 112), antibond N4-C5 (NBO 106) \rightarrow C7-C12 antibond (NBO 110), lone pair N1 (NBO 39) \rightarrow N4-C5 antibond (NBO 106) has the highest stabilization energy are 212.8, 69.47, 50.93kcal/mol Respectively.`

7.11 CONCLUSION

The present investigation thoroughly analyzed the HOMO-LUMO, and vibration spectra, both infrared and Raman of 5MPTZ molecules with B3LYP method with standard 6-31G and 6-311+G basis sets. All the vibration bands are observed in the FT-IR and FT-Raman spectra of the compound are assigned to various modes of vibration and most of the modes have wave numbers in the expected range. The complete vibration assignments of wave numbers are made on the basis of potential energy distribution (PED). The electrostatic potential surfaces (MEPS) together with complete analysis of the vibration spectra, both IR and Raman and help to identify the structure and symmetry. The excellent agreement of the calculated and observed vibration spectra reveals the advantages over the other method. Finally, calculated HOMO-LUMO energies show that the charge transfer occurs in the molecule, which are responsible for the bioactive properly of the biomedical compound 5MPTZ.

Table 7.1: Geometry Optimization Parameter of 5(4 methyl phenyl)tetrazole (5MPTZ) based on B3LYP/6-31G and B3LYP/6-311+G method and basis set.

Во	ondLength(Å)		BondAngle(°)					
Atom	6-31G	6-311+G	Atom	6-31G	6-311+G			
C10-C17	1.51	1.51	C5-N1-H6	131.076	131.348			
C5-C7	1.46	1.46	N1-C5-C7	126.995	126.910			
C7-C8	1.41	1.41	N4-C5-C7	125.406	125.550			
C9-C10	1.41	1.41	C5-C7-C12	122.300	122.211			
C7-C12	1.41	1.40	C8-C9-C10	121.259	121.342			
C10-C11	1.40	1.40	C11-C10-C17	121.104	121.250			
C11-C12	1.40	1.39	C10-C11-C12	121.068	121.120			
N3-N4	1.39	1.39	C9-C8-H13	120.957	120.821			
C8-C9	1.39	1.39	C9-C10-C17	120.797	120.776			
N1-N2	1.39	1.39	C7-C12-H16	120.709	120.758			
N1-C5	1.36	1.36	C7-C12-C11	120.464	120.543			
N4-C5	1.35	1.34	C7-C8-C9	120.287	120.345			
N2-N3	1.32	1.32	N2-N1-H6	119.550	119.503			
C17-H18	1.10	1.09	C10-C11-H15	119.469	119.410			
C17-H20	1.10	1.09	C12-C11-H15	119.463	119.377			
C17-H19	1.09	1.09	C10-C9-H14	119.396	119.248			
C12-H16	1.09	1.08	C8-C9-H14	119.345	119.130			
C9-H14	1.09	1.08	C5-C7-C8	118.874	119.110			
C11-H15	1.09	1.08	C11-C12-H16	118.826	118.897			
C8-H13	1.08	1.08	C8-C7-C12	118.826	118.678			
N1-H6	1.01	1.00	C7-C8-H13	118.756	118.637			
			C9-C10-C11	118.095	117.972			
			C10-C17-H19	111.510	111.460			
			C10-C17-H20	111.392	111.377			

C10-C17-H18	111.099	111.138
N2-N3-N4	110.866	110.610
N2-N1-C5	109.374	109.523
H19-C17-H20	108.043	107.892
N1-C5-N4	107.599	107.584
H18-C17-H19	107.485	107.541
H18-C17-H20	107.106	107.188
N3-N4-C5	106.612	106.712
N1-N2-N3	105.549	105.614

Table 7.2: HOMO-LUMO energy (eV) and other related properties of 5(4 methyl phenyl)tetrazole (5MPTZ) based on B3LYP/6-31G and B3LYP/6-311+G method and basis set

Parameters	6-31G	6-311+G
rarameters	(eV)	(eV)
Homo(I)	-6.8600	-7.1484
Lumo(A)	-1.6599	-2.0000
Energy gap(ΔE)	5.2001	5.1484
Electronegativity	4.2599	4.5742
Global hardness	2.6000	2.5742
Global softness(eV ⁻¹)	0.3846	0.3885
Chemical potential	-4.2599	-4.5742
Electriphilicity	3.4898	4.0641

Table 7.3: Mulliken charge (charge/e) of 5(4 methyl phenyl)tetrazole (5MPTZ) based on B3LYP/6-31G and B3LYP/6-311+G method and basis set.

Atom	6-31G	6-311+G				
Atom —	Charge/e					
N1	0.6088	0.5648				
N2	0.0148	0.1788				
N3	-0.0822	-0.1907				
N4	-0.3317	-0.3710				
C5	0.4033	1.0604				
Н6	0.3623	0.4352				
C7	0.1626	1.7626				
C8	-0.1369	-0.2400				
C9	-0.1635	-0.5421				
C10	0.1262	1.1972				
C11	-0.1665	-1.1517				
C12	-0.1386	-0.5323				
H13	0.1839	0.2560				
H14	0.1362	0.2139				
H15	0.1321	0.2051				
H16	0.1165	0.1870				
C17	-0.4836	-1.3766				
H18	0.1660	0.2596				
H19	0.1497	0.2312				
H20	0.1582	0.2416				

Table 7.4: Dipole moment(μ), Polarizability(α), Anisotropy polaraizability($\Delta\alpha$) and First order polarizability(β_{tot}) of 5(4 methyl phenyl)tetrazole (5MPTZ) based on B3LYP/6-31G and B3LYP/6-311+G method and basis set.

Parameters	6-31G	6-311+G
μ_{x}	6.0797	6.2633
$\mu_{ m y}$	3.5941	3.6175
μ_{z}	0.0489	0.0429
$\alpha_{ ext{XX}}$	-82.6947	-84.9573
α_{YY}	-63.8621	-65.4107
α_{ZZ}	-71.5172	-73.5735
α_{XY}	-9.0345	-9.1645
$\alpha_{\rm XZ}$	0.1748	0.0651
α_{YZ}	-0.0015	-0.0182
$oldsymbol{eta_{XXX}}$	130.0165	135.7744
$oldsymbol{eta_{YYY}}$	20.1929	21.203
β_{ZZZ}	0.5809	0.4321
eta_{XYY}	7.982	9.1765
eta_{XXY}	17.6595	17.3876
eta_{XXZ}	0.708	0.462
eta_{XZZ}	-6.36	-6.5217
β_{YZZ}	-0.1262	-0.2017
$oldsymbol{eta_{YYZ}}$	-0.3797	-0.2368
$oldsymbol{eta_{XYZ}}$	-0.0077	-0.0152
μ(debye)	7.0628	7.2331
α(esu)	-10.7583 X10 ⁻²⁴	-11.0478 X10 ⁻²⁴
$\Delta \alpha(esu)$	144.1678 X10 ⁻²⁴	148.1296 X10 ⁻²⁴
$\beta_{tot}(esu)$	1.1830 X10 ⁻³⁰	1.2410 X10 ⁻³⁰

Table 7.5: Observed Frequency (cm⁻¹), Theoretical Frequency (cm⁻¹) and Vibrational assignment with PED(%) of 5(4 methyl phenyl)tetrazole (5MPTZ) based on B3LYP/6-31G and B3LYP/6-311+G method and basis set.

	Ol	oserved		Theo	retical		
Se Freque	Frequ	ency(cm ⁻¹)		Frequen	ncy(cm	⁻¹)	Vibrational assignment
	ET ID	FT-Raman	6-31G		6-3	11+G	(PED %)
	r 1-Kaman	Calc	scaled	Calc	Scaled		
A	3407	-	3710	3524	3687	3502	ν NH(100)
A	3082	-	3241	3097	3206	3046	ν CH(95)
A	-	-	3210	3067	3176	3018	ν CH(73)
A	-	3050	3201	3058	3165	3007	ν CH(93)
A	3045	-	3186	3044	3153	2995	ν CH(75)
A	-	-	3134	2994	3097	2942	ν CH(69)
A	2924	-	3103	2965	3069	2915	ν CH(47)
A	-	2910	3041	2906	3013	2862	ν CH(58)
A	1613	1630	1678	1603	1656	1574	ν CC(29)
A	1580	1595	1631	1558	1611	1530	ν CC(27)
A	1505	-	1605	1533	1587	1508	ν CC(18)
A	1458	-	1539	1471	1528	1452	β HNN(10)+ β HCC(11)
A	-	-	1536	1468	1527	1451	β HCH(28)
A	-	-	1533	1464	1524	1448	β HCH(39)+ τ HCCC(14)
A	-	-	1477	1451	1460	1435	ν CC(17)+ $β$ HCC(10)
A	1404	1400	1464	1438	1454	1429	β HCH(43)
A	1377	-	1396	1372	1384	1360	β HCC(21)
A	-	-	1378	1354	1365	1341	β HNN(19)+v CC(14)
A	-	1310	1370	1346	1348	1325	β HNN(35)
A	1285	-	1321	1298	1302	1279	ν NC(33)+ν CC(16)

A	1258	1250	1258	1237	1247	1225	ν CC(39)+β HCC(12)
A	-	1217	1247	1226	1237	1215	β HCC(27)+ β HCC(11)
	1187	1196					β HNN(19)+ β HCC(12) + ν
A	110/	1190	1178	1158	1172	1151	NN(23)
	1162						v CC(14)+v CC(10)+v
A	1163	-	1167	1147	1159	1139	NN(49)
A	1116	-	1151	1131	1141	1121	ν NC(22)
A	-	1070	1101	1082	1092	1073	τ HCCC(30)+β HCH(14)
A	1054	-	1059	1041	1050	1032	β CCC(37)
A	-	1049	1049	1031	1041	1023	β NNN(65)
A	1027	-	1037	1019	1027	1009	τ HCCC(34)+ν CC(10)
A	1013	-	1030	1012	1026	1008	τ HCCC(51)
A	992	980	1022	1004	1017	999	β NCN(26)
A	-	-	984	967	982	965	τ HCCC(37)
A	-	-	955	938	974	957	ν NN(64)
A	-	-	918	902	923	907	β NCN(27)+ β NNN(17)
A	-	-	885	870	878	863	τ HCCC(51)
A	823	-	858	843	850	835	τ CCC(44)
A	-	800	824	809	818	803	ν CC(24)
A	744	740	768	755	737	725	τ NNCN(15)+δ CNNC(17)
A	698	700	734	721	720	708	τ CCCC(26)+ τ CCCC(26)
A	-	-	696	683	687	675	τ NNNC(71)
A	-	-	672	660	669	657	τ HNNN(64)
A	-	650	671	659	645	634	β CCC(30)
A	615	-	630	619	626	615	τ CCCC(23)
A	506	-	531	522	520	511	β CCC(31)
A	-	-	467	458	465	457	τ CCCC(37)
A	-	-	422	415	427	420	δ CCCC(27)+ τ CCCC(26)

A	-	360	367	361	342	336	τ CCCC(22)
A	-	350	337	331	336	330	β CCC(68)
A	-	-	325	319	323	317	ν CC(31)
A	-	-	213	209	207	204	δ CNNC(34)
A	-	-	139	136	136	133	β CCC(49)
A	-	-	83	81	80	79	τ CCCC(55)
A	-	-	44	44	42	41	τ HCCC(26)
A	-	-	39	39	32	31	τ CCCN(75)

v-Stretching;β-Bending;δ-out-of-plane bending;τ-Torsion.

Table 7.6: NBO Analysis of 5(4 methyl phenyl)tetrazole (5MPTZ)

S.No	No Donor NBO (i)				nontor	NRO (i)	E(2)	E(j)-E(i)	F(i,j)
5.110	L	OHOI 1	ADO (I)	A	AcceptorNBO (j)		kcal/mol	a.u.	a.u.
1	110	BD*	C7-C12	117	BD*	C10-C11	275.79	0.01	0.08
2	110	BD*	C7-C12	112	BD*	C8-C9	212.8	0.01	0.08
3	106	BD*	N4-C5	110	BD*	C7-C12	69.47	0.04	0.073
4	39	LP	N1	106	BD*	N4-C5	50.93	0.28	0.108
5	103	BD*	N2-N3	106	BD*	N4-C5	37.48	0.04	0.055
6	39	LP	N1	103	BD*	N2-N3	36.38	0.24	0.084
7	12	BD	C7-C12	106	BD*	N4-C5	25.04	0.24	0.07
8	8	BD	N4-C5	103	BD*	N2-N3	24.11	0.26	0.074
9	19	BD	C10-C11	110	BD*	C7-C12	23.67	0.27	0.071
10	14	BD	C8-C9	117	BD*	C10-C11	22.17	0.28	0.07
11	14	BD	C8-C9	110	BD*	C7-C12	19.47	0.27	0.065
12	12	BD	C7-C12	112	BD*	C8-C9	19.17	0.29	0.067
13	12	BD	C7-C12	117	BD*	C10-C11	18.16	0.29	0.065
14	19	BD	C10-C11	112	BD*	C8-C9	17.53	0.28	0.064

Summary of Conclusion

Molecular studies play vital role in enhance the development of industrial and pharmaceutical field. Vibration spectroscopy is a essential tool for the determination of vibrational spectroscopic signature of some organic compounds. Also, Quantum Chemical Calculation methods are tremendous implements for the computation of a vast variety of properties of molecules such as ground state geometry, vibrational wavenumber calculations, simulation of Raman and IR Spectra, characterization of the molecular orbitals and predictions of reactivity, electronic excitations, calculation of NLO properties and reaction mechanism.

The work reported in the thesis for calculations of spectroscopic profile and molecular properties of small organic molecules is based on the density functional theory. Four different organic compounds have been studied here and they were selected on the basis of their pharmaceutical and biological or industrial importance.

Chapter four deals with spectroscopic signature of Pentylenetetrazole (PTZ)] on the basis of both experimental and theoretical IR and Raman spectra. The normal coordinate analysis and subsequent scaling procedure identify the functional group's wave numbers of the molecule. The complete vibrational assignments, along with the observed and theoretical vibrational wave numbers are presented and interpreted in detail.

In Chapter five The detailed experimental and theoretical FT-IR and FT-Raman spectra of 5-Methyl-1H-tetrazole(5MTZ). are analysed based on density functional theory (DFT) calculation. Detailed vibrational assignments of observed experimental peaks are

done on the basis of PED results. The calculated Mulliken atomic charges at different levels are also presented.

Chapter Six includes the vibrational FT-IR and FT- Raman spectra of 5-Chloro-1-phenyl-1H-tetrazole(5clptz). The completed assignments of vibrational normal modes associated with the molecule are made on the basis of PED results. The electronic properties were studied by DFT calculation with various basis set which helps to determine the chemical hardness, reactivity and softness.

Chapter seven concerns the detailed experimental and theoretical FT-IR and FT-Raman spectra of 5(4 methyl phenyl)tetrazole (5MPTZ) along with NBO, HOMO-LUMO energy gap. The molecular polarizability and Mulliken properties are also discussed.

The results of our analysis are consistent with the experimental observations of similar kind of molecules and DFT quantum chemical computations implemented in this work are well suited for all the selected Tetrazole derivatives.

References

- [1] .P. Coates, The Interpretation of Infrared Spectra: Published Reference Sources, Appl. Spectrosc. Rev., 31, (1996) 179.
- [2] L.J. Bellamy, "Infrared Spectra of Complex Molecules", Chapman & Hall, New York, Vol. 1, 1975.
- [3] L.J. Bellamy, Advances in Infrared Group Frequencies, Infrared Spectra of Complex Molecules, Chapman & Hall, New York, Vol. 2, 980.
- [4] D. Steele, Interpretation of Vibrational Spectra, Chapman & Hall, London, 1971.
- [5] N.B. Colthup, L.H. Daly, S.E. Wiberley, Introduction to Infrared and Raman Spectroscopy, Academic Press, San Diego, CA, 1990.
- [6] G. Socrates, Infrared Characteristic Group Frequencies, John Wiley & Sons, NeG. Socrates, Infrared Characteristic Group Frequencies, John Wiley & Sons, New York, (1994), 11.
- [7] D. Lin-Vien, N.B. Colthup, W.G. Fateley, J.G. Grasselli, Infrared and Raman Characteristic Frequencies of Organic Molecules, Academic Press, San Diego, CA, 1991.
- [8] B. Smith, Infrared Spectral Interpretation a Systematic Approach, CRC Press, Boca Raton, FL, 1999.
- [9] R.A. Nyquist, C.L. Putzig, M.A. Leugers, Handbook of Infrared and Raman Spectra of Inorganic Compounds and Organic Salts, Academic Press, San Diego, CA, 1997.

- [10] P. Griffiths, J.A. de Hasseth, (18 May 2007) Fourier Transform Infrared Spectrometry, 2nd Ed., Wiley-Blackwell.
- [11] J.B. Foresman, A. Frisch, Exploring Chemistry with Electronic Structure Methods,2nd Ed., Gaussian, Inc., Pittsburg PA, 1996.
- [12] F. Jensen, Introduction to Computational Chemistry, 2nd Ed., Wiley, Inc., New York, 2001.
- [13] D. Young, Computational Chemistry, 1st Ed., Wiley, Inc., New York, 2001.
- [14] C.J. Cramer, Essentials of Computational Chemistry, 1st Ed., Wiley, Inc., New York, 2002.
- [15] D.R. Hartree, Proc. Cambridge Phil. Soc. 4 (1928) 111.
- [16] D.A. McQuarrie, Quantum Chemistry, 1st Ed., University Science Books, Sausalito CA, 1983.
- [17] C.J. Roothaan, Rev. Mod. Phys. 23 (1951) 69.
- [18] P. Hohenberg, W. Kohn, Phys. Rev. 136 (1964) 864.
- [19] A.D. Becke, J. Chem. Phys. 98 (1993) 5648.
- [20] C. Lee, W. Yang, R. G. Parr, Phys. Rev. B37 (1988) 785.
- [21] B. Miehlich, A. Savin, H. Stoll, H. Preuss, Chem. Phys Lett. 157 (1989) 200.
- [22] J.P. Perdew, J.A. Chevary, S.H. Vosko, K.A. Jackson, M.R. Pederson, J. Singh, C. Fiolhais, Phys. Rev. B 46 (1992) 523.
- [23] J.P. Perdew, K. Burke, Y. Wang, Phys. Rev. B 54 (1996) 16533.
- [24] E. D. Glendening, A. E. Red, J. E. Carpenter, F. Weinhold. NBO version 3. 1, TCL, university of Wisconsin. Madison, WI, 1998.

- [25] R. Gunasekaran, R. A. Balaji, S. Kumeresan, G. Anand, S. Srinivasan. can. J. Anal. sci. spectrosc. 53 (2008) 149.
- [26] B. Kosar, C. Albayrak. Spectrochim. Acta 78A, 2011, 160–167.
- [27] A.D. Buckingham. Adv. Chem. Phys. 12 (1967) 107.
- [28] Ervand G Paronikyan, Anthi Petrou, Maria Fesatidou, Athina Geronikaki, Shushanik Sh Dashyan, Suren S Mamyan, Ruzanna G Paronikyan, Ivetta M Nazaryan, Hasmik H Hakopyan. MedChemComm, 10(8), 1399-1411 (2019-9-20)
- [29] Morgane Boillot, Clément Huneau, Elise Marsan, Katia Lehongre, Vincent Navarro, Saeko Ishida, Béatrice Dufresnois, Ekim Ozkaynak, Jérôme Garrigue, Richard Miles, Benoit Martin, Eric Leguern, Matthew P Anderson, Stéphanie Baulac. Brain: a journal of neurology, 137(Pt 11), 2984-2996 (2014-9-23)
- [30] Ming-Xia Song, Yuping Huang, Shiben Wang, Zeng-Tao Wang, Xian-Qing Deng.

 Archiv der Pharmazie, 352(8), e1800313 (2019-7-23)
- [31] Phedias Diamandis, Jan Wildenhain, Ian D Clarke, Adrian G Sacher, Jeremy Graham, David S Bellows, Erick K M Ling, Ryan J Ward, Leanne G Jamieson, Mike Tyers, Peter B Dirks. Nature chemical biology, 3(5), 268-273 (2007-4-10)
- [32] Nikita Zabinyakov, Garrett Bullivant, Feng Cao, Matilde Fernandez Ojeda, Zheng Ping Jia, Xiao-Yan Wen, James J Dowling, Gajja S Salomons, Saadet Mercimek-Andrews. PloS one, 12(10), e0186645 (2017-10-21)
- [33] Mehwish Anwer, Riikka Immonen, Nick M E A Hayward, Xavier Ekolle Ndode-Ekane, Noora Puhakka, Olli Gröhn, Asla Pitkänen. Scientific reports, 9(1), 11819 (2019-8-16)

- [34] A. Ramu, M.K. Murali, M.karnan, M.Karunanithi. Journal of Information and Computational Science. ISSN: 1548-7741. Volume 9 Issue 11 2019.P: 1290-1314. DOI: http://www.joics.org/gallery/ics-1805.pdf.
- [35] K. Fukui, Science 218 (1982) 474.
- [36] K. Fukui, T. Yonesawa, H. Shingu, J. Chem. Phys. 20 (1952) 722.
- [37] C.H. Choi, M. Kertesz, J. Phys. Chem. 101 (1997) 3823.
- [38] R.G. Parr, L. Szentpaly, S. Liu, J. Am. Chem. Soc. 121 (1999) 1922.
- [39] P.K. Chattaraj, B. Maiti, U. Sarkar, J. Phys. Chem. 107A (2003) 4973.
- [40] R.G. Parr, R.A. Donnelly, M. Ley, W.E. Palke, J. Chem. Phys. 68 (1978) 3801.
- [41] R.G. Parr, R.G. Pearson, J. Am. Chem. Soc. 105 (1983) 7512.
- [42] R.G. Parr, P.K. Chattaraj, J. Am. Chem. Soc. 113 (1991) 1854.
- [43] R. Parthasarathi, J. Padmanabhan, M. Elango, V. Subramanina, P. Chattaraj, Chem. Phys. Lett. 394 (2004) 225.
- [44] R. Parthasarathi, J. Padmanabhan, V. Subramanian, B. Maiti, P. Chattaraj, Curr. Sci. 86 (2004) 535.
- [45] R. Parthasarathi, J. Padmanabhan, V. Subramanian, U. Sarkar, B. Maiti, P. Chattaraj, Internet Electron J. Mol. Des. 2 (2003) 798.
- [46] S. Chidangil, M.K. Shukla, P.C. Mishra, J. Mol. Model. 4 (1998) 250.
- [47] R.S. Mulliken, Electronic Population Analysis on LCAO-MO Molecular Wave Functions., J. Chem. Phys. 23 (1995) 1833-1840.
- [48] P. N. Prasad, D. J. Williams, "Introduction to Nonlinear Optical Effects in Molecules and Polymers" Wiley: New York, 1991.

- [49] R.M. Silverstein, G.C. Bassler, T.C. Morril, Spectrometric Identification of Organic Compounds, fifth ed., John Wiley and Sons Inc., Singapore, 1991.
- [50] R. Shanmugam, D. Sathyanarayana, Spectrochim. Acta 40 (1984) 764–773.
- [51] S. Genc, N. Dege, A. Cetin, A. Cansiz, M. Sekerci, M. Dincer, Acta Crystallogr. E60 (2004) o1340–o1342.
- [52] S. Kundoo, A.N. Banerjee, P. Saha, K.K. Chattopadhyay, Mater. Lett. 57 (2003) 2193–2197.
- [53] N.P.G. Roeges, A Guide to the Complete Interpretation of IR Spectra of Organic Compounds, Wiley, New York, 1994.
- [54] N.B. Colthup, L.H. Daly, S.E. Wiberly, Introduction to Infrared and Raman Spectroscopy, Academic Press, New York, 1990.
- [55] S. Muthu, J. Uma Maheswari, Tom Sundius. Spectrochimica acta part

 A.Molecular And Biomolecular spectroscopy 106, (2013)299-309.
- [56] A. E. Reed, F. Weinhold. J. Chem. Phys. 83 (1985) 1736-1740.
- [57] A. E. Reed, R. B. Weinstock, F. Weinhold. J. Chem. Phys. 83 (1985) 735-746.
- [58] A. E. Reed, F. Weinhold. J. Chem. Phys. 78 (1983) 4066-4073.
- [59] J. P. Foster, F. Weinhold. J. Am. Chem. Soc. 102 (1980) 7211-7218.
- [60] P. Singh, S. S. Islam, H. Ahmad, A. Prabakaran. J. Mol. Struct. 1154 (2018) 39-50.
- [61] K. R. Santhy et al. J. Mol. Struct. (2018). DOI.10. 1016/j. molstruc. 2018. 09. 058.
- [62] Jack Peter Green, Carl L. Johnson, and Sungzong Kang. Annu. Rev. Pharmacol. 1974.14:319-342. Downl d from www.annualreviews.org

- [63] S. Wang, Z. Fan, D. Wang, Y. Li, X. Ji, X. Hua, Y. Huang, T. Kalinina,V. Bakulev, Y. Morzherin, Chinese Chem. Lett., 2013; 24: 889.
- [64] H. Kavitha, N. Balasubramanian, Ind. J. Chem. Tech., 2002; 9: 361.
- [65] K. Chauhan, P. Singh, V. Kumar, P. Shukla, M. Siddiqi, P. Chauhan, Eur. J. Med. Chem., 2014; 78: 442. 7. S. George, P. Shanmugapandiyan, Int. J. Chem Tech Res., 2013; 5: 2603.
- [66] S. Rostom, H. Ashour, H. Abd El Razik, A. Abd El Fattah, N. El-Din, Bioorg. Med. Chem., 2009; 17: 2410.
- [67] R. Herbst, C. Roberts, H. Givens, E. Harvill, J. Org. Chem., 1952; 17: 262. 10. D.Wu, R. Herbst, J. Org. Chem., 1952; 17: 1216.
- [68] A.F. Holleman, E. Wiberg, N. Wiberg, in: W. de Gruyter (Ed.), Lehrburch der Anorganischen Chemie, Berlin, New York, 2007.
- [69] D.Durgadevi, S.Manivarman, S.Subashchandrabose.j. Karbala International Journal Of Modern Science 3 (2017) 18-28
- [70] V.Balachandran, A.Lakshmi, A.Janaki, i.Mol Struct 1013(2012)75-85
- [71] H.Tanaka, H.Takashima, M.Ubasawa, K.Sekiya, I.Nitta, M.Baba, S.Shigeta, R.T.Walker, E.De Clercq, T.Miyasaka, j.Med,chem. 35 (1992)337-345
- [72] V.Balachandran, A.Lakshmi, A.Janaki. j. Spectrocheimica Acta Part A 81(2011) 1-7
- [73] A.Natraj, V.Balachandran, T.Karthick, j.Mol.Struct. 1022(2012)94-108
- [74] N. Choudhary, S. Bee, A. Gupta, P. Tandon, Comp. Theor. Chem. 1016 (2013) 8–21.
- [75] N. Sinha, O. Prasad, V. Narayan, S.R. Shukla, J. Mol. Simul. 37 (2011) 153–163.

- [76] D.F.V. Lewis, C. Loannides, D.V. Parke, Xenobiotica 24 (1994) 401–408.
- [77] E. Scrocco, J. Tomasi, Adv. Quantum Chem. 11 (1979) 115–121.
- [78] F.J. Luque, J.M. Lopez, M. Orozco, Theor. Chem. Acc. 103 (2000) 343–345.
- [79] P. Politzer, J.S. Murray, in: D.L. Beveridge, R. Lavery (Eds.), Theoretical Biochemistry and Molecular Biophysics: A Comprehensive Survey, Protein, vol. 2, Adenine Press, Schenectady, New York, 1991.
- [80] E. Scrocco, J. Tomasi, Curr. Chem. 42 (1973) 95–170.
- [81] H. Kobinyi, G. Folkers, Y.C. Martin, 3D QSAR in Drug Design, Recent Advances, vol. 3, Kluwer Academic Publishers., 1998.
- [82] S. Moro, M. Bacilieri, C. Ferrari, G. Spalluto, Curr. Drug Discovery Technol. 2 (2005) 13–21.
- [83] Y.R. Shen, The Principles of Nonlinear Optics, Wiley, New York, 1984.
- [84] P.V. Kolinsky, Opt. Eng. 31 (1992) 11676–11684.
- [85] D.F. Eaton, Science 25 (1991) 281–287.
- [86] D.A. Kleinman, Phys. Rev. 126 (1962) 1977–1979.
- [87] P.Vennila, M.Govindaraju, G.Venkatesh, C.Kamal J.mol structure. 1111 (2016) 151-156.
- [88] K.Parimala, V.Balachandran, Spectrochim. Acta 81A(2011) 711-723
- [89] M.karnan, V.Balachandran, M.Murugan, Spectrochim. Acta A:mol and biomol Spec 96(2012) 51-62
- [90] L.J.Bella my. *The IR Spectra of complex Molecules*, John Wiley and sons, New York, 1975.

- [91] R.Minitha, Y.S.Mary, H.T.Varghese, C.Y.Panicker, R.Rauindran, K.Raju, V.M.Nair, FT-IR, FT -Raman and computational study of 1H-2, 2-dimethl-3H-phenothazin-4[IOH]- one, J.Mal, struct.985(2011)316-322.
- [92] R.M. Silverstein, G.C. Bassler, T.C. Morril, Spectrometric Identification of Organic Compounds, fifth ed., John Wiley and Sons Inc., Singapore, 1991.
- [93] S. Genc, N. Dege, A. Cetin, A. Cansiz, M. Sekerci, M. Dincer, Acta Crystallogr. E60 (2004) 1340–1342.
- [94] Wittenberger, S.J. Organic Preparations and Procedures Int., 1994,26, 499.
- [95] Butler, R.N. Adv. Heterocycl. Chem., 1977,21, 323; Singh, H.; Chawla, A.S.; Kapoor, V.K.; Paul, D. and Malhotra, R.K. "Progress in Medicinal Chemistry", Vol. 17, Eds: Ellis, G.P. and West, G.B., Elsevier, Biomedical PRSS, North-Holland, 1980, p. 151
- [96] Wazir, V.; Singh, G.B.; Gupta, R. and Kachroo P.L. J. Ind. Chem SOC., 1991.68, 305.
- [97] George, E.F. and Riddell, W.D. U.S. Pat. 3,865,570, Chem. Abstr., 1975.83,
 54601; Theodoridis, G.; Hotzman, F.W.; Schcrer, L.W.; Smith, B.A.; Tymonko,
 J.M. and Wyle, M.J. Pestic. Sci., 1990, 30, 259, Chem. Abstr., 1991,114,159059v.
- [98] Barratt, A.J.; Bates, L.R.; Jenkins, J.M. and White, J.R. U.S. Nut. Tech. Inform Serv., AD Rep., 1971, No. 752370, Chem. Abstr., 1973, 78, 124508; Astashinsky, V.M.; Kostyukevich, E.A.; Ivashkevich, O.A.; Lesnikovich, A.I. and Krasitsky, V.A. Combust. Flame, 1994, 96, 286, Chem. Abstr., 1994,120,248733.

- [99] Schwartz, N.V. J. Appl. Polym. Sci., 1972,16, 2715; Shelkovnikov, V.V.; Myakishev, K.G.; Kovalev, D. V.; Eroshkin, V.I. and Volkov, V.V. Chem. Abstr., 1990,112,207625j.
- [100] R. Alcala, Acta Cryst. 28B (1972) 1671–1677.
- [101] J.L. Derissen, Acta Cryst. 30B (1974) 2764–2765.
- [102] .R.Dennington II, T.Keith, J. Millam, Gauss View, Version 4.1.2, Semichem, Inc., Shawnee Mission, KS(2007).
- [103] R. S. Mulliken, J. Chem. Phys., 1955, 23, 1841–1846.
- [104] R. S. Mulliken, J. Chem. Phys., 1955, 23, 2338–2342.
- [105] C. W. Kern and M. Karplus, Journal of Chemical Physics, 1964, 40, 1374–1389.
- [106] L. C. Cusachs and P. Politzer, Chemical Physics Letters, 1968, 1, 529–531.
- [107] C. Andraud, T. Brotin, C. Garcia, F. Pelle, P. Goldner, B. Bigot, A. Collet, Theoretical and experimental investigations of the nonlinear optical properties of vanillin, polyenovanillin, and bisvanillin derivatives, J. Am. Chem. Soc. 116 (1994) 2094-2103.
- [108] Arivazhagan, M., Jeyavijayan, S., 2011. Vibrational spectroscopic, first order hyperpolarizability and HOMO, LUMO studies of 1,2-dichloro-4-nitrobenzene based on Hartree-Fock and DFT calculations. Spectrochim. Acta. 79, 376-383.
- [109] Roeges, N.P.G., 1994. A Guide to the Complete Interpretation of IR Spectra of Organic Compounds. Wiley, New York.
- [110] H. M. Nanjundaswamy and H. Abrahamse, Hetrocycles, 2014, 89, 2137-2150.

- [111] T. Jin, F. Kitahara, S. Kamijo, and Y. Yamamoto, Tetrahedron Lett., 2008, 49, 2824-2827.
- [112] B. Sreedhar, A. Suresh Kumar, and D. Yada, Tetrahedron Lett., 2011, 52, 3565-3569.
- [113] L. V. Myznikov, A. Hrabalek, and G. I. Koldobskii, Chem. Hetrocyclic Chem., 2007, 43, 1-9
- [114] L. Zamani, B.B.F. Mirjalili, K. Zomorodian and S. Zomorodian, 133 S. Afr. J. Chem., 2015, 68, 133–137.
- [115] M.J. Frisch, G.W. Trucks, H.B. Schlegal, G.E. Scuseria, M.A. Robb, J.R. Cheesman, V.G. Zakrzewski, J.A. Montgomery Jr., R.E. Stratmann, J.C. Burant, S. Dapprich, J.M. Millam, A.D. Daniels, K.N. Kudin, M.C. Strain, O. Farkas, J. Tomasi, V. Barone, M. Cossi, R. Cammi, B. Mennucci, C. Pomkelli, C. Adamo, S. Clifford, J. Ochterski, G.A. Petersson, P.Y. Ayala, Q. cui, K. Morokuma, N. Rega, P. Salvador, J.J. Dannenberg, D.K. Malilck, A.D. Rabuck, K. Raghavachari, J.B. Foresman, J. Cioslowski, J.V. Ortiz, A.G. Baboul, B.B. Stefanov, G. Liu, A. Liashenko, P. Piskorz, I.Komaromi, R.Gomperts, R.L. Martin, D.J. Fox, T.Keith, M.A. Al-Laham, C.Y. Peng, A.Nanayakkara, M. Challa-Combe, P.M.W. Gill, B. Johnson, W. Chen, M.W. Wong, J.L. Andres, C. Gonzalez, M. Head-Gordon, E.S. Replogle, J.A. Pople, Gaussian 98, Revision A 11.4, Gaussian Inc., Pittsburgh, PA, 2002.
- [116] Dong-Yue Hu, Xiao-Wei Chu and Zhi-Rong Qu. Acta Cryst. (2009). E65, o2463. doi:10.1107/S1600536809036411

- [117] Mehmet Karabacak, Mehmet Cinar, Mustafa Kurt, Spectrochim. Acta Part A Mol. Biomol. Spectrosc. 74 (2009) 1197–1203.
- [118] Z. Zhou, R.G. Parr, J. Am. Chem. Soc. 112 (1990) 5720–5724.
- [119] R. Ditchfield, Mol. Phys. 27 (1974) 789–807.
- [120] S. Fliszar, Charge Distributions and Chemical Effects, Springer, New York, 1983.
- [121] E. Smith, J. Am. Chem. Soc. 113 (1991) 6029–6037.
- [122] Fleming, Frontier Orbitals and Organic Chemical Reactions, John Wiley and Sons, New York, pp. 5–27, 1976.
- [123] J.S. Murray, K. Sen, Molecular Electrostatic Potentials, Concepts and Applications, Elsevier, Amsterdam, 1996.
- [124] J.M. Seminario, Recent Developments and Applications of Modern Density Functional Theory, Vol.4, Elsevier, pp 800–806, 1996.
- [125] T. Yesilkaynak, G. Binzet, F. Mehmet Emen, U. Florke, N. Kulcu, H. Arslan, Eur. J. Chem. 1 (2010)
- [126] Teimouri, A.N. Chermahini, K. Taban, H.A. Dabbagh, Spectrochim. Acta A 72 (2009) 369–377
- [127] G. Keresztury, Raman spectroscopy: theory, in: J.M. Chalmers, P.R. Griffiths(Eds.), Handbook of Vibrational Spectroscopy, vol. 1, John Wiley &Sons Ltd., 2002, p. 71
- [128] D.N. Sathyanarayana, Vibrational Spectroscopy Theory and Applications, second ed., New Age International (P) Limited Publishers, New Delhi, 2004.

- [129] R. M. Silverstein, G. Clayton Basseler, C. Morril. Spectrometric Identification of Organic Compounds, John Wiley, New York, USA, (1991).
- [130] F. R. Dollish, W. G. Fateley, F. F. Bentely. Characterestic Raman Frequencies On Organic Compounds, Wiley, New York.
- [131] S. Muthu, J. Uma Maheswari, Tom Sundius. Spectrochimica acta part

 A. Molecular And Biomolecular spectroscopy 106, (2013)299-309.



Clear filters

Apply

Sources

ISSN	Enter l	ISSN	l or ISSNs	5		Fin	d sources				
ISSN: 01934120 × 0913412	20 ×										
which provides an indi calculation of CiteScore	CiteScore is cation of it e, as well a ues have b	resea as ret been r	rch impact, roactively fo	ensure a more robust, stable ar earlier. The updated methodolo r all previous CiteScore years (i d are no longer available.	ogy will be ap	plied to	the				×
Filter refine list Apply Clear filters			1 result		业 Dov	wnload S	Scopus Source List	(i) Learn m	nore about Sco	opus Source I	List
Apply Clear filters			☐ All ∨	Export to Excel Save	e to source lis	t		View metrics for year:		2020	~
Display options	^		Sou	irce title $igstyle$	Cite	Score 🗸	Highest percentile ↓	Citations 2017-20 \downarrow		% Cited ↓	>
Display only Open Access journals				t Engineering and Managemer	a+ NI/A		N1/A	NI/A	NI/A	N/A	
Counts for 4-year timeframe			1 les	t Engineering and Managemen	nt N/A		N/A	N/A	N/A	N/A	
No minimum selected				_							
Minimum citations	_	*	^ Top	o of page							
Minimum documents											
Citescore highest quartile											
Show only titles in top 10 percent											
1st quartile											
2nd quartile											
3rd quartile											
4th quartile											
Source type	^										
Journals											
Book Series											
Conference Proceedings											
Trade Publications											

About Scopus

What is Scopus

Content coverage

Scopus blog

Scopus API

Privacy matters

Language

日本語に切り替える

切换到简体中文

切換到繁體中文

Русский язык

Customer Service

Help

Tutorials

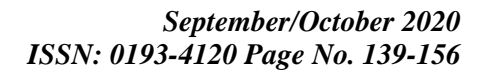
Contact us

ELSEVIER

 $Copyright \textcircled{$\otimes$ Elsevier B.V $$ \urcorner}. \ All \ rights \ reserved. \ Scopus @ is a \ registered \ trademark \ of \ Elsevier B.V.$

We use cookies to help provide and enhance our service and tailor content. By continuing, you agree to the use of cookies.







Quantum mechanics calculation and Vibrational Spectra FT-IR and FT-Raman (theoretical, Experimental) studies of 5-**Methyl-1H-Tetrazole (5MTZ)**

A.Rajeswari^a, M.K. Murali^a,* A.Ramu^b.

^a PG and Research department of physics, JJ. College of Arts & Science (Autonomous), Pudukottai-622422, Tamil Nadu, India.(Affiliated bharathidasan university. Thiruchirapalli-620024.)

Article Info Volume 83

Page Number: 139-156

Publication Issue:

September/October 2020

Abstract

The spectra of 5-Methyl-1H-tetrazole(5MTZ) have been recorded in the regions 4000-400 cm⁻¹ for FT-IR and 3500-100 cm⁻¹ for FT-Raman. The geometry optimization, vibrational frequencies were obtained by the density functional theory (DFT) using B3LYP method with 6-31G and 6-311+G basis sets. The complete assignments were performed on the basis of the potential energy distribution (PED) of the vibrational modes, calculated and the scaled values were compared with experimental FT-IR and FT-Raman spectra. The HOMO and LUMO energy gap reveals that the energy gap reflects the chemical activity of the molecule. The dipole moment (μ) , polarizability (α) , anisotropy polarizability ($\Delta \alpha$) and first hyperpolarizability (β_{tot}) of the molecule have been reported. Information about the size, shape, charge density distribution and site of chemical reactivity of the molecule has been obtained by molecular electrostatic potential (MEP).

Keywords: 5-Methyl-1H-tetrazole, DFT, FT-IR,FT-Raman,

MEP

Article History Article Received: 4 June 2020

Revised: 18 July 2020 Accepted: 20 August 2020 Publication: 15 September 2020

Introduction

The Quantum mechanics is used as a tool to learn the molecular forces determining drug activity. This information can be used to infer the nature of the biological substances with which the drug reacts and

^b Department of Physics, Ganesar College of Arts and Science, melaisiva puri-622403, Tamil Nadu, India.



hopefully as a guide to the synthesis of useful new agents[1].the complete investigation of the 5-Methyl-1H-tetrazole(5MTZ) has been carried by DFT method, which belongs to the quantum mechanics.

In recent years, tetrazole and their derivatives have been extensively studied they exhibit effective biological activities such as anti-inflammatory[2], antiviral[3], analgesic[4], antibacterial[5], antitubercular[6], anticonvulsant[7] etc. the title molecule 5-Methyl-1H-tetrazole is one of the tetrazole derivatives which used in the preparation of novel antifungal based agents derived from N-Niodopropargylazoles and triiodoallylazoles. 5-Methyl Tetrazole also in the preparation of novel quinoline derivatives against mycobacterium tuberculosis. these studies, In molecular structure, vibrational spectra and HOMO-LUMO energy gap of 5-Methyl-1H-tetrazole(5MTZ) investigated by a concerted approach using matrix isolation vibrational spectroscopy and high-level DFT-based theoretical calculations. Regarding their studies, tetrazoles have been found to be extremely interesting and challenging molecules.

Experimental Details:

The fine sample of 5-Methyl-1H-tetrazole(5MTZ) was obtained from Lancaster Chemical Company.UK, with a stated purity of 99% and it was used as such without further purification.The FT-Raman Spectrum of PTZ was recorded using 1064 nm line of ND: YAG laser for excitation wavelength in the region 3500-100 cm⁻¹ on Thermo Electron Corporation model Nexus spectrometer equipped with FT-Raman module accessory. The FT-IR

Spectrum of the title compound was recorded in the region 4000-400 cm⁻¹ on Perking Elmer Spectrophotometer in KBr pellet.

Computational Details:

The combination of Vibration spectra with quantum chemical calculation is effective for understanding the fundamental mode of vibration of the compound. The structural characteristic, stability and energy of the compound under investigation are determined by DFT with the three-parameter hybrid functional (B₃) for the exchange part and the Becke Three Lee Yong-Pare (LYP) and 6-31G,6basis sets with Gaussian 09 311+G Program Package. The Cartesian representation of the theoretical force constants has been compound at the fully optimized geometry by assuming the molecule belongs to C₁ point group symmetry. The Transformation of force field from Cartesian to internal local symmetry coordinates, the scaling, and the subsequent normal coordinate analysis (NCA) Calculation of potential energy distributions (PED) has been done on a PC with the VEDA program.

Geometrical parameter.

The calculated C-N distances areN1-C7 = 1.36 Å, N4-C5=1.34 Å, this value indicate that the bond N4-C5 is stronger than the bond N1-C7 and these values indicate that the bond distances were found to be much smaller than the average value for a single C-N bond (1.47 Å) [7]. The bond lengths of N3-N4, N1-N2 were found to be elongated to 1.40 Å, 1.39 Å respectively, compared to N2-N3 values of 1.32 Å. Because bond order of N2-N3 is higher than N3-N4, N1-N2 bond order [8]. table-1



report the detailed data of geometrical optimization of the isolated title molecule. Functional group methyl substituted in ring structure with C5 atom which made longest bond length in that molecule structure because C-C bond shaped a nonpolar covalent bond[9] and the hyper conjugation causes the interaction of the orbital of the methyl group with the π orbital of a ring. in methyl group ,C-H bond length1.10Å, (6-31G),1.09 Å, (6-311+G) are good agreement with other literature values 1.09 Å [10]1.08 Å,1.09 Å [11]1.09 Å [12]. this cooperation caused to discharging electronic charge from methyl group[13].highest bond angle occurred at C5-N1-H6 whereas lowest bond angle occurred at N1-N2-N3.

Electronic properties

To explain several types of reactions and for predicting the most reactive position in conjugated systems, molecular orbital and their properties such as energy are used [14]. The highest occupied molecular orbital (HOMO) and lowest unoccupied molecular orbital (LUMO) are the most important orbital in a molecule. The eigen values of HOMO and LUMO and their energy gap reflect the biological activity of the molecule. A molecule having a small frontier orbital gap is more polarizable and is generally associated with a high chemical reactivity and low kinetic stability [15,16]. HOMO, which can be thought the outer orbital containing electrons, tends to give these electrons as an electron donor and hence the ionization potential is directly related to the energy of the HOMO. On the other hand LUMO can accept electrons and the LUMO energy is directly related to electron affinity [17]. Two important molecular orbital (MO)

were examined for the title compound, the occupied molecular highest orbital (HOMO) and the lowest unoccupied molecular orbital (LUMO) which are given in Fig. 3. In the title compound, the HOMO of π nature is delocalized over the tetrazole ring. By contrast, the LUMO is located over the tetrazole ring and methyl group. For understanding various aspects of pharmacological sciences including drug design and the possible ecotoxicological characteristics of the drug molecules, several new chemical reactivity descriptors have been proposed. Conceptual DFT based descriptors have helped in many ways to understand the structure of molecules and their reactivity by calculating the chemical potential, global hardness and electrophilicity. Using HOMO and LUMO orbital energies, the ionization energy and electron affinity can be expressed as: $I = E_{HOMO}$, A =E_{LUMO}.table shows global reactor values of the title compound. It is seen that the chemical potential of the title compound is negative and it means that the compound is stable. They do not decompose spontaneously into the elements they are made up of. The hardness signifies the resistance towards the deformation of electron cloud of chemical systems under small perturbation encountered during chemical process. The principle hardness works in Chemistry and Physics but it is not physical observable. Soft systems are large and highly polarizable, while hard systems are relatively small and much less polarizable.

Molecular electrostatic potential (MEP)

MEP is related to the ED and is a very useful descriptor in understanding sites for electrophilic and nucleophilic reactions as



well as hydrogen bonding interactions [18,19]. The electrostatic potential V(r) is also well suited for analyzing processes based on the "recognition" of one molecule by another, as in drug-receptor, enzyme-substrate interactions, and because it is through their potentials that the two species first "see" each other [20,21]. To predict reactive sites of electrophilic and nucleophilic attacks for the investigated molecule, MEP at the B3LYP level optimized geometry was calculated. The different values of the electrostatic potential at the MEP surface are represented by different colours1: red, blue and green represent the regions of most negative, most positive and zero electrostatic potential respectively. The negative electrostatic potential corresponds to an attraction of the proton by the aggregate electron density in the molecule (shades of red), while the positive electrostatic potential corresponds to the repulsion of the proton by the atomic nuclei (shade of blue). The negative (red and yellow) regions of MEP were related to electrophilic reactivity and the positive (blue) regions to nucleophilic reactivity (Fig. 4). From the MEP it is evident that the negative charge covers the N atoms which presence in tetrazole group. the positive region is over the H atoms. The value of the electrostatic potential is largely responsible for the binding of a substrate to its receptor binding sites since the receptor and the corresponding ligands recognize each other at their molecular surface [22,23].

NLO properties

Nonlinear optics deals with the interaction of applied electromagnetic fields in various materials to generate new electromagnetic fields. altered in wavenumber, phase, or other physical properties [24]. Organic molecules able to manipulate photonic signals efficiently are of importance in technologies such as optical communication, optical computing, and dynamic image processing [25,26]. In this context. the dynamic first hyperpolarizability of the title compound is also calculated in the present study. The first hyperpolarizability (b0) of this novel molecular system is calculated using DFT method, based on the finite field approach. In the presence of an applied electric field, the energy of a system is a function of the electric field. First hyperpolarizability is a third rank tensor that can be described by a 3 X 3X 3 matrix. The 27 components of the 3D matrix can be reduced to 10 components due to the Kleinman symmetry [27]. The components of b are defined as the coefficients in the Taylor series expansion of the energy in the external electric field. When the electric field is weak and homogeneous, this expansion become

$$E{=}E_0$$
 - $\mu_\alpha F_\alpha$ - $1/2\alpha_{\alpha\beta}F_\alpha F_\beta$ - $1/6\beta_{\alpha\beta\gamma}F_\alpha F_\beta F_\gamma + \dots$

Where E_0 is the vitality of the unperturbed atoms, F_{α} the field at the source μ_{α} , $\alpha_{\alpha\beta}$ and $\beta_{\alpha\beta\Upsilon}$ are the segments of dipole moment, polarizability and the first order hyper polarizabilities. The aggregate static dipole moment (μ) , polarizability (α) , anisotropy polarizability ($\Delta \alpha$) and the mean first first order hyperpolarizability (β_{tot}) utilizing x,y,z, The segments are characterized as follows ,The calculated first hyperpolarizability of the title compound is 0.3199×10^{-30} esu/6-31G,0.3458 $\times 10^{-30}$ esu/6-311+G. The calculated hyperpolarizability of the title compound is superior than that of the standard NLO



material urea (0.13 X 10⁻³⁰ esu) [28]. We conclude that the title compound is an attractive object for future studies of nonlinear optical properties.

Mulliken Atomic charge

Mulliken atomic charge calculation has important role in the application quantum of mechanics calculations to molecular system: the atomic charge calculation of molecule plays an important role [28]. The electron distribution in 5MTZ is compared in two different quantum chemical methods and the sensitivity of the calculated charges to charge in the choice of methods is studies. By determining the electron population of each atom in the define basis function, the Mulliken charges are calculated. An estimated Mulliken charges at both levels are lists in Table 3.The results can be represented in graphical form as given in Fig 7.In this molecule all the hydrogen atoms have got positive charge.N1, N3 and N4 have negative charge. Tetrazole carbon atom has negative charge and methyl carbon atom has positive charge.

Vibrational Assignment

The detailed vibrational data of the c1 point group title molecule were tabulated in table. The higher valu of theoretical vibrations have been reduced by scaled factor 0.9555 for >1500 cm-1,0.9826 for <1500cm-1 in 6-31G basis set. as well as 0.9642 for >1500 cm-1,0.9860 for <1500cm-1 in 6-311+G basis set.

The C-H linear vibration in methyl group occurs in the range 3000 - 2900 cm⁻¹ [29]. The methyl groups vibrational frequencies depend upon the connecting atom. For example, the stretching

frequency of C-OCH₃ is higher than that of C-CH₃ [30]. The C-H vibration frequencies also differ in their position. K.Parimala et assigned asymmetric [31] stretching frequency band at 2943 cm⁻ ¹,2896 cm⁻¹ and,2940 cm⁻¹,2900 cm⁻¹ respective in the FT-IR and FT-Raman. Other literature values assigned to the frequency band stretching for CH₃ molecule is 2833cm⁻¹, 2875cm⁻¹, 2991cm⁻¹ in FT-IR 2937, 2975 cm⁻¹ in FT-Raman[29], 2967 cm⁻¹, 2925 cm⁻¹ in FT-IR, 2976 cm⁻¹, 2930 cm⁻¹ in FT-Raman(32). In this investigation all the vibration frequencies of the methyl group are in accordance with literature values those found in the characteristic group frequency as shown in Table V. The calculated values by B3LYP methods are fit with experimental values.

NH stretching is in the region 3500-3400cm⁻¹ [33] and theoretically assigned at 3490cm⁻¹ and 3458cm⁻¹ [34]. In this molecule,in this work,the NH band occurred at 3420 cm⁻¹ in FT-IR,3550 cm⁻¹ in FT-Raman.theoretically,this band observed at 3535 cm⁻¹(6-31G),3553 cm⁻¹(6-311+G).

B3LYP computation gives mode arising from the N-N stretching at 1162 cm⁻¹ in 6-31G and 1162 cm-1 in 6-311+G basis set corresponding to the peak at 1113 cm-1 in IR spectrum. The C-N vibrations is a very critical task, since the mixing of vibrations is possible in this region. Silverstein et al. [35] attributed C-N stretching absorption in the region 1266-1382 cm-1 for aromatic amines. In benzamide the band observed at 1368 cm-1 is assigned to the CN stretching band [36]. In 1,2,4-triazole the band observed at 1390 and 1327 cm-1 are assigned to CN stretching [37]. The C-N stretching modes



are reported in the range 1000–1400 cm-1 [38] and in the present case these bands are assigned at 1008, 1354, 1508 (6-31G) 1007,1345, 1510 (6-311+G) cm-1 theoretically. 1001, 1366, 1566 cm-1 in IR and 1380, 1570 cm-1 in Raman.

Natural Bond Analysis

The Natural bond ortbital [39] analyzes is used to understand the delocalization of electron density and second order donor-acceptor energy. Typically, the stabilization of orbital interaction is high for higher energy differences between interacting orbitals. Effective donor and effective acceptor have this strong stabilization [40-43]. According to the second order perturbation approach, the stabilization energy is derived [44]. The energy from (donor) i → (acceptor) j is calculated as

$$E^{2} = \Delta E_{ij} = q_{i} \frac{F(i, j)^{2}}{\varepsilon_{i} - \varepsilon_{i}}$$

Where, q_i is the donor orbital occupancy, ε_i , ε_j are diagonal elements (orbital energies) and F(i,j) is the off-diagonal NBO Fock matrix element. The NBO analysis gives valuable information about the intra and inters molecule interaction of the molecule [45].

The current work summarizes second order perturbative calculation donor-acceptor interactions based on NBO. This analysis was carried out by observing all possible interaction between lewis and non-lewis NBOs and calculated their stabilization energy (E2). Donor NBO (i), acceptor NBO (j) and stabilization energy (E2) are

tabulated in Table 5.7. From this table, it is show that the interaction between the bonded N2-N3 (NBO 55) and N4-C5 antibond (NBO 58) gives the strongest stabilization, 27.74 kcal/mol and also, lonepair N1 (NBO 19) → N2-N3 antibond (NBO 55), lonepair N1 (NBO 19) → N4-C5 antibond (NBO 58), bonded N4-C5 (NBO 8) → N2-N3 antibond (NBO 55) has the highest stabilization energy are 18.98, 18.32, 16.27kcal/mol Respectively.`

Conclusion

The present investigation thoroughly analyzed the HOMO-LUMO, and vibration spectra, both infrared and Raman of 5MTZ molecules with B3LYP method with standard 6-31G and 6-311+G basis sets. All the vibration bands are observed in the FT-IR and F-Raman spectra of the compound are assigned to various modes of vibration and most of the modes have wave numbers in the expected range. The complete vibration assignments of wave numbers are made on the basis of potential energy distribution (PED). The electrostatic potential surfaces (MEP) together with complete analysis of the vibration spectra, both IR and Raman and help to identify the structure symmetry. The excellent agreement of the calculated and observed vibration spectra reveals the advantages over the other calculated method. Finally, HOMO-LUMO energies show that the charge transfer occurs in the molecule, which are responsible for the bioactive properly of the biomedical compound 5MTZ.



References

- [1]. Jack Peter Green, Carl L. Johnson, and Sungzong Kang. Annu. Rev. Pharmacol. 1974.14:319-342. Downl d from www.annualreviews.org
- [2]. S. Wang, Z. Fang, Z. Fan, D. Wang, Y. Li, X. Ji, X. Hua, Y. Huang, T. Kalinina, V. Bakulev, Y. Morzherin, Chinese Chem. Lett., 2013; 24: 889.
- [3]. H. Kavitha, N. Balasubramanian, Ind. J. Chem. Tech., 2002; 9: 361.
- [4]. K. Chauhan, P. Singh, V. Kumar, P. Shukla, M. Siddiqi, P. Chauhan, Eur. J. Med. Chem., 2014; 78: 442. 7. S. George, P. Shanmugapandiyan, Int. J. Chem Tech Res., 2013; 5: 2603.
- [5]. S. Rostom, H. Ashour, H. Abd El Razik, A. Abd El Fattah, N. El-Din, Bioorg. Med. Chem., 2009; 17: 2410.
- [6]. R. Herbst, C. Roberts, H. Givens,E. Harvill, J. Org. Chem., 1952; 17: 262. 10.D. Wu, R. Herbst, J. Org. Chem., 1952; 17: 1216.
- [7]. A.F. Holleman, E. Wiberg, N. Wiberg, in: W. de Gruyter (Ed.), Lehrburch der Anorganischen Chemie, Berlin, New York, 2007.
- [8]. **A.Ramu**, M.K. Murali, M.karnan, M.Karunanithi. Journal of Information and Computational Science. ISSN: 1548-7741. Volume 9 Issue 11 2019.P: 1290- 1314. DOI: http://www.joics.org/gallery/ics-1805.pdf.
- [9]. D.Durgadevi,S.Manivarman,S.Sub ashchandrabose.j.Karbala International Journal Of Modern Science 3 (2017) 18-28 [10]. V.Balachandran,A.Lakshmi,A.Jana ki.j.Mol Struct 1013(2012)75-85
- [11]. H.Tanaka, H.Takashima, M.Ubasawa, K.Sekiya, I.Nitta, M.Baba,

- S.Shigeta, R.T.Walker, E.De Clercq, T.Miyasaka, j.Med,chem. 35 (1992)337-345 [12]. V.Balachandran,A.Lakshmi,A.Jana ki.j.Spectrocheimica Acta Part A 81(2011) 1-7
- [13]. A.Natraj, V.Balachandran, T.Karthic k.j.Mol.Struct.1022(2012)94-108
- [14]. N. Choudhary, S. Bee, A. Gupta, P. Tandon, Comp. Theor. Chem. 1016 (2013) 8–21.
- [15]. N. Sinha, O. Prasad, V. Narayan, S.R. Shukla, J. Mol. Simul. 37 (2011) 153–163.
- [16]. D.F.V. Lewis, C. Loannides, D.V. Parke, Xenobiotica 24 (1994) 401–408.
- [17]. B. Kosar, C. Albayrak, Spectrochim. Acta 78 (2011) 160–167.
- [18]. E. Scrocco, J. Tomasi, Adv. Quantum Chem. 11 (1979) 115–121.
- [19]. F.J. Luque, J.M. Lopez, M. Orozco, Theor. Chem. Acc. 103 (2000) 343–345.
- [20]. P. Politzer, J.S. Murray, in: D.L. Beveridge, R. Lavery (Eds.), Theoretical Biochemistry and Molecular Biophysics: A Comprehensive Survey, Protein, vol. 2, Adenine Press, Schenectady, New York, 1991.
- [21]. E. Scrocco, J. Tomasi, Curr. Chem. 42 (1973) 95–170.
- [22]. H. Kobinyi, G. Folkers, Y.C. Martin, 3D QSAR in Drug Design, Recent Advances, vol. 3, Kluwer Academic Publishers., 1998.
- [23]. S. Moro, M. Bacilieri, C. Ferrari, G. Spalluto, Curr. Drug Discovery Technol. 2 (2005) 13–21.
- [24]. Y.R. Shen, The Principles of Nonlinear Optics, Wiley, New York, 1984.
- [25]. P.V. Kolinsky, Opt. Eng. 31 (1992) 11676–11684.
- [26]. D.F. Eaton, Science 25 (1991) 281–287.



- [27]. D.A. Kleinman, Phys. Rev. 126 (1962) 1977–1979.
- [28]. R.S. Mulliken, Electronic Population Analysis on LCAO-MOMolecular Wave Functions., J. Chem. Phys. 23 (1995) 1833-1840.
- [29]. A.Natraj, V.Balachandar, T.Karthick . J.mol struc 1022(2012)94-108.
- [30]. P.Vennila,M.Govindaraju,G.Venka tesh,C.Kamal J.mol structure.1111(2016)151-156.
- [31]. K.Parimala, V.Balachandran, Spectrochim. Acta 81A(2011) 711-723
- [32]. M.karnan, V.Balachandran, M.Muru gan, Spectrochim. Acta A:mol and biomol Spec 96(2012) 51-62
- [33]. L.J.Bella my. *The IR Spectra of complex Molecules*, John Wiley and sons, New York, 1975.
- [34]. R.Minitha, Y.S.Mary, H.T.Varghese, C.Y.Panicker, R.Rauindran, K.Raju, V.M.Nair, FT-IR, FT -Raman and computational study of 1H-2, 2-dimethl-3H-phenothazin- 4[IOH]- one, J.Mal, struct.985(2011)316-322.
- [35]. R.M. Silverstein, G.C. Bassler, T.C. Morril, Spectrometric Identification of Organic Compounds, fifth ed., John Wiley and Sons Inc., Singapore, 1991.

- [36]. R. Shanmugam, D. Sathyanarayana, Spectrochim. Acta 40 (1984) 764–773.
- [37]. S. Genc, N. Dege, A. Cetin, A. Cansiz, M. Sekerci, M. Dincer, Acta Crystallogr. E60 (2004) 1340–1342.
- [38]. S. Kundoo, A.N. Banerjee, P. Saha, K.K. Chattopadhyay, Mater. Lett. 57 (2003) 2193–2197.
- [39]. S. Muthu, J. Uma Maheswari, Tom Sundius. Spectrochimica acta part A.Molecular And Biomolecular spectroscopy 106, (2013)299-309.
- [40]. A. E. Reed, F. Weinhold. J. Chem. Phys. 83 (1985) 1736-1740.
- [41]. A. E. Reed, R. B. Weinstock, F. Weinhold. J. Chem. Phys. 83 (1985) 735-746.
- [42]. A. E. Reed, F. Weinhold. J. Chem. Phys. 78 (1983) 4066-4073.
- [43]. J. P. Foster, F. Weinhold. J. Am. Chem. Soc. 102 (1980) 7211-7218.
- [44]. P. Singh, S. S. Islam, H. Ahmad, A. Prabakaran. J. Mol. Struct. 1154 (2018) 39-50.
- [45]. K. R. Santhy et al. J. Mol. Struct. (2018). DOI.10. 1016/j. molstruc. 2018. 09. 058.



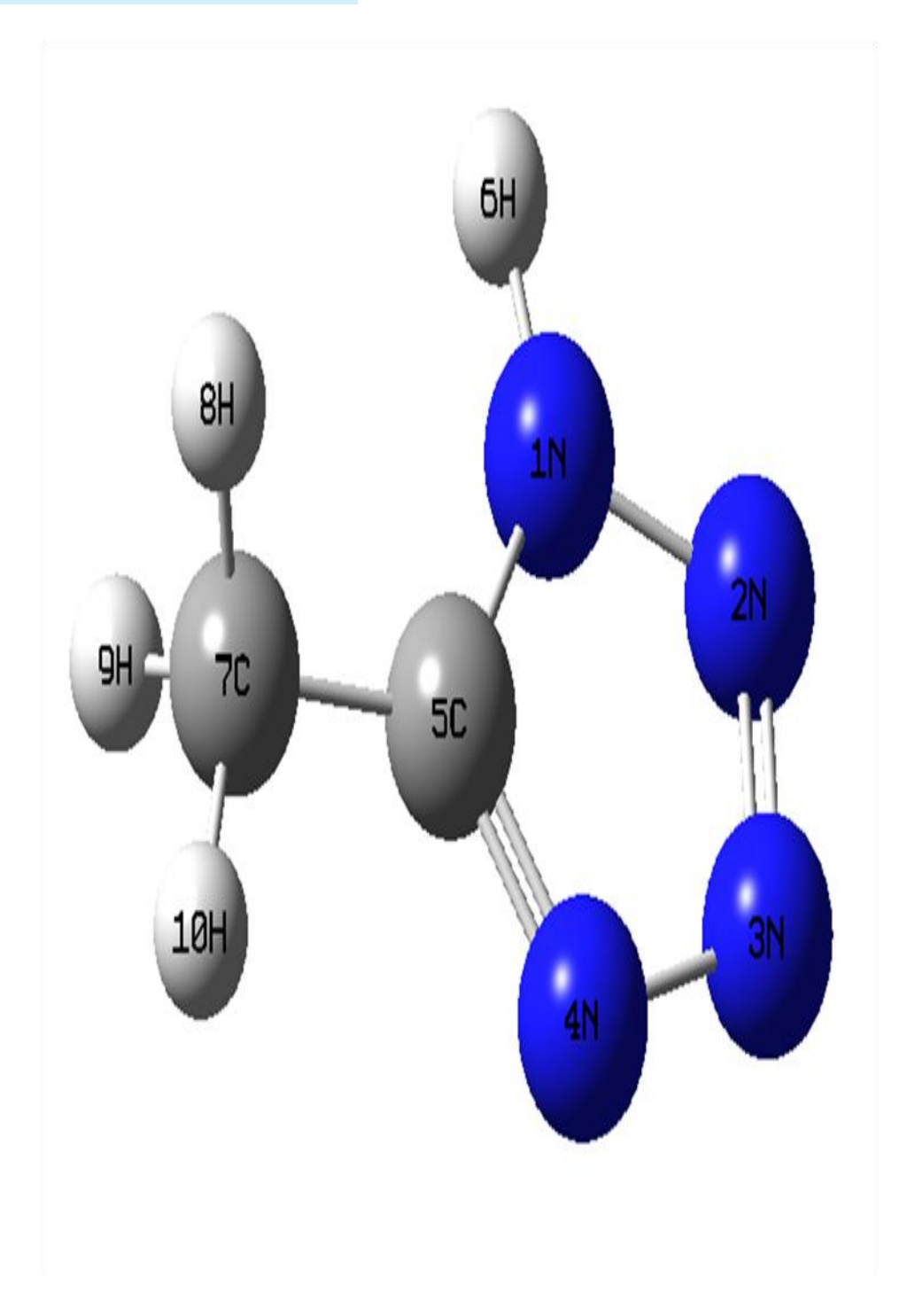


Fig 1. The theoretical geometry structure and atomic numbering scheme of 5-Methyl-1H-tetrazole (5MTZ).



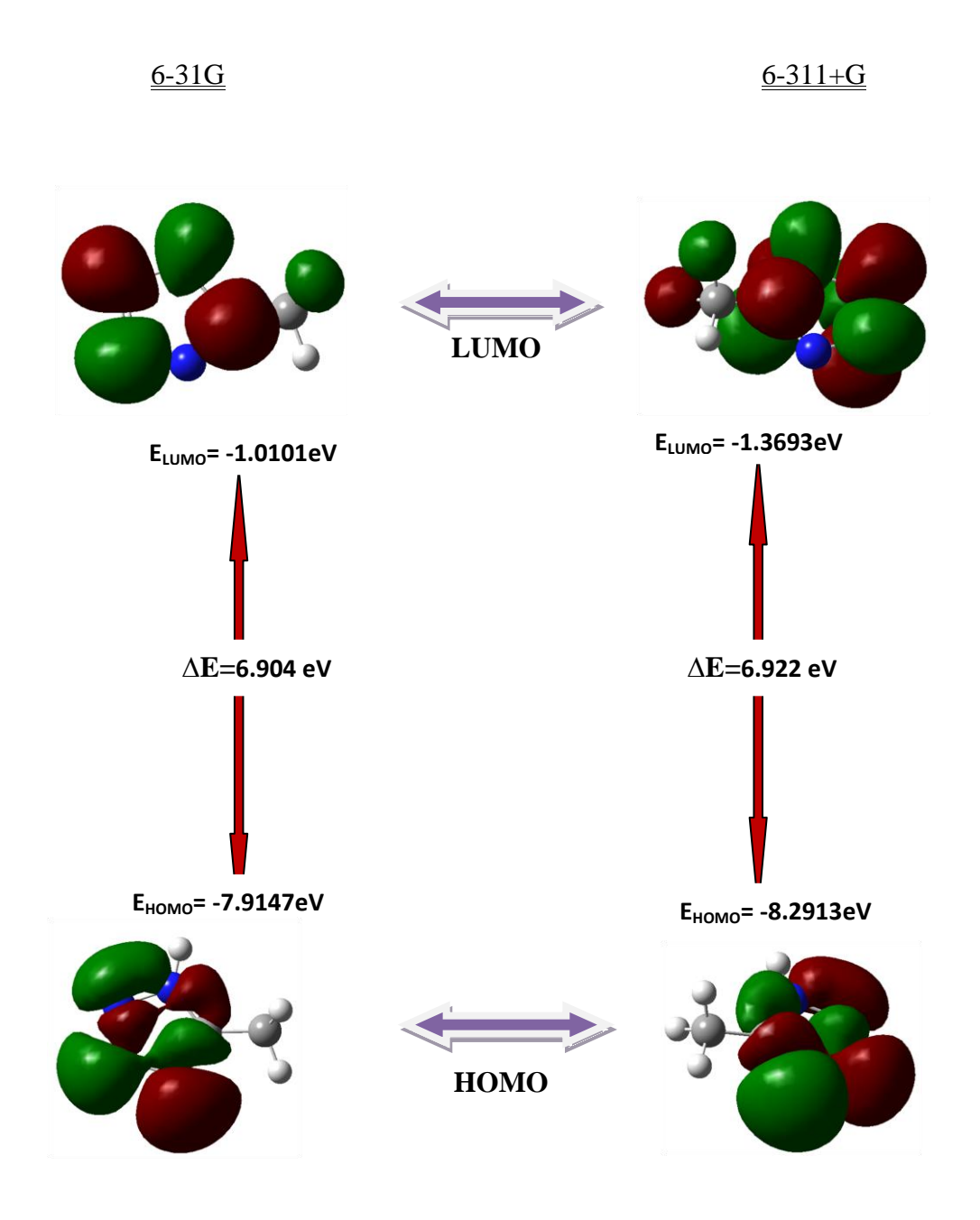


Fig 2: The atomic orbital compositions of the frontier molecular orbital for 5-Methyl-1H-tetrazole (5MTZ).



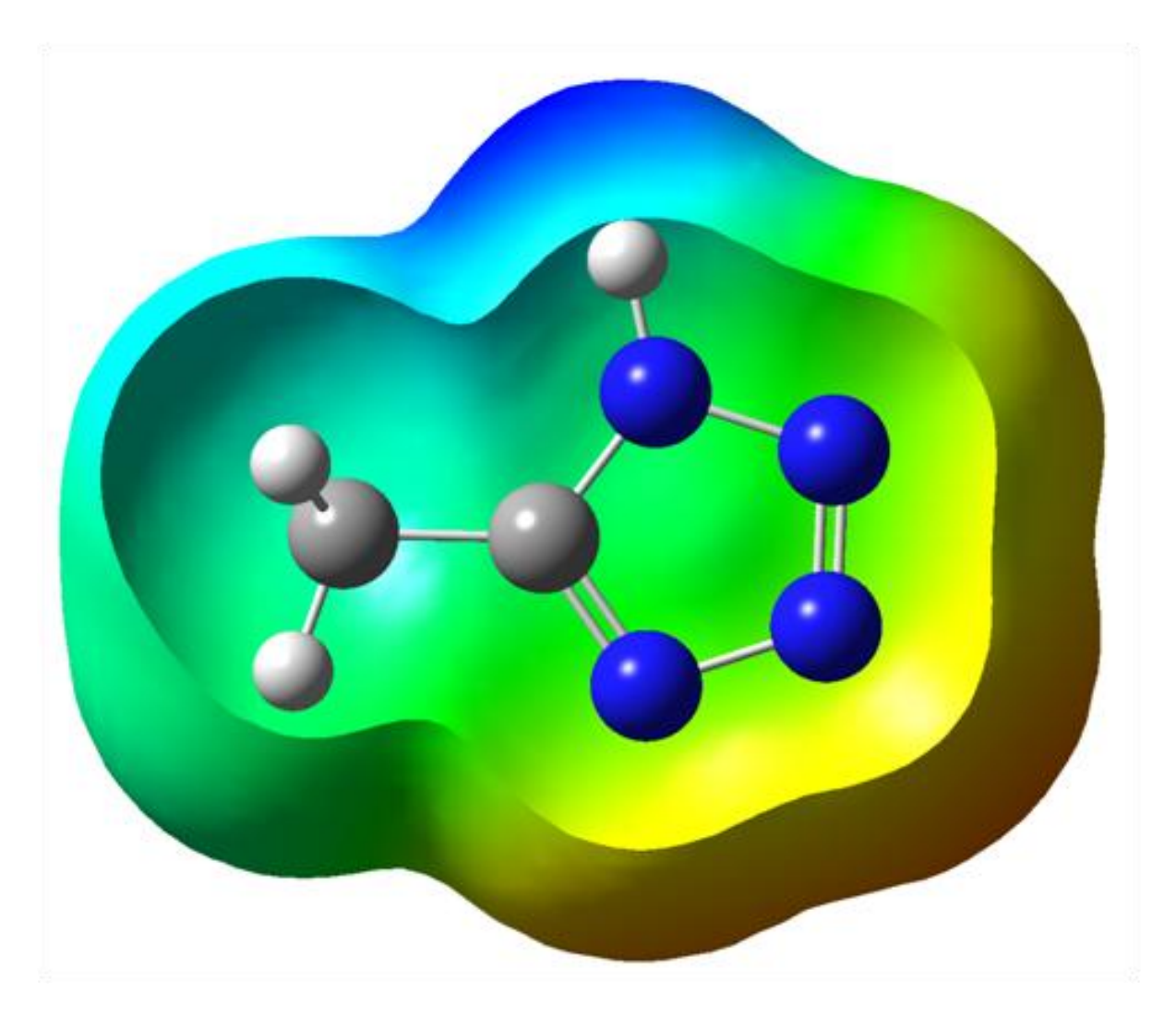


Fig 3. The total electron density surface mapped with of 5-Methyl-1H-tetrazole (5MTZ).



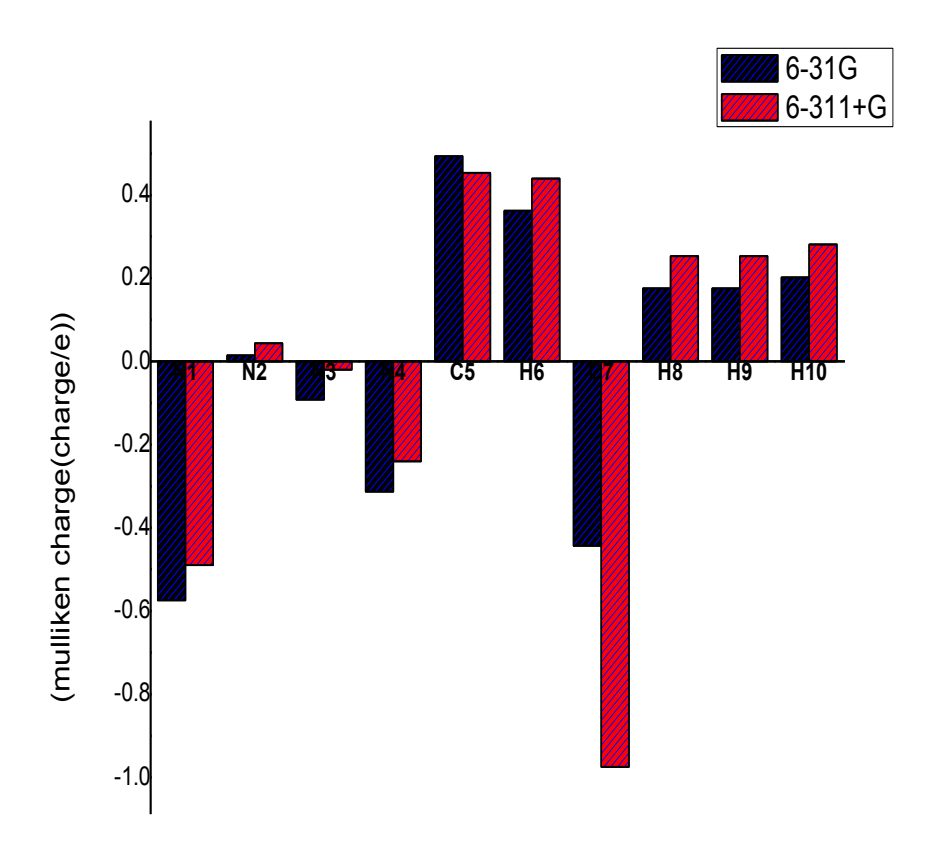


Fig 4 Bar diagram representing the Mulliken atomic charge distribution of 5-Methyl-1H-tetrazole (5MTZ).



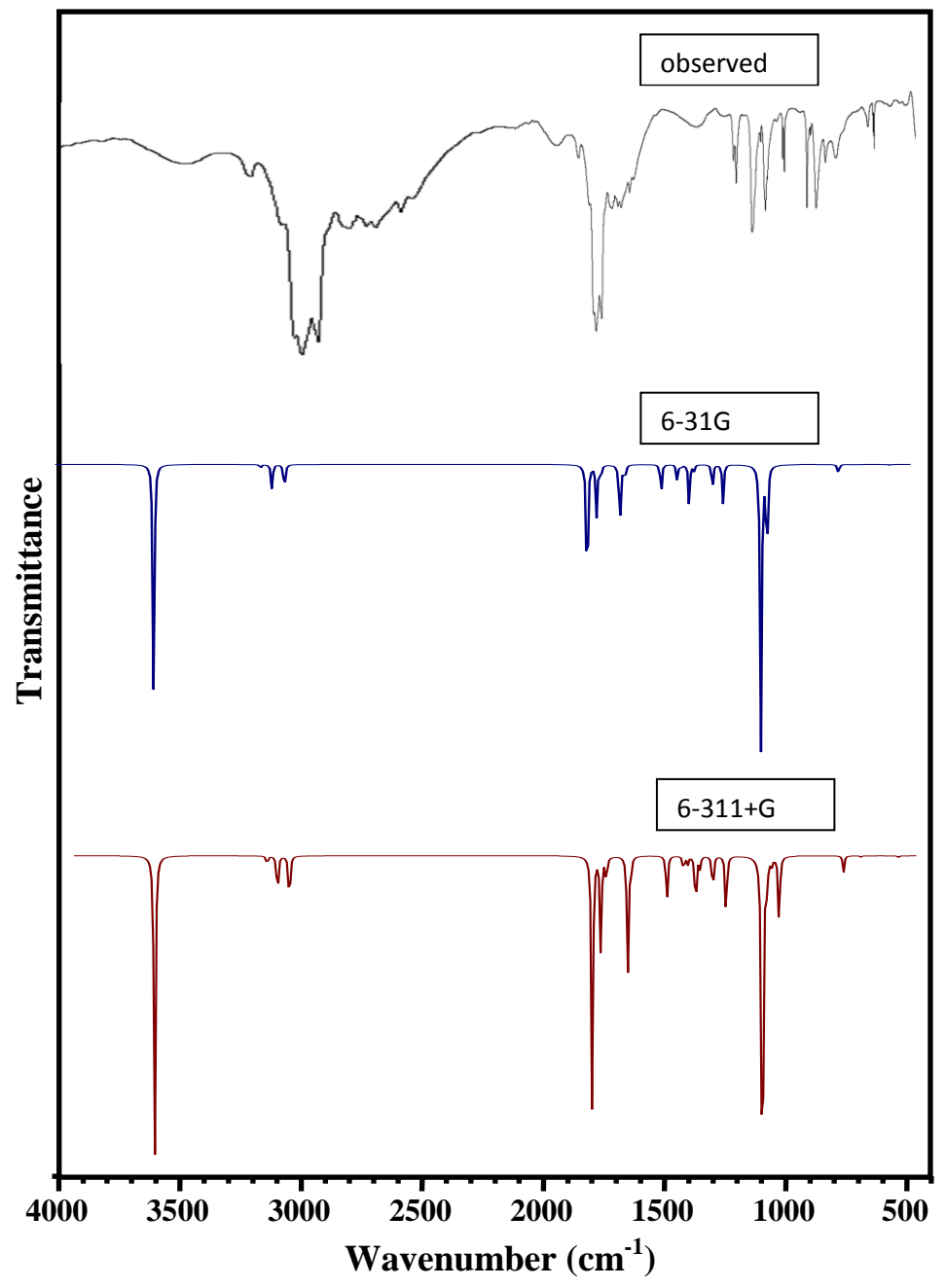


Fig 5. Comparative representation of FT-IR spectra for **5-Methyl-1H-tetrazole** (**5MTZ**).



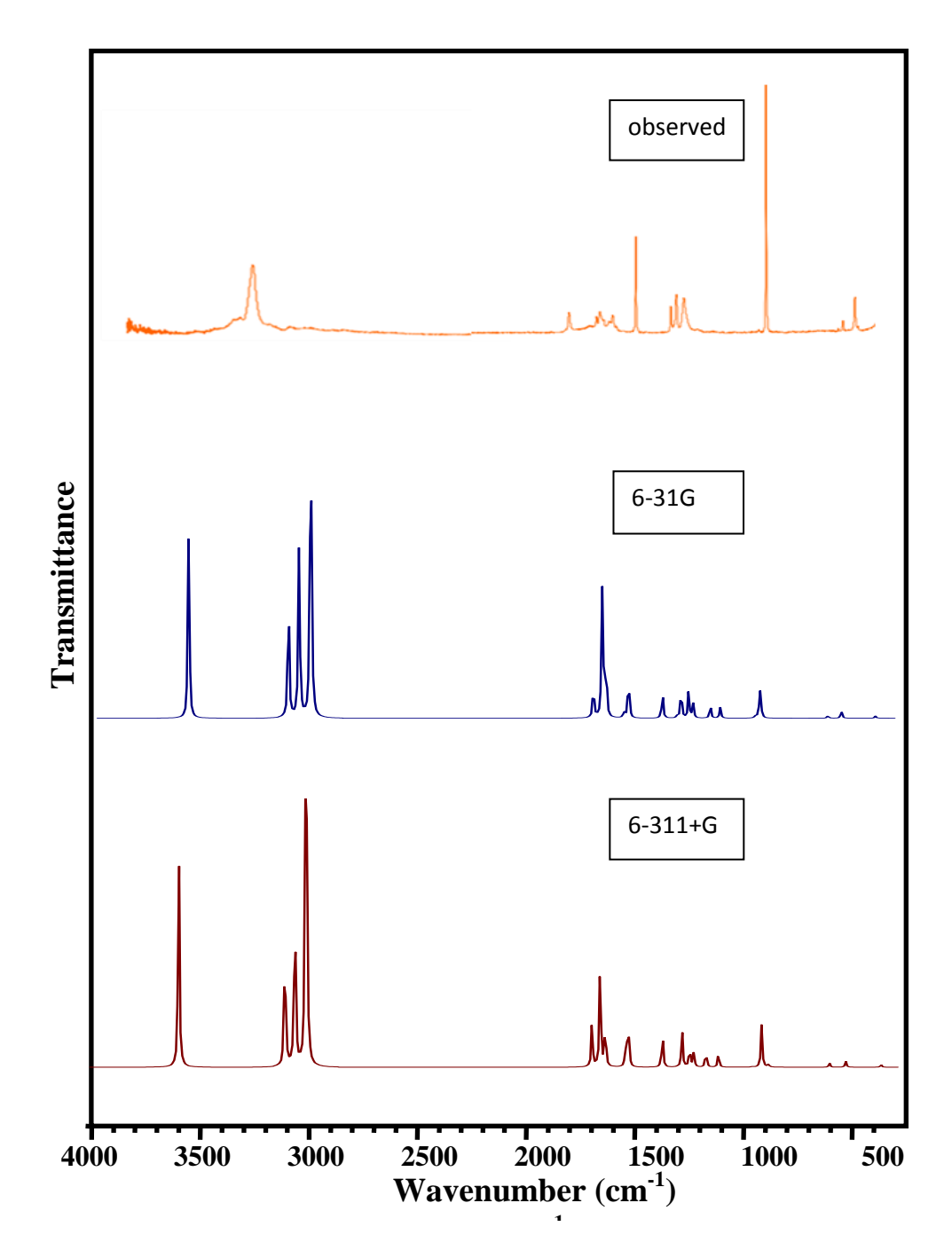


Fig 6. Comparative representation of FT-Raman spectra for **5-Methyl-1H-tetrazole (5MTZ)**.



Table 1: Geometry Optimization Parameter of 5-Methyl-1H-tetrazole (5MTZ) based on B3LYP/6-31G and B3LYP/6-311+G method and basis set.

	BondLength(Å))	BondAngle(°)			
Atom	6-31G	6-311+G	Atom	6-31G	6-311+G	
C5-C7	1.49	1.48	C5-N1-H6	130.75	130.85	
N3-N4	1.40	1.40	N1-C5-C7	126.12	126. 10	
N1-N2	1.39	1.39	N4-C5-C7	125.90	126.01	
N1-C5	1.36	1.36	N2-N1-H6	119.91	119.60	
N4-C5	1.34	1.34	C5-C7-H8	111.56	111.62	
N2-N3	1.32	1.32	C5-C7-H9	111.54	111.57	
C7-H9	1.10	1.09	N2-N3-N4	110.77	110.54	
C7-H8	1.10	1.09	N2-N1-C5	109.35	109.55	
C7-H10	1.09	1.09	C5-C7-H10	108.65	108.81	
N1-H6	1.01	1.00	H8-C7-H10	108.47	108.30	
			H9-C7-H10	108.47	108.29	
			H8-C7-H9	108.06	108.15	
			N1-C5-N4	107.98	107.89	
			N3-N4-C5	106.36	106.49	
			N1-N2-N3	105.54	105.54	

Table 2: HOMO-LUMO energy (eV) and other related properties of 5-Methyl-1H-tetrazole (5MTZ) based on B3LYP/6-31G and B3LYP/6-311+G method and basis set.

Parameters	6-31G (eV)	6-311+G (eV)	
Homo(I)	-7.9147	-8.2913	
Lumo(A)	-1.0101	-1.3693	
Energy gap(ΔE)	6.9046	6.9220	
Electronegativity	4.4624	4.8303	
Global hardness	3.4523	3.4610	
Global softness(eV ⁻¹)	0.2897	0.2889	
Chemical potential	-4.4624	-4.8303	
Electriphilicity	2.8840	3.3706	



Table 3: Dipole moment(μ), Polarizability(α), Anisotropy polaraizability($\Delta\alpha$) and First order polarizability(β_{tot}) of 5-Methyl-1H-tetrazole (5MTZ) based on B3LYP/6-31G and B3LYP/6-311+G method and basis set.

Parameters	6-31G	6-311+G
μ_{x}	-4.7921	4.9639
$\mu_{ m y}$	4.0155	4.1044
$\mu_{\mathbf{z}}$	0.0001	0.0003
$a_{ ext{XX}}$	-37.5178	-38.5207
$a_{ m YY}$	-34.8592	-35.9312
α_{ZZ}	-34.6744	-35.4883
$a_{ ext{XY}}$	0.054	0.0135
$a_{ extbf{XZ}}$	-0.001	-0.001
$lpha_{ m YZ}$	0.0002	0.0007
$oldsymbol{eta_{XXX}}$	-23.2569	24.9565
$oldsymbol{eta_{YYY}}$	21.6646	22.7176
$oldsymbol{eta_{ZZZ}}$	0.0017	0.0013
$oldsymbol{eta_{XYY}}$	-5.3476	5.8671
$oldsymbol{eta_{XXY}}$	-0.165	-0.2122
$oldsymbol{eta_{XXZ}}$	0.0009	-0.0028
$oldsymbol{eta_{XZZ}}$	-0.6815	1.2008
$oldsymbol{eta_{YZZ}}$	1.1585	1.5009
$oldsymbol{eta_{YYZ}}$	-0.0006	0.0004
$oldsymbol{eta_{XYZ}}$	-0.0007	-0.001
μ(debye)	6.2521	6.4410
α(esu)	-5.2812X10 ⁻²⁴	-5.4237 X10 ⁻²⁴
$\Delta \alpha(esu)$	65.0411X10 ⁻²⁴	66.7801 X10 ⁻²⁴
$\beta_{tot}(esu)$	0.3199X10 ⁻³⁰	0.3458X10 ⁻³⁰

Table 4: Mulliken charge (charge/e) of 5-Methyl-1H-tetrazole (5MTZ) based on B3LYP/6-31G and B3LYP/6-311+G method and basis set.

A 4 0 200	6-31G	6-311+G			
Atom	Charge/e				
N1	-0.5748	-0.4897			
N2	0.0143	0.0438			
N3	-0.0924	-0.0203			
N4	-0.3128	-0.2401			
C5	0.4934	0.4534			
Н6	0.3618	0.4396			
C 7	-0.4437	-0.9744			
H8	0.1759	0.2534			
H9	0.1759	0.2534			
H10	0.2023	0.2809			

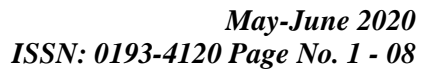




Table 5: Observed Frequency (cm⁻¹)- Theoretical Frequency (cm⁻¹) and Vibrational assignment with PED(%) of 5-Methyl-1H-tetrazole (5MTZ) based on B3LYP/6-31G and B3LYP/6-311+G method and basis set.

	-			I IICO	retical		
	Frequency(cm ⁻¹)			Freque	ncy(cm	·1)	Vibrational aggignment (DED 0/)
cis	FT-IR	FT-Raman	6-3	6-31G 6-311+G		11+G	- Vibrational assignment (PED %)
Spe cis			Calc	scaled	Calc	Scaled	
A	3420	3550	3700	3535	3684	3553	v NH (100)
A	3146	-	3176	3035	3140	3028	ν CH(86)+ν CH(14)
A	2955	-	3121	2982	3090	2979	v CH(99)
A	2923	-	3060	2923	3032	2924	ν CH(14)+ν CH(86)
A	1566	1570	1578	1508	1566	1510	v NC(23)+v CC(23)
A	1464	-	1532	1464	1526	1471	β HCH(78)+τ HCCN(21)
A	-	-	1529	1461	1523	1469	β HCH(71)+τ HCCN(21)
A	1409	1410	1469	1444	1465	1444	β HCH(97)
A	1366	1380	1378	1354	1364	1345	v NC(30)+v NC(19)+β NNC(11)
A	1269	1270	1355	1331	1350	1331	ν CC(14)+β HNN(57)
A	1113	1105	1182	1162	1178	1162	v NN(73)
A	1089	1090	1106	1087	1099	1084	β HCH(20)+τ HCCN(60)+τ HCCN(10)
A	1064	1070	1087	1068	1080	1065	v NC(32)+v NC(14)+β NCN(14)
A	-	-	1049	1031	1042	1027	β NNN(71)
A	1001	-	1026	1008	1022	1007	ν NC(11)+β HCH(15)+β NNC(15)
A	928	-	939	922	961	947	v NN(68)+β NCN(11)
A	723	-	888	872	897	885	ν NC(19)+β NCN(43)+β NNN(16)
A	690	-	711	699	726	716	τ NNNC(31)+τ NNCN(58)
A	683	-	706	694	703	694	τ HNNN(79)+τ NNNC(19)
A	-	-	686	674	681	672	v NC(10)+v CC(52)+β NCN(11)
A	-	490	679	667	646	637	τ HNNN(15)+τ NNNC(44)+τ NNCN(19)



May-June 2020 ISSN: 0193-4120 Page No. 1 - 08

A	-	330	339	333	341	336	β CCN(86)

A - 270 270 265 260 256 τ NNCN(19)+δ CNNC(65) A - 96 94 83 81 τ HCCN(77)+δ CNNC(11)

Table 6: Natural Bond Orbital Calculation of 5-Methyl-1H-tetrazole (5MTZ)

S.No	D	onor	NBO (i)	Acce	eptorN	BO (j)	E(2) kcal/mol	E(j)-E(i) a.u.	F(i,j) a.u.
1	55	BD	N2-N3	58	BD*	N4-C5	27.74	0.04	0.04
2	19	LP	N1	55	BD*	N2-N3	18.98	0.34	0.34
3	19	LP	N1	58	BD*	N4-C5	18.32	0.38	0.38
4	8	BD	N4-C5	55	BD*	N2-N3	16.27	0.3	0.3
5	21	LP	N3	51	BD*	N1-N2	12.15	0.68	0.68



Clear filters

Apply

Sources

ISSN	Enter l	ISSN	l or ISSNs	5		Fin	d sources				
ISSN: 01934120 × 0913412	20 ×										
which provides an indi calculation of CiteScore	CiteScore is cation of it e, as well a ues have b	resea as ret been r	rch impact, roactively fo	ensure a more robust, stable ar earlier. The updated methodolo or all previous CiteScore years (i d are no longer available.	ogy will be ap	plied to	the				×
Filter refine list Apply Clear filters			1 result		业 Dov	wnload S	Scopus Source List	(i) Learn n	nore about Sco	opus Source l	List
Apply Clear filters			☐ All ∨	Export to Excel Save	e to source lis	t		\/:	.: (2020	~
Display options	^		Sou	urce title $igspace$	Cite	Score 🗸	Highest percentile ↓	Citations 2017-20 ↓	oics for year: Documents 2017-20 ↓	% Cited ↓	>
Display only Open Access journals				t Engineering and Managemer	a+ NI/A		N1/A	NI/A	NI/A	N/A	
Counts for 4-year timeframe			1 les	t Engineering and Managemen	nt N/A		N/A	N/A	N/A	N/A	
No minimum selected				_							
Minimum citations	_	*	^ Top	o of page							
Minimum documents											
Citescore highest quartile											
Show only titles in top 10 percent											
1st quartile											
2nd quartile											
3rd quartile											
4th quartile											
Source type	^										
Journals											
Book Series											
Conference Proceedings											
Trade Publications											

About Scopus

What is Scopus

Content coverage

Scopus blog

Scopus API

Privacy matters

Language

日本語に切り替える

切换到简体中文

切換到繁體中文

Русский язык

Customer Service

Help

Tutorials

Contact us

ELSEVIER

Terms and conditions $\ \ \,$ Privacy policy $\ \ \,$

 $Copyright \textcircled{$\otimes$ Elsevier B.V $$ \urcorner}. \ All \ rights \ reserved. \ Scopus @ is a \ registered \ trademark \ of \ Elsevier B.V.$

We use cookies to help provide and enhance our service and tailor content. By continuing, you agree to the use of cookies.





Non Linear Optical Properties, Optimized Structure, Global Reactivates and Mulliken Atomic Charge Studies on 5-Chloro-1-Phenyl-1H-Tetrazole Based on Density Functional Theory with Vibrational Assignment

A.Rajeswari^a, M.K. Murali^a,* A.Ramu^b.

- ^a PG and Research department of physics, JJ. College of Arts & Science (Autonomous), Pudukottai-622422, Tamil Nadu, India. .(Affiliated bharathidasan university. Thiruchirapalli-620024.)
- ^b Department of Physics, Ganesar College of Arts and Science, melaisivapuri-622403, Tamil Nadu, India.

Article Info Volume 83 Page Number: 252 - 268 Publication Issue:

November/December 2020

Article History

Article Received: 25 October 2020 Revised: 22 November 2020 Accepted: 10 December 2020 Publication: 31 December 2020

Abstract

The vibrational spectra of 5-Chloro-1-phenyl-1H-tetrazole (5ClPTZ) have been recorded in the regions 4000–400 cm⁻¹ for FT-IR and 3500-100 cm⁻¹ for FT-Raman. The molecular structure, geometry optimization, vibrational frequencies were obtained by the density functional theory (DFT) using B3LYP method with 6-31G and 6-311+G basis sets. The complete assignments were performed on the basis of the potential energy distribution (PED) of the vibrational modes, calculated and the scaled values were compared with experimental FT-IR and FT-Raman spectra. The HOMO and LUMO energy gap reveals that the energy gap reflects the chemical activity of the molecule. The dipole moment (μ) , polarizability (α), anisotropy polarizability ($\Delta\alpha$) and first hyperpolarizability (β_{tot}) of the molecule have been reported. Information about the size, shape, charge density distribution and site of chemical reactivity of the molecule has been obtained by molecular electrostatic potential (MEP).

Keywords: 5-Chloro-1-phenyl-1H-tetrazole,DFT, FT-IR,FT-

Raman, MEP

Introduction

5-Chloro-1-aryl-1H-tetrazoles are widely used in several disparate areas of research and, commercially, in a variety of drug and herbicide manufactures[1]. Biological

activity is encountered due to the special metabolism of disubstituted tetrazoles and also because, in 5-substituted tetrazolyl compounds, the heterocyclic ring is isosteric with a carboxy group and of similar acidity[3]. Some typical uses of



such tetrazoles are in anti-inflammatory herbicides[4], drugs[2], rocket propellants[5] and photography and polymers[6]. Due to this importance, the title 5-Chloro-1-phenyl-1H-tetrazole molecule (5ClPTZ) was investigated by method.since density functional theory (DFT) has recently emerged compromise between the desired level of accuracy and the demand on computational time.

In these studies, the molecular structure, vibrational spectra and HOMO-LUMO energy gap of Pentylenetetrazole (PTZ) were investigated by a concerted approach using matrix isolation vibrational spectroscopy and high-level DFT-based theoretical calculations. Regarding their studies, tetrazoles have been found to be extremely interesting and challenging molecules.

Experimental Details:

The fine sample of 5ClPTZ was obtained from Lancaster Chemical Company.UK, with a stated purity of 99% and it was used as such without further purification. The FT-Raman Spectrum of 5ClPTZ was recorded using 1064 nm line YAG laser for excitation of ND: wavelength in the region 3500-100 cm⁻¹ on Thermo Electron Corporation model Nexus spectrometer equipped with FT-Raman module accessory. The FT-IR Spectrum of the title compound was recorded in the region 4000-400 cm⁻¹ on Perking Elmer Spectrophotometer in KBr pellet.

3. Computational Details:

The combination of Vibration spectra with quantum chemical calculation is effective for understanding the fundamental mode of vibration of the compound. The structural

characteristic, stability and energy of the under investigation compound determined by DFT with the threeparameter hybrid functional (B₃) for the exchange part and the Becke Three Lee Yong-Pare (LYP) and 6-31G ,6-311+G basis sets with Gaussian 09 Program Package. The Cartesian representation of the theoretical force constants has been compound at the fully optimized geometry by assuming the molecule belongs to C₁ point group symmetry. The Transformation of force field from Cartesian to internal local symmetry coordinates, the scaling, and the subsequent normal coordinate analysis (NCA) Calculation of potential energy distributions (PED) has been done on a PC with the VEDA program.

Molecular geometry

The optimised geometry of 5ClPTZ with atom numbering is shown in Fig. 3. The more stable 5CITZ molecule has C1 point group symmetry. The theoretical and experimental C-C bond lengths in the benzene ring of 5ClPTZ are in the range of 1.40 Å. The Alcala [7] and Derissen [8] reported that the C-C bond length of the isophthalic acid was in the range of 1.391–1.402 Å and well agreed with the theoretical bond length of the title molecule. The C-H bond lengths are calculated as 1.09-1.08 Å, experimentally reported as 0.930 Å. The substitution of halogen reduces the electron density at the ring carbon atom. The C-Cl bond length is calculated as 1.76 Å .which is longest bond length in the molecule. The theoretical bond in harmony angles are with experimental bond angles. In particular, the C-C-C bond angles of benzene ring in the molecule in range title 120.253-121.162 and well agreed with the



experimental range of bond angles 116.2–124.80. the calculated C-N distance in the tetrazole ring is 1.36 Å.where as 1.43 Å for C7-N1 bond.N-N bonds are assigned at 1.40 Å.

Frontier molecular orbital analysis

The study of frontier molecular orbital is important that ionization potential (I), electron affinity (A), electrophilicity index (ω), chemical potential electronegativity (χ) and hardness (η) to be put into a MO frame work [9]. These global descriptors η,μ and χ are defined as $\eta = (I - I)^{-1}$ A)/2, $\mu = -(I + A)/2$, $\chi = (I + A)/2$, where I and A denote the ionization potential and electron affinity of the compounds respectively. The ionization energy (I) and electron affinity (A) can be expressed through HOMO and LUMO orbital energies as I = -EHOMO and A = -ELUMO. Parr et al. [9] have defined a new quantity the descriptor to global electrophilic power of the compound as electrophilicity index ($\omega = \mu 2/2\eta$.) which defines a quantitative classification of global electrophilic nature of a compound. The calculated values have tabulated in table. HOMO is localized over the entire molecule and LUMO is localized over the entire compound .the small value of energy gap reveals the title molecule has more reactive.

Molecular Electrostatic Potential (MEP):

Molecular electrostatic potential (MEP) is most helpful descriptor in understanding sites for electrophilic attack and nucleophilic reactions and for the study of biological recognition process [10] and to predict reactive sites of electrophilic and nucleophilic attacks for the title molecule, MEP at the B3LYP optimized geometry was calculated. Potential value increases in the order red < orange < yellow < green < blue. The negative (red and yellow) regions of MEP were related to electrophilic reactivity and the positive (blue) regions to nucleophilic reactivity. From the MEP of the title compound it is evident that the negative charge covers the N atoms which belongs to tetrazole molecule group and the positive region is over the H group in phenyl ring.

Mulliken Atomic charge

Although atomic charges in a molecule are not experimentally observable quantities, they are fundamental and useful tools to understand and relate properties molecules to their structures. Even though Various methods are available to assigning charges have been proposed, Mulliken method is widely used due to its convenient. Mulliken atomic charge [11-13] is defined based on orbitals. For each atom, all electronic charge contributions from orbitals centered at that atom are summed up, and electronic overlap clouds between two atoms are divided equally to the two atoms. However, they extremely basis-function dependent: changing basis functions could result in a big difference for the charge on the same atom[14,15].In this study two different basis sets were used to find the muliiken atomic charge of title molecule. They are tabulated in table.All the N atoms got negative charge except N2 atom. As well as all the C atoms got negative charge except C12 atom. Further, all the H atoms got positive charge and Cl atom got negative charge.



Nonlinear optical properties

In the current study, the nonlinear optical (NLO) effect is considered most important because it provides key functions of optical modulation, optical switching, optical logic, and optical memory for the emerging technologies in the areas telecommunications, optical interconnections, and signal processing [16]. In order to investigate the effects of the HF and DFT/B3LYP methods on the NLO properties of the studied compound, the dipole moments (μ) , the polarizabilities (α) , the anisotropy of the polarizabilities $(\langle \Delta \alpha \rangle)$, and the mean first- order hyperpolarizabilities (β) of 5ClTZ were calculated using the finite-field approach and are presented in Table 5.

The dipole moment, the mean polarizability of the title compound are calculated using Gaussian 09 software and are found to be 6.4941,6.4675 Debye 6-31G,6-311+G basis set respectively. The magnitude of the first hyperpolarizability from Gaussian 09 output is 0.9636×10^{-30} , 0.9552×10^{-30} esu 6-31G, 6-311+G basis set respectively. The β value calculated by the DFT/B3LYP method shows that the title compound is an attractive molecule for future studies of NLO properties. Based on NLO properties of (common values) urea; the mean firstorder hyperpolarizability and polarizability values of the studied molecule are bigger than those of urea.

Vibrational assignment

The detailed vibration assignments of fundamental modes of 5ClPTZ with observed and calculated frequencies and normal modes description are reported in Table 2. The observed experimental FT-IR, FT-Raman spectra are shown in Fig 2 and 3 respectively. The higher valu of theoretical

vibrations have been reduced by scaled factor 0.9555 for >1500 cm-1,0.9826 for <1500cm-1 in 6-31G basis set. as well as 0.9642 for >1500 cm-1,0.9860 for <1500cm-1 in 6-311+G basis set.

Typically, the C-Cl frequency band is absorbed between 850 and 550 cm-1 [17]. For the title compound the bands occured at 490 cm-1 in the IR spectrum are assigned as C-Cl stretching mode. According to the DFT theory, these bands are calculated at 479,440 cm-1 (6-31G) and 465,430(6-311+G) cm-1. The PED value of the CCl stretching modes is 45 and 16%. In this case the deformation modes of C-Cl are assigned at 235 cm-1 at Raman spectrum, whereas this bands have been observed at 228,218 cm-1 (6-31G) ,218,212 cm-1(6-311+G) in theoretically.

The C-H stretching vibrational modes of the title compound are expected in the region 3120-3000 cm-1[18]. This study reveals the CH stretching modes are assigned at 3073 cm-1 in the Raman spectrum, 3065 cm-1 in the IR spectrum and at 3096,3091,3081,3072,3062 cm-1 (6-31G) and 3166,3160,3150,3140,3129 cm-1 (6-311+G) theoretically. The ring stretching vibrational modes are expected in the region 1615-1260 cm-1[18]. In the present case,the ring modes are occured at 1691,1339,1116 cm-1 in the IR spectrum and 1599 cm-1 in the Raman spectrum. The theoretical calculation showed that mode at 1578, 1569,1104 cm-1 (6-31G) and 1616,1606,1291cm-1(6-311+G). **PED** contribution of the phenyl ring stretching modes were assigned at 29%, 44% and 62%. The C-H in-plane deformation of Clptz is expected in the range 1270-1045 cm-1[18]. For the title compound the phenyl C-H indeformation CH(Phenyl) plane observed at 1244, 1174 cm-1 in the in the



IR spectrum. The DFT calculation gives modes at 1209,1202 cm-1 (6-31G) and 1179,1171cm-1 (6-311+G). The C-H out-of-plane deformations are expected in the range [18] 980-740 cm-1[18]. These CHPh modes are observed at 853 cm-1 in the IR spectrum, corresponding calculated values are 1022,1000,860 cm-1 (6-31G) and 998,980,873 cm-1(6-311+G).

DFT computational method gives mode arising from the N-N stretching at 966,937 cm⁻¹ in 6-31G and 957,923 cm-1 in 6-311+G basis set corresponding to the peak at 975,924 cm-1 in IR spectrum. The C-N vibrations is a very critical task, since the mixing of vibrations is possible in this region. Silverstein et al. [19] attributed C-N stretching absorption in the region 1266for aromatic amines. In 1382 cm-1 benzamide the band observed at 1368 cm-1 is assigned to the CN stretching band [20]. In 1,2,4-triazole the band observed at 1390 and 1327 cm-1 are assigned to CN stretching [21]. The C-N stretching modes are reported in the range 1000-1400 cm-1 [22] and in the present case these bands are assigned at 1418,1382 (6-31G)1387,1347 (6-311+G) cm-1 theoretically. 1431,1410 cm-1 in IR and 1433 cm-1 in Raman.

Natural Bond Analysis

The Natural bond ortbital [23] analyzes is used to understand the delocalization of electron density and second order donor-acceptor energy. Typically, the stabilization of orbital interaction is high for higher energy differences between interacting orbitals. Effective donor and effective acceptor have this strong stabilization [24-27]. According to the second order perturbation approach, the

stabilization energy is derived [28]. The energy from (donor) $i \rightarrow$ (acceptor) j is calculated as

$$E^{2} = \Delta E_{ij} = q_{i} \frac{F(i, j)^{2}}{\varepsilon_{j} - \varepsilon_{i}}$$

Where, q_i is the donor orbital occupancy, ε_i , ε_j are diagonal elements (orbital energies) and F(i,j) is the off-diagonal NBO Fock matrix element. The NBO analysis gives valuable information about the intra and inters molecule interaction of the molecule [29].

The current work summarizes second order perturbative calculation donor-acceptor interactions based on NBO. This analysis was carried out by possible observing all interaction between lewis and non-lewis NBOs and calculated their stabilization energy (E2). Donor NBO (i), acceptor NBO (j) and stabilization energy (E2) tabulated in Table 5.7. From this table, it is show that the interaction between the Antibonded N2-N3 (NBO 152) and N4-C5 antibond (NBO 155) gives the strongest stabilization, 79.87 kcal/mol and also, antibond C7-C8 (NBO 158) \rightarrow C11-C12 antibond (NBO 168), antibond $C7-C8 \text{ (NBO 158)} \rightarrow C9-C10 \text{ antibond}$ (NBO 163), lone pair N1 (NBO 40) \rightarrow N2-N3 antibond (NBO 152) has the highest stabilization energy are 72.4, 69.1, 20.72kcal/mol Respectively.

CONCLUSION

The present investigation thoroughly analyzed the HOMO-LUMO, and vibration spectra, both infrared and Raman of PTZ



molecules with B3LYP method with standard 6-31G and 6-311+G basis sets. All the vibration bands are observed in the FT-IR and F-Raman spectra of the compound are assigned to various modes of vibration and most of the modes have wave numbers in the expected range. The complete vibration assignments of wave numbers are made on the basis of potential energy distribution (PED). The electrostatic potential surfaces (MEP) together with complete analysis of the vibration spectra, both IR and Raman spectra help to identify the structure and symmetry. The excellent agreement of the calculated and observed vibration spectra reveals the advantages over the other method. Finally, calculated HOMO-LUMO energies show that the charge transfer occurs in the molecule, which are responsible for the bioactive properly of the biomedical compound PTZ.

References

- [1]. Wittenberger, S.J. Organic Preparations and Procedures Int., 1994,26, 499. [2]. Butler, R.N. Adv. Heterocycl. Chem., 1977,21, 323; Singh, H.; Chawla, A.S.; Kapoor, V.K.; Paul, D. and Malhotra, R.K. "Progress in Medicinal Chemistry", Vol. 17, Eds: Ellis, G.P. and West, G.B., Elsevier, Biomedical PRSS, North-Holland, 1980, p. 15
- [3]. Wazir, V.; Singh, G.B.; Gupta, R. and Kachroo P.L. J. Ind. Chem SOC., 1991.68, 305. [4]. George, E.F. and Riddell, W.D. U.S. Pat. 3,865,570, Chem. Abstr., 1975.83, 54601; Theodoridis, G.; Hotzman, F.W.; Schcrer, L.W.; Smith, B.A.; Tymonko, J.M. and Wyle, M.J. Pestic. Sci., 1990, 30, 259, Chem. Abstr., 1991,114,159059v.
- [5]. Barratt, A.J.; Bates, L.R.; Jenkins, J.M. and White, J.R. U.S. Nut. Tech. Inform Serv., AD Rep., 1971, No. 752370, Chem. Abstr.,

- 1973. 78. 124508; Astashinsky, V.M.: Kostyukevich, Ivashkevich, O.A.; E.A.; Lesnikovich, A.I. and Krasitsky, V.A. Combust. Flame, 1994, 96, 286, Chem. Abstr., 1994,120,248733.
- [6]. Schwartz, N.V. J. Appl. Polym. Sci., 1972,16, 2715; Shelkovnikov, V.V.; Myakishev, K.G.; Kovalev, D. V.; Eroshkin, V.I. and Volkov, V.V. Chem. Abstr., 1990,112,207625j.
- [7]. R. Alcala, Acta Cryst. 28B (1972) 1671–1677.
- [8]. J.L. Derissen, Acta Cryst. 30B (1974) 2764–2765.
- [9]. Parr, R.G., Szentpaly, L.V., Liu, S., 1999. Electrophilicity index. J. Am. Chem. Soc. 121, 1922-1924.
- [10]. R.Dennington II, T.Keith, J. Millam, Gauss View, Version 4.1.2, Semichem, Inc., Shawnee Mission, KS(2007).
- [11]. R. S. Mulliken, J. Chem. Phys., 1955, 23, 1833–1840.
- [12]. R. S. Mulliken, J. Chem. Phys., 1955, 23, 1841–1846.
- [13]. R. S. Mulliken, J. Chem. Phys., 1955, 23, 2338–2342.
- [14]. C. W. Kern and M. Karplus, Journal of Chemical Physics, 1964, 40, 1374–1389.
- [15]. L. C. Cusachs and P. Politzer, Chemical Physics Letters, 1968, 1, 529–531.
- [16]. C. Andraud, T. Brotin, C. Garcia, F. Pelle, P. Goldner, B. Bigot, A. Collet, Theoretical and experimental investigations of the nonlinear optical properties of vanillin, polyenovanillin, and bisvanillin derivatives, J. Am. Chem. Soc. 116 (1994) 2094-2103.
- [17]. Arivazhagan, M., Jeyavijayan, S., 2011. Vibrational spectroscopic, first order hyperpolarizability and HOMO, LUMO studies of 1,2-dichloro-4-nitrobenzene based on Hartree-Fock and DFT calculations. Spectrochim. Acta. 79, 376-383.



- [18]. Roeges, N.P.G., 1994. A Guide to the Complete Interpretation of IR Spectra of Organic Compounds. Wiley, New York.
- [19]. R.M. Silverstein, G.C. Bassler, T.C. Morril, Spectrometric Identification of Organic Compounds, fifth ed., John Wiley and Sons Inc., Singapore, 1991.
- [20]. R. Shanmugam, D. Sathyanarayana, Spectrochim. Acta 40 (1984) 764–773.
- [21]. S. Genc, N. Dege, A. Cetin, A. Cansiz,M. Sekerci, M. Dincer, Acta Crystallogr. E60(2004) o1340-o1342.
- [22]. Kundoo, A.N. Banerjee, P. Saha, K.K. Chattopadhyay, Mater. Lett. 57 (2003) 2193–2197
- [23]. S. Muthu, J. Uma Maheswari, Tom Sundius. Spectrochimica acta part

- A.Molecular And Biomolecular spectroscopy 106, (2013)299-309.
- A. E. Reed, F. Weinhold. J. Chem. Phys. 83 (1985) 1736-1740.
- [24]. E. Reed, R. B. Weinstock, F. Weinhold. J. Chem. Phys. 83 (1985) 735-746.
- [25]. E. Reed, F. Weinhold. J. Chem. Phys. 78 (1983) 4066-4073.
- [26]. J. P. Foster, F. Weinhold. J. Am. Chem. Soc. 102 (1980) 7211-7218.
- [27]. P. Singh, S. S. Islam, H. Ahmad, A. Prabakaran. J. Mol. Struct. 1154 (2018) 39-50.
- [28]. K. R. Santhy et al. J. Mol. Struct. (2018). DOI.10. 1016/j. molstruc. 2018. 09. 058.

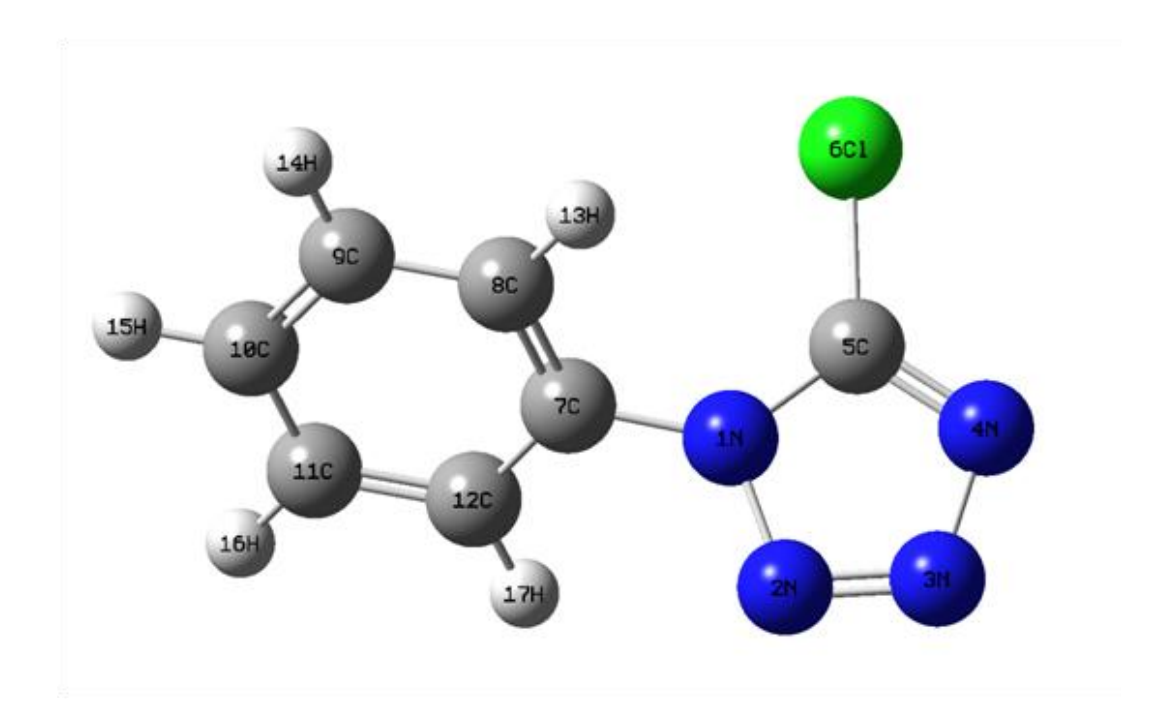


Fig 1. The theoretical geometry structure and atomic numbering scheme of 5-Chloro-1-phenyl-1H-tetrazole (5ClPTZ)



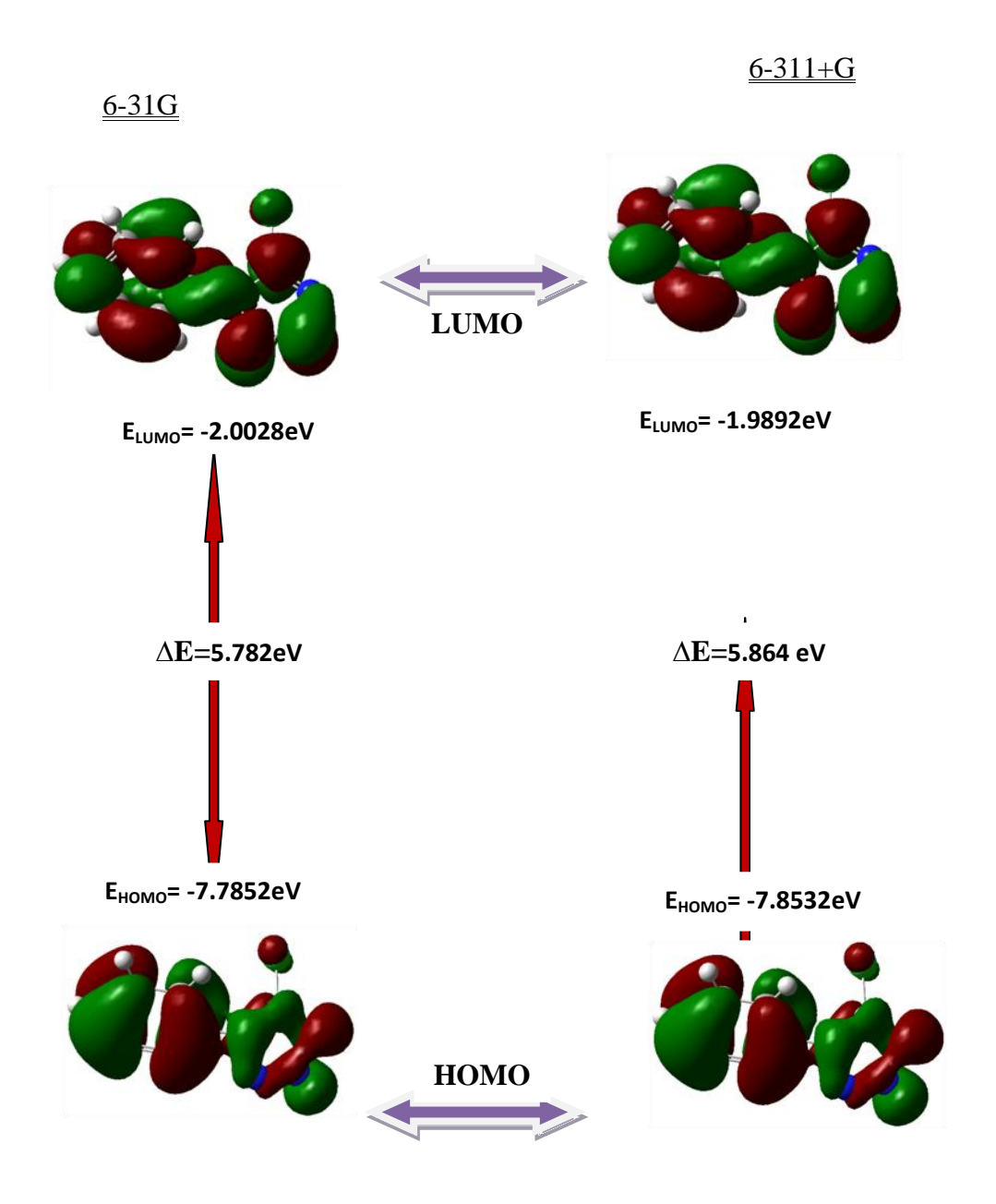


Fig 2: The atomic orbital compositions of the frontier molecular orbital for5-Chloro-1-phenyl-1H-tetrazole (5ClPTZ)..



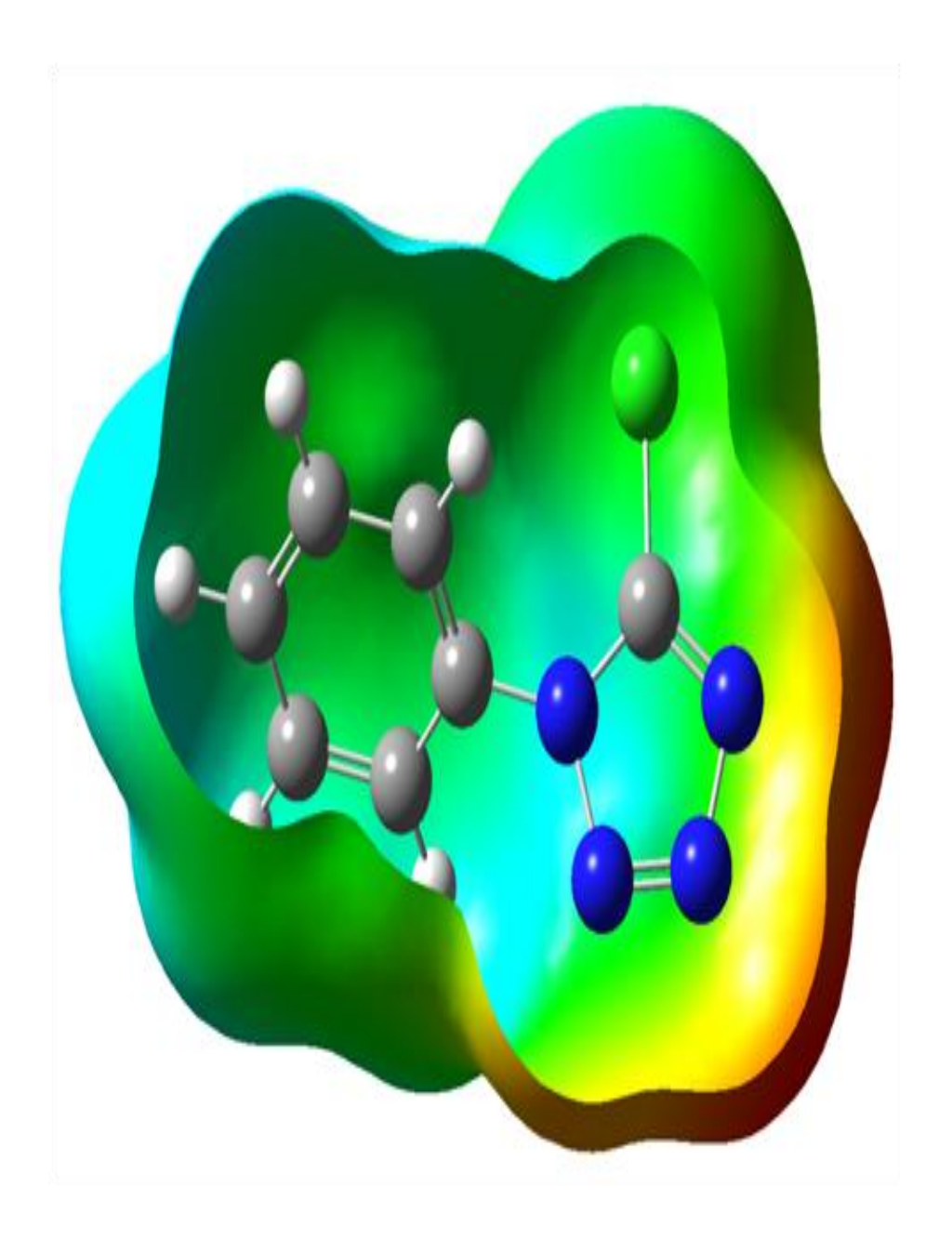


Fig 3. The total electron density surface mapped with of 5-Chloro-1-phenyl-1H-tetrazole (5ClPTZ)



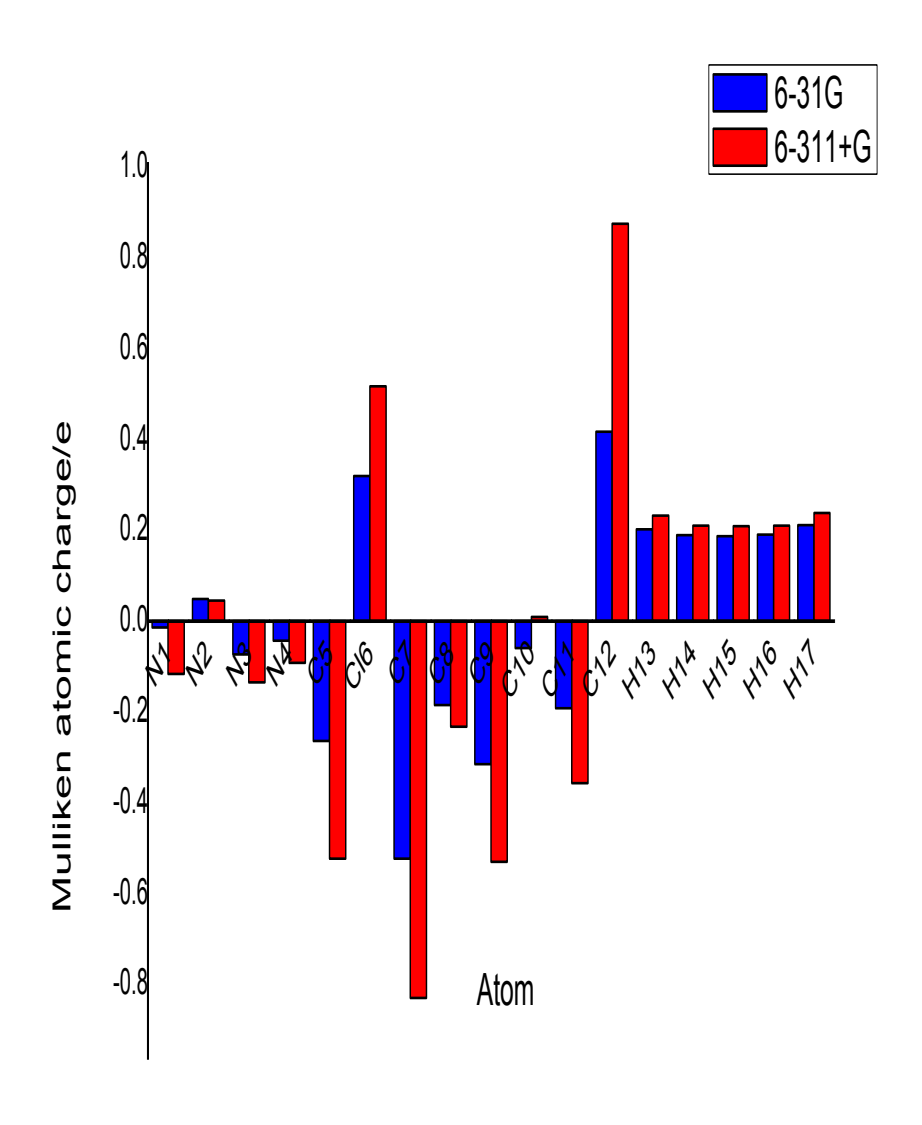


Fig 4 Bar diagram representing the Mulliken atomic charge distribution of 5-Chloro-1-phenyl-1H-tetrazole (5ClPTZ)



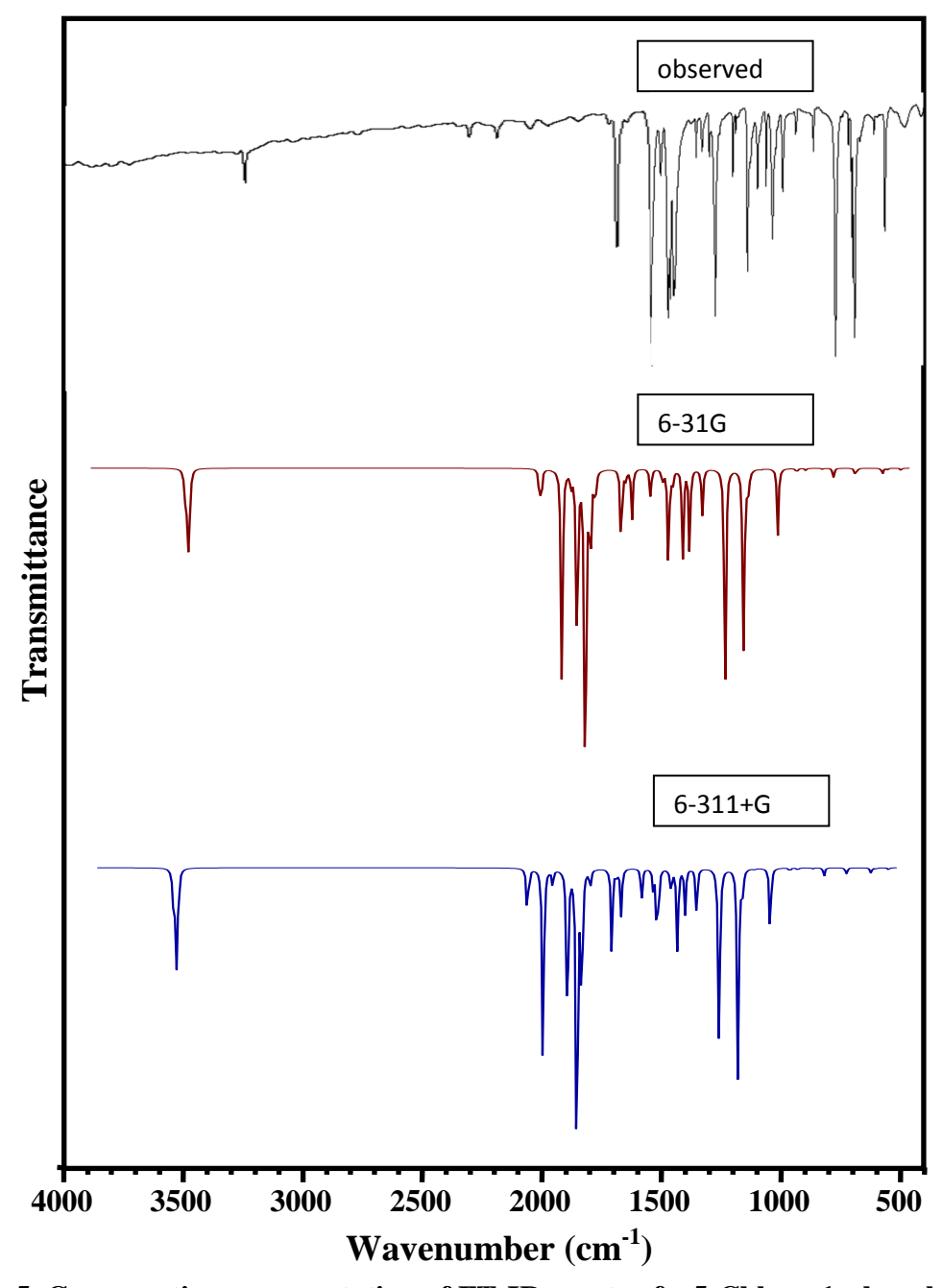


Fig 5. Comparative representation of FT-IR spectra for 5-Chloro-1-phenyl-1H-tetrazole (5ClPTZ).



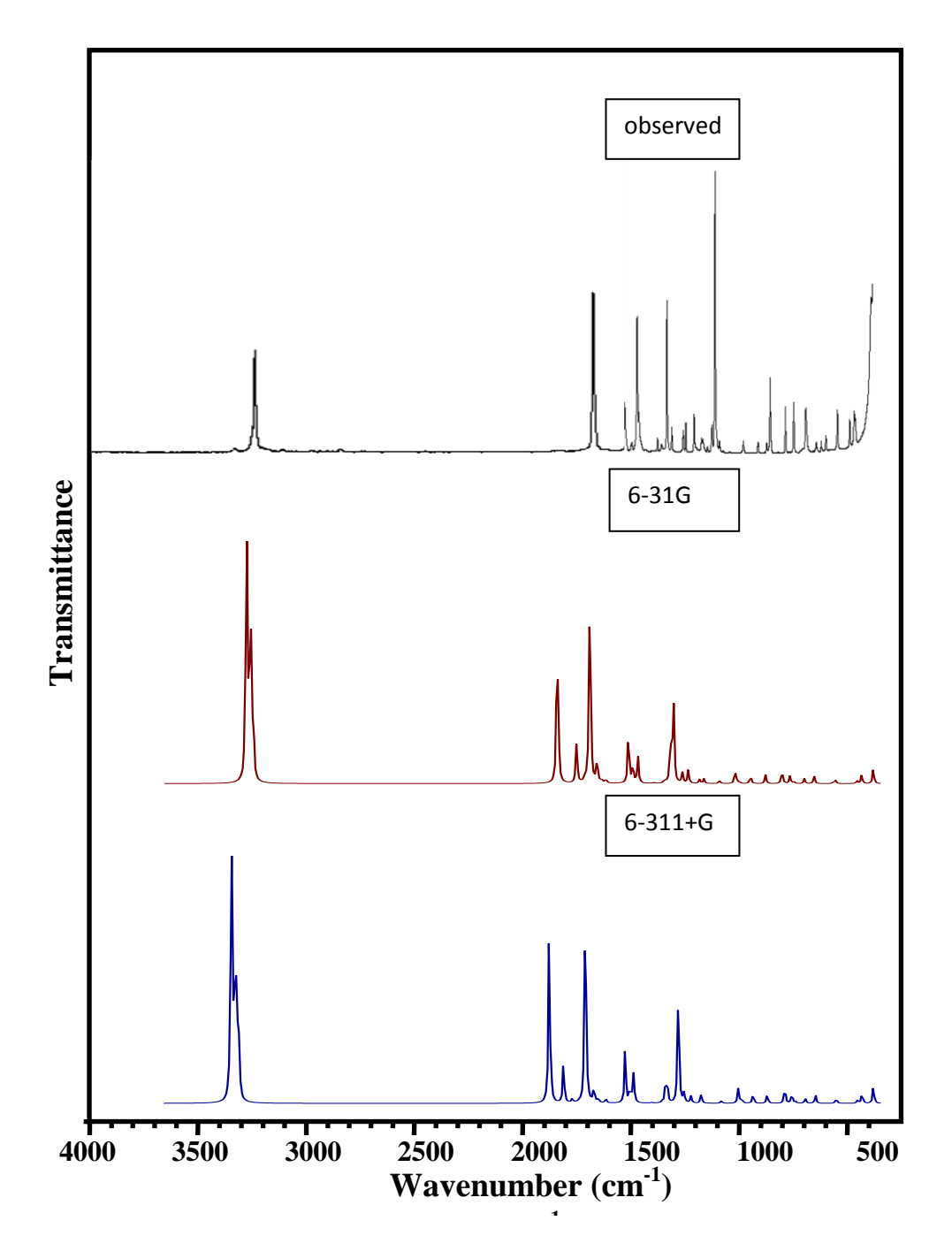


Fig 6. Comparative representation of FT-Raman spectra for 5-Chloro-1-phenyl-1H-tetrazole (5ClPTZ)



Table 1: Geometry Optimization Parameter of 5-Chloro-1-phenyl-1H-tetrazole (5ClPTZ) based on B3LYP/6-31G and B3LYP/6-311+G method and basis set.

BondLength(Å)			BondAngle(°)			
Atom	6-31G	6-311+G	Atom	6-31G	6-311+G	
C5-Cl6	1.76	1.76	C5-N1-C7	131.744	131.538	
N1-C7	1.43	1.43	N1-C5-Cl6	124.968	124.831	
N3-N4	1.40	1.40	N4-C5-Cl6	124.536	124.704	
C10-C11	1.40	1.40	N2-N1-C7	121.239	121.269	
C9-C10	1.40	1.40	C8-C7-C12	121.214	121.202	
N1-N2	1.40	1.40	C11-C12-H17	121.162	121.134	
C7-C8	1.40	1.40	C9-C8-H13	120.584	120.593	
C7-C12	1.40	1.40	C7-C8-H13	120.296	120.269	
C8-C9	1.40	1.40	C8-C9-C10	120.253	120.232	
C11-C12	1.40	1.40	C10-C9-H14	120.224	120.213	
N1-C5	1.36	1.36	C10-C11-H16	120.217	120.211	
N4-C5	1.33	1.32	C10-C11-C12	120.238	120.204	
N2-N3	1.32	1.32	C9-C10-C11	120.018	120.039	
C10-H15	1.09	1.08	N1-C7-C8	120.087	120.033	
C9-H14	1.08	1.08	C11-C10-H15	120.011	120.001	
C11-H16	1.08	1.08	C9-C10-H15	119.970	119.959	
C8-H13	1.08	1.08	C7-C12-H17	119.687	119.683	
C12-H17	1.08	1.08	C12-C11-H16	119.544	119.585	
			C8-C9-H14	119.519	119.551	
			C7-C12-C11	119.150	119.181	
			C7-C8-C9	119.118	119.134	
			N1-C7-C12	118.678	118.754	
			N2-N3-N4	110.949	110.785	
			N1-C5-N4	110.470	110.443	
			N2-N1-C5	107.004	107.178	
			N1-N2-N3	106.266	106.175	
			N3-N4-C5	105.311	105.419	



Table 2: HOMO-LUMO energy (eV) and other related properties of 5-Chloro-1-phenyl-1H-tetrazole (5ClPTZ) based on B3LYP/6-31G and B3LYP/6-311+G method and basis set.

Parameters	6-31G (eV)	6-311+G (eV)	
Homo(I)	-7.7852	-7.8532	
Lumo(A)	-2.0028	-1.9892	
Energy gap(ΔE)	5.7824	5.8641	
Electronegativity	4.8940	4.9212	
Global hardness	2.8912	2.9320	
Global softness(eV ⁻¹)	0.3459	0.3411	
Chemical potential	-4.8940	-4.9212	
Electriphilicity	4.1420	4.1299	

Table 3: Mulliken charge (charge/e) of 5-Chloro-1-phenyl-1H-tetrazole (5ClPTZ) based on B3LYP/6-31G and B3LYP/6-311+G method and basis set.

Atom	6-31G	6-311+G
Atom	Charge/e	
N1	-0.0142	-0.1162
N2	0.0482	0.0448
N3	-0.0734	-0.1347
N4	-0.0431	-0.0923
C5	-0.2643	-0.5233
Cl6	0.3190	0.5174
C7	-0.5227	-0.8294
C8	-0.1844	-0.2327
C9	-0.3151	-0.5296
C10	-0.0595	0.0095
C11	-0.1920	-0.3567
C12	0.4169	0.8746
H13	0.2016	0.2319
H14	0.1899	0.2097
H15	0.1873	0.2090
H16	0.1906	0.2103
H17	0.2117	0.2381



Table 4: Dipole moment(μ), Polarizability(α), Anisotropy polaraizability($\Delta\alpha$) and First order polarizability(β_{tot}) of 5-Chloro-1-phenyl-1H-tetrazole (5ClPTZ) based on B3LYP/6-31G and B3LYP/6-311+G method and basis set.

DSL 11/0-311+G memou and basis set.						
Parameters	6-31G	6-311+G				
μ_{x}	-5.8148	-5.8211				
$\mu_{ m y}$	2.8346	2.7621				
μ_{z}	-0.5722	-0.5609				
a_{XX}	-81.805	-81.9707				
α_{YY}	-80.4211	-80.7151				
α_{ZZ}	-75.0133	-74.632				
α_{XY}	5.8718	5.6262				
α_{XZ}	-0.2512	-0.202				
α_{YZ}	6.3594	6.4021				
β_{XXX}	-85.5234	-85.3691				
eta_{YYY}	31.8908	31.1578				
β_{ZZZ}	-1.4118	-1.2158				
β_{XYY}	-13.4878	-12.2542				
eta_{XXY}	21.7629	21.499				
$eta_{ ext{XXZ}}$	-7.532	-7.3829				
$eta_{\mathbf{XZZ}}$	4.4195	3.4289				
eta_{YZZ}	3.2261	3.0377				
$oldsymbol{eta_{YYZ}}$	-7.1489	-7.2038				
eta_{XYZ}	-7.499	-7.6444				
μ(debye)	6.4941	6.4675				
α(esu)	-11.7038 X10 ⁻²⁴	-11.7077 X10 ⁻²⁴				
$\Delta \alpha(esu)$	141.8267 X10 ⁻²⁴	142.1401 X10 ⁻²⁴				
$\beta_{tot}(esu)$	0.9636 X10 ⁻³⁰	$0.9552 \text{ X} 10^{-30}$				



Table 5: Observed Frequency (cm⁻¹), Theoretical Frequency (cm⁻¹) and Vibrational assignment with PED(%) of 5-Chloro-1-phenyl-1H-tetrazole (5ClPTZ) based on B3LYP/6-31G (0.9555, 0.9826)and B3LYP/6-311+G (0.9642, 0.9860)method and basis set.

		Observe	ed		retical	<u> </u>				
		Frequer	ncy(cm ⁻¹)	Freq	uency(cr	n ⁻¹)	Vibrational			
s.no	cis		FT-Raman	6-31G		6-311+G		Assignment (PED %)		
	Spe cis			Calc	scaled	Calc	Scaled			
1	A	_	-	3240	3096	3211	3166	ν CH(55)		
2	A	-	-	3235	3091	3205	3160	ν CH(44)		
3	A	-	-	3225	3081	3194	3150	ν CH(50)		
4	A	-	3073	3215	3072	3185	3140	ν CH(72)		
5	A	3065	-	3204	3062	3173	3129	v CH(85)		
6	A	1691	-	1651	1578	1639	1616	v CC(29)		
7	A	-	1599	1642	1569	1629	1606	ν CC(44)		
8	A	-	-	1552	1483	1545	1524	β HCC(36)		
9	A	1502	1503	1511	1444	1503	1482	β HCC(32)		
10	A	1431	1433	1443	1418	1439	1387	v NC(35)		
11	A	1410	-	1406	1382	1397	1347	ν NC(44)		
12	A	1404	-	1384	1360	1376	1327	β HCC(22)		
13	A	1339	-	1363	1340	1339	1291	ν CC(62)		
14	A	1267	1269	1251	1229	1245	1200	β NCN(18)		
15	A	1244	-	1231	1209	1223	1179	β HCC(37)		
16	A	1174	-	1223	1202	1215	1171	β HCC(61)		
17	A	1164	1165	1203	1182	1203	1160	$v NN(65) + \beta CNN(16)$		
18	A	1116	1119	1123	1104	1114	1074	ν CC(21)		
19	A	1041	-	1071	1052	1064	1026	β CCC(27)		
20	A	1015	-	1046	1028	1047	1010	β NNN(54)		
21	A	1003	1004	1042	1024	1039	1002	β CCC(53)		
22	A	-	-	1040	1022	1035	998	τ HCCC(50)+ τ CCCC(31)		
23	A	-	_	1028	1010	1021	984	ν CC(61)		
24	A	-	-	1018	1000	1017	980	τ HCCC(37)		
25	A	975	-	983	966	992	957	v NN(39)		
26	A	924	-	953	937	957	923	ν NN(19)		
27	A	-		898	882	905	873	ν NCN(41)		
28	A	853	-	876	860	877	873	τ HCCC(55)		
29	A	755	-	799	785	803	774	τ HCCC(52)		
30	A	-	-	718	705	718	696	τ CCCC(28)		
31	A	714	-	717	710	717	694	τ CCCC(38)		
32	A	702	-	709	697	701	676	β CCN(47)		
33	A	696	699	696	684	696	671	δ NNNC(60)		
34	A	612	614	644	633	643	620	τ CCC(46)		
35	A	570	568	569	559	571	551	β NCCC(19)		
36	A	490	-	487	479	483	465	v ClC(45)		
37	A	-	-	448	440	446	430	ν ClC(16)		



38	A	-	-	427	420	428	413	ν CCCC(69)
39	Α	-	-	377	370	379	365	β NCC(13)
40	A	-	327	327	322	327	315	τ CCCC(18)
41	A	-	235	232	228	226	218	β ClCN(21)+ $δ$ ClNNC(39)
42	A	-	-	222	218	220	212	β ClCN(20)
43	Α	-	-	115	113	114	110	β NCC(24)+ $δ$ NCNC(37)
44	A	-	-	92	90	91	88	β NNC(30)
45	A	-	-	34	33	34	33	δ NNCC(86)

Table 6: Natural Bond Orbital Calculation of 5-Chloro-1-phenyl-1H-tetrazole (5ClPTZ).

S.No	Donor NBO (i)			Acce	ptorNE	30 (j)	E(2)	E(j)-E(i)	F(i,j)
							kcal/mol	a.u.	a.u.
1	152	BD*	N2-N3	155	BD*	N4-C5	79.87	0.02	0.059
2	158	BD*	C7-C8	168	BD*	C11-C12	72.4	0.01	0.062
3	158	BD*	C7-C8	163	BD*	C9-C10	69.1	0.01	0.063
4	40	LP	N1	152	BD*	N2-N3	20.72	0.33	0.075
5	40	LP	N1	155	BD*	N4-C5	19.44	0.34	0.074
6	8	BD	N4-C5	152	BD*	N2-N3	14.11	0.32	0.062
7	45	LP	Cl6	161	BD*	C8-H13	14.11	0.88	0.1
8	46	LP	Cl6	161	BD*	C8-H13	14.02	0.87	0.1
9	16	BD	C9-C10	158	BD*	C7-C8	11.82	0.28	0.052
10	21	BD	C11-C12	158	BD*	C7-C8	11.69	0.29	0.052
11	46	LP	Cl6	155	BD*	N4-C5	11.25	0.33	0.057
12	16	BD	C9-C10	168	BD*	C11-C12	11.1	0.3	0.051
13	40	LP	N1	158	BD*	C7-C8	10.92	0.41	0.062
14	21	BD	C11-C12	163	BD*	C9-C10	10.83	0.3	0.051
15	42	LP	N3	148	BD*	N1-N2	10.66	0.69	0.076
16	11	BD	C7-C8	168	BD*	C11-C12	10.39	0.32	0.051

Author search

Sources



Create account

Sign in

Sources

Scopus API

Privacy matters

ISSN	Enter IS	SN or ISSNs	Fi	nd sources					
ISSN: 0011-9342 ×									
which provides an in calculation of CiteSco	e CiteScore modication of resore, as well as alues have been	ethodology to ensure a more robust, stable and consearch impact, earlier. The updated methodology retroactively for all previous CiteScore years (ie. 2 en removed and are no longer available.	will be applied t	to the				×	
Filter refine list	1 result		t. Davida	h. Dayunlaad Caanus Cayusa List		① Learn more about Scopus Source List			
Apply Clear filters		☐ All ✓		a Scopus Source List	View metrics for year:		2020		
Display options	^	Source title $igspace$	CiteScore		Citations 2017-20 ↓	Documents 2017-20 \downarrow	% Cited ↓	>	
Display only Open Access journals Counts for 4-year timeframe No minimum selected		Design Engineering (Toronto)	1.0	35% 191/297 General Engineering	57	58	19		
Minimum citations Minimum documents	·	↑ Top of page							
Citescore highest quartile Show only titles in top 10 percent									
1st quartile									
2nd quartile 3rd quartile 4th quartile									
Source type	^								
☐ Journals ☐ Book Series									
Conference Proceedings Trade Publications									
Apply Clear filters									
About Scopus		Language		Custome	r Service				
What is Scopus Content coverage Scopus blog		日本語に切り替える 切换到简体中文 切換到繁體中文		Help Contact us					

Русский язык

ISSN: 0011-9342 | Year 2021 Issue: 7 | Pages: 10815 - 10830

Vibrational Spectra(Theoretical, Experimental) and Optimized Structure, Frontire Molecular Orbital, Mulliken Atomic Charge Studies on Pentylenetetrazole (PTZ) Based on Density Functional Theory

A.Rajeswari^a, M.K. Murali^a*A.Ramu^b

^a PG and Research department of physics, JJ. College of Arts & Science (Autonomous), Pudukottai-622422, Tamil Nadu, India.

*aramusir80@gmail.com

Abstract

The vibrational spectra of Pentylenetetrazole (PTZ) have been recorded in the regions $4000-400~\text{cm}^{-1}$ for FT-IR and $3500-100~\text{cm}^{-1}$ for FT-Raman. The molecular structure, geometry optimization, vibrational frequencies were obtained by the density functional theory (DFT) using B3LYP method with 6-31G and 6-311+G basis sets. The complete assignments were performed on the basis of the potential energy distribution (PED) of the vibrational modes, calculated and the scaled values were compared with experimental FT-IR and FT-Raman spectra. The HOMO and LUMO energy gap reveals that the energy gap reflects the chemical activity of the molecule. The dipole moment (μ), polarizability (α), anisotropy polarizability ($\Delta\alpha$) and first hyperpolarizability (β_{tot}) of the molecule have been reported. Information about the size, shape, charge density distribution and site of chemical reactivity of the molecule has been obtained by molecular electrostatic potential (MEP).

Key words: Pentylenetetrazole, DFT, FT-IR, FT-Raman, MEP

Introduction

The biological potential molecule Pentylenetetrazole (PTZ) is a tetrazole derivative and inhibitor of the γ aminobutyric acid (GABAA) and its receptor complex[1,2]. PTZ is a convulsing agent used for inducing seizures. It can traverse the blood-brain barrier[3]. As well as Pentylenetetrazole has been used to induce seizures in zebra fish larvae[4], mice[5], and male wistar rats[6]. This extensive applications of tetrazoles derivatives stimulated research in areas such as the reactivity of various tetrazolyl derivatives and the design of synthetic methodologies. In these studies, the molecular structure, vibrational spectra and HOMO-LUMO energy gap of Pentylenetetrazole (PTZ) were investigated by a concerted approach using matrix isolation

^b Department of Physics, Ganesar College of Arts and Science, Melaisivapuri-622403, Tamil Nadu, India.

Design Engineering

ISSN: 0011-9342 | Year 2021 Issue: 7 | Pages: 10815 - 10830

vibrational spectroscopy and high-level DFT-based theoretical calculations. Regarding their studies, tetrazoles have been found to be extremely interesting and challenging molecules.

Experimental Details:

The fine sample of PTZ was obtained from Lancaster Chemical Company.UK, with a stated purity of 99% and it was used as such without further purification. The FT-Raman Spectrum of PTZ was recorded using 1064 nm line of ND: YAG laser for excitation wavelength in the region 3500-100 cm⁻¹ on Thermo Electron Corporation model Nexus spectrometer equipped with FT-Raman module accessory. The FT-IR Spectrum of the title compound was recorded in the region 4000-400 cm⁻¹ on Perking Elmer Spectrophotometer in KBr pellet.

3. Computational Details:

The combination of Vibration spectra with quantum chemical calculation is effective for understanding the fundamental mode of vibration of the compound. The structural characteristic, stability and energy of the compound under investigation are determined by DFT with the three-parameter hybrid functional (B₃) for the exchange part and the Becke Three Lee Yong-Pare (LYP) and 6-31G ,6-311+G basis sets with Gaussian 09 Program Package. The Cartesian representation of the theoretical force constants has been compound at the fully optimized geometry by assuming the molecule belongs to C₁point group symmetry. The Transformation of force field from Cartesian to internal local symmetry coordinates, the scaling, and the subsequent normal coordinate analysis (NCA) Calculation of potential energy distributions (PED) has been done on a PC with the VEDA program.

Molecular geometry

The optimized structures of the title compounds along with numbering of atoms are shown in Figure 1. Due to the global minimum energy all the calculated vibrational wavenumbers using the optimized geometry were found to be positive for the title compounds. The bond lengths, bond angles and the optimized parameters calculated using the DFT method is shown in the Supplementary material (Tables 1).

An organic heterobicyclic compound that is 1H-tetrazole in which the hydrogens at positions 1 and 5 are replaced by a pentane-1,5-diyl group. Further, in TPZ, the bond lengths of C6-C7, C7-C8, C8-C9, C9-C10, C8-C10 were found to be elongated to 1.55 Å, 1.54 Å, 1.54 Å, 1.54 Å respectively compared to pentamethylene and tetrazole connection bond C5-C6 values of 1.49 Å. In this structure, C-C bond length has longer value and C-H bond length has shorter value (1.10 Å). The bond lengths of N3-N4, N1-N2 were found to be elongated to 1.40 Å, 1.39 Å respectively, compared to N2-N3 values of 1.32 Å. Because bond order of N2-N3 is higher than N3-N4, N1-N2 bond order [7]. The two different basis set good agreement with each other.

Design Engineering

ISSN: 0011-9342 | Year 2021 Issue: 7 | Pages: 10815 - 10830

Frontier molecular orbital analysis

The highest occupied molecular orbital (HOMO) and lowest unoccupied molecular orbital (LUMO) and their properties are very useful to analyze the chemical reaction of molecule. The HOMO and LUMO energies are directly related to the ionization potential and electron affinity respectively [8, 9].those is also used by the frontier electron density for predicting the most reactive position in pi-electron systems and also explains several types of reaction in conjugated system [10]. The conjugated molecules are characterized by a small energy gap, which is the result of a significant degree of intra-molecular charge transfer from the endcapping electron-donor groups to the efficient electron-acceptor group through pi-conjugated path [11]. The HOMO and LUMO plots of the title compound are shown in Figs. 2. The energy gap(ΔE) is a critical parameter in determining molecular electrical transport properties because it is a measure of electron conductivity. By using the HOMO and LUMO energy values, the global chemical reactivity descriptors such as hardness, chemical potential, electronegativity and electrophilicity index as well as local reactivity have been defined. Pauling introduced the concept of electronegativity as the power of an atom in a molecule to attract electrons to it. Hardness (η) , chemical potential (μ) , electrophilicity (ω) and electronegativity (γ) are defined using Koopman's theorem as $\eta = (I - A)/2$, $\mu = -(I + A)/2$ and $\gamma = (I + A)/2$ A)/2, where $I = -E_{HOMO}$ and $A = -E_{LUMO}$ are the ionization potential and electron affinity of the molecule. Considering the chemical hardness, large energy gap denotes a hard molecule and small gap denotes a soft molecule. One can also relate the stability of the molecule to hardness, which means that the molecule with least energy gap means, it is more reactive. Parr et al. [12] have defined a descriptor to quantify the global electrophilic power of the molecule as electrophilicity index, $\omega = \mu^2/2\eta$. The usefulness of this new reactivity quantity has been recently demonstrated in understanding the toxicity of various pollutants in terms of their reactivity and site selectivity [13-19]. The global parameters of compound PTZ are given in Table 2.

Molecular Electrostatic Potential (MEP):

The molecular electrostatic potential (MEP) method is used to study the interaction of a molecular system with its surroundings which is used for predicting sites and relative reactivity towards electrophilic attack and in studies of biological recognition. The MEP surface which is a method of mapping electrostatic potential on to the isoelectron density surface and it provides a visual method to understand the relative polarity [20]. To predict reactive sites of electrophilic and nucleophilic attacks for the investigated molecule, MEP at the B3LYP level optimized geometry was calculated. The different values of the electrostatic potential at the MEP surface are represented by different colors; red, blue and green represent the regions of most negative, most positive and zero electrostatic potential respectively. The MEP plots of the title compound PTZ is shown in Fig. 3and it provides a visual representation of the chemically active sites and comparative reactivity of atoms. The negative electrostatic potential corresponds to an attraction of proton by the aggregate electron density in the molecule (shades of red and yellow) and the positive electrostatic potential corresponds to the repulsion of proton by the nuclei (shades of blue). The electrophilic attack, nucleophilic attack and zero region of the title compound are depicted by Fig 3.

Design Engineering

ISSN: 0011-9342 | Year 2021 Issue: 7 | Pages: 10815 - 10830

Mulliken Atomic charge

The Mulliken atomic charge calculation has vital role in the application of quantum mechanics calculations to molecular system: the calculation of effective atomic charge plays an important role [21]. The electron distribution in PTZ is compared in two different quantum chemical methods and the sensitivity of the calculated charges to charge in the choice of methods is studies. By determining the electron population of each atom in the define basis function, the Mulliken charges are calculated. An estimated Mulliken charges at both levels are lists in Table 3. The results can be represented in graphical form as given in Fig 4.

Nonlinear optical properties

Theoretical evaluation of the polarizability (a), and the first order hyperpolarizabilities (b) is used to the design of new compounds for nonlinear optical applications and to understand the interaction between electromagnetic field and matter [22]. The calculation of hyperpolarizability and related properties have been carried out at DFT level by finite field approach.

The dipole moment, the mean polarizability of the title compound are calculated using Gaussian 09 software and are found to be 7.1416,7.3831 Debye 6-31G,6-311+G basis set respectively. The magnitude of the first hyperpolarizability from Gaussian 09 output is 0.6177X10⁻³⁰, 0.6692 X10⁻³⁰esu 6-31G, 6-311+G basis set respectively.

Vibrational assignment

The title compound belongs to C1 symmetry, consists of 20 atoms species and get 54 fundamental vibrations. The detailed vibration assignments of fundamental modes of PTZ with observed and calculated frequencies and normal modes description are reported in Table 2. The observed experimental FT-IR, FT-Raman spectra are shown in Fig 2 and 3 respectively. The higher valu of theoretical vibrations have been reduced by scaled factor 0.9555 for >1500 cm-1,0.9826 for <1500cm-1 in 6-31G basis set. as well as 0.9642 for >1500 cm⁻¹,0.9860 for <1500cm-1 in 6-311+G basis set.

B3LYP computation gives mode arising from the N-N stretching at 1129 cm⁻¹in 6-31G and 1119 cm⁻¹ in 6-311+G basis set corresponding to the peak at 1115 cm⁻¹ in IR spectrum. The C-N vibrations is a very critical task, since the mixing of vibrations is possible in this region. Silverstein et al. [23] attributed C-N stretching absorption in the region 1266–1382 cm⁻¹ for aromatic amines. In benzamide the band observed at 1368 cm⁻¹ is assigned to the CN stretching band [24]. In 1,2,4-triazole the band observed at 1390 and 1327 cm⁻¹are assigned to CN stretching [25]. The C-N stretching modes are reported in the range 1000–1400 cm⁻¹[26] and in the present case these bands are assigned at 1194, 1269, 1533 (6-31G) 1191,1268, 1530(6-311+G) cm⁻¹ theoretically. 1171,1246,1530 cm⁻¹ in IR and 1242,1531 cm⁻¹ in Raman.

ISSN: 0011-9342 | Year 2021 Issue: 7 | Pages: 10815 - 10830

The vibrations of the CH_2 group (attached with the tetrazole ring), the asymmetric stretch CH_2 , symmetric stretch CH_2 , scissoring vibration CH_2 and wagging vibration CH_2 appear in the regions, 3000 ± 50 , 2965 ± 30 , 1455 ± 55 and 1350 ± 85 cm⁻¹, respectively [27,28]. The B3LYP calculations give stretching vibration of CH_2 at 3007-2885 cm⁻¹ in 6-31G basis set, 3003-2860 cm⁻¹ in 6-311+G basis set. Experimentally bands are observed at 2946-2821 cm⁻¹ in IR and at 3005-2869 cm⁻¹ in the Raman spectrum as CH_2 stretching modes. All the bands were also found well within the characteristic region and presented in.

Table 1: Geometry Optimization Parameter of Pentelyenetetrazole (PTZ) based on B3LYP/6-31G and B3LYP/6-311+G method and basis set.

Be	ondLength(A)	Å)	BondAngle(°)			
Atom	6-31G	6-311+G	Atom	6-31G	6-311+G	
C6-C7	1.55	1.55	C5-N1-C10	130.49	130.37	
C7-C8	1.54	1.54	N4-C5-C6	125.87	125.85	
C8-C9	1.54	1.54	N1-C5-C6	125.56	125.56	
C9-C10	1.54	1.53	N2-N1-C10	120.94	120.97	
C5-C6	1.49	1.49	C7-C8-C9	115.96	116.05	
N1-C10	1.46	1.46	C8-C9-C10	115.2	115.20	
N3-N4	1.40	1.40	C6-C7-C8	115.07	115.10	
N1-N2	1.39	1.39	C5-C6-C7	114.17	114.14	
N1-C5	1.36	1.36	N1-C10-C9	112.95	112.91	
N4-C5	1.34	1.34	C9-C10-H20	111.04	111.04	
N2-N3	1.32	1.32	N2-N3-N4	110.61	110.69	
C6-H11	1.10	1.10	C9-C10-H19	110.56	110.41	
C7-H13	1.10	1.10	C8-C9-H18	110.16	110.23	
C7-H14	1.10	1.09	C7-C6-H12	110.12	110.04	
C8-H15	1.10	1.09	C8-C7-H14	109.77	109.81	
C8-H16	1.10	1.09	C5-C6-H11	109.73	109.77	
C9-H17	1.10	1.09	C6-C7-H14	109.21	109.26	
C9-H18	1.10	1.09	C7-C6-H11	109.13	109.24	
C10-H19	1.10	1.09	C7-C8-H15	109.13	109.12	
C6-H12	1.09	1.09	C9-C8-H15	109.06	109.06	
C10-H20	1.09	1.09	C10-C9-H18	108.94	108.97	
			N1-C10-H19	108.76	108.68	
			N2-N1-C5	108.58	108.66	
			N1-C5-N4	108.56	108.58	
			C8-C9-H17	108.56	108.54	
			C8-C7-H13	108.31	108.30	
			C7-C8-H16	108.14	108.14	
			H19-C10-H20	108.00	107.99	

C9-C8-H16	107.97	107.86
C6-C7-H13	107.59	107.58
C10-C9-H17	106.94	106.96
H11-C6-H12	106.8	106.71
H17-C9-H18	106.66	106.63
C5-C6-H12	106.62	106.55
H13-C7-H14	106.53	106.42
N3-N4-C5	106.2	106.26
H15-C8-H16	106.14	106.09
N1-N2-N3	106.04	106.02
N1-C10-H20	105.28	105.40

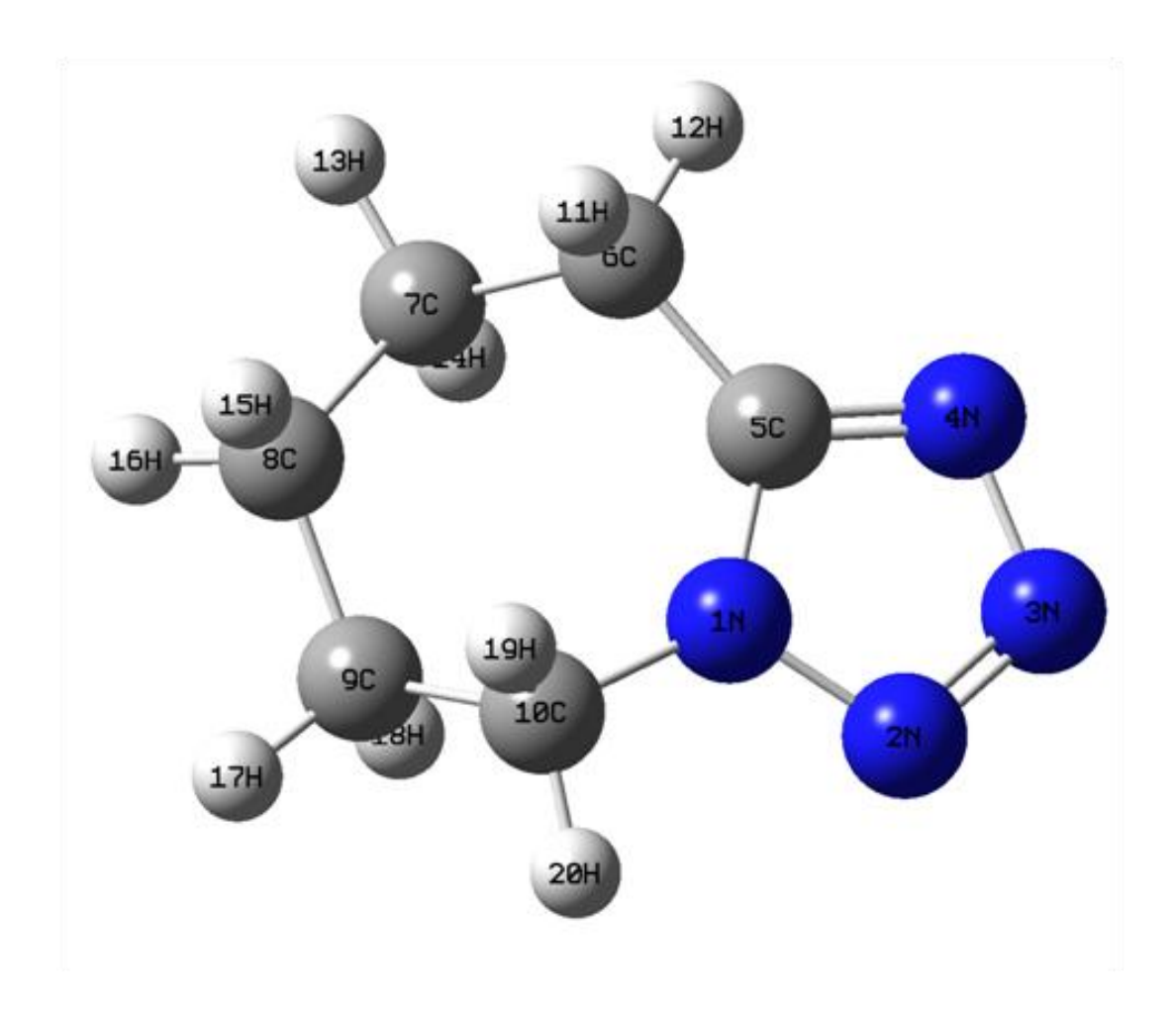


Fig. 1. The theoretical geometry structure and atomic numbering scheme of Pentylenetetrazole (\mbox{PTZ})

Table 2: HOMO-LUMO energy (eV) and other related properties of Pentelyenetetrazole (PTZ) based on B3LYP/6-31G and B3LYP/6-311+G method and basis set.

Parameters	6-31G (eV)	6-311+G (eV)
Homo(I)	-7.5293	-7.8994
Lumo(A)	-0.6585	-1.0204
Energy gap(ΔE)	6.8708	6.8790
Electronegativity	4.0939	4.4599
Global hardness	3.4354	3.4395
Global softness(eV ⁻¹)	0.2910	0.2907
Chemical potential	-4.0939	-4.4599
Electriphilicity	2.4393	2.8915

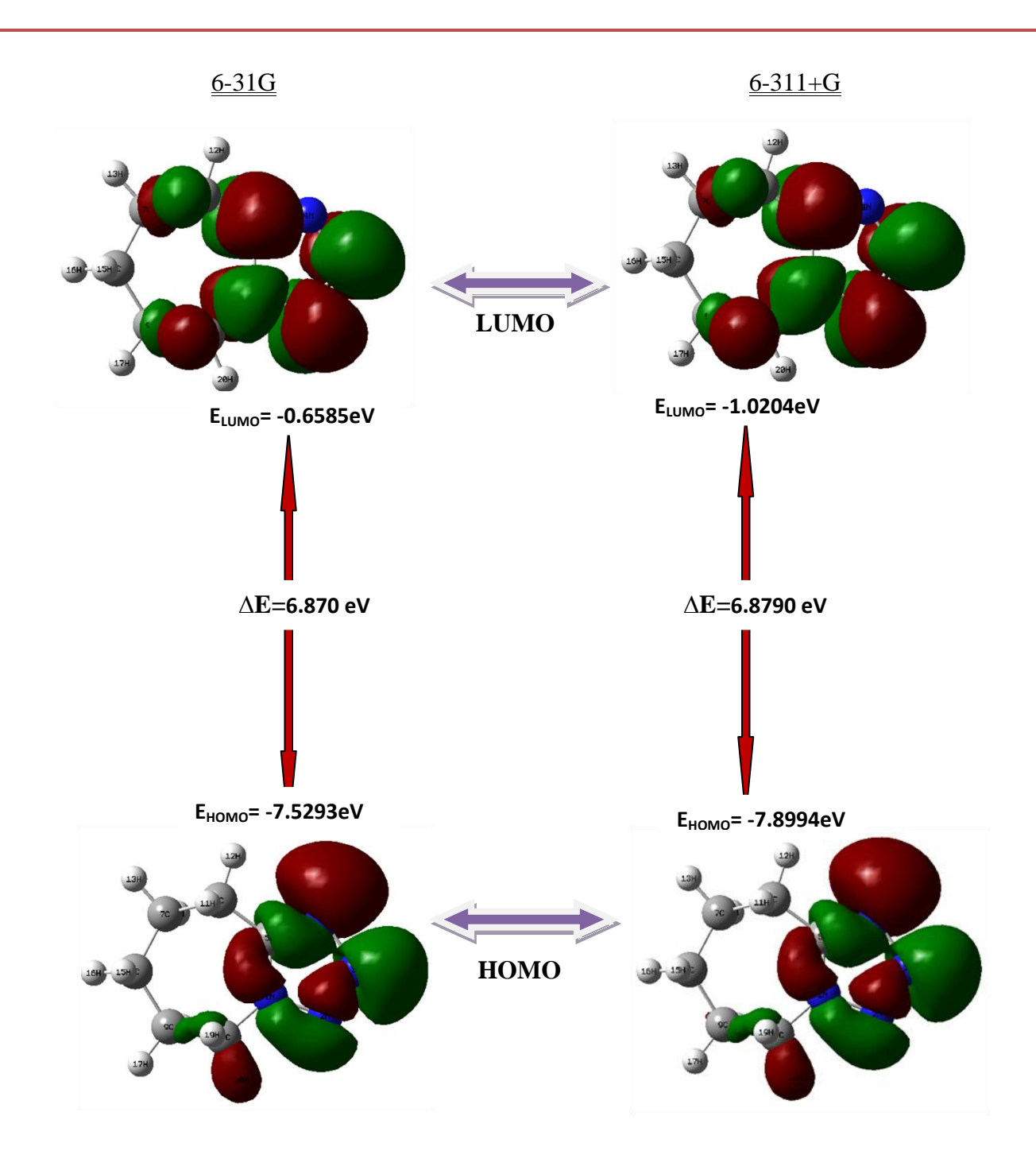


Fig 2:The atomic orbital compositions of the frontier molecular orbital for pentelyenetetrazole (PTZ).

Table 3: Mulliken charge (charge/e) of Pentelyenetetrazole (PTZ) based on B3LYP/6-31G and B3LYP/6-311+G method and basis set.

	6-31G	6-311+G
Atom	Cl	narge/e
N1	-0.5433	-0.2775
N2	0.0042	0.2422
N3	-0.0973	-0.0681
N4	-0.3257	-0.1392
C5	0.5090	0.1250
C6	-0.2788	-0.5999
C7	-0.2482	-0.3476
C8	-0.2519	-0.5628
C9	-0.2522	-0.2626
C10	-0.0793	-0.6035
H11	0.1598	0.2747
H12	0.1825	0.2706
H13	0.1440	0.2357
H14	0.1471	0.2496
H15	0.1277	0.2357
H16	0.1427	0.2325
H17	0.1474	0.2393
H18	0.1539	0.2510
H19	0.1683	0.2467
H20	0.1901	0.2581

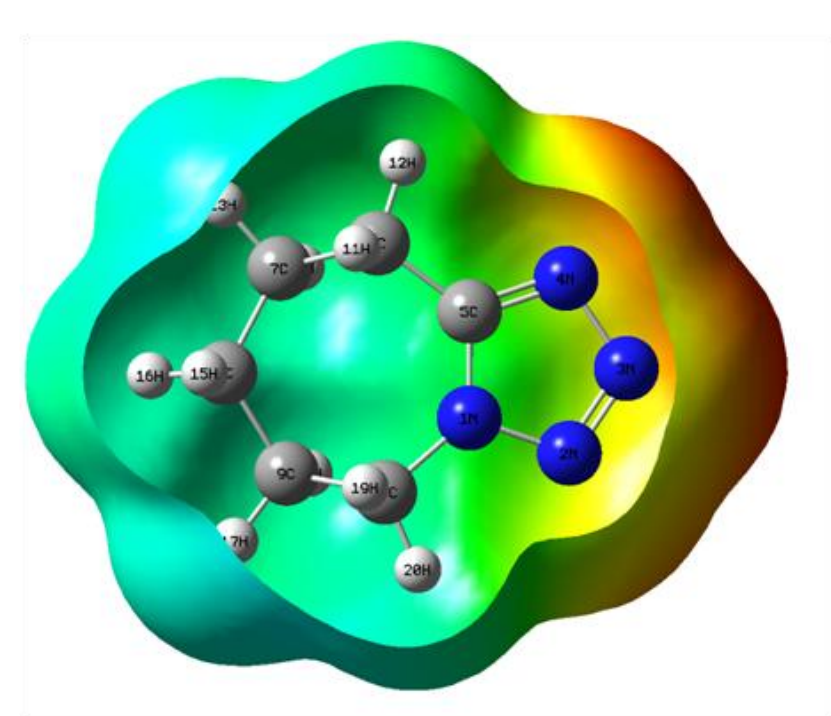


Fig. 3. The total electron density surface mapped with of Pentylenetetrazole (PTZ).

Table 4: Dipole moment(μ), Polarizability(α), Anisotropy polaraizability($\Delta\alpha$) and First order polarizability(β_{tot}) of Pentelyenetetrazole (PTZ) based on B3LYP/6-31G and B3LYP/6-311+G method and basis set.

Parameters	6-31G	6-311+G
μ_{x}	-6.9613	-7.1981
$\mu_{ m y}$	-0.8587	-0.8722
μ_{z}	1.3437	1.3917
a_{XX}	-73.8034	-75.6721
a_{YY}	-59.1621	-60.6258
a_{ZZ}	-58.4211	-59.6432
a_{XY}	-0.9227	-0.9443
$a_{ ext{XZ}}$	2.2679	2.3738
$a_{ m YZ}$	-0.0276	-0.0363
$eta_{ extbf{XXX}}$	-52.1379	-55.563
$oldsymbol{eta_{YYY}}$	-5.5846	-5.9735
$oldsymbol{eta_{ZZZ}}$	1.3902	1.8947
$oldsymbol{eta_{XYY}}$	-16.5269	-18.1617
$oldsymbol{eta_{XXY}}$	-3.4782	-3.5951
$oldsymbol{eta_{XXZ}}$	5.5513	5.6818
$oldsymbol{eta_{XZZ}}$	-1.3562	-2.1705
$oldsymbol{eta_{YZZ}}$	-1.0458	-1.2285

$oldsymbol{eta_{YYZ}}$	3.3821	3.5901
$oldsymbol{eta_{XYZ}}$	0.3376	0.2452
μ(debye)	7.1416	7.3831
α(esu)	-9.4417X10 ⁻²⁴	-9.6664 X10 ⁻²⁴
$\Delta \alpha(esu)$	19.0493X10 ⁻²⁴	19.5343 X10 ⁻²⁴
$\beta_{tot}(esu)$	$0.6177X10^{-30}$	$0.6692 \text{ X} 10^{-30}$

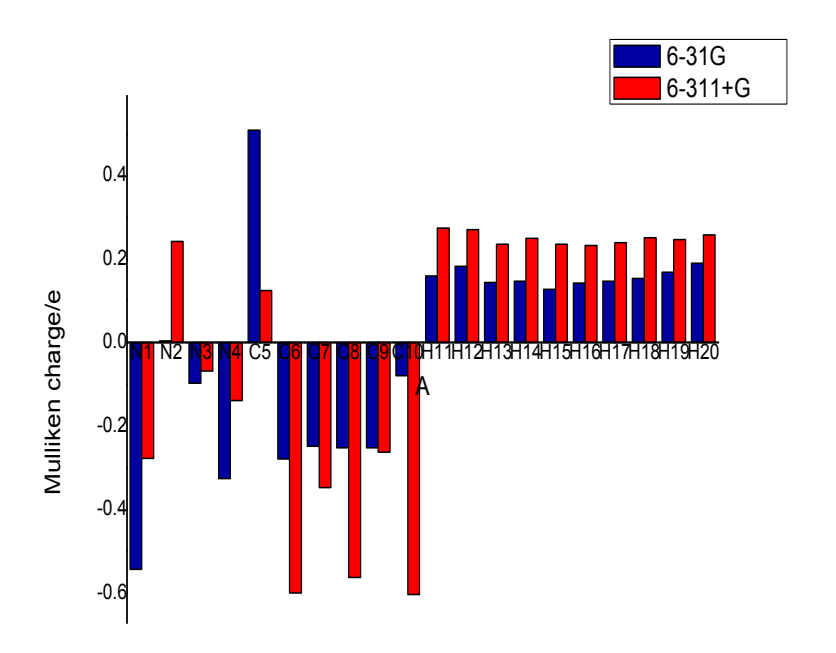


Fig. 4 Bar diagram representing the Mulliken atomic charge distribution of Pentylenetetrazole (PTZ)

Table 5:Observed Frequency (cm $^{-1}$),TheoreticalFrequency (cm $^{-1}$) and Vibrational assignment with PED(%) of Pentelyenetetrazole (PTZ) based on B3LYP/6-31G(0.9555,0.9826)and B3LYP/6-311+G(0.9642,0.9860)method and basis set.

cis		served nency(cm ⁻¹)		Theoretical Frequency(cm ⁻¹)			Vibrational
e C	FT-	FT-	6-3	6-31G 6-311+G		- assignment (PED %)	
Spe	IR	Raman	Calc	scaled	Calc	Scaled	
Α	-	3005	3147	3007	3114	3003	ν CH(91)
A	-	2983	3125	2986	3094	2983	ν CH(94)
A	-	-	3094	2956	3060	2951	ν CH(82)
A	-	-	3088	2951	3054	2945	ν CH(88)
A	-	-	3077	2940	3045	2936	v CH(76)+v CH(15)
A	2946	2951	3056	2920	3024	2916	ν CH(84)

A	2929	2927	3044	2909	3013	2905	ν CH(93)
A	-	2911	3042	2907	3010	2902	ν CH(12)+ν CH(78)
A	2863	2869	3029	2894	3000	2893	ν CH(88)
A	2821	-	3019	2885	2987	2860	ν CH(84)+ν CH(11)
	1530	1531	1560	1533	1552	1530	ν NC(27)+ β HCH(12)+ β
A	1330	1331	1300	1333	1332	1550	HCH(25)
A	-	-	1541	1514	1531	1510	β HCH(59)
A	-	-	1536	1509	1527	1506	β HCH(70)
A	-	-	1530	1503	1521	1500	β HCH(58)
A	1468	1474	1527	1500	1517	1496	β HCH(68)
A	1439	1449	1524	1477	1514	1473	β HCH(54)+ $β$ HCH(10)
A	1428	-	1463	1438	1456	1436	$v CC(17)+\tau HCNC(19)$
A	1378	1375	1427	1402	1420	1400	β HCC(12)+τ HCCC(60)
							β HCC(13)+ τ
	1370	-	1420	1395	1413	1393	$HCCN(14)+\tau$
A							$HCCN(13)+\tau HCNC(12)$
A	1382	-	1408	1382	1402	1382	β HCC(12)+ τ HCCC(33)
A	1355	-	1407	1382	1398	1378	β HCN(25)+ τ HCCN(21)
A	1344	1347	1388	1364	1380	1361	β HCC(26)+ τ HCCN(30)
A	1334	-	1344	1321	1346	1327	β HCC(44)+ $τ$ HCNC(18)
	1302	1307	1310	1287	1309	1291	β HCC(14)+ β HCN(12)+ τ
A	1302	1507	1310	1207	1307	1231	HCNC(13)
	1271	1274	1306	1283	1305	1287	β HCC(10)+ β HCC(12)+ β
A							$HCC(17)+\tau HCCN(13)$
	1246	1241	1292	1269	1286	1268	v NC(10)+ $β$ HCC(12)+ $τ$
A	4407		1010	4400	1015	4400	HCCC(12)
A	1187	-	1219	1198	1215	1198	β HCC(16)
A	1171	-	1215	1194	1208	1191	v NC(31)
A	1115	-	1210	1129	1206	1119	v NN(55)
A	1097	1100	1138	1118	1132	1116	τ CCCC(30)
A	1088	1092	1128	1108	1119	1103	v CC(56)
A	1078	1079	1064	1045	1062	1047	β NNN(66)
A	-	1028	1059	1041	1053	1038	$v CC(41) + \beta CNN(11)$
	993	997	1038	1020	1040	1025	v NN(24)+ $β$ CCC(11)+ $τ$
A	060		006	070	000	074	HCCC(10)
A	968	-	996	979	988	974	v CC(15)
A	962	-	968	951	973	959	v NN(22)
A	894	-	925	909	926	913	v NC(14)+β NCN(44)
A	864	-	911	895	912	899	β NNC(22)
A	832	-	873	858	869	857	v CC(14)+β CCN(15)
	805	802	870	835	863	841	τ HCCC(31)+τ
A	700					700	NCNN(14)
A	799	-	807	793	801	790	v CC(51)

A	744	-	751	738	738	728	τ NNNC(13)+δ CNNC(53)
	676	679	704	692	699	689	τ NNNC(74)+ δ
A							CNNC(12)
A	633	635	675	663	670	661	v NC(54)
A	504	501	643	632	635	626	ν CC(21)+β NNC(11)+τ NCNN(11)
A	-	-	509	500	507	500	β CCC(38)+ τ HCCC(10)
A	-	395	449	441	448	432	β CNN(19)
A	-	349	390	383	388	383	β CCC(28)+ τ CCNC(12)
A	-	273	355	309	354	319	β CCN(40)
A	-	-	343	298	341	296	β CCN(12)+β CNN(27)+τ HCCC(10)
A	-	245	268	263	265	261	β CCN(21)+β CCC(13)+τ CCNC(18)
A	-	155	234	168	234	168	τ CCNC(13)+ $δ$ CCNN(21)
A	-	-	156	153	155	153	τ CCCN(65)
A	-	-	101	99	100	99	τ NCNN(10)+τ CCCN(10)+δ CCNN(30)

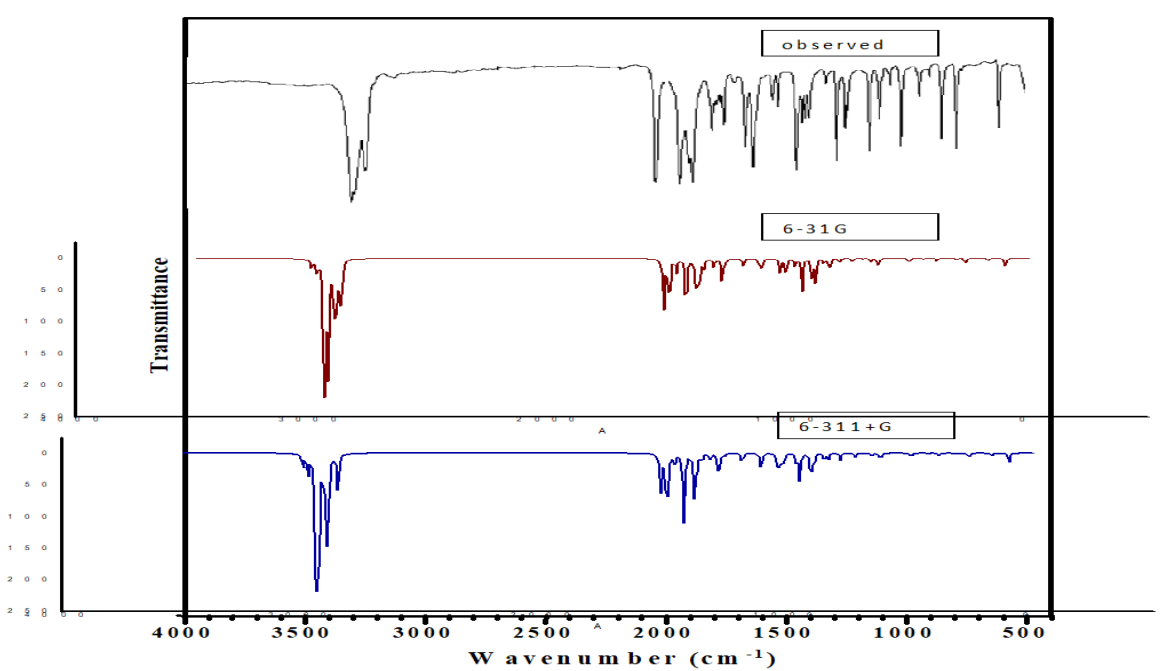


Fig. 5. Comparative representation of FT-IR spectra for Pentylenetetrazole (PTZ)

ISSN: 0011-9342 | Year 2021 Issue: 7 | Pages: 10815 - 10830

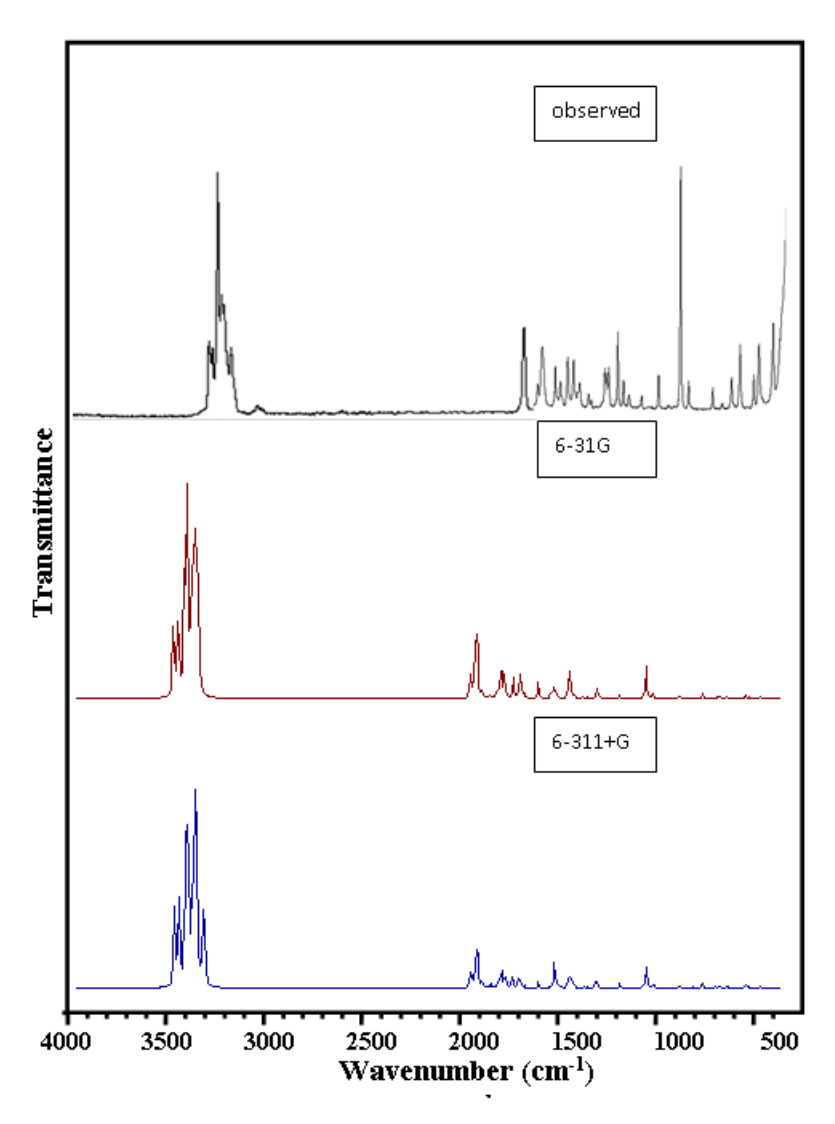


Fig. 6. Comparative representation of FT-Raman spectra for Pentylenetetrazole (PTZ)

CONCLUSION

The present investigation thoroughly analyzed the HOMO-LUMO, and vibration spectra, both infrared and Raman of PTZ molecules with B3LYP method with standard 6-31G and 6-311+G basis sets. All the vibration bands are observed in the FT-IR and F-Raman spectra of the compound are assigned to various modes of vibration and most of the modes have wave numbers in the expected range. The complete vibration assignments of wave numbers are made on the basis of potential energy distribution (PED). The electrostatic potential surfaces (MEP) together with complete analysis of the vibration spectra, both IR and Raman spectra help to identify the structure and symmetry. The excellent agreement of the calculated and observed vibration spectra reveals the advantages over the other method. Finally, calculated HOMO-LUMO energies show that the charge transfer occurs in the molecule, which are responsible for the bioactive properly of the biomedical compound PTZ.

ISSN: 0011-9342 | Year 2021 Issue: 7 | Pages: 10815 - 10830

References

- [1]Ervand G Paronikyan, Anthi Petrou, Maria Fesatidou, Athina Geronikaki, Shushanik Sh Dashyan, Suren S Mamyan, Ruzanna G Paronikyan, Ivetta M Nazaryan, Hasmik H Hakopyan.MedChemComm, 10(8), 1399-1411 (2019-9-20)
- [2]Morgane Boillot, Clément Huneau, Elise Marsan, Katia Lehongre, Vincent Navarro, Saeko Ishida, Béatrice Dufresnois, Ekim Ozkaynak, Jérôme Garrigue, Richard Miles, Benoit Martin, Eric Leguern, Matthew P Anderson, Stéphanie Baulac. Brain: a journal of neurology, 137(Pt 11), 2984-2996 (2014-9-23)
- [3]Ming-Xia Song, Yuping Huang, Shiben Wang, Zeng-Tao Wang, Xian-Qing Deng. Archiv der Pharmazie, 352(8), e1800313 (2019-7-23)
- [4]Phedias Diamandis, Jan Wildenhain, Ian DClarke, Adrian G Sacher, Jeremy Graham, David S Bellows, Erick K M Ling, Ryan J Ward, Leanne G Jamieson, Mike Tyers, Peter B Dirks. Nature chemical biology, 3(5), 268-273 (2007-4-10)
- [5]Nikita Zabinyakov, Garrett Bullivant, Feng Cao, Matilde Fernandez Ojeda, Zheng Ping Jia, Xiao-Yan Wen, James J Dowling, Gajja S Salomons, Saadet Mercimek-Andrews. PloS one, 12(10), e0186645 (2017-10-21)
- [6] Mehwish Anwer, Riikka Immonen, Nick M E A Hayward, Xavier Ekolle Ndode-Ekane, Noora Puhakka, Olli Gröhn, Asla Pitkänen. Scientific reports, 9(1), 11819 (2019-8-16)
- [7] **A.Ramu**, M.K. Murali, M.karnan, M.Karunanithi. Journal of Information and Computational Science. ISSN: 1548-7741. Volume 9 Issue 11 2019.P: 1290- 1314. DOI: http://www.joics.org/gallery/ics-1805.pdf.
- [8] K. Fukui, Science 218 (1982) 474.
- [9] S. Gunasekaran, R.A. Balaji, S. Kumaresan, G. Anand, S. Srinivasan, Can. J. Anal. Sci. Spectrosc. 53 (2008) 149.
- [10] K. Fukui, T. Yonesawa, H. Shingu, J. Chem. Phys. 20 (1952) 722.
- [11] C.H. Choi, M. Kertesz, J. Phys. Chem. 101 (1997) 3823.
- [12] R.G. Parr, L. Szentpaly, S. Liu, J. Am. Chem. Soc. 121 (1999) 1922.
- [13] P.K. Chattaraj, B. Maiti, U. Sarkar, J. Phys. Chem. 107A (2003) 4973.
- [14] R.G. Parr, R.A. Donnelly, M. Ley, W.E. Palke, J. Chem. Phys. 68 (1978) 3801.
- [15] R.G. Parr, R.G. Pearson, J. Am. Chem. Soc. 105 (1983) 7512.
- [16] R.G. Parr, P.K. Chattaraj, J. Am. Chem. Soc. 113 (1991) 1854.
- [17] R. Parthasarathi, J. Padmanabhan, M. Elango, V. Subramanina, P. Chattaraj, Chem. Phys. Lett. 394 (2004) 225.
- [18] R. Parthasarathi, J. Padmanabhan, V. Subramanian, B. Maiti, P. Chattaraj, Curr. Sci. 86 (2004) 535.
- [19] R. Parthasarathi, J. Padmanabhan, V. Subramanian, U. Sarkar, B. Maiti, P. Chattaraj, Internet Electron J. Mol. Des. 2 (2003) 798.
- [20] S. Chidangil, M.K. Shukla, P.C. Mishra, J. Mol. Model. 4 (1998) 250.
- [21]R.S. Mulliken, Electronic Population Analysis on LCAO-MO Molecular Wave Functions., J. Chem. Phys. 23 (1995) 1833-1840.

- [22]P. N. Prasad, D. J. Williams, "Introduction to Nonlinear Optical Effects in Molecules and Polymers" Wiley: New York, 1991.
- [23] R.M. Silverstein, G.C. Bassler, T.C. Morril, Spectrometric Identification of Organic Compounds, fifth ed., John Wiley and Sons Inc., Singapore, 1991.
- [24] R. Shanmugam, D. Sathyanarayana, Spectrochim. Acta 40 (1984) 764–773.
- [25] S. Genc, N. Dege, A. Cetin, A. Cansiz, M. Sekerci, M. Dincer, Acta Crystallogr. E60 (2004) o1340–o1342.
- [26] S. Kundoo, A.N. Banerjee, P. Saha, K.K. Chattopadhyay, Mater. Lett. 57 (2003) 2193–2197.
- [27] N.P.G. Roeges, A Guide to the Complete Interpretation of IR Spectra of Organic Compounds, Wiley, New York, 1994.
- [28] N.B. Colthup, L.H. Daly, S.E. Wiberly, Introduction to Infrared and Raman Spectroscopy, Academic Press, New York, 1990.



Science Master Journal Urists
Group

Match Manuscript

Downloads

Help Center

Login

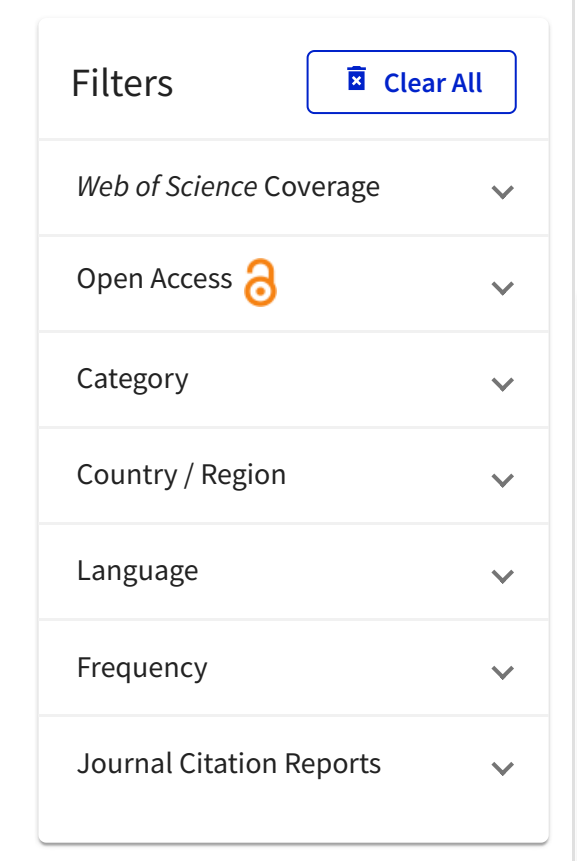


The power of the Web of Science™ on your mobile device, wherever inspiration strikes.

Dismiss

Learn More







0976-0997 Search

Sort By: Title (A-Z) ▼

Search Results

Found 1 results (Page 1) Share These Results

Exact Match Found

INDIAN JOURNAL OF NATURAL SCIENCES

Publisher: TAMIL NADU SCIENTIFIC RESEARCH

ORGANISATION, NO 46-141,

MEENAKSHIPURAM RD, NEAR POST OFFICE, PUDUKKOTTAI DIST, TAMIL NADU, INDIA, ARIMALAM, 622 201

ISSN / eISSN: **0976-0997**

Additional Web of Science Indexes: Zoological Record

Share This Journal
View profile page

* Requires free login.

International Bimonthly (Print)

ISSN: 0976 – 0997

RESEARCH ARTICLE

Simulation of FT-IR and FT-Raman Spectra Based on quantum chemical Calculations, Vibrational Assignments, Hyperpolarizability, and Homo-Lumo Analysis of 5(4 methyl phenyl)tetrazole (5MPTZ)

A.Rajeswari¹, M.K. Murali^{1*} and A.Ramu²

¹PG and Research Department of Physics, JJ.College of Arts & Science (Autonomous), Pudukottai -622422, Affiliated to Bharathidasan University, Trichy, Tamil Nadu, India.

²Department of Physics, Ganesar College of Arts and Science, Melaisivapuri-622403, Affiliated to Bharathidasan University, Trichy, Tamil Nadu, India.

Received: 06 Jun 2021 Revised: 25 Jun 2021 Accepted: 16 July 2021

*Address for Correspondence

M.K. Murali

PG and Research Department of Physics, JJ.College of Arts & Science (Autonomous), Pudukottai - 622422, Affiliated to Bharathidasan University, Trichy, Tamil Nadu, India.



This is an Open Access Journal / article distributed under the terms of the Creative Commons Attribution License (CC BY-NC-ND 3.0) which permits unrestricted use, distribution, and reproduction in any medium, provided the original work is properly cited. All rights reserved.

ABSTRACT

The spectra of 5(4 methyl phenyl)tetrazole (5MPTZ) have been recorded in the regions 4000–400 cm⁻¹ for FT-IR and 3500-100 cm⁻¹ for FT-Raman. The geometry optimization, vibrational frequencies were obtained by the density functional theory (DFT) using B3LYP method with 6-31G and 6-311+G basis sets. The complete assignments were performed on the basis of the potential energy distribution (PED) of the vibrational modes, calculated and the scaled values were compared with experimental FT-IR and FT-Raman spectra. The HOMO and LUMO energy gap reveals that the energy gap reflects the chemical activity of the molecule. The dipole moment (μ), polarizability (α), anisotropy polarizability ($\Delta\alpha$) and first hyperpolarizability (βιοι) of the molecule have been reported. Information about the size, shape, charge density distribution and site of chemical reactivity of the molecule has been obtained by molecular electrostatic potential (MEP).

Keywords: 5(4 methyl phenyl)tetrazole (5MPTZ), DFT, FT-IR, FT-Raman, MEP.

INTRODUCTION

Tetrazole-related molecules have attracted considerable attention due to their biological activities. The synthesis of new members of this family of ligands is an important direction in the development of modern coordination chemistry [1,2]. Tetrazole compounds have a wide range of applications in coordination chemistry, medicinal





Vol.12 / Issue 67 / August / 2021

International Bimonthly (Print)

Rajeswari et al.

chemistry and material science[3,4] . Tetrazole derivatives are used as antibiotics and optically active tetrazole-containing antifungal preparations of azole type was reported. There is always a need for new and effective antifungal and antibacterial agents with broad-spectrum activities. It was decided to develop this interest by ascertaining the molecules features essential for activity and utilizing them to develop a new class of potential drugs [5]. The detailed investigations of the 5(4 methyl phenyl) tetrazole (5MPTZ) were carried out with Gaussian 09 software package [6] using the Beeke-3-Lee-Yang-Parr (B3LYP) functional[7,8] supplemented with the standard 6-31G and 6-311+G basis set.

Experimental Details

The fine sample of 5(4 methyl phenyl) tetrazole (5MPTZ) was obtained from Lancaster Chemical Company.UK, with a stated purity of 99% and it was used as such without further purification. The FT-Raman Spectrum of 5MPTZ was recorded using 1064 nm line of ND: YAG laser for excitation wavelength in the region 3500-100 cm⁻¹ on Thermo Electron Corporation model Nexus spectrometer equipped with FT-Raman module accessory. The FT-IR Spectrum of the title compound was recorded in the region 4000-400 cm⁻¹ on Perking Elmer Spectrophotometer in KBr pellet.

Computational Details

The combination of Vibration spectra with quantum chemical calculation is effective for understanding the fundamental mode of vibration of the compound. The structural characteristic, stability and energy of the compound under investigation are determined by DFT with the three-parameter hybrid functional (B₃) for the exchange part and the Becke Three Lee Yong-Pare (LYP) and 6-31G ,6-311+G basis sets with Gaussian 09 Program Package. The Cartesian representation of the theoretical force constants has been compound at the fully optimized geometry by assuming the molecule belongs to C₁ point group symmetry. The Transformation of force field from Cartesian to internal local symmetry coordinates, the scaling, and the subsequent normal coordinate analysis (NCA) Calculation of potential energy distributions (PED) has been done on a PC with the VEDA program.

Geometrical parameter

The molecular structure along with numbering of atoms of 5(4 methyl phenyl) tetrazole (5MPTZ) was as shown in the Fig.1 . The Global minimum energies of the title molecule calculated by Density Functional Theory structure optimization for different basis sets such as B3LYP/6-31+ G(d,p), B3LYP/6-31++ G(d,p), B3LYP/6-311++ G(d,p) are given in Table 1. Geometry optimization is the procedure that attempts to find the configuration of minimum energy of the molecule. The procedure calculates the wave function and the energy at a starting geometry and then proceeds to search a new geometry of a lower energy. This is repeated until the lowest energy geometry is found. The procedure calculates the force on each atom by evaluating the gradient or the first derivative of the energy with respect to atomic positions. Sophisticated algorithms are then used at each step to select a new geometry, aiming for rapid convergence to the geometry of the lowest energy. In the final, minimum energy geometry the force on each atom is zero. The optimized geometric parameters like bond length, bond angles of 5(4 methyl phenyl) tetrazole (5MPTZ) were calculated and given in Table II .

The title compound is a tetrazole ligand with a toluene substituent in position 5 (Fig. 1). In the solid state structure the molecule possesses crystallographic mirror symmetry, with four C atoms lying on the reflecting plane, which bisects the phenyl and tetrazole rings [9]. The C-C bond lengths in the benzene ring obtained from B3LYP ranges from 1.41 to 1.40 Å and C-H bond length ranges from 1.09 to 1.08 Å. The C-N bond lengths in the tetrazole ring have calculated as 1.36 and 1.35 Å. the N1-N2 and N3-N4 bond length of the tetrazole ring has longer than the N2-N3 bond length in the same ring. the C-H bond lenths of the methyl group were 1.10-1.09 Å. The bond angle of the phenyl ring does not have equal value .it varied from 118° to 121°. All the values were compared with experimental values [9], those are good agreement with each other.





Vol.12 / Issue 67 / August / 2021

International Bimonthly (Print)

Rajeswari et al.

Electronic properties

When we are dealing with interacting molecular orbitals, the two that interact are generally The Highest energy Occupied Molecular Orbital (HOMO) of one molecule, The Lowest energy Unoccupied Molecular Orbital (LUMO) of the other molecule. These orbitals are the pair that lie closest in energy of any pair of orbitals in the two molecules, which allows them to interact most strongly. These orbitals are sometimes called the frontier orbitals, because they lie at the outermost boundaries of the electrons of the molecules. The energy gap between the HOMOs and LUMOs called as energy gap. It is a critical parameter in determining molecular electrical transport properties because it is a measure of electron conductivity [10]. The HOMO energy characterizes the ability of electron giving, the LUMO characterizes the ability of electron accepting, and the gap between HOMO and LUMO characterizes the molecular chemical stability [11]. Surfaces for the frontier orbital's were drawn to understand the bonding scheme of present compound. The features of these Molecular Orbitals can be seen in Figure 2.

This electronic absorption corresponds to the transition from the ground state to the first excited state and is mainly described by one electron excitation from HOMO to LUMO. While the energy of the HOMO is directly related to the ionization potential, LUMO energy is directly related to the electron affinity. There are lots of applications available for the use of HOMO and LUMO energy gap as a quantum chemical descriptor. It establishes correlation in various chemical and bio-chemical systems [12]. The HOMO–LUMO energy gap is an important value for stability index. A large HOMO–LUMO gap implies high stability for the molecule in the sense of its lower reactivity in chemical reactions [13]. According to B3LYP calculation, EHOMO , ELUMO and the energy band gap (translation from HOMO to LUMO) of the title molecule in electron Volt are presented in Table 2 . Considering the chemical hardness, large HOMO-LUMO gap represent a hard molecule and small HOMO-LUMO gap represent a soft molecule. From the Table 2, it is clear that the molecule under investigation is very soft since it has a small HOMO-LUMO gap and also having a high value for softness.

NLO properties

The NLO activity provide the key functions for frequency shifting, optical modulation, optical switching and optical logic for the developing technologies in areas such as communication, signal processing and optical interconnections [14]. The first static hyperpolarizability (β tot) and its related properties (β , α and $\Delta\alpha$) have been calculated using B3LYP/6-31G and 6-311+G level based on finite field approach. In the presence of an applied electric field, the energy of a system is a function of the electric field and the first hyperpolarizability is a third rank tensor that can be described by a 3×3×3 matrix. The 27 components of the 3D matrix can be reduced to 10 components because of the Kleinman symmetry [15]. The matrix can be given in the lower tetrahedral format. It is obvious that the lower part of the 3×3×3 matrices is a tetrahedral.

The values of the polarizabilities (α) and first hyperpolarizability (β tot) of the Gaussian 09 output are reported in atomic units (a.u.). All the calculated values then have been converted into electrostatic units (esu). (For α : 1a.u. = 0.1482 × 10⁻²⁴ esu; For β : 1a.u. = 8.639 ×10⁻³³ esu). The total molecular dipole moment and first order hyperpolarizability are 7.0628 and 7.2331 Debye and 1.1830x10⁻³⁰ and 1.241010⁻³⁰ esu , respectively and are depicted in Table 4.Total dipole moment of title molecule is greater than that of urea and first order hyperpolarizability is very much greater than that of urea (μ and β of urea are 1.3732 Debye and 0.3728×10⁻³⁰ esu) obtained by B3LYP/6-31G and 6-311+G method. This result indicates the nonlinearity of the title molecule.

Mulliken Atomic charge

Atomic charges has been used to describe the process of electronegativety equalization and charge transfer in chemical reactions [16,17]. Mulliken atomic charge calculation has an important role in the application of quantum chemical calculation to molecular system because atomic charges affect dipole moment ,molecular polarizability, electronic structure and a lot of properties of electronic systems. The Mulliken atomic charges are calculated at B3LYP/6-31G and 6-311+G level by determining the electron population of each atom as defined by the basis function and collected in Table 3.





Vol.12 / Issue 67 / August / 2021

International Bimonthly (Print)

Rajeswari et al.

A Graph of Mulliken atomic charge on individual atom of 5MPTZ was drawn and given in Figure 8. it is worthy to mention that N3,N4 and C8,C9,C11and C12,C17 atoms of the title molecule exhibit negative charge where all hydrogen atoms exhibit positive charges.

Molecular Electrostatic Potential

The molecular electrostatic potential is the potential that a unit positive charge would experience at any point surrounding the molecule due to the electron density distribution in the molecule. The electrostatic potential generated in space by charge distribution is helpful to understand the electrophilic and nucleophilic regions in the title molecule. Electrostatic potential maps, also known as electrostatic potential energy maps, or molecular electrical potential surfaces, illustrate the charge distributions of molecules three dimensionally. Knowledge of the charge distributions can be used to determine how molecules interact with one another. Molecular electrostatic potential (MEP) mapping is very useful in the investigation of the molecular structure with its physiochemical property relationships [18-21]. In the electrostatic potential map, the semispherical blue shapes that emerge from the edges of the above electrostatic potential map are hydrogen atoms.

The molecular electrostatic potential surface MESP which is a 3D plot of electrostatic potential mapped onto the iso electron density surface simultaneously displays molecular shape, size and electrostatic potential values. The Electrostatic potential surface of 5MPTZ is shown in Figure 3. The colour scheme for the MESP surface is red electron rich or partially negative charge; blue - electron deficient or partially positive charge; light blue-slightly electron deficient region; yellow–slightly electron rich region, respectively. Areas of low potential, red, are characterised by an abundance of electrons. Areas of high potential, blue, are characterised by a relative absence of electrons. That is negative potential sites are on the electronegative atoms like nitrogen while the positive potential sites around the hydrogen and carbon atoms. Green area covers parts of the molecule where electrostatic potentials are nearly equal to zero . This is a region of zero potential enveloping the π systems of aromatic ring leaving a more electrophilic region in the plane of hydrogen atom. Nitrogen has a higher electronegativity value would consequently have a higher electron density around them. Thus the spherical region that corresponds to nitrogen atom would have a red portion on it. The MESP of 5MPTZ clearly indicates the electron rich centres of nitrogen atom.

Vibrational Assignment

Vibrational spectroscopy has been shown to be effective in the identification of functional groups of organic compounds as well as in studies on molecular conformations and reaction kinetics [22] The symmetry possessed by the title molecule helps to determine and classify the actual number of fundamental vibrations of the system. The observed spectrum is explained on the basis of C1 point group symmetry. The title molecule consists of 20 atoms, which undergo 36 normal modes of vibrations .The total number of 54 fundamental vibrations (3N-6, where N is the number of atoms) are distributed as Γ vib = 37 A' (In plane vibrations;2N-3) 17 A" (out of plane vibrations;N-3) All vibrations are active both in Raman and infrared absorption. The detailed vibrational assignment of fundamental modes of 5MPTZ along with the calculated IR and Raman frequencies, normal mode descriptions using PED (Potential Energy Distribution) are reported in Table III. The calculated frequencies are usually higher than the corresponding experimental quantities, due to the combination of electron correlation effects and basis set deficiencies.

C–H vibrations: The presence of C-H stretching vibrations in the region 3000 - 3200 is common for heteroaromatic structure. In the present study the C-H stretching vibrations of the title compound are observed at 3082 and 3045 cm⁻¹ in the FT-IR spectrum and 3050cm⁻¹ in the FT-Raman spectrum. The calculated wave numbers at 3097,3067,3058,3044 cm⁻¹ are assigned to C-H stretching vibrations. The C-H out of plane bending vibrations are occurring in the region 900-667 cm⁻¹ [23].In the present investigation the computed wave numbers at 1073,1009,1008 are assigned to C-H out of plane vibrations and the scaled values are in good agreement with the experimental values. The assignments of other in-plane and out-of-plane C-H bending vibrations are as shown in Table III.





Vol.12 / Issue 67 / August / 2021

International Bimonthly (Print)

Rajeswari et al.

Ring vibrations: There are six equivalent C-C bonds in benzene and consequently there will be six C-C stretching vibrations. In addition, there are several C-C-C in-plane and out-of-plane bending vibrations of the ring carbons. However, due to high symmetry of benzene, many modes of vibrations are infrared inactive. In general, the bands around 1400 to 1650 cm⁻¹ in benzene derivatives are assigned to skeletal stretching C-C bands[24]. In the case of title compound the carbon stretching vibrations have been observed at 1613,1580,1505 cm⁻¹ in the FT-IR spectrum and 1630.1595 cm⁻¹ in FT-Raman spectrum were assigned to C-C stretching vibration which show good agreement with scaled frequencies. The measured wavenumbers at 1603,1558,1533 cm⁻¹ are assigned to C-C stretching vibrations. It is clear from the above values that the difference between observed and scaled frequencies is very small. In general, the C-C-C out-of-plane and in-plane-bending vibrational wavenumber observed in FT-IR spectrum and FT-Raman spectrum shows good agreement with theoretically computed wavenumber.

C-N Vibrations: The mixing of several bands are possible in this region. The C-N stretching frequency is a rather difficult task. In the present study the band observed at 1285,1116 cm⁻¹ in FT-IR spectrum is attributed to C-N bending vibration. The theoretically calculated value of corresponding C-N bending vibration is predicted at 1298,1131 cm⁻¹. B3LYP computation gives mode arising from the N-N stretching at 1158,1147 cm⁻¹ corresponding to the peak at 1187,1163 cm⁻¹ in IR spectrum. The methyl group CH stretching vibrational frequency band is found in 5MPTZ at 2924, 2910 cm⁻¹ respectively, in the FT-Raman, FT-IR spectrum. The CH stretching mode for methyl is in the zone of 3000-2800 cm⁻¹ [25,26].theoretically found at 2994,2965,2906 cm⁻¹.

CONCLUSION

The present investigation thoroughly analyzed the HOMO-LUMO, and vibration spectra, both infrared and Raman of 5MPTZ molecules with B3LYP method with standard 6-31G and 6-311+G basis sets. All the vibration bands are observed in the FT-IR and FT-Raman spectra of the compound are assigned to various modes of vibration and most of the modes have wave numbers in the expected range. The complete vibration assignments of wave numbers are made on the basis of potential energy distribution (PED). The electrostatic potential surfaces (MEP) together with complete analysis of the vibration spectra, both IR and Raman and help to identify the structure and symmetry. The excellent agreement of the calculated and observed vibration spectra reveals the advantages over the other method. Finally, calculated HOMO-LUMO energies show that the charge transfer occurs in the molecule, which are responsible for the bioactive properly of the biomedical compound 5MPTZ.

REFERENCES

- 1. H. M. Nanjundaswamy, and H. Abrahamse, Hetrocycles, 2014, 89, 2137-2150.
- 2. T. Jin, F. Kitahara, S. Kamijo, and Y. Yamamoto, Tetrahedron Lett., 2008, 49, 2824-2827.
- 3. B. Sreedhar, A. Suresh Kumar, and D. Yada, Tetrahedron Lett., 2011, 52, 3565-3569.
- 4. L. V. Myznikov, A. Hrabalek, and G. I. Koldobskii, Chem. Hetrocyclic Chem., 2007, 43, 1-9
- 5. L. Zamani, B.B.F. Mirjalili, K. Zomorodian and S. Zomorodian, 133 S. Afr. J. Chem., 2015, 68, 133–137.
- M.J. Frisch, G.W. Trucks, H.B. Schlegal, G.E. Scuseria, M.A. Robb, J.R. Cheesman, V.G. Zakrzewski, J.A. Montgomery Jr., R.E. Stratmann, J.C. Burant, S. Dapprich, J.M. Millam, A.D. Daniels, K.N. Kudin, M.C. Strain, O. Farkas, J. Tomasi, V. Barone, M. Cossi, R. Cammi, B. Mennucci, C. Pomkelli, C. Adamo, S. Clifford, J. Ochterski, G.A. Petersson, P.Y. Ayala, Q. cui, K. Morokuma, N. Rega, P. Salvador, J.J. Dannenberg, D.K. Malilck, A.D. Rabuck, K. Raghavachari, J.B. Foresman, J. Cioslowski, J.V. Ortiz, A.G. Baboul, B.B. Stefanov, G. Liu, A. Liashenko, P. Piskorz, I.Komaromi,R.Gomperts, R.L. Martin, D.J. Fox, T.Keith,M.A. Al-Laham, C.Y. Peng, A.Nanayakkara, M. Challa-Combe, P.M.W. Gill, B. Johnson,W. Chen,M.W.Wong, J.L. Andres, C. Gonzalez, M. Head-Gordon, E.S. Replogle, J.A. Pople, Gaussian 98, Revision A 11.4, Gaussian Inc., Pittsburgh, PA, 2002.
- 7. A.D. Becke, J. Chem. Phys. 98 (1993) 5648.
- 8. C. Lee, W. Yang, R.C. Parr, Phys. Rev. B 37 (1998) 785.





Vol.12 / Issue 67 / August / 2021

International Bimonthly (Print)

- 9. Dong-Yue Hu, Xiao-Wei Chu and Zhi-Rong Qu. Acta Cryst. (2009). E65, o2463. doi:10.1107/S1600536809036411
- 10. D.F.V. Lewis, C. Loannides, D.V. Parke, Xenobiotica 24 (1994) 401-408.
- 11. Mehmet Karabacak, Mehmet Cinar, Mustafa Kurt, Spectrochim. Acta Part A Mol. Biomol. Spectrosc. 74 (2009) 1197–1203.
- 12. Z. Zhou, R.G. Parr, J. Am. Chem. Soc. 112 (1990) 5720-5724.
- 13. R. Ditchfield, Mol. Phys. 27 (1974) 789-807.
- 14. C. Andraud, T. Brotin, C. Garcia, F. Pelle, P. Goldner, B. Bigot, A. Collet, J. Am. Chem. Soc. 116 (1994) 2094–2101
- 15. D.A. Kleinman, Phys. Rev. 126 (1977) 1962-1979.
- 16. S. Fliszar, Charge Distributions and Chemical Effects, Springer, New York, 1983.
- 17. E. Smith, J. Am. Chem. Soc. 113 (1991) 6029-6037.
- 18. I. Fleming, Frontier Orbitals and Organic Chemical Reactions, John Wiley and Sons, New York, pp. 5–27, 1976.
- 19. J.S. Murray, K. Sen, Molecular Electrostatic Potentials, Concepts and Applications, Elsevier, Amsterdam, 1996.
- 20. J.M. Seminario, Recent Developments and Applications of Modern Density Functional Theory, Vol.4, Elsevier, pp 800–806, 1996.
- 21. T. Yesilkaynak, G. Binzet, F. Mehmet Emen, U. Florke, N. Kulcu, H. Arslan, Eur. J. Chem. 1 (2010)
- 22. A. Teimouri, A.N. Chermahini, K. Taban, H.A. Dabbagh, Spectrochim. Acta A 72 (2009) 369-377
- 23. G. Keresztury, Raman spectroscopy: theory, in: J.M. Chalmers, P.R. Griffiths(Eds.), Handbook of Vibrational Spectroscopy, vol. 1, John Wiley &Sons Ltd., 2002, p. 71
- 24. D.N. Sathyanarayana, Vibrational Spectroscopy Theory and Applications, second ed., New Age International (P) Limited Publishers, New Delhi, 2004.
- 25. R. M. Silverstein, G. Clayton Basseler, C. Morril. Spectrometric Identification of Organic Compounds, John Wiley, New York, USA, (1991).
- 26. F. R. Dollish, W. G. Fateley, F. F. Bentely. Characterestic Raman Frequencies On Organic Compounds, Wiley, New York.

Table 1: Geometry Optimization Parameter of 5(4 methyl phenyl)tetrazole (5MPTZ) based on B3LYP/6-31G and B3LYP/6-311+G method and basis set

Bond Length(Å)			Bond Angle(°)		
Atom	6-31G	6-311+G	Atom	6-31G	6-311+G
C10-C17	1.51	1.51	C5-N1-H6	131.076	131.348
C5-C7	1.46	1.46	N1-C5-C7	126.995	126.910
C7-C8	1.41	1.41	N4-C5-C7	125.406	125.550
C9-C10	1.41	1.41	C5-C7-C12	122.300	122.211
C7-C12	1.41	1.40	C8-C9-C10	121.259	121.342
C10-C11	1.40	1.40	C11-C10-C17	121.104	121.250
C11-C12	1.40	1.39	C10-C11-C12	121.068	121.120
N3-N4	1.39	1.39	C9-C8-H13	120.957	120.821
C8-C9	1.39	1.39	C9-C10-C17	120.797	120.776
N1-N2	1.39	1.39	C7-C12-H16	120.709	120.758
N1-C5	1.36	1.36	C7-C12-C11	120.464	120.543
N4-C5	1.35	1.34	C7-C8-C9	120.287	120.345
N2-N3	1.32	1.32	N2-N1-H6	119.550	119.503
C17-H18	1.10	1.09	C10-C11-H15	119.469	119.410
C17-H20	1.10	1.09	C12-C11-H15	119.463	119.377
C17-H19	1.09	1.09	C10-C9-H14	119.396	119.248
C12-H16	1.09	1.08	C8-C9-H14	119.345	119.130
C9-H14	1.09	1.08	C5-C7-C8	118.874	119.110





International Bimonthly (Print)

int) ISSN: 0976 – 0997

C11-H15	1.09	1.08	C11-C12-H16	118.826	118.897
C8-H13	1.08	1.08	C8-C7-C12	118.826	118.678
N1-H6	1.01	1.00	C7-C8-H13	118.756	118.637
			C9-C10-C11	118.095	117.972
			C10-C17-H19	111.510	111.460
			C10-C17-H20	111.392	111.377
			C10-C17-H18	111.099	111.138
			N2-N3-N4	110.866	110.610
			N2-N1-C5	109.374	109.523
			H19-C17-H20	108.043	107.892
			N1-C5-N4	107.599	107.584
			H18-C17-H19	107.485	107.541
			H18-C17-H20	107.106	107.188
			N3-N4-C5	106.612	106.712
			N1-N2-N3	105.549	105.614

Table 2: HOMO-LUMO energy (eV) and other related properties of 5(4 methyl phenyl)tetrazole (5MPTZ) based on B3LYP/6-31G and B3LYP/6-311+G method and basis set

Parameters	6-31G	6-311+G
	(eV)	(eV)
Homo(I)	-6.8600	-7.1484
Lumo(A)	-1.6599	-2.0000
Energy gap(ΔE)	5.2001	5.1484
Electronegativity	4.2599	4.5742
Global hardness	2.6000	2.5742
Global softness(eV-1)	0.3846	0.3885
Chemical potential	-4.2599	-4.5742
Electriphilicity	3.4898	4.0641

Table 3: Mulliken charge (charge/e) of 5(4 methyl phenyl)tetrazole (5MPTZ) based on B3LYP/6-31G and B3LYP/6-311+G method and basis set.

Atom	6-31G	6-311+G			
Atom	Charge/e				
N1	0.6088	0.5648			
N2	0.0148	0.1788			
N3	-0.0822	-0.1907			
N4	-0.3317	-0.3710			
C5	0.4033	1.0604			
H6	0.3623	0.4352			
C7	0.1626	1.7626			
C8	-0.1369	-0.2400			
C9	-0.1635	-0.5421			
C10	0.1262	1.1972			
C11	-0.1665	-1.1517			





International Bimonthly (Print)

ISSN: 0976 - 0997

C12	-0.1386	-0.5323		
H13	0.1839	0.2560		
H14	0.1362	0.2139		
H15	0.1321	0.2051		
H16	0.1165	0.1870		
C17	-0.4836	-1.3766		
H18	0.1660	0.2596		
H19	0.1497	0.2312		
H20	0.1582	0.2416		

Table 4: Dipole moment(μ), Polarizability(α), Anisotropy polaraizability($\Delta\alpha$) and First order polarizability($\beta\omega$) of 5(4 methyl phenyl)tetrazole (5MPTZ) based on B3LYP/6-31G and B3LYP/6-311+G method and basis set

Parameters	6-31G	6-311+G			
μx	6.0797	6.2633			
μ	3.5941	3.6175			
μz	0.0489	0.0429			
axx	-82.6947	-84.9573			
α_{YY}	-63.8621	-65.4107			
αzz	-71.5172	-73.5735			
axy	-9.0345	-9.1645			
αxz	0.1748	0.0651			
αyz	-0.0015	-0.0182			
Вххх	130.0165	135.7744			
βγγγ	20.1929	21.203			
βzzz	0.5809	0.4321			
Вхүү	7.982	9.1765			
Вххч	17.6595	17.3876			
βxxz	0.708	0.462			
βxzz	-6.36	-6.5217			
βyzz	-0.1262	-0.2017			
βyyz	-0.3797	-0.2368			
βxvz	-0.0077	-0.0152			
μ(debye)	7.0628	7.2331			
α(esu)	-10.7583 X10 ⁻²⁴	-11.0478 X10 ⁻²⁴			
Δα(esu)	144.1678 X10 ⁻²⁴	148.1296 X10 ⁻²⁴			
βtot(esu)	1.1830 X10 ⁻³⁰	1.2410 X10 ⁻³⁰			





Vol.12 / Issue 67 / August / 2021

International Bimonthly (Print)

Table 5: Observed Frequency (cm⁻¹), Theoretical Frequency (cm⁻¹) and Vibrational assignment with PED(%) of 5(4 methyl phenyl)tetrazole (5MPTZ) based on B3LYP/6-31G (0.9555, 0.9826)and B3LYP/6-311+G (0.9642, 0.9860)method and basis set

Specis	Observed Frequency		Theoretical				
	(cm ⁻¹)		Frequency(cm ⁻¹) 6-31G 6-311+G			11.0	Vibrational assignment (PED %)
	FT-IR	FT-Raman	Calc	scaled	Calc	Scaled	
Α	3407	_	3710	3524	3687	3502	ν NH(100)
Α	3082	_	3241	3097	3206	3046	ν CH(95)
Α	-	_	3210	3067	3176	3018	ν CH(73)
Α	_	3050	3201	3058	3165	3007	ν CH(93)
Α	3045	-	3186	3044	3153	2995	ν CH(75)
Α	-	_	3134	2994	3097	2942	ν CH(69)
Α	2924	_	3103	2965	3069	2915	ν CH(47)
Α	-	2910	3041	2906	3013	2862	ν CH(58)
Α	1613	1630	1678	1603	1656	1574	ν CC(29)
A	1580	1595	1631	1558	1611	1530	ν CC(27)
A	1505	-	1605	1533	1587	1508	ν CC(18)
Α	1458	_	1539	1471	1528	1452	β HNN(10)+β HCC(11)
Α	-	-	1536	1468	1527	1451	β HCH(28)
Α	-	_	1533	1464	1524	1448	β HCH(39)+τ HCCC(14)
Α	_	_	1477	1451	1460	1435	ν CC(17)+β HCC(10)
Α	1404	1400	1464	1438	1454	1429	β HCH(43)
Α	1377	_	1396	1372	1384	1360	β HCC(21)
Α	-	_	1378	1354	1365	1341	β HNN(19)+ν CC(14)
Α	-	1310	1370	1346	1348	1325	β HNN(35)
Α	1285	_	1321	1298	1302	1279	ν NC(33)+ν CC(16)
Α	1258	1250	1258	1237	1247	1225	ν CC(39)+β HCC(12)
Α	-	1217	1247	1226	1237	1215	β HCC(27)+β HCC(11)
Α	1187	1196	1178	1158	1172	1151	β HNN(19)+β HCC(12) + ν NN(23)
Α	1163	-	1167	1147	1159	1139	ν CC(14)+ν CC(10)+ ν NN(49)
Α	1116	-	1151	1131	1141	1121	v NC(22)
Α	-	1070	1101	1082	1092	1073	τ HCCC(30)+β HCH(14)
Α	1054	-	1059	1041	1050	1032	β CCC(37)
Α	-	1049	1049	1031	1041	1023	β NNN(65)
Α	1027	-	1037	1019	1027	1009	τ HCCC(34)+ν CC(10)
Α	1013	-	1030	1012	1026	1008	τ HCCC(51)
Α	992	980	1022	1004	1017	999	β NCN(26)
Α	-	-	984	967	982	965	τ HCCC(37)
Α	-	-	955	938	974	957	ν NN(64)
Α	-	-	918	902	923	907	β NCN(27)+β NNN(17)
Α	-	-	885	870	878	863	τ HCCC(51)
Α	823	-	858	843	850	835	τ CCC(44)
Α	-	800	824	809	818	803	ν CC(24)
Α	744	740	768	755	737	725	τ NNCN(15)+δ CNNC(17)
Α	698	700	734	721	720	708	τ CCCC(26)+τ CCCC(26)



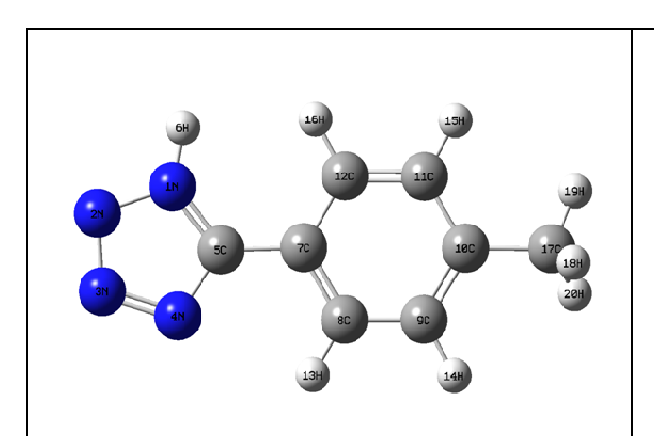


International Bimonthly (Print)

ISSN: 0976 – 0997

Α	ı	ı	696	683	687	675	τ NNNC(71)
Α	-	=	672	660	669	657	τ HNNN(64)
Α	-	650	671	659	645	634	β CCC(30)
Α	615	=	630	619	626	615	τ CCCC(23)
Α	506	-	531	522	520	511	β CCC(31)
Α	-	-	467	458	465	457	τ CCCC(37)
Α	-	-	422	415	427	420	δ CCCC(27)+τ CCCC(26)
Α	-	360	367	361	342	336	τ CCCC(22)
Α	-	350	337	331	336	330	β CCC(68)
Α	-	=	325	319	323	317	ν CC(31)
Α	-	-	213	209	207	204	δ CNNC(34)
Α	1	-	139	136	136	133	β CCC(49)
Α	-	=	83	81	80	79	τ CCCC(55)
Α	-	-	44	44	42	41	τ HCCC(26)
Α	=	=	39	39	32	31	τ CCCN(75)

 $v\text{-}Stretching; \beta\text{-}Bending; \delta\text{-}out\text{-}of\text{-}plane\ bending}; \tau\text{-}Torsion$



E₁₀₀₀= -1.6599eV

E₁₀₀₀= -2.0000eV

ΔE=5.2001eV

ΔE=5.1484 eV

HOMO

Fig. 1. The theoretical geometry structure and atomic numbering scheme of 5(4 methyl phenyl)tetrazole (5MPTZ)

Fig 2: The atomic orbital compositions of the frontier molecular orbital for 5(4 methyl phenyl)tetrazole (5MPTZ).

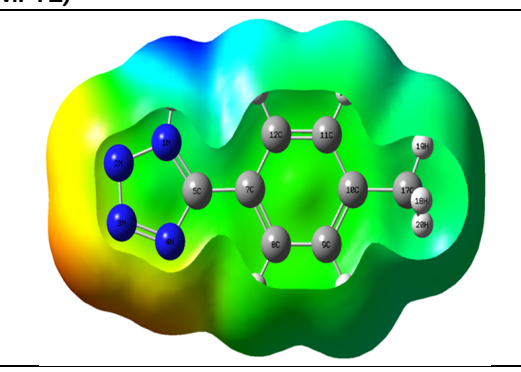


Fig. 3. The total electron density surface mapped with of 5(4 methyl phenyl)tetrazole (5MPTZ)

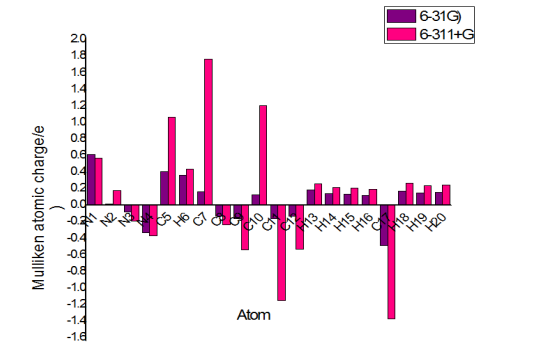


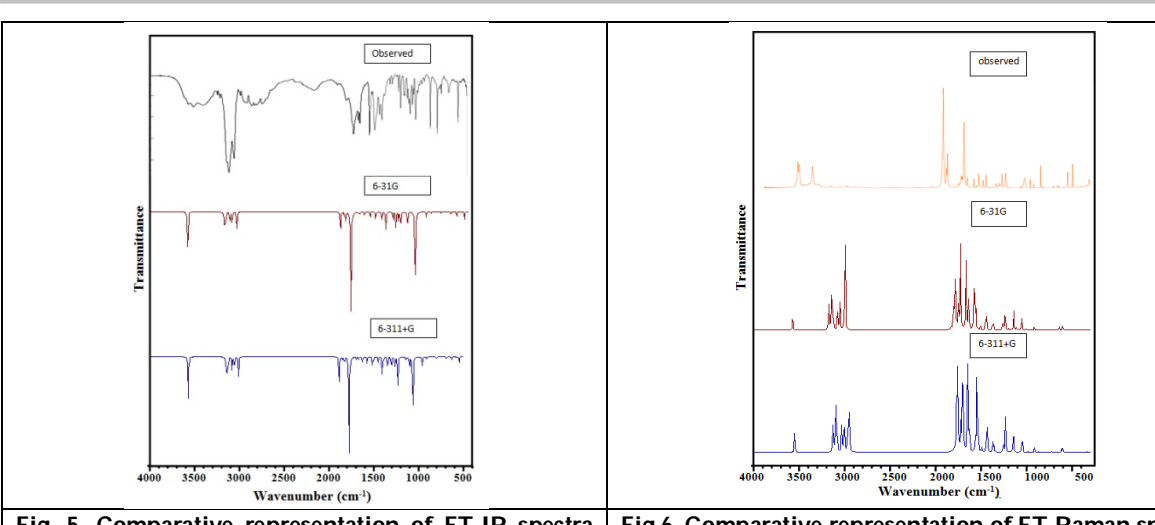
Fig. 4 Bar diagram representing the Mulliken atomic charge distribution of 5(4 methyl phenyl)tetrazole (5MPTZ)





International Bimonthly (Print)

ISSN: 0976 – 0997



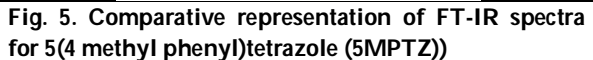


Fig.6. Comparative representation of FT-Raman spectra for 5(4 methyl phenyl)tetrazole (5MPTZ)

